

Tectonically-controlled emplacement mechanisms in the upper crust
under specific stress regimes: case studies

Dissertation
zur Erlangung des Doktorgrades
der Mathematisch-Naturwissenschaftlichen Fakultäten
der Georg-August-Universität zu Göttingen

vorgelegt von

Nadine Friese

aus Leinefelde

Göttingen 2009

D 7

Referentin/Referent: Prof. Dr. Siegfried Siegesmund
Geowissenschaftliches Zentrum der Georg-August Universität Göttingen

Korreferentin/Korreferent: Dr. David C. Tanner
Leibnitz Institut für Angewandte Geophysik, Hannover

Tag der mündlichen Prüfung: 15.7. 2009

Writing a PhD thesis has been a challenge for me and my time as a PhD student included many “ups” and “downs”. Without the support and company of the following people the result, this PhD thesis, would not have been possible.

First of all, I thank Siegfried Siegesmund for taking over the main supervision. I am grateful to him for allowing a certain freedom to carry out my projects.

Secondly, I want to thank my co-supervisor David C. Tanner. He put enormous effort into planning and supporting this work. Not only that he taught me 3D modelling and how to sum up scientific goals concisely, he was always available for inspiring discussions and brought me back on track. I thank him for his patience and many personal and scientific advises.

The major part of my PhD projects was only possible with the collaboration, help and support of many colleagues from the Structural Geology and Isotope Geology Department. Above all, I want to thank Axel Vollbrecht and Bernd Leiss for being very motivated co-authors and colleagues. Thanks go to Nicole Nolte and Ilka Schönberg for long scientific talks, a nice time in Sweden, and for sharing the “passion” for granites. I am grateful to the Structural Geology and Isotope Geology Departments for the financial support to realise my fieldtrips and to attend conferences. I also want to acknowledge Gudrun Asic, Ines Ringel, Marie-France Hesse and Brigitte Hinz for their help concerning administrative things.

Several people helped me especially at the end of my PhD time: Melanie von Drachenfels is thanked for the permission to use several of her CLM figures. Alfons van den Kerkhof and Axel Müller are acknowledged for their discussion on CLM images. I am grateful to all the authors that sent requested papers. The manuscripts included in this thesis benefited from constructive reviews of Sven Egenhoff, Michele Cook, Nicolas Houlié and several anonymous reviewers.

This thesis is based upon the help of several students and colleagues as regards field work and technical support. Asdis Oelrich is thanked for introducing “first steps” to work with GoCad and reducing my confusion with the program in the beginning. Special thanks go to Frithjof Bense for his company in Iceland, for handling and explaining the sometimes mysterious GPS system in the field, its data output and finally realising the 3D reconstruction. Working in the Jökulsargljúfur National Park in NE Iceland was only possible with the permission of the ranger team on-site. I am grateful to the managers Sigprúður Stella Jóhannsdóttir and Þorstein Hymer, all other rangers and volunteers for their support and interest they showed in our field work. I also want to thank them for the offer to live in the historical ranger house; special thoughts go to Jóna and Kristin for their company, evening talks, and for their introduction to Asbyrgi’s cultural highlights.

The adventurous work in Iceland would not have been possible without the help of Ludvik E. Gustafsson. I greatly acknowledge the effort he put into the realisation of the project, his patience, the help with literature research (and its translation into German), and for being a critical co-author. His field experience that he shared with us during his family holidays in the Hljodarklettur area was very valuable.

Thanks go to Wiebke Fahlbusch and Miriam Weidemann for their supportive work in SE Sweden. I am grateful for their persistent data collection on the Götemar Pluton (under partly adverse and adventurous conditions), their always positive thinking and interesting scientific discussions.

I can also not forget to thank Ines Galindo and Ruth Andrew for their support and company during an earlier field study in Iceland, in summer 2007.

Without my friends at university and at home, the last three years would not have been the same. Malte Drobe, Judith Sippel, Anne LeMellec, Annett Reinhardt, Sabine Kammermeier, but especially France Albero, Luisa Becker, Antje Schneeberg and Rahel Odermatt are thanked for having discussions not primarily centred on geosciences, for helpful distractions, and moral support. Special thanks go to Steffi Burchardt and Michael Krumbholz for their friendship and help in many ways, not only during the last exciting and difficult three years. Thank you for your support, patience and believe in me. I enjoyed the coffee breaks and discussions we had, and the time we spent together.

I would not be at this point, at the end of my PhD, without the support that I received from my parents and my sister Franziska. I want to thank them for encouraging me and for the understanding, when I had only little time for them during busy weeks and months.

Finally, I want to thank Chris for his support in many ways, his understanding and patience in the last years. He was always there for me when I needed him. Thank you for guarding my back.

Abstract

With regards to emplacement controlled by tectonic activity, sedimentary, metamorphic, and igneous materials share many similarities. This is not only because that most of the features are associated with pre-existing structures (e.g. joints, bedding planes, faults), but also the physical occurrence of intrusions in the upper crust, regardless of which material (i.e. salt, shale, clastic deposits, magma), show similar shapes, distribution and emplacement mechanisms, which are mainly controlled by regional tectonics.

Four field studies deal with the conditions of opening of tectonic fractures in the upper crust, their propagation, interaction and final emplacement. The following examples aim to better understand (1) the influence of pre-existing tectonic features on emplacement mechanisms in the upper crust; (2) tectonic effect on magma movement and location of eruption sites; (3) the feedback between faulting and magmatism; and (4) conditions and mechanisms of dyke emplacement. The features addressed in the presented case scenarios include clastic, eruptive, and plutonic bodies, which were studied using field work, 2D numerical, 3D dynamic, geometric modelling, and macro- and microstructural fabric analyses.

The first case study, located in SE Sweden (Chapter 3), describes the tectonically-controlled emplacement of the circular, in map view, Götömar Pluton ahead of a propagating shear zone. The emplacement is consistent with the concept of an inflating sill, that was trapped by mechanical and structural heterogeneities in the Transscandinavian Igneous Belt. Due to episodic replenishments with silicic, crystal-poor magma batches from a deeper magma chamber and amalgamation of sheets, the intrusion grew by roof uplift to form a layered body that consists of alternating sequences of fine- and coarse-grained granite. Boundaries between the layers are commonly smudged and diffuse suggesting rapid injections of magma into the initial sill. To explain the internal stratigraphy, at least two independent pathways from the magma chamber are proposed, one is additionally connected to a fracture network that developed at the margin of the growing pluton. Structural field data, e.g. joints, magmatic dykes, and microfabrics indicate magma mixing in the magma chamber and rapid magma ascent (combined with decompression). The final emplacement and the shape of the Götömar Pluton were modified by horizontal extension of the individual intrusive sheets (as the pluton cooled from the roof and margin), minor floor subsidence, magmatic stoping, and a thickening of the root zone as the last magma batches arrived. Rapid emplacement of the intrusion within a timeframe of 20 ka-30 ka, might be an explanation for the missing deformation pattern in the intrusion and thus elucidate why the body is inferred to be anorogenic, even though the Götömar Pluton was subjected to a regional deviatoric stress field at the time of emplacement.

The second case study (Chapter 4) outlines the results for a multi-stage emplacement of clastic dykes in the Palaeoproterozoic basement in SE Sweden. Sedimentary dykes in crystalline basement that were formed by downward fracture opening and filled with siliciclastic material supplied from the surface have been rarely described. Therefore, the field-related example closes a gap in literature by combining macro- and microfabric analyses to determine the evolutionary history of sedimentary dykes in basement rocks. A conceptual emplacement model reveals that the downward propagation of the dyke was controlled by an alternating stress regime and an episodic repetition of opening/filling, cementation/lithification, and alteration. Pre-existing joints in the basement rocks were used as pathways for dyke intrusion during NW-SE directed Cambrian rifting. Clastic dyke orientations can thus be used as a palaeostress indicator.

The third field example (Chapter 6) describes the Holocene segmented monogenetic Raudholar crater cones in the northern rift zone of Iceland that offers the opportunity to study a cross-section through the inner workings of the uppermost few hundred metres of a crater row in an active volcanic rift zone. A 3D reconstruction, based on high-precision GPS mapping, of the geometry of the plugs and scoria cones is used as a tool to determine the magma flow under a small edifice, segmentation, and the influence of the re-activation of pre-existing faults underlying the crater row on the localisation of the eruptive centres. Volcanic deposit analysis suggests a diversified eruption style and intensive water-magma interaction. Flow indicators reveal a dominantly horizontal magma transport through dykes connecting the eruptive vents along the fissure. The Raudholar cones represent individual eruptive events, i.e., they are decoupled from a shallow magma chamber associated with a central volcano, but connected to a temporal glacial rebound effect and enhanced mantle melting in early Holocene times.

The fourth case study, located in the northern rift zone of Iceland (Chapter 7), focuses on the feedback between dyke emplacement and fault slip processes and provides insight into magma feeding relationships, the mechanical conditions of dyke emplacement, and the mechanical effect of its emplacement on the surroundings. The results of the field study show that dyke-induced surface deformation during unrest periods in volcanoes and rift zones are complex, and that existing grabens may capture feeder dykes. The field observations and numerical models also indicate that a dyke entering a rift zone graben may cause large reverse displacement on a nearby boundary fault, and that the displacement, in turn, may contribute to an increasing dyke thickness close to and at the surface.

Zusammenfassung

Bezogen auf eine tektonisch kontrollierte Platznahme in der Oberkruste, besitzen sedimentäre, metamorphe und magmatische Materialien viele Gemeinsamkeiten; nicht nur, dass diese Strukturen meist an tektonische Vorzeichnungen (z.B. Klüfte, Störungen, Schichtgrenzen) gebunden sind, so zeigen sie auch Übereinstimmungen in ihrer Erscheinungs-, und Intrusionsform, sowie in Bezug auf Platznahmemechanismen, und einer räumlichen Verteilung unabhängig von ihren Materialien (z.B. Salz, Ton, klastisches Material, Magma).

Hintergrund der hier vorgestellten Fallbeispiele ist die Bedingung für die Öffnung tektonisch induzierter Brüche in der oberen Erdkruste, deren Ausbreitung, Interaktion und finale Platznahme. Die Ergebnisse tragen zum Verständnis der folgenden Fragestellungen bei: (1) die Rolle bereits existierender tektonischer Vorzeichnungen auf die Platznahmemechanismen in der oberen Kruste; (2) tektonischer Einfluss auf den Magmentransport und die Lokation von eruptiven Zentren; (3) die Interaktion zwischen Magmatismus und Störungen; und (4) Bedingungen für die Platznahme von Gängen. In vier Fallbeispielen wird die tektonisch kontrollierte Platznahme verschiedener Materialien, d.h. klastische Gänge, Extrusiv- und Intrusivkörper, untersucht. Hierbei werden die Ergebnisse auf Geländebeobachtungen, strukturgeologische Daten, Mikro- und Makrogefügeanalysen, sowie auch auf die 2D numerische, und 3D geometrische Modellierung gestützt.

Das erste Fallbeispiel in Kapitel 3, beschäftigt sich mit der tektonisch kontrollierten Platznahme des im Kartenbild runden Götömar Plutons in SE Schweden, der an eine propagierende Scherzone gebunden ist. Die Platznahme stimmt mit dem in der Literatur oft beschriebenen Konzept eines sich „aufblähenden“ Lagerganges, der an Heterogenitäten im umgebenden Transmagmatischen Gürtel gebunden ist, überein. Durch episodische Injektionen von kristallarmem, saurem Magma, dass durch einen Fördergang aus einer tiefer liegenden Magmenkammer gespeist wurde, und durch die Vermischung früherer Magmenpulse, wuchs der Pluton nach oben (Dachhebung). Der so entstandene intern geschichtete Magmenkörper besteht aus sich abwechselnden Sequenzen aus fein- und grobkörnigem Granit. Die Grenzen zwischen den individuellen Granitlagen sind meist diffus und verwischt, was auf schnell aufeinander folgende Magmeninjektionen schließen lässt. Um die alternierende Stratigraphie erklären zu können, wird ein Modell vorgeschlagen, welches die Speisung des Lakkolithen mittels mindestens zweier unabhängig voneinander agierenden Fördergängen beschreibt; einer ist der im Gravimetrieprofil erkennbare vertikalen Fördergang, und ein zweites System ist an ein Bruchnetzwerk am Rand des wachsenden Plutons gebunden. Strukturgeologische Daten (magmatische Gänge, Kluftsysteme) und die Untersuchung der Mikrogefüge belegten eine

Magmenmischung in der Magmenkammer und einen relativ schnellen Aufstieg des Magmas verbunden mit Dekompression. Die finale Platznahme, und letztlich die Form des Götömar Pluton, wurde durch eine Kombination aus horizontaler Ausbreitung der Internlagen, einer untergeordneten Absenkung des Plutonbodens, magmatischem Stopping und einer Verdickung des Förderanges bestimmt. Eine schnelle Platznahme, die einen Zeitraum von etwa 20 ka-30 ka umfasste, könnte eine Erklärung für die Abwesenheit von Deformationsstrukturen sein, und zeigt eine Möglichkeit auf, warum der Götömar Pluton als anorogen bezeichnet wird, obwohl der Körper während einer Zeit mit regionaler Deformation Platz genommen hat.

Das zweite Geländebeispiel (Kapitel 4) behandelt die passive Platznahme von Kambrischen Sedimentgängen entlang von vorgezeichneten Kluftsystemen im Paleoproterozoischen Basement in SE Schweden. Klastische Gänge in Kristallingesteinen, die von der Erdoberfläche ausgehend nach unten propagieren sind selten beobachtet worden. Diese Studie, gestützt auf die Interpretation von Mikro- und Makrogefügen, schließt somit eine Lücke in der bisherigen Literatur. Das vorgestellte konzeptionelle Modell zeigt, dass die Platznahme der Sedimentgänge von einem wechselnden Spannungsfeld beeinflusst wurde, welches sich in alternierenden Phasen von Öffnung/Füllung, Zementation/Verfestigung und Alteration des nach unten propagierenden Ganges äußert. Die Lokation der klastischen Gänge ist an bereits angelegte Kluftsysteme geknüpft, die auf Grund des NW-SE gerichteten Kambrischen Riftings reaktiviert wurden. Somit ist die Orientierung von Sedimentgängen ein aussagekräftiger Paleospannungsindikator.

Das dritte Fallbeispiel (Kapitel 6) beschäftigt sich mit der Holozänen monogenetischen Raudholar-Kraterkegelreihe in der nördlichen Riftzone Islands. Das Gebiet gibt Einblick in einen Querschnitt durch die oberen hundert Meter dieser segmentierten Kraterreihe in einem aktiven Extensionsgebiet. Die 3D-Rekonstruktion basiert auf einer präzisen GPS-Vermessung der erodierten Förderkanäle und intakten Kraterkegel, sowie auf der Aufnahme strukturgeologischer Elemente. Somit konnten Aussagen über den Magmenfluss unter einem relativ kleinen Vulkangebäude getroffen werden, als auch der Einfluss der Reaktivierung von bereits unter der Kraterreihe bestehenden Störungen auf die Lokalisierung der Eruptionsschlote bestimmt werden. Vulkanische Ablagerungsprodukte zeigen zudem eine variable Eruptionsgeschichte der Kraterkegel und eine intensive Wasser-Magma-Interaktion. Fließgefüge in (Förder)Gängen lassen einen vorwiegend horizontalen Magmenfluss erkennen. Die untersuchten Raudholar Krater stellen ein separates Spalteneruptionsereignis dar, welches, anders als die meisten Spaltenschwärme in Island, nicht an eine Magmenkammer unterhalb eines Zentralvulkans gekoppelt ist. Aufgrund des Alters der Raudholar-Kraterreihe (frühes Holozän) könnte dieses Riftsegment zeitlich an das Abschmelzen der nördlichen Riftzone gebunden sein, was seine außergewöhnliche Lage am

Rande des Spaltenschwarmes und eine eventuelle Magmenzufuhr von der Kruste/Mantelgrenze erklären würde.

Das vierte Fallbeispiel (Kapitel 7) beschäftigt sich mit der Interaktion zwischen Gangintrusionen und Verwerfungen, und zeigt Bedingungen für die Magmenzufuhr für Gangintrusionen auf, sowie welche mechanische Auswirkung eine Intrusion auf das Nebengestein haben kann. Die Studie zeigt, dass der durch Gangintrusionen induzierten Oberflächendeformationen in Vulkanen und Riftzonen komplex sind und existierende Grabensysteme vorhandene Fördergänge lenken und an sich binden können. Feldbeobachtungen und numerische Modelle machen deutlich, dass Gangintrusionen nahe gelegene Störungen reaktivieren können, und dass der Versatz wiederum zu einer Vergrößerung der Gangmächtigkeit nahe der Oberfläche beiträgt.

Acknowledgements	i
Abstract	iii
Zusammenfassung	v
Table of contents	ix
Table of figures	xiii
List of publications	xvi
1. General introduction	1
Preface	1
1.1 The connection between volcanism and plutonism	4
1.2 Tectonic influence on ascent and emplacement – presentation of case scenarios	5
1.3 Emplacement mechanisms	8
1.3.1 Diapirism and ballooning	9
1.3.2 Cauldron subsidence, ring faulting and caldera collapse	9
1.3.3 Formation of dykes, sills, laccoliths and lopoliths	11
1.3.4 Magmatic stoping	13
2. Geological and tectonic framework of Sweden	15
2.1 Geological and tectonic framework of Sweden	15
2.2 Tectonic and magmatic evolution of Southeast Sweden– the Göttemar region	18
2.3 Case studies Sweden	20
3. Multi-stage emplacement of the Göttemar Pluton - case study Southeast Sweden	23
Preface	23
Abstract	25
3.1 Introduction	26
3.2 State of the art	28
3.3 Geological Setting	29
3.4 Field relationships and internal structure of the Göttemar Pluton	31
3.4.1 The host rock	31
3.4.2 Contact features and internal structure of the Göttemar Pluton	31
3.4.3 Jointing in and around the Göttemar Pluton	32

3.4.4 Mineral veins and hydrothermal alteration associated with the Götemar Pluton	34
3.4.5 Minor intrusion associated with the Götemar Pluton	34
3.5 Mineralogy, microfabrics, and cathodoluminescence analysis of the Götemar Pluton	36
3.5.1 Mineralogy and microfabrics of the Götemar Granite	36
3.5.2 Cathodoluminescence analysis	39
3.5.2.1 CL colours and deformation pattern in quartz grains	39
3.5.2.2 CL colours of K-feldspar and plagioclase	40
3.6 Interpretation and discussion-a model for the multistage emplacement of the Götemar Pluton	43
3.7 Conclusions	51
Acknowledgements	51
4. Episodic formation of Cambrian clastic dykes - case study Southeast Sweden	53
Preface	53
Abstract	55
4.1 Introduction	55
4.2 Geological setting	56
4.3 Macrofabrics	58
4.4 Microfabrics	59
4.4.1 Detrital components	59
4.4.2 In-situ formed fabrics and mineralisations	62
4.5 Interpretation	68
4.6 Conclusions	71
Acknowledgements	71
5. Geological and tectonic framework of Iceland	73
5.1 Location of Iceland - mantle plume and Mid-Atlantic Ridge	73
5.2 Geological structure and stratigraphy of Iceland	74
5.3 Rift jumps and spreading episodes	77
5.4 Case studies Iceland	80
6. Tectonic feedback on magma emplacement - case study Northeast Iceland	81
Preface	81
Abstract	82
6.1 Introduction	83

6.2 Regional setting	83
6.3 Methodology	86
6.4 Results from the 3D mapping and reconstruction of the crater row	87
6.5 Raudholar and Hljodaklettur eruptive vents and deposits	87
6.5.1 Lithofacies of weakly welded, scoriaceous red and brown lapilli	88
6.5.2 Lithofacies of twisted, fluidally-shaped, welded spatter	89
6.5.3 Lithofacies of volcanic bombs	90
6.5.4 Dykes at the eroded part Hljodaklettur	91
6.5.5 Lava flows at the eroded part Hljodaklettur	93
6.6 Reconstruction of the eruption style	95
6.7 Discussion	99
6.7.1 Structural control on eruptive fissure location	99
6.7.2 Plumbing system of the eruptive fissure	100
6.7.3 Magma source and vertical versus horizontal magma flow in the fissure swarm	101
6.8 Conclusions	102
Acknowledgements	103
7. Dyke-induced reverse faulting in a graben - case study Northeast Iceland	105
Preface	105
Abstract	107
7.1 Introduction	107
7.2 Graben and feeder dyke	108
7.3 Dyke-induced reverse faulting	110
7.4 Discussion	112
7.5 Conclusion	113
Acknowledgements	113
8. Discussion and conclusion	115
8.1 Multi-stage emplacement of the Götömar Pluton, Southeastern Sweden	115
8.2 Reconstruction of a monogenetic crater cone row in the northern rift zone of Iceland	117
8.3 Dyke-induced reverse faulting in the northern rift zone of Iceland	119
8.4 Episodic formation of Cambrian clastic dykes in the basement of Southeast Sweden	120

References cited	123
Curriculum vitae	169
Appendix	The CD includes a movie of the three-dimensional model of the reconstructed Raudholar Crater Row, NE Iceland (Chapter 6), as well as the already published manuscript about dyke-induced reverse faulting in a graben (Chapter 7).

Chapter 1		
Figure 1.1	Examples of salt structures	1
Figure 1.2	Field examples of magmatic features	2
Figure 1.3	Components of a mud volcano plumbing system with eruptive field example	3
Figure 1.4	3D representation of saucer-shaped Gamma field sand injective and Golden Valley sill	3
Figure 1.5	Schematic illustration of the mechanisms diapirism and ballooning	9
Figure 1.6	Stages of ring fault initiation and caldera collapse	10
Figure 1.7	Laccolith models of a punched laccolith and a christmas-tree laccolith	12
Figure 1.8	Intrusion thickness (T) and width (L) result in an S-style curve relating the dimensions of crack to batholith	13
Figure 1.9	Schematic illustration of the initiation of stoping	14
Chapter 2		
Figure 2.1	Late Palaeoproterozoic to Early Neoproterozoic tectonic complexes in the East European Craton (Baltica)	15
Figure 2.2	The ‘traditional’ model of Rodinia	16
Figure 2.3	The postulated positions of Baltica in relationship to the surrounding terranes	17
Figure 2.4	Simplified geological map of SE Sweden	19
Figure 2.5	Active tectonics during geological time in the Götömar area	20
Chapter 3		
Figure 3.1	Geological map of SE Sweden and the Götömar Pluton	27
Figure 3.2	N-S and E-W gravity profiles of the Götömar and Uthammar Plutons	29
Figure 3.3	Field examples of joint, faults and host rock-pluton contacts	33
Figure 3.4	Data of joint measurements in the host rock and the Götömar Pluton	33
Figure 3.5	Field examples of mineral veins and magmatic dykes in the Götömar area	35
Figure 3.6	Microfabrics of the coarse-grained Götömar Granite	37
Figure 3.7	Microfabrics of the fine-grained granitic variety of the Götömar Pluton	38
Figure 3.8	Summary of the different quartz generations identified in the granites of the Götömar Pluton as observed in CLM	40
Figure 3.9	CL images of quartz crystals in the Götömar Granite	41

Figure 3.10	Summary of identified plagioclase generations in the granites of the Götemar Pluton as observed with CLM	43
Figure 3.11	CL images of plagioclase crystals in the Götemar Granite	44
Figure 3.12	Schematic model of the multi-stage emplacement of the Götemar Pluton	46
Chapter 4		
Figure 4.1	Geological map of SE Sweden and the Västervik area, with occurrence of sedimentary dykes	57
Figure 4.2	Outcrop photograph showing the studied sedimentary dyke	58
Figure 4.3	Pole plot of the orientation of joints in granites and corresponding strike direction of main sets and pole plot of the orientation of sedimentary dykes occurring in Scandinavia	58
Figure 4.4	Macrofabrics in hand specimens	60
Figure 4.5	Thin section observation: spectrum of detrital components	61
Figure 4.6	In-situ formed fabrics I: Mechanical compaction, pressure solution, overgrowth	64
Figure 4.7	In-situ formed fabrics II: Calcite mineralisation	66
Figure 4.8	In-situ formed fabrics III: Matrix	67
Figure 4.9	Schematic illustration of the Cambrian tectonic framework	69
Figure 4.10	Model for polyphase dyke development	70
Chapter 5		
Figure 5.1	The principal elements of the geology in Iceland, outlining the distribution of the major geological subdivisions, including the main fault structures and volcanic zones and belts.	73
Figure 5.2	Distribution of active volcanic systems among volcanic zones and belts in Iceland	75
Figure 5.3	Crustal accretion, relocation and propagation of the Icelandic rift zones in the last 12 Ma	78
Figure 5.4	Location of the Askja and Krafla volcanoes and swarms of the same name at the divergent plate boundary in North Iceland.	79
Figure 5.5	Observations with time during the Krafla episode 1974–1989	80
Chapter 6		
Figure 6.1	Geological map of the fissure swarms in Northeastern Iceland	84

Figure 6.2	Detailed geological map of the northern part of the Fremrinamur Fissure Swarm	85
Figure 6.3	Dataset of accomplished measurements in the field area and DEM of the mapped area showing the reconstructed crater row in GoCad 2.0.8, as well as faults.	87
Figure 6.4	Results from reconstructing the cone row in three dimensions	88
Figure 6.5	Lithofacies of fallout deposits	89
Figure 6.6	Lithofacies of welded spatter	90
Figure 6.7	Lithofacies of volcanic bombs	91
Figure 6.8	Dykes and flow indicators	92
Figure 6.9	Distinction between colonnade and entablature in the lava flow	94
Figure 6.10	Thin sections of tholeiitic basalt from the field area	96
Figure 6.11	Topographic profile in N-S direction (194°) along the Raudholar Cone Row and evolution of the fissure swarm and fissure eruption	98
Figure 6.12	Stereogram of structural data in Raudholar and Hljodaklettur	100
Figure 6.13	Field example of Sveinar Cone Row, southwest of Raudholar Cone Row	102
Chapter 7		
Figure 7.1	Location of the Sveinar Graben and Sveinar-Randarholar Crater Row in the Holocene rift zone of northern Iceland.	109
Figure 7.2	Schematic illustration of part of the 8000 yr old Sveinar-Randarholar Crater Row and Sveinar Graben	110
Figure 7.3	Photograph and drawing show feeder-dyke segment to the Sveinar-Randarholar Crater row being connected to one of its spatter cones.	111
Figure 7.4	Boundary-element model of effects of dyke on nearby graben faults	111
Chapter 8		
Figure 8.1	Schematic emplacement history of the Götömar Pluton	116
Figure 8.2	Opening of tectonic fractures and magma intrusion in the Raudholar fissure, northern rift of Iceland	118
Figure 8.3	Illustrations of graben faults capturing a dyke in the northern rift zone of Iceland	119
Figure 8.4	Illustration of active and passive clastic dyke emplacement in crystalline host rock	121

This doctoral thesis includes the following papers

Paper I Multi-stage emplacement of the Götömar Pluton, SE Sweden - a layered laccolith intrusion

N. Friese, A. Vollbrecht, D. C. Tanner, W. Fahlbusch, M. Weidemann, 2009
(submitted to Tectonophysics)

Paper II Cambrian sedimentary dykes in the Proterozoic basement of the Västervik area (Southeast Sweden): cyclic formation inferred from macro- and microfabrics.

N. Friese, A., Vollbrecht, B. Leiss, O. Jacke, 2008
(submitted in revision, International Journal of Earth Sciences)

Paper III Reconstruction of a monogenetic basaltic cinder cone row in the rift zone of North Iceland: tectonic control on magma emplacement and eruption dynamics.

N. Friese, F. A. Bense, D.C. Tanner, L.E. Gustafsson, S. Siegesmund, 2009
(submitted to Journal of Volcanology and Geothermal Research)

Paper IV Dike-induced reverse faulting in a graben.

A. Gudmundsson, N. Friese, I. Galindo, S.L. Philipp, 2008
(Geology 36, p. 123-126)

1. General introduction: preface

With regards to emplacement controlled by tectonic activity, sedimentary, metamorphic and igneous materials share many similarities. This is because not only are most of the features associated with pre-existing structures (e.g. joints, faults), but also the physical occurrence of intrusions in the upper crust, regardless of which material (i.e. salt, shale, clastic deposits, magma, Figs. 1.1-1.4) show similar shapes, distribution and emplacement mechanisms, which are mainly controlled by regional tectonics (e.g. Morley et al., 1998; Capozzi and Picotti, 2002; Dimitrov, 2002; Marco et al., 2002; Mazzini et al., 2003a,b; Tucker, 2003; Stewart and Davies, 2006; Hudec and Jackson, 2007; Cartwright et al., 2008, Polteau et al., 2008 a,b; Zhigulev et al., 2008).

The emplacement of (shallow) intrusions of different types of material is of economic interest, e.g. deposits of ore (e.g. Eckstrand and Hulbert, 2007; Ramirez et al., 2006; Vignerresse, 2007), diamonds (Sparks et al., 2006), and dimension stones (Kalvig et al., 2002; Rasmussen and Olsen, 2003; Hoffmann and Siegesmund, 2007; Oyhantçabal et al., 2007; Härmä and Selonen, 2008). Shallow magma emplacement, salt and shale tectonics (Figs. 1.1, 1.3) play a significant role in the spatial distribution of hydrocarbon reservoirs as well as hydrocarbon generation, migration, and entrapment (e.g. Davison et al., 2000; Petford and McCaffrey, 2003; Planke et al., 2003;

Rowan et al., 2003; Schutter, 2003; Lee et al., 2006; Jones et al., 2007; Rohrman, 2007; Filho et al., 2008; Løseth et al., 2008; Polteau et al., 2008 a,b; Galland et al., 2009; Fig. 1.4).

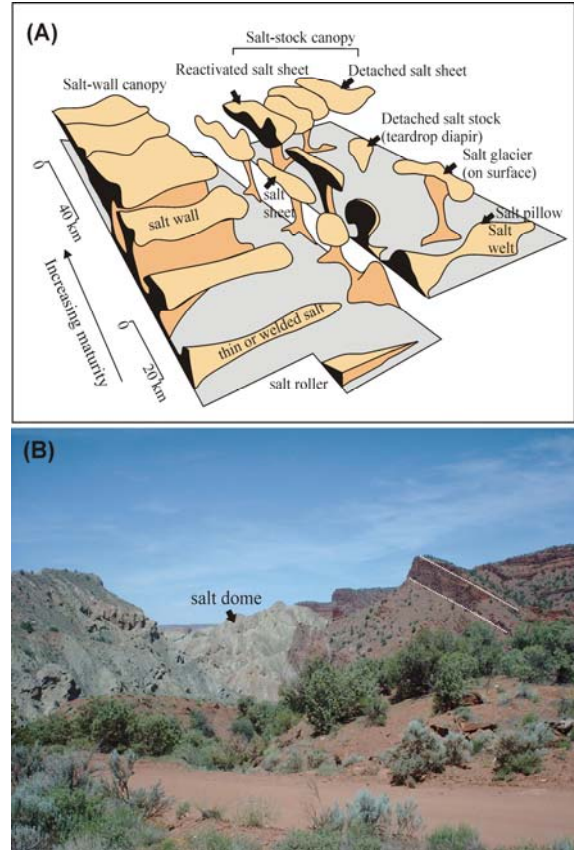


Figure 1.1: (A) Salt structures (simplified after Jackson and Talbot, 1991). (B) Cretaceous salt dome at Fisher Towers (USA). Photograph by Ken Leonard (<http://en.wikipedia.org>).

Shallow magma emplacement is the most direct geological record of the magmatic plumbing systems beneath volcanic centres (e.g. Coleman et al., 2004) and thus an important volcanic-plutonic link (e.g. Metcalf, 2004). The occurrence and monitoring of shallow-emplaced bodies, associated volcanic activity and influence of tectonic forces (Figs. 1.2-1.3) have been intensively studied to understand geological hazards. For example, there is a curtain of

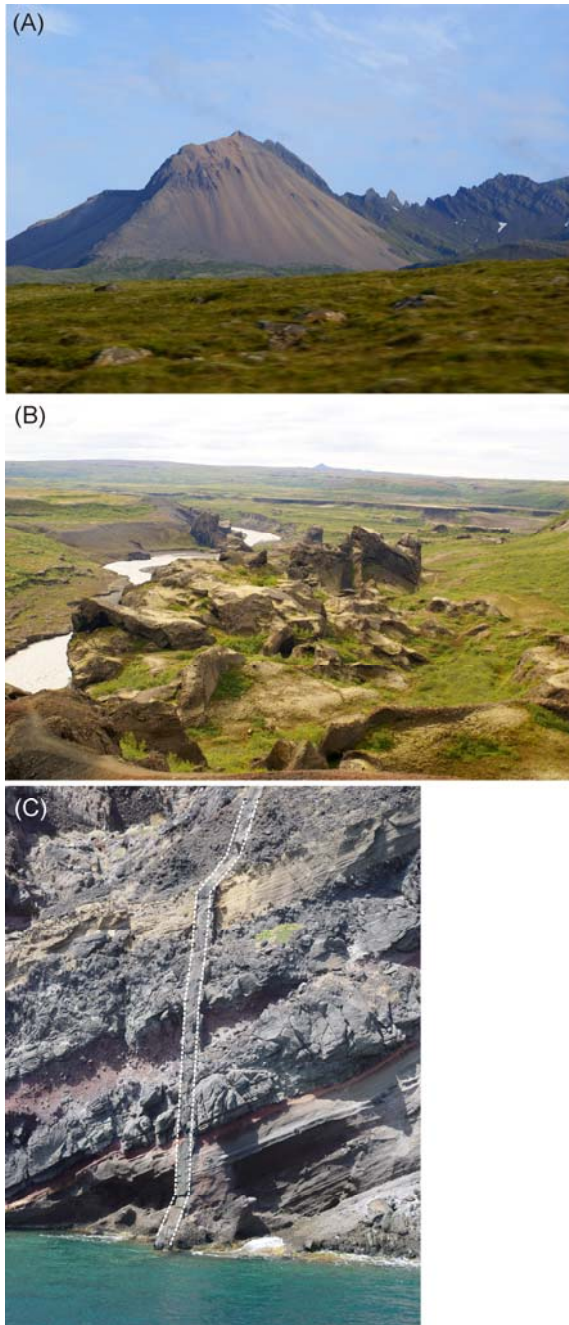


Figure 1.2: (A) Rhyolitic Sandfell laccolith, SE Iceland. Steeply dipping strata on either side of Sandfell were pushed up by the intrusion. View towards SE. (B) Hljodarklettur, eroded scoria cone row part, rift zone N Iceland. View towards south. (C) Basaltic dyke (dotted line) cross-cutting sedimentary and lava layers at the Santorini Caldera rim, Greece.

mud volcanoes aligned along the plate margins in N Italy, the Mediterranean Sea, the Black Sea, and the Caspian Sea to Indonesia (e.g. Blinova et al., 2003; Planke et al., 2003; Mazzini et al., 2007; Bonini, 2008), that have forced human relocation and have had an impact on human health and environment (e.g. Davies et al., 2008; Kopf et al., 2008; Fig. 1.3). While volcanic threats from volcanoes such as Vesuvius (Italy), La Soufrière (Guadeloupe), Teide (Spain), and Etna (Italy), to name a few, have been known for a long time (e.g. Chester et al., 2002; Macedonio et al., 2008; Marti et al., 2008; Komorowski et al., 2008; Andronico et al., 2009), hazards from small volume scoria-cone eruptions are often overlooked (Ort et al., 2008), although these features are the most abundant volcanic landforms on Earth (Wood, 1980). Studying their eruptions, deposits, and plumbing systems help to forecast eruptions and minimise vulnerability especially in densely populated areas such as Mexico (e.g. Siebe et al., 2004; Martin and Nemeth, 2006; Guilbaud et al., 2009). Areas of scoria cone occurrence became a research object lately (in terms of dyke injections, a possible volcano formation) connected to radioactive waste repository sites e.g. at Yucca Mountain (USA; e.g. Crowe et al., 1983; Wells et al., 1990; Doubik and Hill, 1999; Ho et al., 2006; Valentine and Keating, 2007). But also other shallow emplaced materials are targets for waste deposits, such as salt structures in Northern Germany (e.g. Langer, 1999; Behlau and Mingerzahn, 2001;

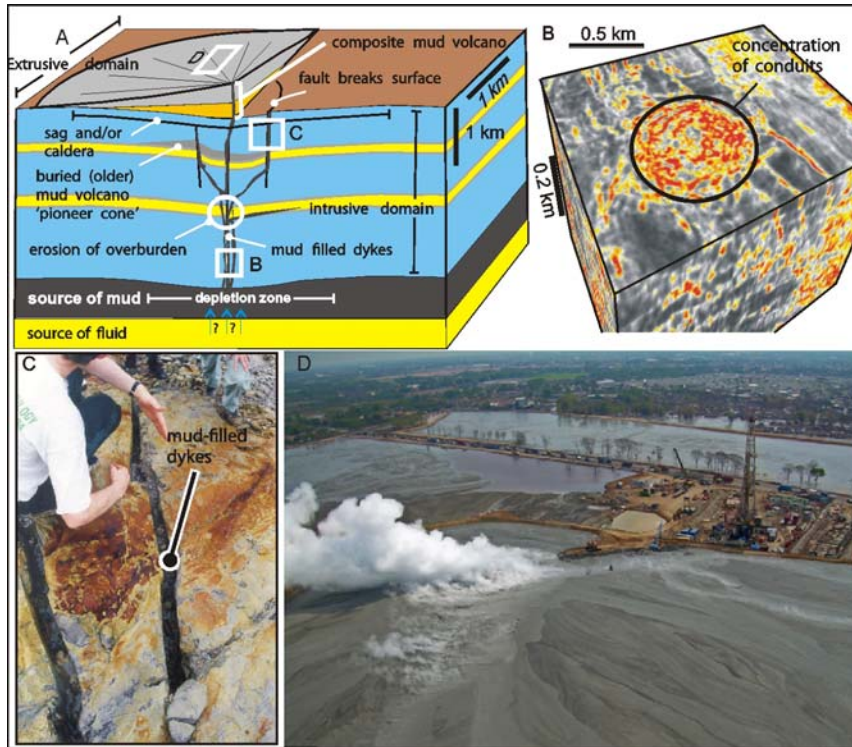


Figure 1.3: Components of a mud volcano system revealed by 3-dimensional seismic data and outcrop: A- Schematic illustration of the main components of a mud volcano system. Mud volcano systems can be divided into intrusive and extrusive structural domains. Fluid may either co-exist with the mud source or enter from a deeper source (blue arrows) causing remobilisation of shallower mud and entrainment of

other overburden lithologies. The mud-fluid mix is transported through fractures and faults to the surface, where stacked cones form due to episodic eruptive and quiescent periods. B - Seismic coherency cube (see Bahorich and Farmer, 1995) across a mud volcano (South Caspian Sea, from Davies and Stewart, 2005), showing feeder conduits, the detailed internal structure of which is unknown. C - Mud-filled dykes from the Jerudong anticline in Brunei (see Morley, 2003). These types of mud-filled fractures the transport of the mud-fluid mix to the surface. (From Davies et al. (2007), reprinted with permission of GSA Today. D-Photograph of mud volcano LUSI in Indonesia (from Davies et al., 2008).

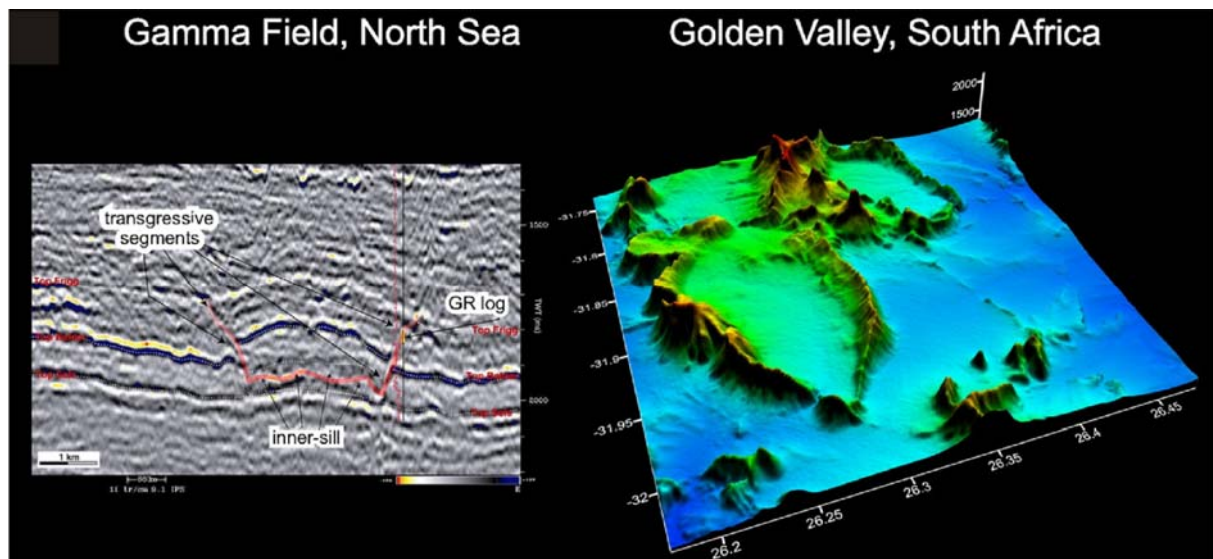


Figure 1.4: 3D representation of saucer-shaped Gamma field sand injective (left, Huuse et al., 2004) and Golden Valley sill (Karoo, right). Figure reprinted from Polteau et al. (2008a) with permission of Elsevier.

Koyi, 2001; Brewitz and Rothfuchs, 2007; Hornschemeyer, 2008) and basement rocks in the vicinity of the Götömar Pluton (SE Sweden; e.g. Tiren et al., 1999; Cruden, 2008; SKB report, 2008; Drake et al., 2009) have been studied with regards to tectonically-controlled emplacement.

In attempt to understand the relationship between the emplacement of fluids and faulting, this thesis consists of several field-based studies that focus on the tectonically-controlled emplacement of features of different scales and materials in the upper crust (i.e. sedimentary dykes, granitic pluton, and basaltic plugs) in two different tectonic settings. The basic idea behind the following emplacement studies is the opening of tectonically-established cracks at different crustal levels, their propagation and growth. The four case studies, located in Sweden and Iceland, address the following research topics:

- (1) influence of pre-existing tectonic features on emplacement mechanisms in the upper crust;
- (2) tectonic effect on magma movement and location of eruptive sites;
- (3) feedback between faulting and magmatism (i.e. reactivation of faults, faults as conduits for magma ascent);
- (4) conditions and mechanisms of (clastic) dyke emplacement.

As an introduction to the topic, Chapter 1 focuses on how the different topics are related in the context of tectonically-controlled emplacement mechanisms in the upper crust. As the field examples occur within a sequence of extrusive and intrusive rocks, the connection between plutonism and volcanism is outlined. Furthermore, an overview of the mechanisms that control material emplacement is given.

The case studies are located in Sweden and Iceland, so the Chapters 2 and 5 give a short overview of the geological framework of both areas, followed by the corresponding field studies. The different methods applied to each study, namely 2D numerical, 3D geometric and dynamic modelling, and microstructural (e.g. cathodoluminescence microscopy) analysis, are introduced in the corresponding chapters. Finally, Chapter 8 summarises the main results and discusses them in the context of recent research on the related topics.

1.1 The connection between volcanism and plutonism

The connection between plutonic and volcanic rocks is fundamental to understanding magma chamber processes and the evolution of magma systems (e.g. Barnes et al., 1990; Wiebe and Collins, 1998; Hawkins and Wiebe, 2004; Metcalf, 2004; Coleman et al., 2004; Kemp et al., 2006; Bachmann et al., 2007). Volcanic and plutonic rocks are clearly linked petrogenetically, but the nature of this

connection is still a matter of debate. One of the controversial questions discussed is: Are volcanic and plutonic rocks mutually complementary or do they evolve along separate pathways?

Plutonic rocks mostly document the final stages of multiple intrusive events (at varying depths) and can be overprinted by late, near-, and subsolidus processes (e.g. textural coarsening, metamorphic reactions, deformation; e.g. Zieg and Marsh, 2005). In contrast, volcanic rocks provide an instantaneous “snapshot” of the state of the magmatic system at the time of eruption. Moreover, they record the peak of magmatic activity in a certain area, rather than late, waning stages, as plutons do (Bachmann et al., 2007).

In magma systems, plutons might represent a cross-section of magma conduits and magma chambers where magmatic processes produce cogenetic magmas reaching the Earth’s surface as a volcanic eruption (Metcalf, 2004). Venting and eruption of magmas is regarded as essential to the evolution of high-level granitic plutons (e.g. Langmuir, 1989; Bachmann and Bergantz, 2004; Vasquez and Reid, 2005). Shallow magmatic intrusions (with roofs < 8 km deep) are closely connected to their volcanic counterparts. Examples include exposed resurgent plutons (e.g., Johnson et al., 1990; Fig. 1.2), dyke and sills within volcanic edifices, and very shallow laccoliths (Fig. 1.2) At deeper levels, dykes that end beneath the surface, small pods, plugs, and

sills can also be regarded as parts of volcanic systems (Figs. 1.2-1.3; see also field studies Chapters 6 and 7).

1.2 Tectonic influence on ascent and emplacement – presentation of case scenarios

Pre-existing structures, e.g. joints, foliation, bedding planes, folds and faults influence the ascent and emplacement of different materials such as salt, shale, and clastics (e.g. Hutton et al., 1990; Paterson and Fowler, 1993a,b; Morley et al., 1998; Beacom et al., 1999; Lafrance and John, 2001; Rowan et al., 2001; Kavanagh et al., 2006; Levi et al., 2006; Hudec and Jackson, 2007; Galland et al., 2009). Case studies in the literature mainly deal with plutonic bodies (e.g. Johnson and Pollard, 1973; Hutton, 1982; Kalakay et al., 2001; Pinotti et al., 2002; Thomson and Hutton, 2004; O’Driscoll et al., 2006; Polteau et al., 2008a,b). Even though there is a debate whether ascent mechanisms via diapirs or dykes occur (e.g. Clemens and Mawer, 1992; Rubin, 1993; Petford et al., 1994; Petford, 1996; Clemens, 1998; Miller and Paterson, 1999; Vigneresse, 2004; Burg and Gerya, 2008), a lithosphere-wide fracturing that provides sieve-like pathways for magma ascent in the upper crust seems to be most effective (Petford et al., 1993; Collins and Sawyer, 1996; Clemens, 1998). Not only are rapid ascent rates of approximately 10^{-2} m/s predicted for granite melts in dykes (m/a for diapirs), which means that felsic magmas can be transported through

the continental crust in months rather than thousands (or even millions) of years (Petford et al., 2000), also that large plutons can in principle be filled in 10^1 - 10^5 yrs (e.g. Petford, 1996; Petford et al., 2000; de Saint-Blanquat et al., 1998; 2001; Michel et al., 2008). According to Hutton (1982) and Vigneresse (1995a), a displacement gradient along a shear zone can not only cause dilation of the zone to allow the space needed for the pluton, but can also create differential stresses in the wall rocks of the zone (Vigneresse, 1995b), thus controlling the emplacement.

Furthermore, the presence of melt has a secondary feedback effect, on e.g. strike-slip systems, since they act as lubricants and enhance displacement along faults. The stress field in the emplacement level may be decoupled from the regional stress field, triggers strain localisation (Tommasi et al., 1994; Brown and Solar, 1998) and magma emplacement occurs as e.g. laccolith or sill (Breitkreuz and Mock, 2004). Laccoliths, for example, occur in locations associated with faulting in extensional (e.g. Basin and Range Province; Neumann et al., 1992; Paterson and Fowler, 1993a; Hawkesworth et al., 1995; Hogan et al., 1998; Huffman and Taylor, 1998), transcurrent (e.g. Saar-Nahe Basin, Permo-Carboniferous Europe; Wang et al., 2000; Breitkreuz and Mock, 2004; Girard and van Wyk de Vries, 2005) and compressional (e.g. Mazzarini et al., 2004) tectonic regimes. However, the ascent must be in locally extensional near-field setting because the magma has to overcome the tectonic stresses

(Vigneresse, 1995a). The amount of displacement, the regional stress field and the amount of melt rising influence type and size of the laccolith complex at shallow crustal levels (Hogan et al., 1998; Vigneresse et al., 1999).

The first case study (Chapter 3) deals with the emplacement of a granitic laccolith into the upper crust controlled by deep regional faults: the Götömar intrusion, SE Sweden. This chapter discusses (1) space creation at depth; (2) influence of the tectonics on magma transport and final emplacement; (3) magma mixing processes and; (4) to a minor amount, the role of stoping as final emplacement mechanism. The strikingly round shape of the Götömar laccolith in map view, its special mineralogy, geochemistry, and its relationship to the surrounding rocks leave room for further data input and discussion in terms of origin and evolution of the hosting Transscandinavian Igneous Belt granites in connection with a broader tectonic scenario of SE Sweden.

As previously mentioned, the geometrical occurrence of magma intrusions (e.g. as diapirs, volcanoes, dyke and sill complexes) is transferable to materials such as shale (e.g. Dimitrov, 2002; Clari et al., 2004) and other clastic materials (e.g. Hillier and Cosgrove, 2002; Jolly and Lonergan, 2002; Röshoff and Cosgrove, 2002; Mazzini et al., 2003a; Tucker, 2003; Cartwright et al., 2008, Polteau et al., 2008 a,b; Fig. 1.3) with

respect to emplacement mechanisms and formation conditions. A clastic sill or dyke can be considered as an example of a opening-mode, hydraulic fracture (Lorenz et al., 1991; Cosgrove, 2001; Marco et al., 2002). Chapter 4 describes Cambrian sedimentary dykes, which formed during polyphase downward propagation and active suction-controlled infill of sediments within a changing stress regime in the Paleoproterozoic granitic basement of SE Sweden. Pre-existing joints determine the location of sedimentary dykes in this area. Sandstone dykes are thus tectonic markers revealing the geological setting, stress regime, and depositional conditions at the time of formation.

Magma propagation and near surface (< 1 km) dyke emplacement can be observed in rift zones and crater cones. The third case study, presented in Chapter 6, deals with the three-dimensional reconstruction and emplacement history of a Holocene scoria cone row in the rift zone of N Iceland. The deposits consist of basaltic scoria and lava flows. The intrusive complex includes plugs and dykes. Careful field observation of an exposed feeding system connected to a crater cone shed light on the mechanics of dyke propagation and magma emplacement near the surface. This combined field-based and 3D dynamic modelling study describes (1) the influence of faulting on the location of the crater row, (2) the tectonic effect on magma movement, and (3) the influence of tectonics

and pre-existing structures on the eruption style. Its location in a volcanic system, the possible connection to other eruptive fissures and its overall arrangement are important observations for magma transport (and the magma source) and an indication of the possible relationship between faults and volcanic features in the area. Both kinematically and dynamically, volcanic activity may be completely dependent on tectonic factors for accumulation, storage, and eruption of magma.

The fourth case scenario (Chapter 7) presents an example of the feedback between emplacement and faulting processes in a rift zone. Dyke-induced uplift is a common feature in both, rift graben and the flanks of rift zones (Rubin and Pollard, 1988). Field observations in the northern rift zone of Iceland and a simple two-dimensional numerical model of the tectonic situation show that dyke emplacement can cause reverse slip along a nearby normal fault. The exposure of the graben and its connected feeder dyke give further insight into the feeding system of a small volume volcano (cinder cone), the shape, and mechanical emplacement conditions of a dyke and therefore allows inferences about its mode of emplacement. The results show (1) how a graben boundary fault capture a potential feeder dyke and (2) why reverse faults are only rarely observed or absent in grabens related to dyke injection.

1.3 Emplacement mechanisms

Traditionally, emplacement mechanisms have been subdivided into “active” forceful mechanisms that result in a distortion of the host rock and “passive” mechanisms that take advantage of space created by regional deformation (e.g. Hutton, 1988; Vendeville and Jackson, 1992a,b; Hudec and Jackson, 2007). This separation into “passive” and “active” mechanisms is retained in the field of e.g. salt tectonics and emplacement of clastic materials (see Chapter 4), for example, so-called Neptunian clastic dykes formed by gravitational controlled, passive deposition into pre-existing fractures (e.g. Stanton and Pray, 2004). Actively-emplaced clastic dykes describe injections by host rock fracturing and injection of sediment mainly from above, connected to high fluid pressure or pressure gradients (e.g. Röshoff and Cosgrove, 2002).

In contrast, a more recent classification by Paterson and Fowler (1993b) separates the magmatic emplacement mechanisms into space creating, i.e. increase the crustal volume, and material-transfer processes. While the crustal volume can only be increased by surface uplift or by lowering the crust-mantle boundary, most classic magma-emplacement mechanisms can be classified as material-transfer processes that do not change the volume in the crust (Paterson and Vernon, 1995). The final emplacement, however, is controlled by the temperature through its effect on rheology, the magma driving pressure, the local and regional stress field,

and physical parameters such as viscosity and density of the intruding material (e.g. Breikreuz and Petford, 2004).

Currently, the following emplacement mechanisms have been proposed and partially accepted: diapirism and ballooning, dyke and sill emplacement along fractures, ring faulting and cauldron subsidence, laccolith and lopolith formation (i.e. floor subsidence and roof lifting). Although magmatic stoping is not regarded as a true emplacement mechanism, it has a great importance as a material-transfer process (e.g. Clarke et al., 1998; Dumond et al, 2005; Zak et al., 2006).

One has to distinguish emplacement in the lower, ductile from emplacement in the upper, brittle crust. Emplacement in the ductile regime is mainly by ballooning and diapirism (especially when dealing with salt material). Plutons in the upper crust are mainly emplaced by roof uplift and floor sinking. The emplacement of intrusive bodies is always controlled by a combination of several mechanisms, interacting and influencing each other (e.g. Paterson and Fowler, 1993b; Paterson and Vernon, 1995; Wang et al., 2000; Burchardt et al., 2009).

These emplacement mechanisms can be influenced by the local creation of space in areas of faulting and folding (Paterson and Fowler, 1993a). All the mechanisms have been vividly debated for more than a century, mainly because field observations tend to be inconclusive: e.g. wall-rock xenoliths and discordant wall-rock contacts may reflect either stoping or sequential injection of dykes

and/or sills, and an ovoid intrusion surrounded by concentrically-foliated wall rocks could result from diapirism, ballooning, or laccolith emplacement. In the following, the most important ductile and brittle emplacement mechanisms are briefly introduced.

1.3.1 Diapirism and ballooning

Diapirism is the upward movement of magma into or through country rock driven by buoyancy (Roberts, 1970), whereas ballooning describes the symmetrical and radial in-situ expansion of a body during ductile shortening of the country rock (e.g. Sylvester et al., 1978; Bateman, 1985; Ramsay, 1989; Fig. 1.5). In terms of magma emplacement, these mechanisms require that a magma chamber with at least 50 vol% liquid throughout a volume comparable to the size the pluton is present (Glazner et al., 2004). Diapiric ascent cannot overcome the brittle-ductile transition (Clemens, 1998; Vigneresse and Clemens, 2000). Also, the common emplacement mechanism for salt, diapirism (e.g. Hudec and Jackson, 2007), is mainly driven by tectonics (Talbot et al., 2000).

Features that are commonly assigned to diapirism and ballooning include e.g. (1) the vertical displacement of country rocks (England, 1990), (2) radial structures and rim synclines, (3) an elliptical pluton shape in map view, (4) concentric compositional zoning of the pluton, (5) flattened enclaves near the pluton margin, (6) an increased

intensity of the internal foliation towards the margin, (7) narrow, high-temperature shear zones and steep lineations in the aureole (e.g. Paterson and Vernon, 1995). However, several of these listed features can be also explained by other material-transfer processes (e.g. Schmeling et al., 1988; Paterson and Vernon, 1995).

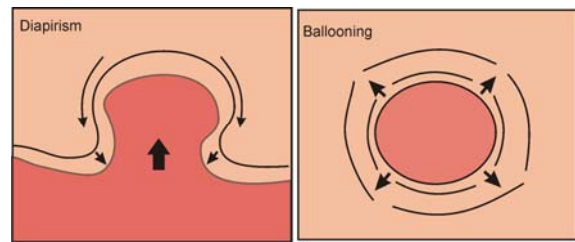


Figure 1.5: Schematic illustration of the mechanisms diapirism and ballooning.

Controversially discussed examples in this context include the Ardara Pluton (Ireland; e.g. Pitcher and Berger, 1972; Sanderson and Meneilly, 1981; Molyneux and Hutton, 2000; Siegesmund and Becker, 2000; Hutton and Siegesmund, 2001), the Cannibal Creek Granite (Australia; e.g. Bateman, 1985; Castro, 1987), the Papoose Flat Pluton (California, USA; e.g. Sylvester et al., 1978; Hibbard, 1987; de Saint-Blanquat et al., 2001), and the Sausfjellet Pluton (Norway, Dumond et al., 2005). The La Bazana Pluton (Spain) has been interpreted as a magmatic diapir (Galadi-Enriquez et al., 2003).

1.3.2 Cauldron subsidence, ring faulting and caldera collapse

Cauldron subsidence is described as subterranean or plutonic version of caldera

collapse by Clough et al. (1909). It involves the sinking of a large piston of rock, bounded by ring faults and dykes, into a magma chamber, to be replaced by magma from the latter (Clough et al. 1909; Anderson 1936; Fig. 1.6). Ring-dyke emplacement is the initial stage, during which magma intrudes along ring faults (shear fractures), in response to the decrease of pressure in an underlying magma reservoir (Roberts, 1970), resulting in a ring-shaped intrusion (e.g. Anderson 1936).

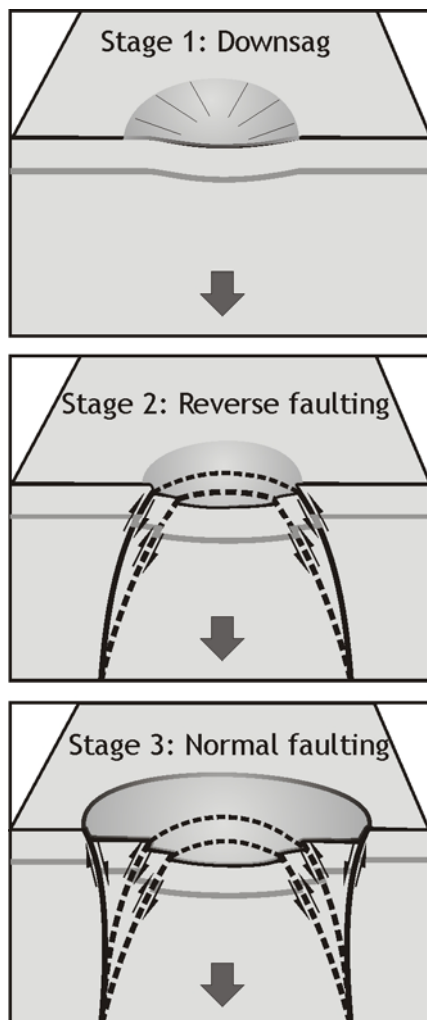


Figure 1.6: Stages of ring fault initiation and caldera collapse (modified from Burchardt and Walter, 2009).

The structural pattern of ring faults is known from field studies of eroded calderas (e.g. Lipman, 1984), geophysical monitoring of active calderas (e.g. Saunders, 2001), and analogue modelling (e.g. Anderson, 1936; Komuro, 1987; Kusumoto and Takemura, 2003, Burchardt and Walter, 2009).

When ring faults reach the surface, a collapse caldera forms and magma, transported along the ring dykes, can be extruded. The contacts crosscut the host rock structure (i.e. they are discordant), implying brittle deformation. Thus, cauldron subsidence is regarded as a passive emplacement mechanism, where passive upwelling of magma fills the space previously occupied by the subsided block (e.g. Stevenson et al., 2007).

Since the recognition of the formation mechanisms of the Glencoe Caldera (Scotland) by Clough et al. (1909), numerous studies have recognised a genetic relationship between ring dykes and plutons in ring complexes and calderas. Field examples include the Chita Pluton (Argentina; Yoshinubo et al., 2003), the Red Mountain Creek Pluton (California; Zak and Paterson, 2006), as well as ring complexes in the Tertiary Igneous Province of Britain such as Mull, Rum, and Ardnamurchan (e.g. Skelhorn and Elwell, 1971; Sparks, 1988; Troll et al., 2000; Nicoll et al., 2009; Holohan et al., 2009). However, some ring dyke complexes are being reinterpreted as lopoliths or inverted cone-shaped intrusions (O'Driscoll et al., 2006; Mathieu et al., 2008).

1.3.3 Formation of dykes, sills, laccoliths and lopoliths

Dykes are steep, cross-cutting intrusions. Brittle rocks can fail in tension under the pressure exerted by magma and fluid filled fractures form (Hubbert and Willis, 1957; Jaeger, 1972). Hydraulic fracturing of rocks is the only mechanism that transports magma fast enough before it solidifies (Spence and Turcotte, 1990). However, many intrusions are emplaced in fault zones (Morris and Hutton, 1993) and there are examples of intrusions propagating through associated brittle and ductile faults (Pollard, 1973). Pollard (1973) suggested that dykes can be emplaced by three main mechanisms: tensional fracturing (a shallow-depth intrusion splits the host rocks and propagates along tensional fracture), brittle faulting (deeper intrusions propagate along brittle faults, which form at their termination), and ductile faulting (at high confining pressure and high temperature, ductile faulting occurs near terminations and the intrusion grows by ductily displacing the host rock). Dyke propagation by fracturing has been modelled by numerical and analogue models (e.g. Pollard, 1973; Spence and Turcotte, 1990; Lister and Kerr, 1991; Heimpel and Oison, 1994; Takada, 1994; Mathieu et al., 2008).

Sills commonly intrude parallel to bedding planes (Francis, 1982), into basement rocks (Holness and Humphreys, 2003), pre-existing lavas, and steeply dipping rocks, or other unconformities (e.g. Mudge, 1968;

Sylvester et al., 1978). Consequently, there are conflicting hypotheses of sill formation, with their emplacement controlled either by buoyancy forces or by tectonic stress systems. The hypothesis that sills are emplaced at the level of neutral buoyancy of magma (Bradley, 1965; Corry, 1988) is not consistent with field observations and 3D seismic data of sills that intrude different stratigraphic levels and feed each other (e.g. Francis, 1982; Thomson and Hutton, 2004; Cartwright and Hansen, 2006). Robert's (1970) tectonic hypothesis states that sills are emplaced during conditions of horizontal compression. The transition from dyke to sill is attributed to a rotation of the principal stress from horizontal tension ($\sigma_x < \sigma_z$), which favours dyke propagation at depth, to horizontal compression ($\sigma_x > \sigma_z$), which promotes sill propagation at shallow crustal levels (e.g. Roman et al., 2004). Field observations of sills at lithologically contrasting boundaries (John, 1988; Cruden, 1998; de Saint-Blanquat et al., 2001, 2006; Rocchi et al., 2002; Breitzkreuz and Mock, 2004; Mazzarini et al., 2004; Westerman et al., 2004; Valentine and Krogh, 2006; Burchardt, 2008) and experimental results by e.g. Kavanagh et al. (2006) and Menand (2008) underline the importance of a rigidity contrast for sill formation.

Once a sill has formed, it propagates laterally by tensile fracturing (Anderson, 1938) in the direction of least resistance. As the size of the sill becomes comparable to its depth and thus has the ability to inflate

vertically (bending the overburden or lifting the roof), it becomes a laccolith (e.g. Pollard and Johnson, 1973; Pollard and Holzhausen, 1979; Habert and de Saint-Blanquat, 2004; Menand, 2008). This also implies that laccolith formation is limited to the uppermost kilometres of the crust. At deeper structural levels, floor sinking by ductile downward flow will result in the formation of lopoliths (Cruden, 1998). Cauldron or floor subsidence differs from lopolith formation by floor depression by the lack of broadly-distributed deformation of low strain magnitude (Cruden, 1998); the shear deformation is instead localised on the boundary fault.

The punched laccolith and the christmas-tree laccolith, a series of concordant intrusions connected by narrow feeder dykes, are considered as end members of laccoliths (Corry, 1988; Fig. 1.7). A punched laccolith is an epizonal intrusion that can form by a single sill that acts mechanically as a vertical punch. A simple laccolith grows from a sill that intrudes along crustal heterogeneities by vertical inflation, lifting of the overburden (roof uplift; Johnson and Pollard, 1973; Corry, 1988; Cruden, 1998; de Saint-Blanquat et al., 2001), and amalgamation of smaller sheet-like bodies (Rocchi et al., 2002; Coleman et al., 2004; Glazner et al., 2004); it is characterised by flat tops, peripheral faults and steep vertical sides. A christmas-tree laccolith may evolve from a series of stacked sills and smaller laccoliths that are interconnected by

vertically extending feeder dykes (Corry, 1988; Westerman et al., 2004; Fig. 1.7).

To summarise, a sill grows mainly by lateral propagation, whereas laccoliths grow by vertical thickening, before extending laterally again to form plutons (Menand, 2008). Regarding laccolith and lopolith formation, the growth of the intrusion results from successive supply of magma in the form of successive sheet- or sill-like units (e.g. Horsman et al., 2005; de Saint-Blanquat et al., 2006) favoured by the creation of a local stress field around the initial intrusion (Vigneresse et al., 1999; Horsman et al., 2005).

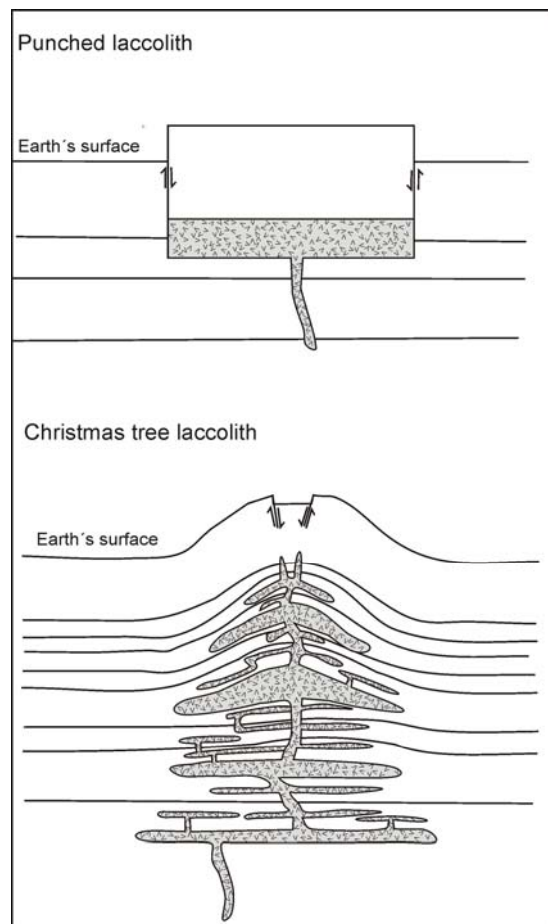


Figure 1.7: Laccolith models (modified after Corry, 1988) of a punched laccolith and a christmas-tree laccolith.

The dimensional similarity between sills, laccoliths, and large plutons (McCaffrey and Petford, 1997; Cruden and McCaffrey, 2001; Westerman et al., 2004) suggests that the emplacement mechanisms of sills and laccoliths play an important role in the emplacement of large plutonic bodies (e.g. Vigneresse, et al., 1999). Laccoliths therefore link lava complexes and plutons (Breitkreuz and Petford, 2004; Fig. 1.8).

Field examples of sills and laccolith intrusions include the igneous complex on the Isle of Elba (Italy; e.g. Rocchi et al., 2002; Westerman et al., 2004), the Black Mesa Pluton (e.g. de Saint-Blanquat et al., 2006), the Trachyte Mesa Laccolith (e.g. Morgan et al., 2005; Horsman et al., 2005), and the Maiden Creek Sill (Utah; e.g. Johnson and Pollard, 1973; Horsman et al., 2005), the Searchlight Pluton (Nevada; e.g. Bachl et al., 2001), the Solsikke Sill Complex, Møre Basin (North Atlantic; e.g. Hansen and Cartwright, 2006), the Great Whin and Midland Valley Sills (United Kingdom; e.g. Francis, 1982; Goult, 2005), and the Golden Valley Sill Complex (South Africa; e.g. Galerne et al., 2008; Polteau et al., 2008b). The Great Eucrite intrusion of Ardnamurchan (Scotland; e.g. O'Driscoll et al., 2006) is an example of a lopolith.

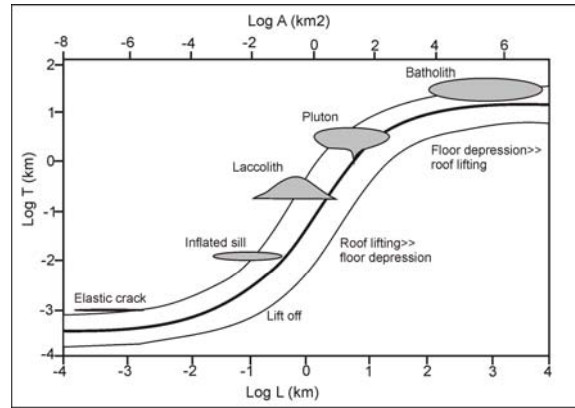


Figure 1.8: Intrusion thickness (T), area (A) and width (L) result in an S-style curve relating the dimensions of crack to batholith (modified after Cruden and McCaffrey, 2001).

1.3.4 Magmatic stoping

The mechanism of magmatic stoping can occur at any crustal level (Pignotta and Paterson, 2007) as a result of shear or tensile failure caused by the interplay of e.g. thermal and mechanical stresses associated with dyke emplacement, fluid migration and expulsion, focused porous flow, and tectonic stresses (e.g. Daly, 1903; Pignotta and Paterson, 2007; Paterson et al., 2008; Fig. 1.9), but is most efficient in the brittle crust mainly due to the large temperature gradients between upper crustal rocks and intruding magma (Zak et al., 2006).

Features that are typically attributed to stoping are described in e.g. Paterson and Fowler, 1993b; Fowler and Paterson, 1997; Yoshinubo et al., 2003; Dumond et al., 2005, and Zak et al., 2006. While the volumetric significance of magmatic stoping is still under discussion (e.g. Clarke et al., 1998; Glazner and Bartley, 2006; Zak et al., 2006; Clarke and Erdmann, 2008; Yoshinubo and

Barnes, 2008), it plays an important role because (1) as a vertical material-transfer process; (2) it may remove evidence of earlier emplacement processes (Paterson and Fowler, 1993b; Paterson and Vernon, 1995; Yoshinubo et al., 2003); (3) it indicates the presence of a magma chamber that allows sinking and removal of stopped blocks and thus rules out emplacement via incremental dyking mechanisms (e.g. Clemens and Mawer 1992; Petford et al. 1994, 2000; Glazner et al. 2004); (4) it contributes to chemical contamination of magma and therefore facilitates the compositional evolution of magma (e.g. Dumond et al., 2005; Yoshinubo and Barnes, 2008); (5) it gives insight into the formation and timing of magmatic fabrics (Fowler and Paterson, 1997) and (6) discrete stopping events may trigger volcanic eruptions (Sparks et al., 1977; Hawkins and Wiebe, 2004).

Examples of intrusions that have been at least partly emplaced by stopping include dykes in Greenland (Bridgwater and Coe, 1969); ring dykes in Glencoe (Scotland; e.g. Clough et al., 1909), sills in Texas (e.g. Barker, 2000), as well as plutons such as the Chita Pluton (Argentina; e.g. Yoshinubo et al., 2003), the Red Mountain Creek Pluton (California; e.g. Zak and Paterson, 2006), Sierra Nevada Batholith (USA; e.g. Pignotta and Patterson, 2007), and some of the Variscan Bohemian plutons (Zak et al., 2006).

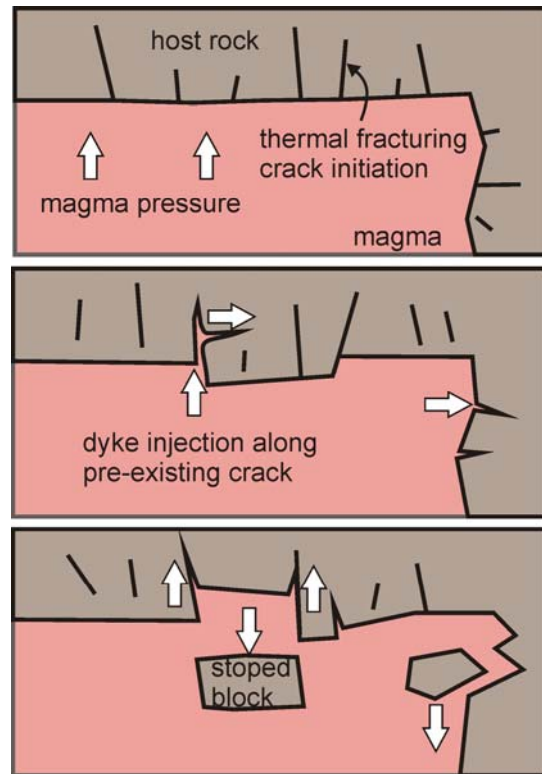


Figure 1.9: Schematic illustration of the initiation of stopping by thermal and mechanical fracturing and magma injection along pre-existing cracks.

2. Geological and tectonic framework of Sweden

2.1 Geological and tectonic framework of Sweden

The Baltic Shield is part of the Precambrian East European Craton, which was formed between 2.0-1.7 Ga by the successive collision of once autonomous crustal segments (Bogdanova et al., 2008 and references therein), namely Fennoscandia, Sarmatia and Volgo-Uralia (Fig. 2.1).

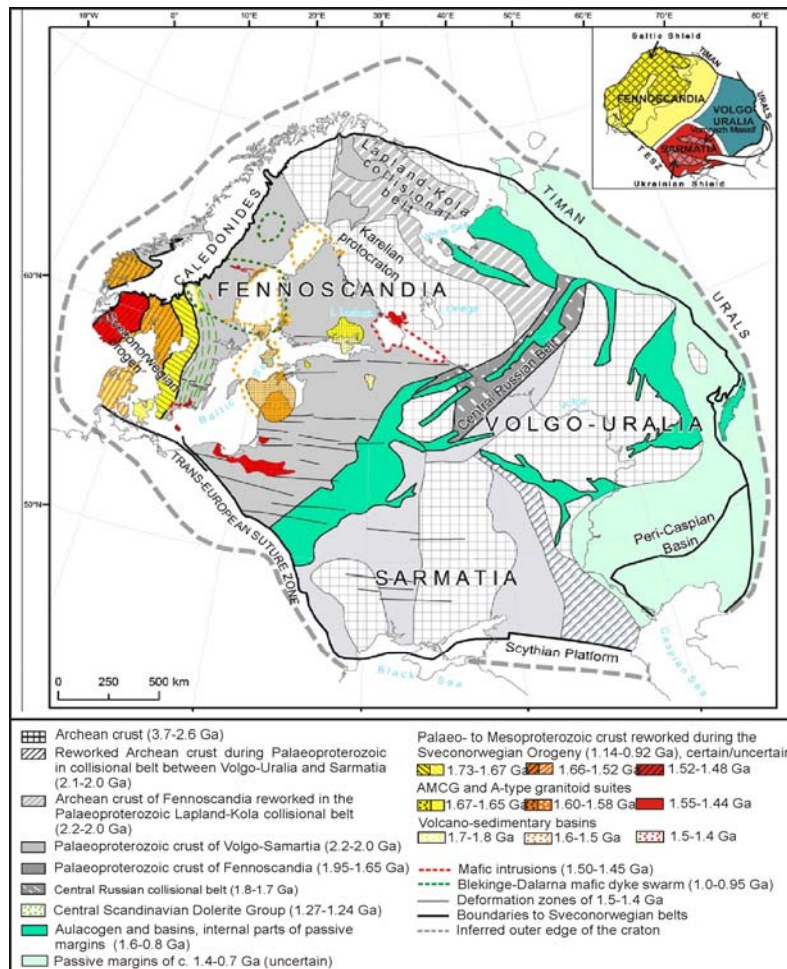


Figure 2.1: Late Palaeoproterozoic to Early Neoproterozoic tectonic complexes in the East European Craton (Baltica). Modified after Bogdanova et al. (2008).

The Archean evolution of Fennoscandia can be traced back to 3.5-3.2 Ga when an Archean continental core was created (Slabunov et al., 2006), now located in the present northwestern-most area (Fig. 2.1). The term “Fennoscandia” includes the Scandinavian Peninsula, the Kola Peninsula, Russian Karelia, Finland, and Denmark (Fig.2.1). Rifting of the Archean craton occurred between 2.45-2.0 Ga, followed by juvenile crust formation in arc systems and

intervening basins outside the craton itself, that range from 2.1-1.93 Ga (e.g. Lundqvist et al., 1998, Rutland et al., 2004).

The oldest crustal block is the Archean domain in the present NE of Fennoscandia, onto which the Svecofennian domain accreted during the Svecofennian Orogeny at 1.95-1.85 Ga (Gaal and Gorbatshev, 1987; Gorbatshev and Bogdanova, 1993; Nironen, 1997; Lahtinen et al., 2005).

The formation of continental crust took place during several episodes of accretion. After 1.85 Ga, Paleoproterozoic growth of the crust continued

semi-simultaneously with the collision between Fennoscandia and Volgo-Sarmatia (Bogdanova et al., 2008), the crust underwent intensive reworking, which resulted in granitoid plutons and the formation of the 1500 km long (N-S extent) and a few hundred

km wide (E-W extent) Transscandinavian Igneous Belt (TIB; Andersson, 1991; Högdahl et al., 2004).

During the Mesoproterozoic, Fennoscandia and Laurentia (represented by Greenland today) were characterised by an extensional stress regime, as is evident from the occurrence of episodic Rapakivi granites, dolerite dykes, continental rift intrusives, sandstone basins, and continental flood basalts (Bingen et al., 2008). The Gothian Orogeny (1.64-1.52 Ga; see Fig. 2.5) caused a continued (oceanward) growth of the Fennoscandian Shield at the southwestern active margins, and reworking during the 1.2-0.9 Ga Sveconorwegian event (Åhall and Gower, 1997; Bingen et al., 2008; see Fig. 2.5), as Baltica and the East European Craton

collided and the supercontinent Rodinia assembled (Meert and Torsvik, 2003; Bogdanova et al., 2008; Li et al., 2008; Fig. 2.2), followed by post-collisional magmatism between 0.96-0.90 Ga.

In contrast to the extensional regime in central Fennoscandia, the south-southwestern margin (including southern Sweden, Bornholm, parts of Lithuania, Poland) was a location of wide-spread granite magmatism between 1.46-1.44 Ga (Čečys and Benn, 2007; Johansson et al., 2004; Obst et al., 2004; Johansson et al., 2006; Motuza et al., 2006; Skridlaite et al., 2007; see Fig. 2.5) and an orogenic event that is referred to as Danopolian (e.g. Bogdanova, 2001; Bingen et al., 2008; Bogdanova et al., 2008; Brander and Söderlund, 2008; Drake et al., 2009).

The Danopolian event (see Fig. 2.5) is defined outside the Sveconorwegian Belt and evidence is provided by syn-tectonic deformation in 1.45 Ga plutons in southern Fennoscandia and 1.49-1.45 Ga hornblende ages ($^{40}\text{Ar}/^{39}\text{Ar}$) from drill cores in Lithuania (Bingen et al., 2008). Structural, geochronological, and geological data suggest that the tectono-magmatic event was (1) related to the collision between Baltica and, presumably, Amazonia or an other South-American terrain (Bogdanova, 2001; Čečys and Benn, 2007), (2) reworking the south-southwestern margin of Fennoscandia, or (3) a change in subduction geometry in an active margin setting (Bingen et al., 2008). Coeval with the Danopolian Orogeny, rifting and the formation of continental basalts and mafic



Figure 2.2: The ‘traditional’ model of Rodinia. Two rifting events, one along the present-day western margin of Laurentia, and a second along the present-day eastern margin of Laurentia are indicated. Reprinted from Meert and Torsvik (2003), with permission from Elsevier.

dykes occurred in various parts of the western East European Craton. Jotnian sediments that have an age of 1.5-1.46 Ga covered central Sweden (Söderlund et al., 2005) and large areas of southern Sweden (Flodén, 1980).

The time interval between 0.85-0.4 Ga was characterised by far-field effects of the break-up of Rodinia and formation of the Iapetus Ocean, rotation and drift of the continent Baltica northwards (e.g. Poprawa et al., 1999; Hartz and Torsvik, 2002; Cocks and Torsvik, 2005; Fig. 2.3).

Later on, Avalonia collided with Baltica at 450 Ma with closure of the Tornquist Sea (SE branch of the Iapetus Ocean) along the Teisseyre-Tornquist Line; Baltica-Avalonia in turn collided with Laurentia to form Laurussia coupled with the closure of the Iapetus Ocean (complete by late Silurian; Pickering, 2008) and the Caledonian Orogeny (see Fig. 2.5). The now opened Rheic Ocean separated Laurussia from Gondwana (Nance and Linnemann, 2008).

After erosion of the sediments in the late Proterozoic the sub-Cambrian peneplane was established (Lidmar-Bergström, 1996); the presently eroded bedrock surface corresponds to this peneplane. Cambrian to Early Silurian marine transgression and sedimentation resulted in the deposition of sandstone, marl, and limestone (Drake et al., 2009). This sedimentary cover had a thickness of at least 2.5-4 km during the Late Paleozoic (Zeck et al., 1988; Larson et al., 1999) partly associated with foreland

sedimentary basins of the Caledonian orogenic belt (SKB report, 2002; Drake et al., 2009 and references therein).

A final closure and subduction of the Rheic Ocean (Variscan orogeny) between 360-295 Ma was connected to accretion of magmatic arcs and docking of microcontinents (Timmermann, 2004).

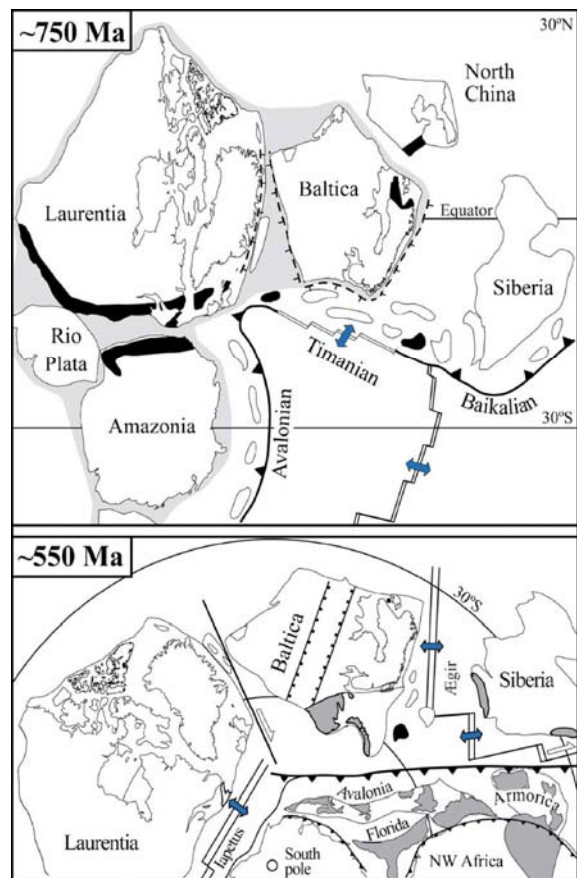


Figure 2.3: The postulated positions of Baltica in relationship to the surrounding terranes (reprinted from Cocks and Torsvik, 2005, with permission of Elsevier). Above, situation at around 750 Ma, shortly after the break up of Rodinia. Protobaltica was still attached to Laurentia, which was in turn attached to the South American terranes. Black shaded areas are 1 Ga mobile belts. Below, equal area polar projection at about 550 Ma, grey areas are mobile belts.

In early Permian, extensional deformation and the main phase of volcanic and intrusive igneous activity took place in the Oslo rift (Norway), and dolerite sills and dyke swarms occurred in Britain and Sweden (Timmermann, 2004). In southern Sweden, mafic dykes and sills were emplaced, connected to transtensional deformation of the Sorgenfrei-Tornquist Zone (Erlstöm and Sivhed, 2001; SKB report, 2002).

From 60 Ma to present, the opening and spreading of the North Atlantic defined the stress field (Slunga, 1989; Gregersen, 1992). Finally, the sedimentary cover was eroded away during uplift in the Tertiary, and the present sub-Cambrian surface was re-exposed (Lidmar-Bergström, 1996). In the last 2 Ma, the area was influenced by glaciations, transgression of the Baltic Sea, land uplift due to glacial rebound and regression of the Baltic Sea (SKB report, 2006).

2.2 Tectonic and magmatic evolution of Southeast Sweden – the Götemar region

Since the research activity of the Swedish Nuclear Fuel and Waste Management Company (SKB) in the coastal area of Southeast Sweden began to search for a potential geological repository for spent nuclear fuel (e.g. Ström et al., 2008), enormous amount of data have been collected in the area south of the Götemar on gravity, geochemical, hydrogeological, and structural geology issues.

The Götemar study area is located in the southeastern province of Sweden that is characterised by 1.8 Ga old intrusions of granitic-syenitic-(quartz) to monozodiorite-dioritic-gabbroic composition belonging to the Transscandinavian Igneous Belt (TIB; Fig. 2.4). The TIB-area is bounded by the older Svecofennian crust to the north and the younger, Southwestern Scandinavian Domain in the west. The TIB-granites in the Götemar area formed during several pulses of magmatism between 1.85 and 1.66 Ga, with the youngest of these rocks to the west (e.g. Larson and Berglund, 1992; Åhäll and Larson, 2000), which is described in the following section.

The NW-SE trending, up to 1600 km long and 130 km wide TIB formed towards the end of the Svecokarelian tectonic cycle at 1.83-1.79 Ga (Stephens and Wahlgren, 2008; Fig. 2.5) by accretion during a phase of magmatic activity in the western Svecofennian Domain and reworking of juvenile Svecofennian crust (Gorbatshev and Bogdanova, 1993; Högdahl et al., 2004). This event was followed by post-orogenic events under increasing lower metamorphic grade conditions until 1.5 Ga (Beunk and Page, 2001). The formation of the TIB towards the present south-southwest is often subdivided into four magmatic periods at 1.85-1.56 Ga, 1.81-1.76 Ga, 1.71-1.69 Ga, and 1.67-1.65 Ga (Andersson et al., 2004, 2007; Mansfeld et al., 2005; Johansson et al., 2006), which led to the formation belts of juvenile crust and

continental magmatic arcs (Bogdanova et al., 2008; Fig. 2.4).

The area of SE Sweden during this time was dominated by dextral transpressive deformation taken up by ductile NW-striking strain zones, with shortening in NE direction (Stephens et al., 1996; Beunk and Page, 2001), coupled with exhumation and erosion, and continued oblique collision to the NE, with N-S to NNW-SSE directed movement (SKB report, 2002).

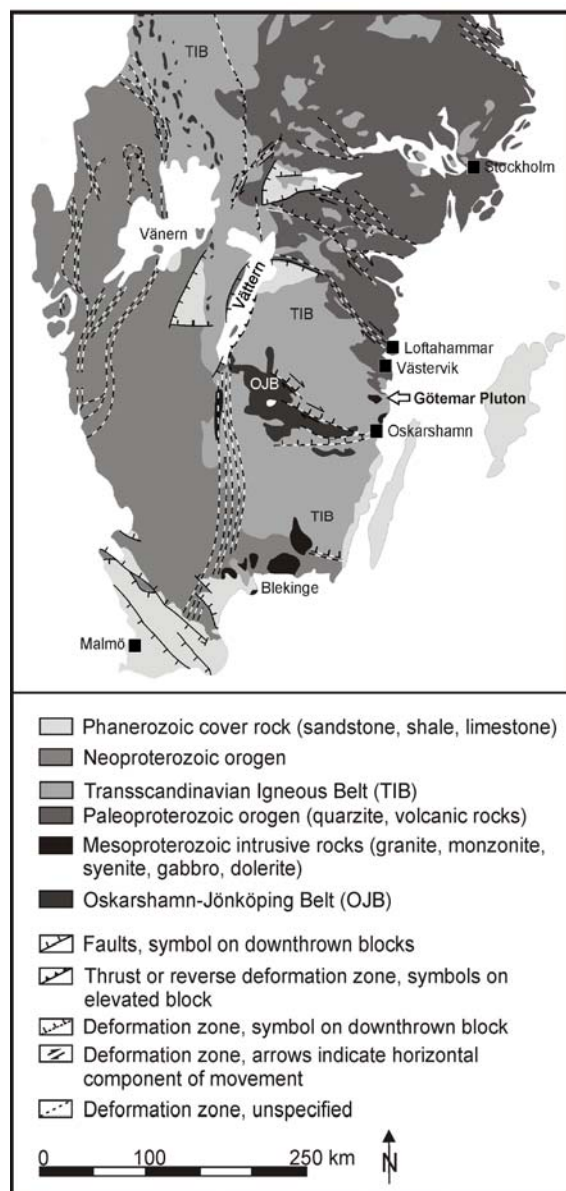


Figure 2.4: Simplified geological map of SE Sweden (modified after Beunk and Page, 2001).

Between 1.40 and 1.53 Ga, the southwestern margin of the East European Craton was subjected to extensive magmatism and deformation. While various suites of e.g. anorthositic and charnockitic-granitic, that are interpreted as A-type magmatic rocks, were emplaced between ca. 1.50 and 1.53 Ga (Brander and Söderlund, 2007; Fig. 2.5), the episode of granitic magmatism around 1.45 Ga (Åhall and Larson, 2000; Skridlaite et al., 2007) was connected to the Danopolian orogenic event. During that event numerous voluminous plutons were intruded in a wide region around the southern Baltic Sea that are geochemically similar, and appear to have originated from slightly different sources.

During the ca. 1.45 Ga Danopolian event (Fig. 2.5), South Sweden experienced a regional compression and ENE-WSW shortening that caused syn- and post-magmatic deformation of the involved granitoids (Čečys and Benn, 2007). In contrast to South Sweden, the coeval plutons (Åhall, 2001) further north, in Småland e.g. the Götemar and Uthammar Plutons (Kresten and Chyessler, 1976; Åberg et al., 1985; Kornfält et al., 1997; Cruden, 2008), seem to occur in an extensional setting that expresses a distal influence of the Danopolian igneous activity. The emplacement might be triggered by changes in the crustal stress field and resulted in time-lapsed magma formation and migration (Čečys, 2004).

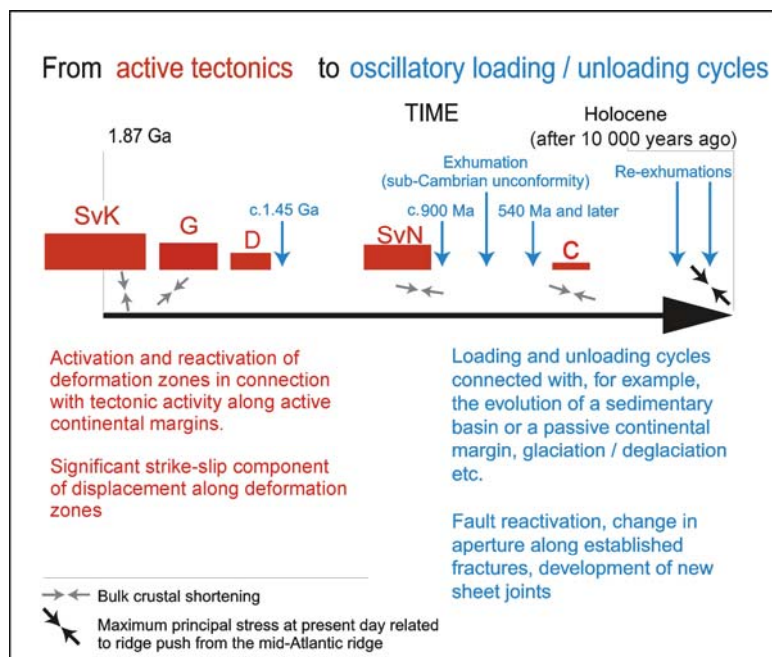


Figure 2.5: Active tectonics (red) and oscillatory loading and unloading cycles (blue) during geological time in the Götömar area (modified from Stephens et al., 2008). SvK: Svecokarelian Orogeny, G: Gothian Orogeny, D: Danopolian Orogeny, SvN: Sveconorwegian Orogeny, C: Caledonian Orogeny.

The time up to 850 Ma was characterised by subsidence and formation of a foreland sediment basin to the east of the Sveconorwegian orogenic belt, exhumation of deeper crustal levels and erosion. Subsequently, the sub-Cambrian peneplane was established, the major unconformity between Proterozoic rocks on the Fennoscandian shield and Paleozoic sedimentary overburden. In Early to Middle Cambrian times the NE-SW trending Baltic Basin developed, related to rifting along the southwestern margin of Baltica and the latest stages of the Precambrian super-continent breakup leading to sea-floor spreading in the Tornquist Sea (SE branch of the Iapetus

Ocean; Poprawa et al., 1999). Faults with NNE and WNW strike control the geometry of outliers of Lower Paleozoic rocks and disturb the sub-Cambrian peneplane, again in Cretaceous times due to marine transgression in SE Sweden (Lidmar-Bergström, 1994; Bergman et al., 1999; SKB report, 2002).

2.3 Case studies Sweden

The circular (in horizontal cross-section) Götömar intrusion is chosen as example of pluton emplacement in the upper crust, influenced by deep rooted faults (Chapter 3). Circular plutons have been often attributed to diapirs or ballooning mechanisms (Marsh, 1982; Bateman, 1985; Hutton, 1997). Studies of other semi-circular plutons in Sweden (Cruden and Aaro, 1992; Cruden et al., 1999) reveal a rather asymmetric, tabular shape of the plutons, like it is assumed for many plutons worldwide (Cruden, 1998; Cruden, 2008). This case study presents a complex emplacement history including episodic granitic injections and build-up of a layered laccolith. Its special mineralogy, geochemistry and hostrock-pluton relationship offers potential for more field work not only in terms of emplacement of the TIB batholith and its individual intrusion, but also towards a petrographic and tectonic model of SE Sweden.

Dyke emplacement mechanisms can be applied to different material, e.g. basalt, granite, gravel, clay, till, breccia, bitumen, and appear in sedimentary, igneous and metamorphic milieu. Along the coast of SE Sweden, including the Götemar Pluton and adjacent areas, hundreds of clastic dykes have been found, attributed to mainly Cambrian to Ordovician activity associated with NW-SE directed rifting and sea floor spreading (e.g. Carlson and Holmqvist, 1968; Bergman, 1982; Tynni, 1982; Katzung and Obst, 1997; Alm and Sundblad, 2002; Chapter 4). The mechanism of clastic dyke formation is poorly understood, and interpretations of field observations are commonly ambiguous. The case study of the emplacement of sedimentary dykes in the coastal area of SE Sweden is an example for downward propagation of a fracture without evidence of hydraulic fracturing in an alternating stress regime.

3. Multi-stage emplacement of the Götömar Pluton – case study Southeast Sweden: preface

Plutons do not necessarily form, and perhaps rarely do form, by crystallisation of a large body of magma emplaced during a single intrusion event (e.g. Cruden and McCaffrey, 2001; Glazner et al., 2004; Annen et al., 2006). Many plutons are thought to be assembled as a series of sheet-like intrusions (e.g., Coleman et al., 1995; Morgan et al., 1998; Wiebe and Collins, 1998; Brown and McClelland, 2000; de Saint-Blanquat et al., 2001; Glazner et al., 2004; Matzel et al., 2006) emplaced at rates several orders of magnitude faster than the long-term average growth rate (Bartley et al., 2006). Such plutons are supposed to be highly composite and may take up to millions of years to grow if magma is delivered in discrete pulses, resulting in a partitioning of single continuous bodies (e.g., Coleman et al., 2004; Condon et al., 2004; Glazner et al., 2004; Matzel et al., 2006; Cruden et al., 2005; Annen et al., 2006).

Ascent of magma by dyking was proposed as a mechanism to build up large granite plutons within a relatively short time in contrast to diapirism (Clemens and Mawer, 1992; Petford et al., 1993; Clemens, 1998). Dyking as a mechanism of magma ascent plays a mayor role for granites related to shear zones (Hutton, 1982; Tobisch and Cruden, 1995; Aranguren et al., 1997), but also for batholiths emplaced at shallow levels in anorogenic settings (Wilson et al., 2000).

With respect to emplacement, major tectonic structures may play an important role by creating dilational space (e.g., Hutton, 1982; 1988; Tikoff and Teyssier, 1992; Grocott et al., 1994; Titus et al., 2005), arresting ascent (e.g., Clemens and Mawer, 1992; Hogan et al., 1998), or controlling the geometry of plutons (Hutton, 1982; Holdsworth et al., 1999; Titus et al., 2005).

Wiebe and Collins (1998), Petford et al. (2000), Vigneresse and Clemens (2000) and Pupier et al. (2008), amongst others, proposed that most granitic intrusions initiated as low-viscosity, crystal-poor magma in tabular intrusions fed from below by small magma batches that ascend either in dykes or are channelled along shear zones. Space for the incoming magma is made by a combination of lateral and vertical material transfer at moderate strain rates (typically $> 10^{-14}/s$) on timescales of less than 100 000 years (Petford et al., 2000).

Formation of laccoliths through upward inflation of original sill-like or tabular intrusions is generally regarded to be mechanically possible at shallow depths, whereas formation of lopoliths via floor sinking is more feasible at greater depths (Corry, 1988; Clemens and Mawer, 1992, Petford, 1996; McCaffrey and Petford, 1997; Clemens, 1998; Cruden, 1998; Cruden et al., 1999). Inflation (vertical and/or horizontal; Brown and McClelland, 2000; Cruden and McCaffrey, 2001) is a general mechanism for pluton growth, which may take different forms depending on (1) the geometry of the

intersection between the evolving pluton and its feeder (point source, linear, etc.), (2) pre-existing structure (anisotropy) of the wall rocks at the emplacement site (heterogeneities, anisotropies), and (3) the regional tectonic stress field (de Saint-Blanquat et al., 2001).

For sub-elliptical and circular pluton shapes in map view, as the following field example of the Götömar Pluton in Sweden, several authors have suggested a tabular or funnel-shaped form that steepens in the directions of one or more feeders (e.g. Vigneresse, 1995a,b; Cruden, 1998). Floors that steepen towards a feeder are also characteristic of a number of layered intrusions (e.g. Irvine, 1980; McBirney, 1996). Models for the development of subhorizontal tabular plutons typically involve: (1) horizontal fracture propagation and/or magma accumulation at anisotropic levels in the crust (e.g., Hogan et al., 1998) (2) lateral growth or ballooning and (3) floor subsidence accommodated by either normal-sense movement on basal shear zones or sinking of the pluton as a deeper source reservoir is drained (Brown and Solar, 1998; Cruden, 1998; Wiebe and Collins, 1998; Dumond et al., 2005). Circular plutons have often been attributed to emplacement by diapirs or ballooning (Marsh, 1982; Bateman, 1985; Hutton, 1997). Recent studies indicate that “inflating” plutons are not necessarily balloon- or bubble-shaped, but are rather tabular (de Saint-Blanquat et al., 2001).

The highly differentiated circular Götömar Pluton is described by earlier studies by Kresten and Chyssler (1976) as the upper part of a diapiric intrusion within the surrounding rocks of the Transscandinavian Igneous Belt batholith emplaced as “crystallised mush with a high volatile content at a subvolcanic level”. The term “crystallised mush” describes a magma that is above its solidus at high crystallinity (Bachmann et al., 2007). Latest studies by Cruden (2008) and Cruden and Wahlgren (2008), based on gravity modelling redefine the intrusion of the Götömar Pluton as a punched laccolith emplaced in a brittle, upper crustal regime by a combination of floor subsidence and roof lifting, and rule out the possibility of diapirism.

Based on additional structural field data, microfabric analysis, and taking into account drill core data and the gravity profiles of the intrusion by Cruden (2008), the following chapter deals with questions regarding the emplacement of the Götömar Pluton: (1) Was the Götömar Pluton emplaced as a steep-walled intrusion or as a subhorizontal tabular body? (2) Is there a possible tectonic influence on emplacement? (3) How was space created for the emplacement?

This work has been submitted to Tectonophysics 2009 as: Friese, N., Vollbrecht, A., Tanner, D.C., Fahlbusch, W., Weidemann, M., Multi-stage emplacement of the Götemar Pluton, SE Sweden - a layered laccolith intrusion

3. Multi-stage emplacement of the Götemar Pluton, SE Sweden - a layered laccolith intrusion

Nadine Friese¹, Axel Vollbrecht¹, David C. Tanner², Wiebke Fahlbusch¹ and Miriam Weidemann¹

¹*Geoscience Centre of the University of Göttingen, Goldschmidtstrasse 1-3, 37077 Göttingen, Germany*

²*Leibniz Institute of Applied Geophysics, Stilleweg 2, 30655 Hannover, Germany*

Abstract

The Götemar Pluton at the coast of SE Sweden is re-examined using a combination of structural, petrographic, and microstructural data of the pluton–wall-rock system. The pluton is circular in plan view and an internally zoned tabular structure, assembled by intrusion of successive pulses of magma at a crustal depth of 4-8 km. Initial pluton formation involved magma ascent in a vertical feeder dyke, which was arrested at stratigraphically-controlled mechanical discontinuities in the Transscandinavian Igneous Belt batholith, leading to the formation of a sill. Subsequent sill inflation, accompanied by horizontal infilling from several magma sources via fractures and a feeder dyke at the base of the laccolith, resulted in deformation of previously emplaced magma pulses and raising of the roof, facilitated by thermal weakening as the wall-rock temperatures progressively rose during emplacement of successive magma pulses. CL analysis emphasise a complex

emplacement history involving magma mixing, decompression through rapid ascent and repeated heating of the laccolith by episodic magma injections. Cooling from the roof downward resulted in the cessation of vertical inflation and probably promoted lateral expansion and minor floor depression. Although no syn-emplacement deformation is recorded in the Götemar Pluton, the emplacement is supposed to be tectonically-controlled by a NNE-SSW trending shear system along which several coeval plutons in SE Sweden are aligned. However, the lack of internal deformation does not preclude that the country rocks were subject to a regional deviatoric stress field at that time. An inferred rapid emplacement, within a timeframe of 20 ka-30 ka, may explain why the pluton appears to be anorogenic even though it was emplaced during a period of regional deformation.

3.1. Introduction

A circular to elliptical shape of plutons is often described (e.g. Cruden and Aaro, 1992; Patterson and Fowler, 1993a,b; Cruden et al., 1999; Molyneux and Hutton, 2000; Pinotti et al., 2002; Galadi-Enriquez et al., 2003; Ciavarella and Wyld, 2008; Raposo and Gastal, 2009) and has been attributed to emplacement by diapirs or ballooning (Marsh, 1982; Bateman, 1985; Hutton, 1997; Galadi-Enriquez et al., 2003). Key elements often interpreted to support ballooning are (1) internal structures (e.g., zoning, dykes, foliations, microstructures); (2) thermal aureoles; (3) country-rock strain fields and near-field material-transfer processes (processes operating in the structural aureole of the pluton; Patterson and Vernon, 1995; e.g., stoping, assimilation); (4) timing of subsolidus deformation in the pluton and country rocks (Patterson and Vernon, 1995). The term “ballooning” often suggested that plutons are associated with radial expansion and oblate strains. A growing number of recent studies indicate that “inflating” plutons are not balloon- or bubble-shaped, but are rather tabular and resemble either laccoliths or lopoliths (de Saint-Blanquat et al., 2001). The circular shape of the plutons is explained as a result of stress field changes from vertical to horizontal related magma flow at shallow crustal levels by Pinotti et al. (2002).

Earlier studies (e.g., Larsen, 1971; Åberg, 1988; Anderson and Morrison, 2005) discuss several Mesoproterozoic Fenno-

scandian plutons as examples of anorogenic intrusions mainly because of their A-type granitoid affinity (e.g., Whalen et al., 1987). New investigations of Mesoproterozoic granitic plutons of similar composition and age to the Götemar Granite in Sweden (e.g. Åhall, 2001; Čečys et al., 2002; Čečys and Benn, 2007; Bogdanova et al., 2008; Brander and Söderlund, 2008) and adjacent areas as e.g. Bornholm and Lithuania (e.g. Kornfält and Vaasjoki, 1999; Söderlund et al., 2002; Obst et al., 2004; Cymerman, 2004; Johansson et al., 2006; Motuza et al., 2006; Skridlaite et al., 2007; Zarins and Johansson, 2008), suggest syntectonic intrusion of a series of Mesoproterozoic plutons during the so called 1.47-1.44 Ga Danopolian compressional event (Bogdanova et al., 2001; 2008, Brander and Söderlund, 2008). Čečys and Benn (2007) proof a ENE-WSW directed compression in this connection. The cogenetic, elliptical Uthammar Pluton (1.44 Ga; Åhall, 2001), and the Götemar Pluton (1.45 Ga; Åhall, 2001) as a focus in this study, are located close to the town Oskarshamn (Fig. 3.1A), SE Sweden. According to studies by Čečys (2004), these plutons are assumed to occur in an extensional setting and seem to express a distal influence of the Danopolian igneous activity. The Götemar Pluton itself shows no signs of deformation or structural control on emplacement at first sight, so the “anorogen component” is a matter of debate and part of this study.

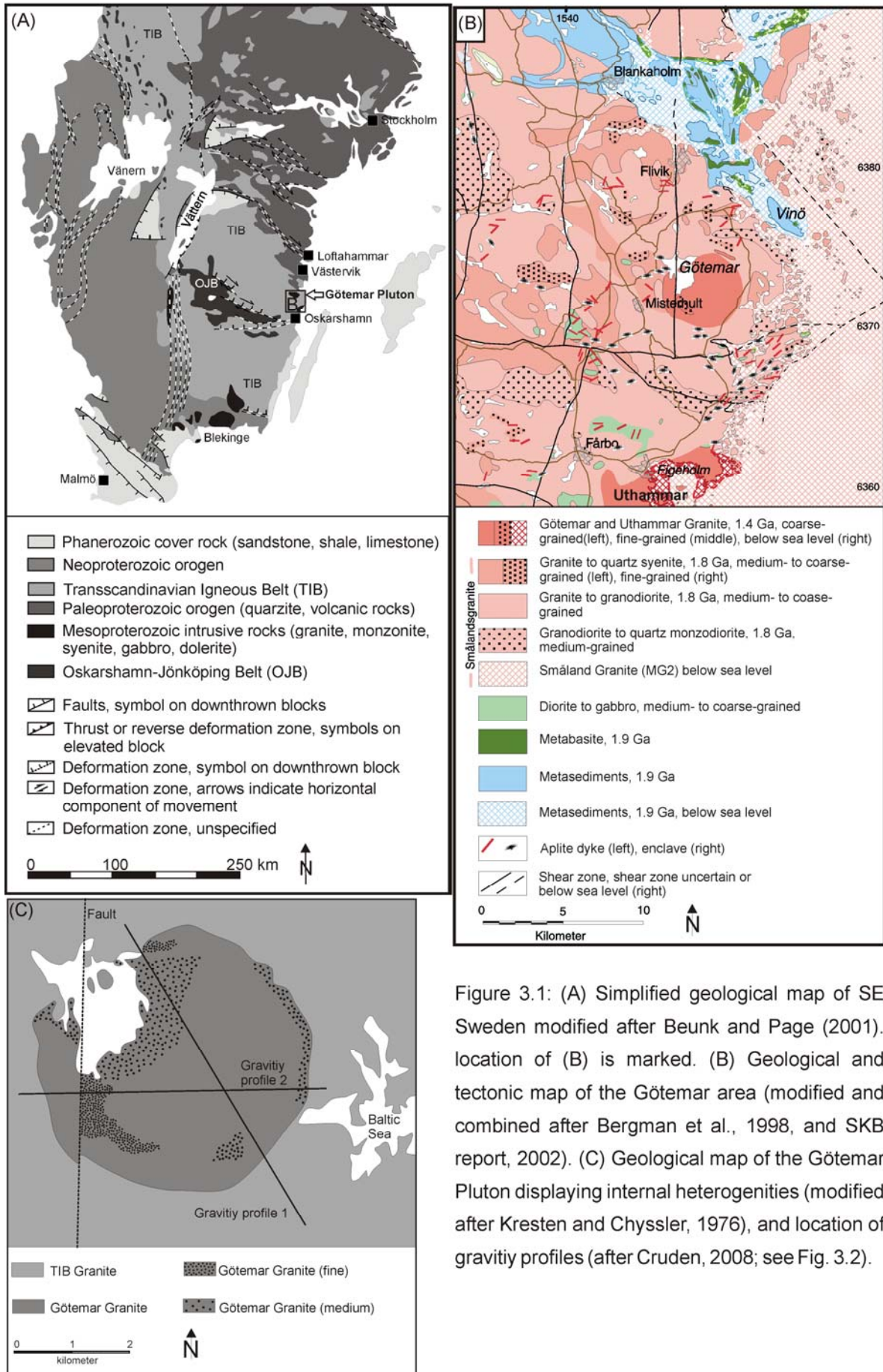


Figure 3.1: (A) Simplified geological map of SE Sweden modified after Beunk and Page (2001). location of (B) is marked. (B) Geological and tectonic map of the Götömar area (modified and combined after Bergman et al., 1998, and SKB report, 2002). (C) Geological map of the Götömar Pluton displaying internal heterogeneities (modified after Kresten and Chyssler, 1976), and location of gravity profiles (after Cruden, 2008; see Fig. 3.2).

In this work, the Götömar Pluton is re-examined for its emplacement mechanism. For this purpose, brittle structures (magmatic dykes, joints, and mineral veins) were mapped to determine the host rock-pluton connection. Microfabric analysis, including cathodoluminescence microscopy, is presented to evaluate grain generations and fabrics in order to show the complex crystallisation and heating history of the intrusion. Available literature data, in particular gravity profiles and drill core data from the Götömar Pluton are used in addition to strengthen the emplacement scenario. We show that the Götömar Pluton grew by recurrent magma injections that caused syn- and postmagmatic deformation of the pluton.

3.2 State of the art

Although the Götömar Granite has been quarried for dimension stone since the 1930s, only little geological work has been done on the pluton and its emplacement. Kresten and Chyssler (1976) were among the first to describe the rock suites and reveal their geochemistry. First dating of the Götömar massif by Åberg (1978) and later by Åberg et al. (1984) yielded ages of 1.4 Ga. After the Swedish Nuclear Fuel and Waste Management Company (SKB) began to investigate the Oskarshamn area for long-term storage of nuclear waste, numerous data on geophysics (e.g. gravity), geochemistry, age dating, and structural geology (e.g. faulting, mineral veins) were collected (reports available on the SKB homepage).

Thus, the around 1.8 Ga old plutonic host rocks of the Götömar Pluton are well studied, in contrast to the 1.4 Ga old granitic intrusions in the area, which have been mostly ignored until now.

With regards to the emplacement, Kresten and Chyssler (1976) interpreted the intrusion as a diapir, a current re-evaluation by Cruden (2008) and Cruden and Wahlgren (2008), based on gravity data, suggest discordant, hybrid plutons modified by floor subsidence and roof lifting. Gravity measurements (Triumpf, 2004; Cruden, 2008) reveal vertical upper contacts of the pluton, and a mid-level body with outward dipping upper, horizontal and lower contacts, that give the pluton a punched tabular shape with a flat roof (Cruden and McCaffrey, 2001; Cruden, 2008; Fig. 3.2). An inferred centrally located feeder extends to depths of around 4 km (Cruden and Wahlgren, 2008; Cruden, 2008; Fig. 3.2) in the gravity models. Gravity modelling indicates that the Götömar Pluton has considerably greater lateral extent in the subsurface (Triumpf, 2004; Cruden, 2008). Numerous drill core data from the host rock (Wahlgren et al., 2008) are used to constrain the gravity profile by Cruden (2008). Drill-core data from three different locations in the Götömar Pluton (Scherman, 1978) identified fine-grained aplitic granite that occurs repeatedly as probably horizontal tabular sheets (with a thickness of 0.2 m–23 m) extending between coarse-grained granite (single increments up to 100 m thick). However, it cannot be reconstructed from the

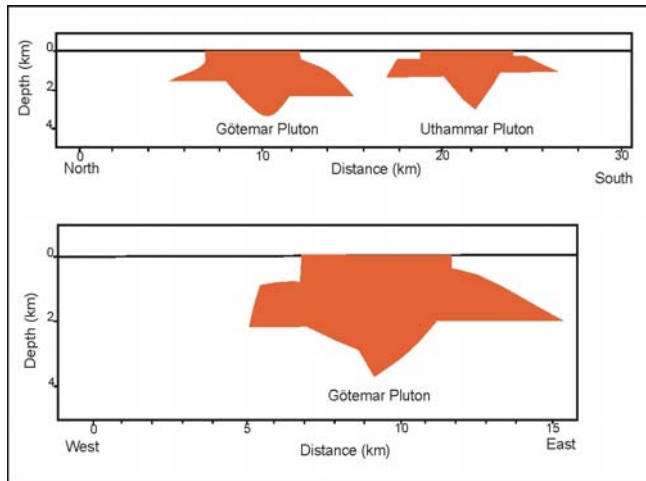


Figure 3.2: N-S and E-W gravity profiles of the Göttemar and Uthammar Plutons modified after Cruden (2008), profiles located in Figure 3.1C.

drill core records whether the granites are multiple intrusions with the resultant great thickness.

Geochemical analyses of the Göttemar Pluton (Åhall, 2001; Alm et al., 2005) reveal geochemical heterogeneities within the overall homogenous pluton, in terms of trace element distribution and SiO₂ content that result in a subdivision into fractionated rest magma (commonly aplites) and two Göttemar Granite varieties. Regarding other contemporaneous plutons in the area, according to Åhall (2001), the Uthammar intrusion has the most primitive magma composition, compared to the three intrusions in the Oskarshamn area, with characteristic high amounts of mafic minerals and a high Fe, Mg, Ti content. Therefore, the coeval intrusions possibly developed from the same magma (Åhall, 2001).

3.3 Geological setting

The study area is located on the Baltic Shield, which is part of the East European Craton. The country rock is formed by metaplutonic rocks of the Trans-scandinavian Igneous Belt batholith (TIB; Fig. 3.1; Andersson et al., 2007; Söderlund et al., 2008), a crustal segment formed in a back-arc environment (Beunk and Page, 2001) in response to a Paleoproterozoic northward directed subduction beneath the WNW-ESE trending Oskarshamn-Jönköping Belt (OJB). The latter is a 1.84-1.83 Ga old island arc complex pre-dating the TIB-rocks, located approximately 100 km to the south (Mansfeld et al., 2005). The TIB is an up to 1600 km long and 130 km wide batholithic complex, which was accreted during a phase of magmatic activity in the western part of the Svecofennian Domain (Gorbatshev and Bogdanova, 1993; Högdahl et al., 2004). It is formed by reworked juvenile Svecofennian crust, supplemented by mantle additions.

Syn- to postkinematic intrusion of various generations of granitoids occurred between 1.85 and 1.65 Ga (Wikman and Kornfält, 1995; Kornfält et al., 1997; Åhall and Larson, 2000; Högdahl et al., 2004; Wahlgren et al., 2006), which represent the southernmost part of the now-exposed TIB. The rocks are affected by the N-S directed Svecofennian Orogeny (Wahlgren et al., 2006). Isotopic data (U/Pb blocking temperature) indicate that the TIB intrusive rocks cooled below 700-500°C in less than 10 Ma after their emplacement (SKB, 2008).

Far-field effects of continental crustal growth and reworking continued during the Gothian (1.61-1.56 Ga) and Danopolian Orogeny (high-grade metamorphism; 1.46 - 1.42 Ga), accompanied by ongoing igneous activity and sedimentation (Bogdanova et al., 2001; SKB report, 2002). The emplacement of 1.47-1.44 Ga intrusions in the Fennoscandian Shield commenced simultaneously with the onset of the Danopolian Orogeny (Bogdanova et al., 2001) and thus point to an orogenic connection (Cecys and Benn, 2007; Möller et al., 2007; Bogdanova et al., 2008; Brander and Söderlund, 2008). Late Sveconorwegian (1.1-0.9 Ga) and Early Cambrian extension in the working area is indicated by dolerite and sandstone dykes (Friese et al., submitted; cf. Chapter 4). The Proterozoic basement was deeply eroded by extensive lithospheric uplift during the Late Proterozoic and probably Early-Paleozoic, and covered by Lower Paleozoic platform sediments of several hundred meters thickness. During the Caledonian Orogeny (510-400 Ma), foreland basins formed and sediments of 2.5–4 km thickness accumulated during the Late Paleozoic (Tullborg et al., 1995; Middleton et al., 1996; Larson et al., 1999; Söderlund et al., 2005). This cover was eroded during the Mesozoic and, to a minor amount, during the Quaternary by glacial erosion, even below the Cambrian unconformity (Lidmar-Bergström, 1997), which is referred to as a key stratigraphic marker horizon.

As the host rock has not been heated to temperatures higher than 350°C since 1.4 Ga (Drake et al., 2009), it can be supposed that only brittle deformation has affected the area. In general, a close relationship between the emplacement of the TIB-granites and the shear zones in that area has been observed (Lundberg and Sjöström, 2006). The transition from ductile to brittle deformation presumably took place during 1.75-1.70 Ga, i.e. during uplift and stabilisation of the crust after the Svecokarelian Orogeny (Carlsson and Christiansson, 2007; Drake et al., 2009). Mylonites older than 1.75 Ga formed at temperatures of around 450-500°C (Lundberg and Sjöström, 2006; Drake et al., 2009), and hence predate the intrusions of Götömar and the neighbored Uthammar intrusions (Drake and Tullborg, 2006, Drake et al., 2009), but were reactivated as these plutons were emplaced. These N-S, NE-SW and E-W striking mylonites are thought to be related to the late stages of the 1.75 Ga old Svecokarelian Orogeny (e.g. Wahlgren et al., 2006; Stephens and Wahlgren, 2008; Söderlund et al., 2008), under a compressive stress regime with ductile shortening in N-S to NNW-SSE direction. The estimated widths of the faults of regional importance range from 5 m to 50 m, their lengths are estimated to be up to 25 km (SKB report, 2002). One of the largest faults, striking N-S, postdates the emplacement of the Götömar intrusion, cuts the pluton, and offers insight into two different emplacement levels. The western block was uplifted and represents the deeper

part of the pluton, whereas the eastern part is regarded as the roof block (Kresten and Chyssler, 1976). The around 25 km long, N-S trending shear zone, and additional minor ones, cutting the western part of the Götömar pluton (Kresten and Chyssler, 1976; SKB report, 2002 and references therein), are not well exposed in the field, and have been primarily inferred from geophysical measurements (magnetic data, VLF, NEMR data by Krumbholz, 2009) and the topology.

3.4 Field relationships and internal structure of the Götömar Pluton

Since our main aim was an evaluation of the mechanisms controlling the emplacement of the Götömar Pluton, fieldwork focused on a study of the emplacement-related structures in the intrusion. This includes data of joints, minor intrusions, and magmatic dykes, mineral veins and hydrothermal alteration associated with the Götömar body (cf. Fahlbusch, 2008; Weidemann, 2008).

3.4.1 The host rock

The main lithological unit of the host rocks is a heterogeneous rock suite of coarse-grained quartzsyenite-granite, to granodiorite (often summarised and named “Småland granites” by e.g., Kornfält et al., 1997; Fig. 3.1B), as well as an equigranular variety of the monzodiorite, which are refined classified by Nolte et al. (2008) and Nolte et al. (in preparation), based on their geochemical and petrographic characteristics as “monzo-

granite”, and “quartzdiorite-tonalite”. The TIB-granites have an age of around 1.8 Ga (Wahlgren et al., 2004), and show intensive magma mingling and mixing features (Söderlund et al., 2008). In addition, N-S striking dolerite dykes (Wahlgren et al., 2006) that are possibly related to the 978-946 Ma Blekinge Dolerites (Söderlund et al., 2005) occur in the Götömar area. Both rock suites show a distinct metaluminous affinity and I-type signature that is typical for island-arc magmas (Nolte et al., in preparation). The area immediately north to the Götömar Pluton is marked by abundant dioritic-tonalitic enclaves (that belong to the “quartzdiorite-tonalite”) and NNW-SSE elongated rhyolite bodies (Küstner, 1997; Nolte et al., 2008). The area southeast of the pluton is characterised by abundant mafic enclaves and NE-SW oriented, fine-grained granitic dykes in close relation to a complex fault zone system (SKB report, 2002; Lundberg and Sjöström, 2006; Wahlgren et al., 2006).

3.4.2 Contact features and internal structure of the Götömar Pluton

The 1.45 Ga old Götömar Pluton (Åhall, 2001) is circular in map view with a diameter of 5 km (Fig. 3.1). The emplacement depth has been calculated, based on extrapolation of $^{40}\text{Ar}/^{39}\text{Ar}$ cooling ages of biotite (Page et al., 2007), to a depth between 4.5–8 km (Cruden, 2008; Cruden and Wahlgren, 2008), which corresponds to a depth above the inferred brittle-ductile transition. The Götömar Pluton is composed

of equigranular, coarse-grained, homogeneous alkali feldspar mesoperthitic granite (Drake et al., 2007) and subordinate fine-grained varieties that preferentially occur in marginal areas (primarily in the NE and NNW), as well as in the central part of the pluton as isolated caps (Fig. 3.1C). The granite is only weakly deformed in a brittle manner (Drake and Tullborg, 2006). The contact between pluton and host rock is sharp and discordant. The intrusion exerted a thermal impact on the surrounding TIB-rocks (Söderlund et al., 2008). Although no indications for a contact aureole were observed in the field, Söderlund et al. (2008) presented geochemical and geochronological data (on biotite and hornblende) on the cooling history of the Proterozoic bedrocks that prove that the Götömar Pluton cooled below 300°C at 1.40 Ga, whereas outside the pluton, the biotite samples show cooling ages of 1.43 Ga (Söderlund et al., 2008), which reflects a rapid cooling of a thermal aureole. Veined, inhomogeneous migmatitic fabrics occur in the host rock at the contact to the Götömar Pluton in the NW and SW sector (Fig. 3.3C). Schlieric magma-mingling structures, as well as polygonal-brecciated xenoliths are found in close vicinity to the NW margin of the pluton, but are rather interpreted as independent xenolith blocks (Fig. 3.3C). Within the western, deeper exposed level of the pluton, scarce angular to rounded, fine-grained granitic enclaves with mafic seams (biotite) are observed that are interpreted as autostoped blocks (autoliths)

and occur as partly-fused blocks (Fig. 3.3D). The pluton experienced brittle faulting observed in the field as narrow shear zones, where localised shear possibly caused slip along mineral plane veins, forming NE-SW striking steeply dipping fractures featuring asymmetric horsetail terminations (Figs. 3.3A, B).

3.4.3 Jointing in and around the Götömar Pluton

The general joint pattern within the Götömar Pluton as observed in the field, is orthogonal (NE-SW and NW-SE striking; Fahlbusch, 2008; Fig. 3.4). This contradicts results of Kresten and Chyssler (1976), who revealed radial and concentric joints in the Götömar Pluton based on aerophotographic lineament analysis. Apart from these steep joint sets, flat-lying joints are very common in and outside the pluton. The “monzogranitic” host rock also displays this orthogonal joint set, but an ESE striking joint set (Fig. 3.4), for which an early formation can be assumed, because they were used as a main migration path for fluids and are occupied by Götömar-related magmatic dykes as well (dominantly flat-lying ones).

In contrast to observations by Kresten and Chyssler (1976), only the host rock seems to show a concentric joint pattern. Outside the Götömar Granite, steep NNW-SSE striking joints are common; near the N-S striking fault zone steep parallel striking joints occur (Fahlbusch, 2008). NNW-SSE trending joints in the host rock contain



Figure 3.3: Field examples of (A) brittle faults in the fine-grained granite variety of the Götemar Pluton; (B) conjugate fracture system and horsetail terminations; (C) migmatic and schlieric structures at the Götemar Pluton-host rock contact; (D) autostopped fine-grained enclave with a mafic seam in the Götemar Granite representing early injections into cold host rock; (E) angular, mafic fragments of a dyke at the Götemar Pluton-host rock contact

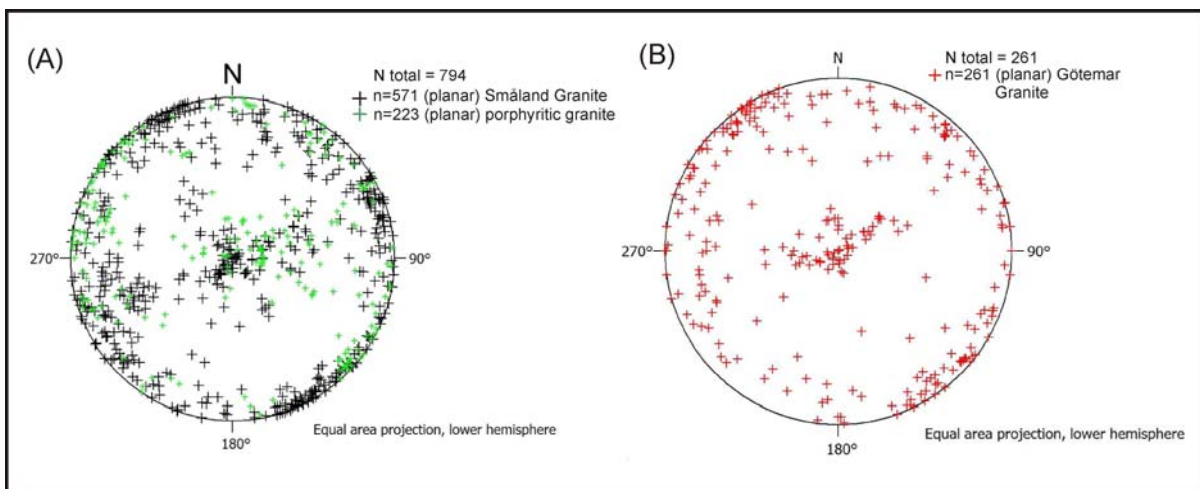


Figure 3.4: (A) Projection of poles to plains of the orientation of joints in the host rock and (B) in the Götemar Pluton.

almost no mineral veins, and are probably older than the Götömar Granite. Horizontally-sheeted joints are common in the Götömar Pluton and in the host rock (Fig. 3.4). Subsequent extension caused thin, vertical, orthogonal fractures that strike NNW and NE.

3.4.4 Mineral veins and hydrothermal alteration associated with the Götömar Pluton

Mineral veins in the Götömar Pluton are related to syn- and postmagmatic circulation of hematite, fluorite, pyrite, calcite, quartz, epidote, muscovite, and kaolinite, revealing a low-temperature genesis (Drake et al., 2009). Fluorite veins, partly associated with calcite and epidote (composite veins) are most common in the Götömar Granite, whereas the surrounding host rock is mainly crosscut by quartz-, epidote- and hematite-rich veins that are usually associated with cataclastic zones and smaller faults. Monomineralic fluorite veins, striking NE-SW, mainly occur within the Götömar Granite (Fig. 3.5). The surrounding bedrock contains rare fluorite veins. One exception is the area immediately south of the Götömar intrusion, where monomineralic fluorite veins in the host rocks are interpreted to be related to a subsurface continuation of the Götömar Granite (Fahlbusch, 2008). The highest density of fracture fillings occurs east of the N-S striking steep shear zone and dips to the ENE (Fahlbusch, 2008), indicating a greater importance of hydrothermal circulation at shallower levels. Drake et al.

(2007, 2009) studied the cross-cutting relationship of mineral veins in TIB-rocks and related fracturing and associated mineralization to at least four different orogenies and the emplacement of the Götömar body.

The widely-occurring red-staining (oxidation) in the host rock, due to hydrothermal alteration especially along fractures, the greisening, and strong sericitisation, as also observed in thin sections (see below; Kresten and Chyssler, 1976), is related to the emplacement of the Götömar pluton (Drake et al., 2007). Mineral veins associated with the greisening are quartz, muscovite, fluorite, pyrite, calcite ± topaz and Fe-Mg chlorite. The greisening is only described north of the Mederhult shear zone (Fig. 3.1), so probably this shear zone acted as a barrier for hydrothermal fluids from the Götömar Granite (Drake et al., 2009) or is a direct result of the juxtaposition of different exposure levels by faulting along the N-S striking shear zone.

3.4.5 Minor intrusion associated with the Götömar Pluton

The most abundant dykes (up to 1 m thick) in the Götömar Pluton are flat-lying tabular pegmatites, exploiting pre-existing joints (Weidemann, 2008). The sharply bordered pegmatites often show internal zonation, multiple intrusions and mainly contain quartz, feldspar, and mica, but also pyrite, apatite, beryl, and topaz, that point to a



Figure 3.5: Mineral veins and magmatic dykes in the Götömar area. (A) Aplite with diffuse boundaries and a pegmatite margin (left side) in the Götömar Pluton. Diffuse boundaries indicate an emplacement into hot host rock. (B) Swarm of subparallel, steeply dipping aplitic dykes in a quarry in the Götömar Pluton (marked by arrows). Fine-grained margins indicate an emplacement into colder host rock. (C) Quartz vein and red staining of the host rock. Hammer for scale. (D) Fluorite vein in the Götömar Pluton (arrow).

formation from volatile-rich residual melt. Quartz and feldspar display graphic intergrowth (Weidemann, 2008), that might be an indication of high pressures at the time of crystallisation of the pegmatite (e.g. Cerny, 1971; Lentz and Fowler, 1992). The high content of volatiles is also reflected by the occurrence of hydrothermal breccias that mainly occur in the eastern, shallower part of the intrusion.

Aplites (thicknesses of 0.2 m-0.75 m), striking NNE-SSW (Weidemann, 2008) in the Götömar intrusion, mainly appear as steeply-dipping sheets in the field, primarily

in the eastern marginal part of the pluton. The aplites have undulating to diffuse boundaries (Fig. 3.5) that suggest injection into hot host rocks. An array of steeply-dipping subparallel aplitic dykes (thickness of 0.05 m-0.2 m) with sharp, fine-grained boundaries, which imply emplacement into cold rocks, is observed at the southeastern margin of the pluton (Weidemann, 2008; Fig. 3.5). Hence, several generations of aplites occur in the Götömar Pluton, but the two sets of aplites do not show preferred strikes.

Within the host rocks, the preferred trend of up to 5 m thick aplitic dykes is ENE-

WSW to NE-SW; in doric (“quartzdiorite-tonalite”) and porphyritic varieties of the “monzogranite”, the dykes strike NNW-SSE (Weidemann, 2008). Thus, the emplacement of dykes seems to be controlled by a local stress field (σ_1 oriented NNW-SSE) and pre-existing older fracture sets. Pegmatite and aplite bodies occur as xenoliths up to 5 m in diameter in the host rock. Steeply-dipping, subparallel (strike NW-SE to NE-SW, and ENE-WSW respectively) fine-grained granitic and mafic (dolerite and metabasite) dykes, with a maximum thickness of 1.5 cm occur exclusively in the host rock.

It is conspicuous that dykes are abundant only in the eastern (marginal) part of the Götömar intrusion. An explanation for this observation might be that dykes, having their origin in late differentiated magmas of the roof, were already eroded in the uplifted block of the pluton.

3.5 Mineralogy, microfabrics, and cathodoluminescence analysis of the Götömar Pluton

3.5.1 Mineralogy and microfabrics of the Götömar Granite

The coarse-grained Götömar Granite is dominated by large K-feldspar laths with perthitic exsolution structures that can even be macroscopically identified (Fig. 3.6A). The K-feldspar display cross-hatched twinning, and usually contains smaller inclusions of plagioclase and quartz (Fig. 3.6). Plagioclase-rimmed megacrysts of K-

feldspar (rapakivi-fabric) occur occasionally (Fig. 3.6A, C).

Polysynthetic, interlocked plagioclase twins, almost idiomorphic due to drifting together of crystals in the melt (synneusis; e.g. Vance, 1969; Stull, 1979) are visible (Figs. 3.6B, E). The albite-rich cores of plagioclase have been strongly altered into epidote and clinozoisite-sericite, while the marginal parts are frequently unaltered, resulting in a strong zoning (Fig. 3.6). Oscillatory zoning is observed in plagioclase grains (Fig. 3.7E). Deformation twins in plagioclase indicating weak deformation in the solid state, occur locally in the coarse-grained granite, but are abundant in the fine-grained granitic caps (Küstner, 1997; Figs. 3.6D, 3.7B). Further evidence for deformation is given by bent biotite flakes (kink bands) and fragmented plagioclase crystals which were partly healed together (Figs. 3.7C, D).

Quartz crystals show two sets of deformation bands (chessboard patterns) indicating weak plastic deformation at high temperatures (Figs. 3.6-3.7). The margins of the grains are often resorbed and show embayments. A few domains show recrystallised quartz and subgrains especially in the fine-grained granite caps (Fig. 3.7). Furthermore, several clusters of anheadral quartz grains are characterised by grain boundary migration that resulted in the nucleation of smaller quartz grains (Figs. 3.6F, 3.7B, F).

Mafic minerals occur only as subordinate, glomerophytic, mainly resorbed

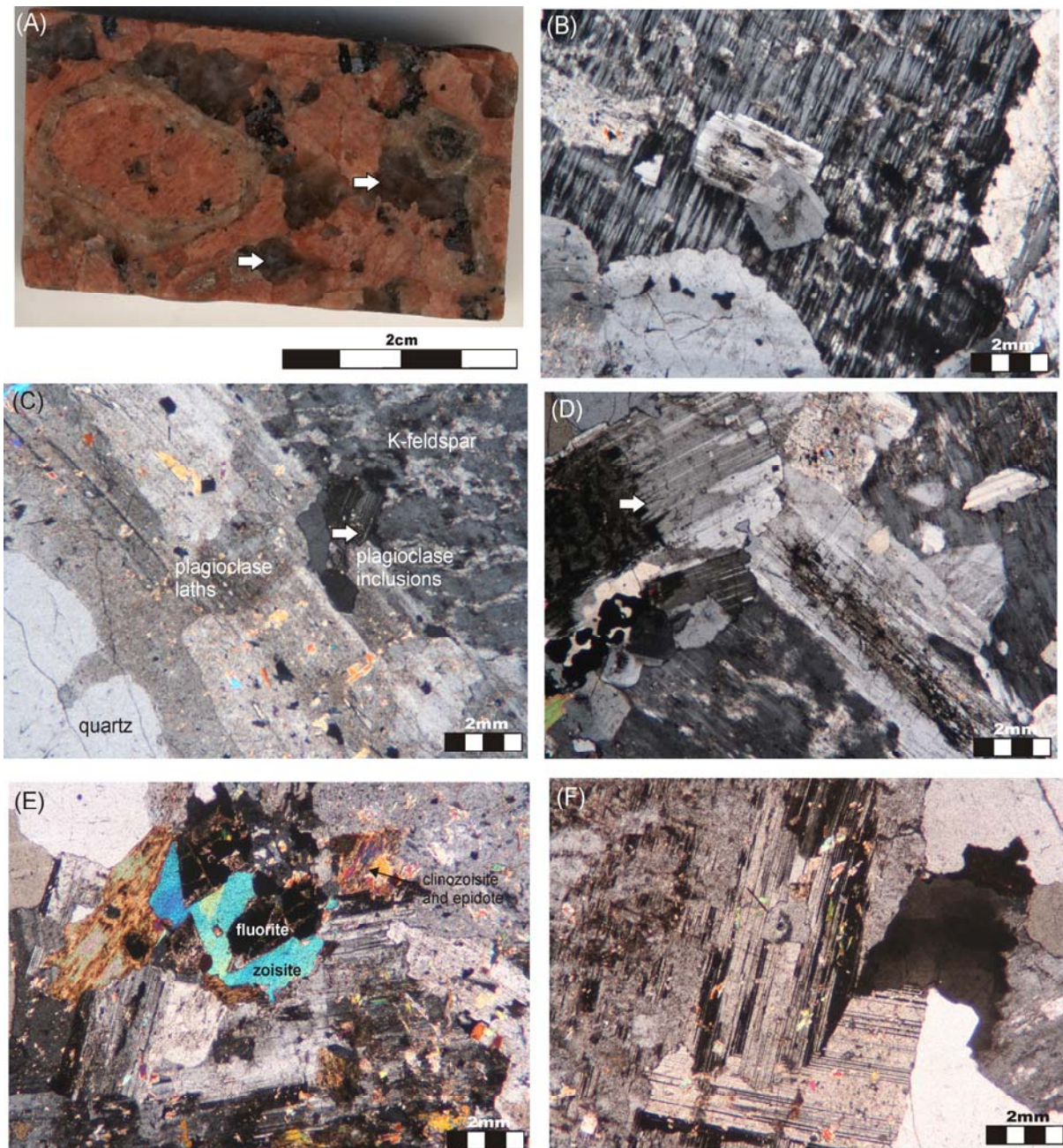


Figure 3.6: Microfabrics of the coarse-grained Götemar Granite. (A) Polished rock sample showing large K-feldspar phenocrysts with a plagioclase rim and hypidiomorphic, zoned quartz grains in the corners (arrows). (B) Intergrown plagioclase crystals embedded in perthite. (C) Plagioclase rim around K-feldspar. (D) Etched and deformed plagioclase (arrow). (E) Intensive sericitisation of plagioclase and occurrence of fluorite crystals. (F) Fine-tinned plagioclase with sericite and clinozoisite. To the right, a deformed quartz grain shows signs of deformation (undulose extinction, chessboard-subgrains). All photographs with crossed nicols.

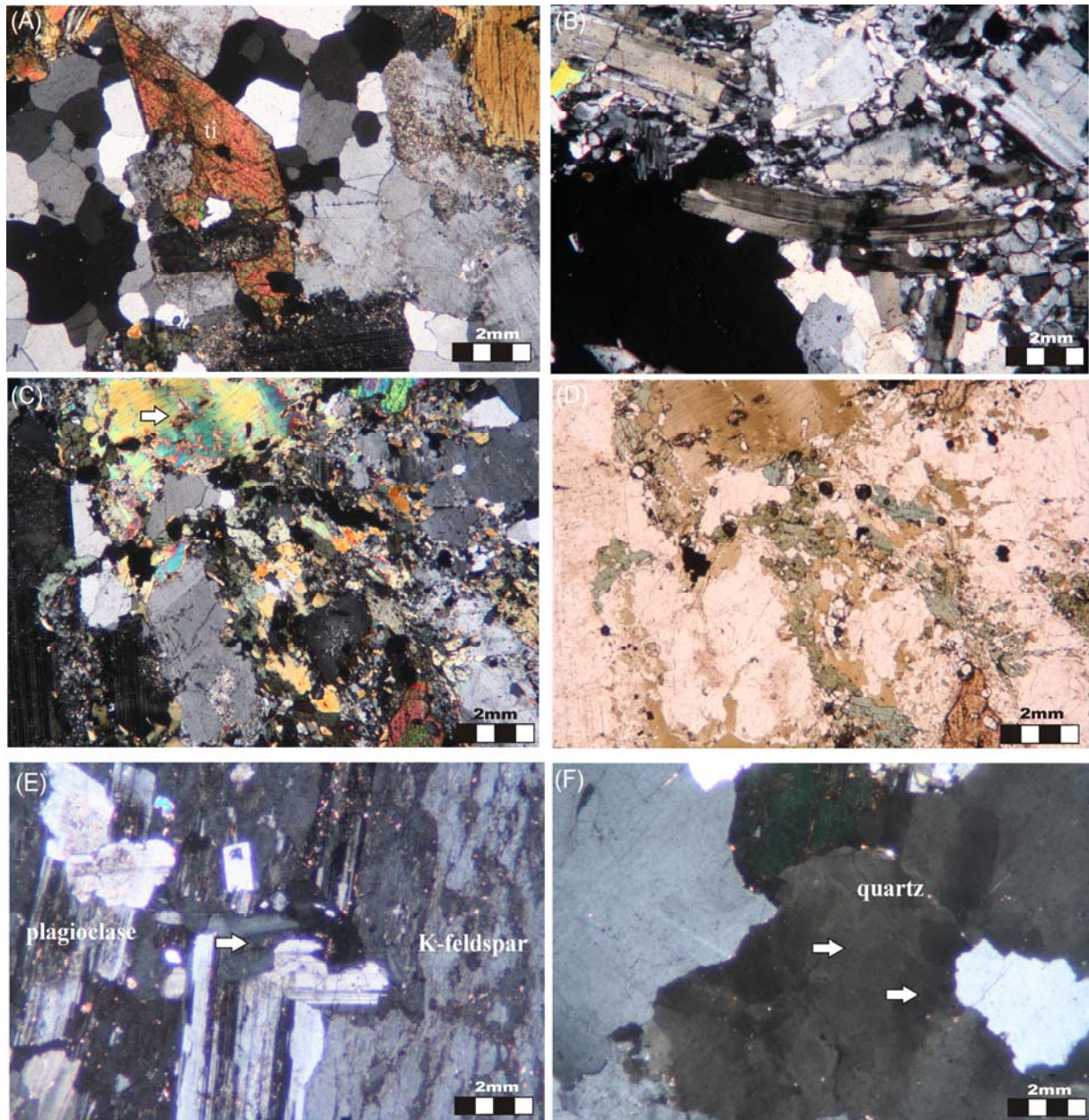


Figure 3.7: Microfabrics of the fine-grained granitic variety of the Götemar Pluton. (A) Hypidiomorphic titanite (ti) occurs as part of mafic nests. (B) Bent, kinked and healed plagioclase in aphanic matrix of recrystallised quartz and plagioclase. (C) Bent and kinked biotite (arrow). (D) Same view as in (C) with parallel polars. (E) Oscillatory zoning in plagioclase (arrow). (F) Two sets of deformation bands in quartz (chess board pattern, arrow).

and chloritised biotite crystals (Figs. 3.6, 3.7) which are rich in (radioactive) solid inclusions (e.g. apatite, zircon). Accessory minerals like apatite, zircon, fluorite, and topaz are common (Figs. 3.6, 3.7). The Götemar Granite is pervaded by hematite and

fluorite microveins and cracks sealed by an unknown black material. A strong hydrothermal overprint (sericitisation, retrograde saussuritisation, e.g. formation of epidote and calcite), and a fluorite pneumatolyse (greisening) is observed.

3.5.2 Cathodoluminescence analysis

In the field of microfabric analysis, the cathodoluminescence microscopy (CLM) is a sensitive method to detect growth zoning, alteration patterns, and cementation/mineral zonation structures that cannot be observed with conventional polarisation microscopy (Müller et al., 2003). Compositional zoning in quartz, visible by cathodoluminescence (CL) colours, can provide information about crystallisation history which may be related to emplacement condition dynamics (e.g. Müller, 2000; Müller et al., 2002, 2005; Wiebe et al., 2007). The CL-intensities and spectra are controlled by activators and sensitiser elements such as Ti, Al, Fe, Mn, and related intrinsic defects (e.g. oxygen and silicon vacancies; e.g. Sprunt, 1981; Pagel et al., 2000; Götze et al., 2001), that substitute for Si. Monovalent ions (such as H, Li, Na, and K) act as compensators for the electric charge at interstitial positions (e.g. Bambauer, 1961; Weil, 1984).

The thin sections of the Göttemar samples were coated with a carbon layer and analysed using a hot-cathode luminescence microscope HC2-LM (Neuser et al., 1995) at an acceleration energy of 14 keV and a filament current of 0.18 mA.

This study focuses on the discrimination of quartz and plagioclase generations in the Göttemar Pluton, growth structures, internal deformation, and crystallisation history of individual crystals to determine the evolution of the Göttemar

Pluton emplacement as well as its syn- to postmagmatic deformation history.

3.5.2.1 CL colours and deformation pattern in quartz grains

The quartz grains in the analysed Göttemar samples are organised in clusters and show several quartz generations that are summarised in the following Figure 3.8.

Generation (1) occurs as matrix and phenocrysts. These quartz crystals possess a wide, dark purple to blue marginal zone followed by alternating lighter bands towards the idiomorphic zone of the grain centre (Figs. 3.9A, F). Grain boundaries between individual quartz crystals are straight and accentuated by slight variations in the CL colour (dark blue to light blue; Fig. 3.9) due to different crystallographic orientations between grains and subgrains. (2) Small idiomorphic, rounded quartz grains that make up the matrix. Idiomorphic, rounded dark blue crystals, with internal deformation bands are abundant in the fine-grained granite in interspaces (Figs. 3.8, 3.9G). (3) Secondary, xenomorphic quartz fillings are found along grain boundaries, microveins, and cataclastic bands tracing healed ruptures, and make up recrystallised domains (Fig. 3.9A-E, G). (4) Xenomorphic to fine-grained quartz result from multiple alteration events, and occur as patchy fields in deformed areas, straight lines tracing fluid migration ways and in close vicinity to deformed and broken quartz grains, and as an orthogonal set primarily at


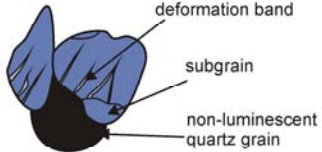
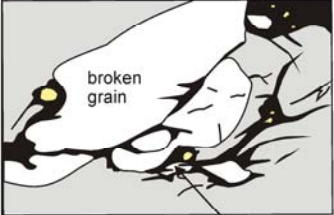
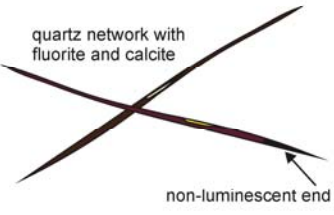
<p>Generation ①</p>	<p>euhedral to polycrystalline, dark blue CL colour, internal straight subgrain boundaries, schlieric occurrence of distinct zonation, several growth bands smudged growth zones</p>	 <p>older quartz grain in centre</p>
<p>Generation ②</p>	<p>idiomorphic, rounded, dark blue CL to non-luminescent, marginal embayments and resorption surfaces, internal deformation bands and subgrain formation</p>	 <p>deformation band subgrain non-luminescent quartz grain</p>
<p>Generation ③</p>	<p>xenomorphic, dark red-brown to black CL colour, no growth zoning, neo-crystallized, radioactive microinclusions with halos</p>	 <p>broken grain secondary quartz with radioactive inclusions</p>
<p>Generation ④</p>	<p>xenomorphic, purple-reddish to greenish CL colour, multiple alteration episodes, associated with calcite and fluorite, non-luminescent ends of network</p>	 <p>quartz network with fluorite and calcite non-luminescent end</p>

Figure 3.8: Summary of the different quartz generations identified in the granites of the Göttemar Pluton as observed in CLM.

the end of veins that cross-cut earlier formed hydrothermal secondary quartz grains. This generation occurs in all earlier described quartz generations (Fig. 3.9).

Brittle deformation structures are observed mainly in the oscillatory zoned quartz grains of generation (1), including convexly banded, broken and later healed cracks that are partly interlocked, cutting each other (Fig. 3.9A-D). Patches of recrystallised grains encompass relic quartz grains (Figs. 3.9A, C-E, and 3.11G). Patchy structures in quartz that occur independently from grain boundaries might indicate deformation

pattern, and are associated with domains of abundant inclusions of accessory minerals (yellow apatite, monazite producing radiation halos and light blue to greenish fluorite) possibly tracing hydrothermal fluid pathways (van den Kerkhof, pers. comm.; Fig. 3.9B-F).

3.5.2.2 CL colours of K-feldspar and plagioclase

Apart from quartz, plagioclase and K-feldspar were studied using CL microscopy (Figs. 3.10, 3.11). In the K-feldspar, perthite exsolution spindles with apatite inclusions occur as scattered fibres in patchy domains

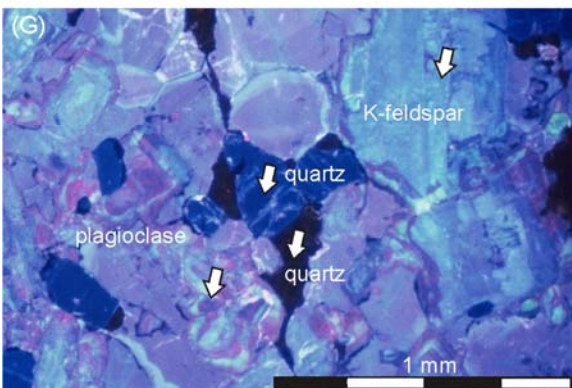
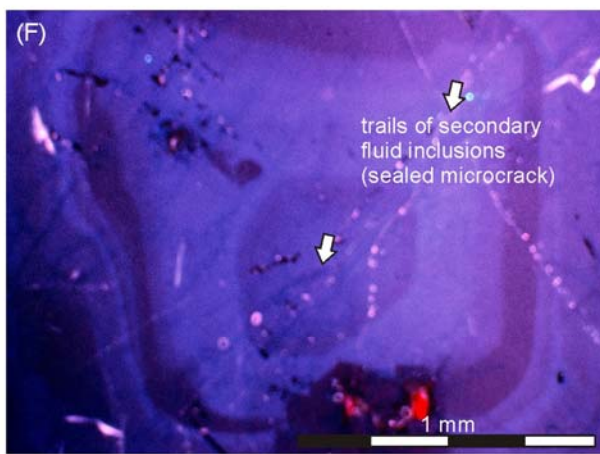
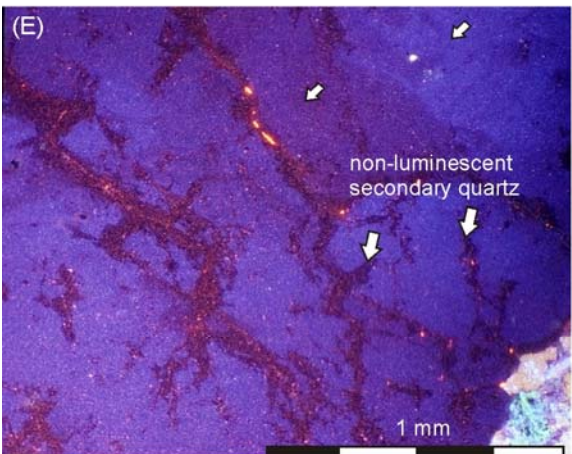
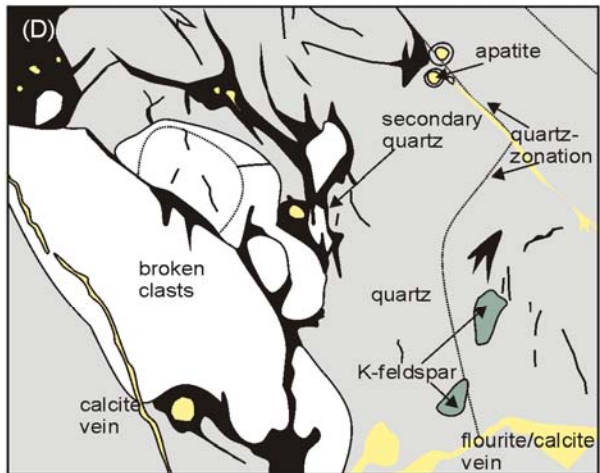
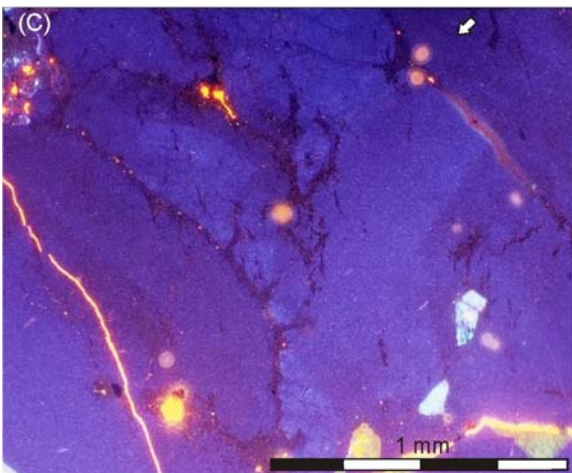
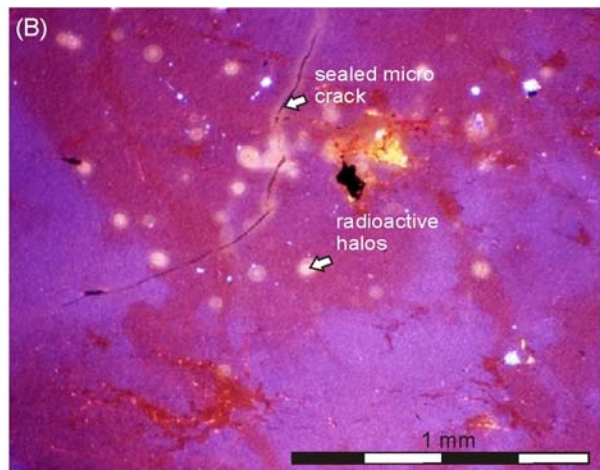
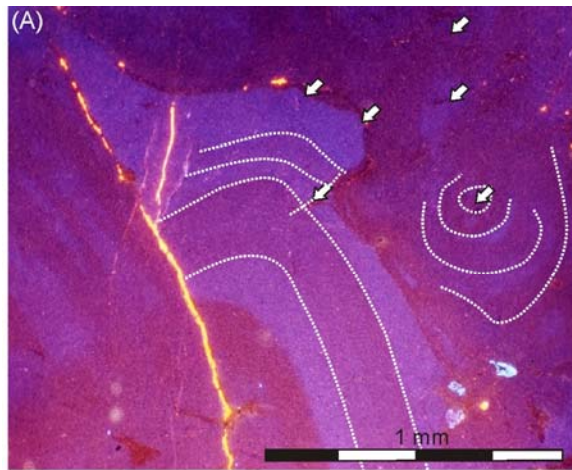


Figure 3.9 overpage: CL images of quartz crystals in the Götömar Granite. (A) Smudged zoning in quartz, boundaries are straight (arrow) and round (dotted lines). An early formed fragment of zoned quartz is overgrown and used as crystallisation nucleus (arrows). Patchy areas are left-over areas of older quartz that has been deformed (arrow). (B) Different quartz generations. Radioactive halos in younger quartz generation with light purple CL colours overgrows older dark purple, patchy quartz mark older and younger generations. (C) Dark blue CL colours with internal zoning (see schema in d, dotted lines). Grains show micro fractures that are sealed with secondary quartz (purple CL) and magma fluids (bright veins). Apatite, calcite and fluorite veins are visible by bright yellow colours. (D) Schematic picture of phenomena shown in (C). (E) Networks of microveins with secondary quartz (arrows). (F) Cyclic zonation of quartz with idiomorphic grain in the centre (Drachenfels pers. comm. 2009, printed with permission). (G) Several quartz generations of the fine-grained granite. Rounded, dark blue quartz grains (with linear deformation bands, embayments, and dissolution features on the margin) next to non-luminescent, xenomorphic, recrystallised quartz. Plagioclase crystals have bluish (anorthite-rich) and pinkish (albite-rich; Slaby et al., 2002) colours with simple zoning. The grains are rounded, deformed and are baked together, while very small grains seem to be recrystallised. The K-feldspar crystal is broken and healed, and appears to be also rounded without zoning (Drachenfels pers. comm. 2009, printed with permission).

with sharp boundaries of varying light blue to light purple CL colours (Fig. 3.11). Large K-feldspar phenocrysts are mantled by plagioclase (Figs. 3.6, 3.11), and contain subhedral inclusions of plagioclase crystals. It is a common observation that idiomorphic plagioclase show irregular zonation and blue CL colours in direct contact with large K-feldspar crystals. The large K-feldspar megacrysts show patchwork fields of different blue-light purple CL colours that are concordant with the occurrence of perthitic albite rich zones.

Plagioclase crystals show, similar to quartz, a complex growth and crystallisation history, summarised in Figure 3.10. Several generations of plagioclase can be identified: (1) Plagioclase as inclusions in the K-feldspar are the most complex generation. An observed rounded grain core of a “filled plagioclase” has a dark brown to bright CL

colour, which points to intensive alteration of the anorthite-rich part into albite, calcite (intensive bright orange CL colour), sericite, and kaolinite (Fig. 3.10). (2) Plagioclase that build up the rim around the K-feldspar shows an combined fine to broad oscillatory zoning with blue CL in the albite-rich margin, while the inner part is greenish due to a higher content of Mn and Ca (e.g. Drachenfels, 2004; Slaby and Götze, 2004; Fig. 3.11), similar to CL colours of feldspar crystals in basaltic magmas. (3) Glomerophytic plagioclase occurs together with the rounded, deformed dark blue quartz of generation (2). The interior shows re-crystallisation and a fibrous core. The mainly greenish-blue to purple CL colours of these plagioclases trade the twin lamella, whereas the greenish-blue colour indicates anorthite and the pinkish CL colour the occurrence of albite (Slaby et al., 2002).

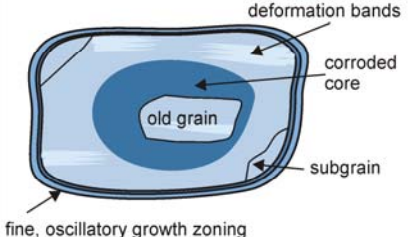
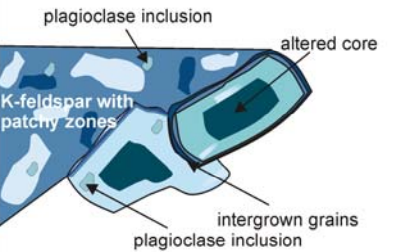
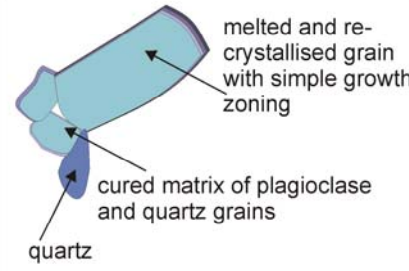
Generation ①	plagioclase inclusion in K-feldspar most complex, rounded grains, altered cores, multiple growth zoning episodes, fine oscillatory bands, patchy zones, subgrain formation	
Generation ②	plagioclase rim around K-feldspar intergrown grains, dissolution of outer grains, reaction rims, patchy zones, irregular contacts	
Generation ③	xenomorphic quartz, radioactive micro- inclusions with halos, dark brown to black CL colour, simple growth zoning	

Figure 3.10: Summary of identified plagioclase generations in the granites of the Götömar Pluton as observed with CLM.

3.6 Interpretation and discussion—a model for the multistage emplacement of the Götömar Pluton

We summarise the following observations, and literature data that are relevant to the discussion of the emplacement of the Götömar Pluton.

(1) Gravity measurements reveal vertical upper contacts of the pluton, and a mid-level body with outward dipping upper and horizontal lower contacts. An inferred centrally-located feeder extends to depths of around 4 km. (2) Drill-core data identified fine-grained aplitic granite that occurs repeatedly as tabular sheets (with a thickness of 0.2 m-23 m) between coarse-grained granite (single increments up to 100 m thick).

(3) Layers of these aplitic granites occur as scattered bodies with gradational and sharp boundaries on subaerial outcrops. (4) The recognised orthogonal and horizontal joint systems support a sheet-like layering of the granite. (5) Intensive metasomatism, localisation and ponding of late-magmatic volatile-rich fluids (now observed as mineral veins), greisen-type alteration, and the lack of deformation of the host rock, point to an exposed near-roof structure of the Götömar Granite. (6) Data from microstructures and CLM indicate a complex emplacement history. Several quartz and plagioclase generations, deformation of grains in a moving magma, heterogeneities in the crystallisation of plagioclase imply multiple

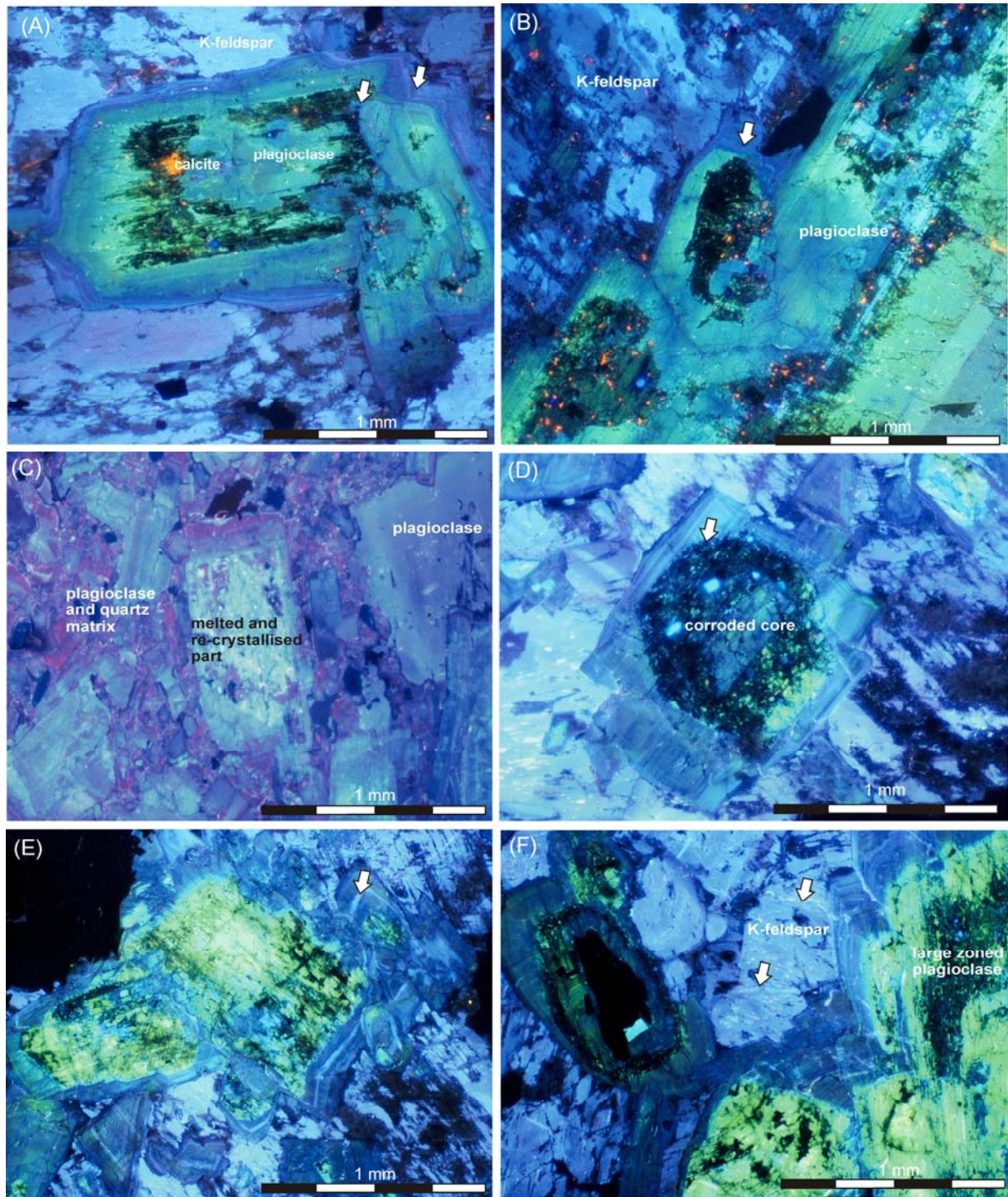


Figure 3.11: CL images of plagioclase crystals in the Göttemar Granite. (A) Intergrown plagioclase (arrows) with alternating blue CL colours at the margin and an intensively altered core (bright colours are secondary calcite) in a perthitic K-feldspar. Both plagioclase grains grew together during a postmagmatic stage (arrow). The patchy colouring is due to perthitic exsolution and marks slight deformation of the grains. (B) Intergrown plagioclase crystals form the margin of the mantled K-feldspar (arrow). (C) Internal zoning of plagioclase. Different CL colours point to chemical variations during crystallisation (Drachenfels, pers. comm., printed with permission). (D) Corroded (arrow) and altered plagioclase crystals with lath-shaped grain mantle (Drachenfels, pers. comm. 2009, printed with permission). The corroded plagioclase probably originates from magma mixing in a chamber, while the mantle of the plagioclase crystallised after

(continuation Figure 3.11) pressing out of the mush and during magma transport into the Göttemar intrusion. (E) Complexly intergrown plagioclase crystals by synneusis. Multiple-stage oscillatory growth can be recognised (arrow), but the process was disturbed several times. A fine zonation (arrow) arises from self-organised growth without intervention of externally-imposed periodicities in the state of the melt, when crystal growth is controlled by cyclic competition of crystal growth rate and diffusion rate of elements (e.g. Sibley et al., 1976; Drachenfels, pers. comm. 2009, printed with permission). (F) Small K-feldspar crystals drifted next to larger plagioclase crystals by synneusis (arrows), an indication for turbulences in the melt (Drachenfels, pers. comm. 2009, printed with permission).

heating episodes and changes in the crystallisation conditions, and decompression through rapid ascent. (7) The occurrence of megacrysts with rapakivi-fabric indicates a special crystallisation history. (8) Internal heterogeneities in the Göttemar Granite detected by geochemical analyses imply a minor fractionation of the magma.

All our observations support a model involving episodic injections of mainly silicic magma of rather homogeneous composition. Magma was transported through a feeder dyke from a magma chamber source. The initial formation of a sill was followed by inflation of multiple pulses of magma intrusions from at least two different sources from a deeper magma chamber to explain the internal layering (Fig. 3.12).

Ascent of magma and initial sill formation

As shown by gravity profiles (Cruden, 2008) the initial ascent of magma occurred through a dyke system. Cruden (1998) calculated that ascent rates for granitic magmas may vary from $3 \cdot 10^{-3}$ to 1 m/s for dykes of 3 m–13 m width, with a typical ascent rate of 0.1 m/s. The initial magma ponding and formation of a sill probably

exploited horizontal structural anisotropies within the heterogeneous TIB-batholith (Fig. 3.12), which acted as trap for the upward-propagating silicic magma in dykes, as underlined by the occurrence of horizontal joints, the shape of the plutons in the gravity model, and as proposed by models for other plutons (e.g. Sylvester et al., 1978; Petford et al., 1993; de Saint-Blanquat et al., 2001). The orthogonal joint system may trace the infilling and inflation axis of a pluton (de Saint-Blanquat et al., 2001).

Sill inflation, laccolith formation and development of internal layering

The formation of the laccolithic complex is consistent with a proposed two-stage model (e.g., Johnson and Pollard, 1973; McCaffrey and Petford, 1997; de Saint-Blanquat et al., 2001) that involves horizontal intrusion of the magma as a sill followed by a thickening of the intrusion by upward inflation.

The formation of the internal layering of the Göttemar Pluton involved magma feeding processes from at least two different locations in a magma chamber, independent from each other, to explain the alternate

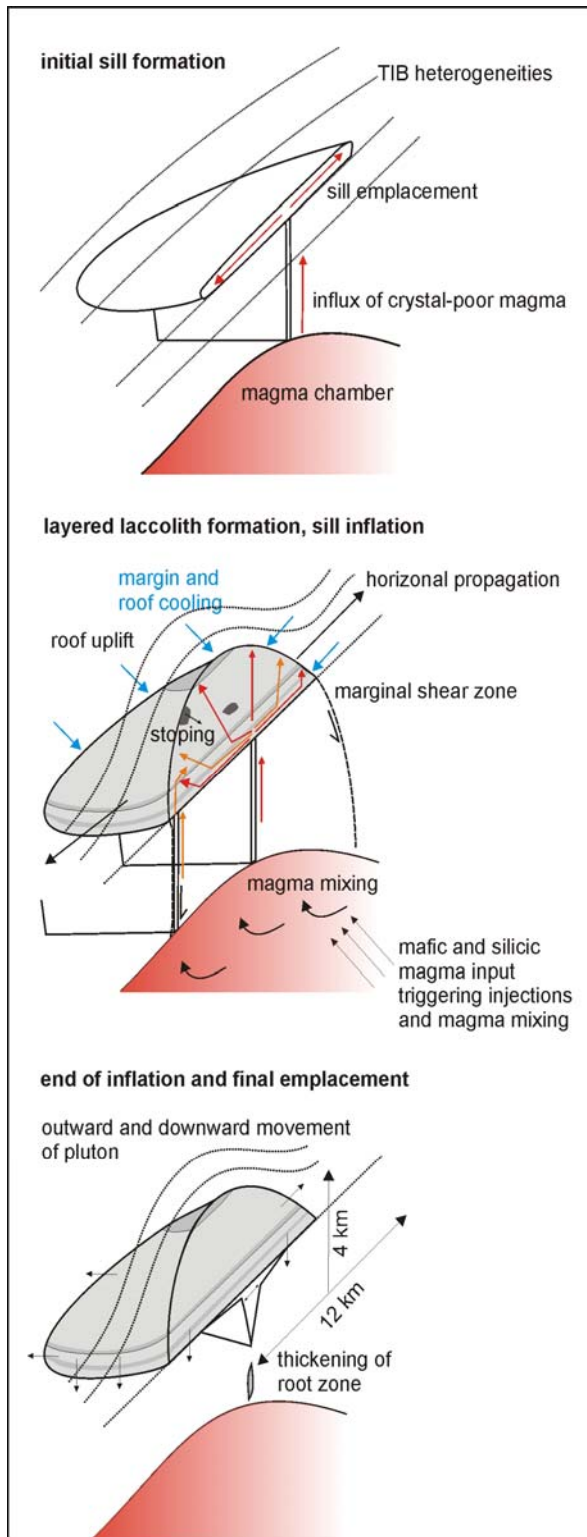


Figure 3.12. Schematic illustration of the multi-stage emplacement of the Götömar Pluton. See text for further explanation.

layering between fine- and coarse-grained granite (Fig. 3.12). A deeper-lying magma chamber filled the feeder dyke connected to

an initially slowly inflating sill with silicic magma. The magma chamber was an open system, replenished by silicic magmas and periodically invaded by mafic magmas, as seen by clustered synmagmatic mafic enclaves (forming a dyke) in the field (Fig. 3.3E). Replenishments buffered the composition of the fractionating magma chamber. Magma mixing processes are mainly triggered by the input of mafic magma (e.g. Wiebe et al., 1997; Miller and Miller, 2002), which transports heat into the system; however, acid-acid magma mixing may have also occurred in the chamber (e.g. Grogan and Reavy, 2002).

In the case that the mafic input was low, the recognition of textures, mainly on quartz and plagioclase, are a useful indication for magma mixing (e.g. Hibbard, 1981; Slaby and Götze, 2004; Slaby et al., 2007) as it has been done by CLM-studies (Figs. 3.8-3.11). Recent studies of several silicic volcanic systems have shown a variety of evidence that the crystal content of magma chambers may wax and wane, possibly depending on the rate of new magma input (Mahood, 1990). This process explains the observed CL-features in plagioclase and K-feldspar, namely the corroded cores and changes in the chemical zonation (from normal broad zonation to narrow, oscillating bands) that suggest chemical disequilibrium in the melt (Drachenfels, 2004; Fig. 3.11). Also the occurrence of a rapakivi-fabric (Figs. 3.6A, C, 3.11B) can be explained by magma mixing and/or decompression due to rapid magma

ascent (e.g. Hibbard, 1981, 1991; Wark and Stimac, 1992; Salonsaari and Haapala, 1994; Dobnikar et al., 2002; Slaby and Götze, 2004; Gagnevin et al., 2005; Müller et al., 2008). Replenishments frequently caused the resident magma to leave the stability field of alkali feldspar (Collins et al., 2006) and cause sporadic rapakivi-textured granite in the melt. Synneusis, as seen in the microfabrics (Fig. 3.11E), is an indication for magma pulsing and turbulence in the magma system (Vance, 1969). Another model, proposed by Dempster et al. (1994), explained the formation of a plagioclase mantle by redistribution of exsolved plagioclase from alkali feldspar phenocrysts linked to the high fluorine contents of magmas.

CL analysis furthermore indicates a rapid ascent of magma by common decompression features observed in microfabrics. Oscillatory-zoned quartz and a schlieric occurrence point to unstable external parameters (temperature, pressure and chemical composition; Vance, 1969; Ginibre et al., 2002), whereas rounded quartz grains, deformation pattern, resorption surfaces (e.g. embayments, reaction rims; Fig. 3.11) in crystals underline decompression by rapid ascent, and that recrystallisation and reheating was triggered by stacking of layered bodies within the pluton (Figs. 3.8-3.9). The occurrence of resorption surfaces is in accordance with a rapid ascent of granitic melts by dyke formation as found by e.g. Clemens and Mawer (1992), Petford et al. (1993), Petford (1996) and Johannes and

Holtz (1996), triggered by extension or shear in the upper crust (Müller, 2000). Calculations by Thomas (1992) and observations by Müller (2000) show that zoned quartz in granites with dominantly (dark) blue CL colours represent a water poor (< 2.5 wt % H₂O) “rhyolitic” crystallisation environment in the crust.

Crystallisation of the initial crystal-poor magma at eutectic composition in the initial sill system formed the coarse-grained Götömar Granite. Higher melt H₂O contents, and an extended temperature range over which crystallisation can proceed, favour both crystallisation of coarser-grained granites. In addition, the potential for the development of late, H₂O-rich melt fractions are significantly enhanced. Upon reaching vapour saturation, these late melt fractions are likely to form aplite and pegmatite dykes (Hogan et al., 2000), which intruded the Götömar Pluton and TIB-granites during late- and postmagmatic stages. Most coarse-grained increments show no sign of chilled margins that might indicate rapid magma pluses without time for solidification. These mechanisms also contributed to heterogeneities in the crystallisation history as observed in plagioclase and quartz.

Fine-grained granite, in contrast, was injected episodically from the magma chamber via a fracture/dyke system, possibly located at the evolving margin of the pluton (Fig. 3.12). Geochemical analyses (Åhall, 2001; Alm et al., 2005) show slight variations from the bulk granite, so that a different

source location within the magma chamber is emphasised. The additional heat that is transferred into the layered sill body by repeated injection of magma, triggers remelting, fractionation, ascent and crystallisation of fine-grained granite. Similar, an absence of solid-state deformation within the injections and at most contacts between aplites and granites which are primarily smudged or are even destroyed by the emplacement of new magma pulses, indicate that the time gap between individual injection pulses was insufficient for a complete solidification of the preceding injections. The observed autoliths in the field might demonstrate how early injections of granitic magma looked like as they intruded into cold TIB-rock and later into hotter sheets where the boundaries are smudged and diffuse, reflecting different ages.

A model by Bachmann and Bergantz (2004) and Bachman et al. (2007) suggests repeated expelling of higher fractionated, crystal-poor melt from “a crystalline mush” into dykes and pods, concentrated in newly-formed fractures and gashes by brittle deformation, as the developing pluton was displaced downwards by gradual floor subsidence. Melt expulsion from crystalline mushes is slow, and it requires a chamber to have a “mush state” that is preserved for a long time (in the order of up to 10^4 - 10^5 years) to produce a sill-like cap of crystal poor magma which can be kept from rapid and thorough crystallisation due to the presence of water (and other volatiles) and heat stored

in the mush (Hildreth, 2004). This model can explain the formation of a sill-like cap, but not the repeated occurrence of the sheets in the proposed time interval. The proposed time interval of 10^4 - 10^5 years (Bachman and Bergantz, 2004; Michel et al., 2008) is rather unlikely when considering the thickness of each of the layers (maximum 100 m). The process of episodic magma injection via dykes happened much faster (Clemens and Mawer, 1992). Consequently, an injection of magma from at least two different sources to form the granite varieties is the more likely model to explain the observation of a rapid emplacement of the Götömar Pluton.

End of inflation, final emplacement stages and modification of the Götömar Pluton

Cooling from the “roof” downwards resulted in cessation of vertical inflation, promoting further lateral expansion and floor subsidence (Fig. 3.12). In addition, contraction of magma due to cooling leads to late-stage sinking of the intrusion due to a density increase (John and Blundy, 1993; Barnes et al., 2004; Ciavarella and Wyld, 2008). Solid deformation observed in the coarse-grained granite might indicate an end of the vertical inflation, and a rather horizontal expansion of the laccolith triggered by solidification of the margin and roofs or depression of the pluton floor during waning stages, which is emphasised by numerous brittle faults in the field and brittle deformation patterns in minerals. The rate of arrival of subsequent melt batches exceeds

the rate of crystallisation at the site of pluton construction, melt pressure ultimately may lead to (sub-) horizontal magma fracture, or viscous flow of wall rocks may allow lateral spreading (Brown and Solar, 1999). Cruden (2008) proposed a combination of floor subsidence and roof uplift for the Göttemar Pluton since neither mechanism alone can explain the occurrence of the root zone underneath the pluton to form a punched laccolith. However, the root zone is assumed to be related to the arrival of last magma batches during progressive locking of the pluton and induced in-situ horizontal inflation of the feeder dyke as proposed by de Saint-Blanquat et al. (2001; Fig. 3.12) for the Papoose Flat pluton (USA). Nevertheless, the proposed final emplacement mechanism was associated with minor floor subsidence, partial melting of existing internal layers and magmatic stoping, as described by e.g. Brown and Solar (1998), Cruden (1998), Hogan et al. (1998), Brown and McClelland (2000), Coulson et al. (2002), Glazner et al. (2004), Matzel et al. (2006), and Michel et al. (2008), for other layered plutons, to solve the room problem. As gravity data shows only minor subsidence of the floor, the emplacement probably required bending of layers, and eventually failure of roof-rock parts (magmatic stoping) associated with reactivation of pre-existing fractures and the formation of new brittle ones, as seen in the field from narrow localised shear zones and the occurrence of autoliths. CL observation underlines a syn- and postmagmatic

modification of the pluton. Secondary quartz developed in multiple temporal and spatial stages. The occurrence of post magmatic alteration features like fluid saturation pattern, healed micro veins, and secondary quartz mixed with alteration products like calcite. These observations strongly indicate a complex, multi-stage magmatic history during emplacement, and a syn- to post magmatic deformation of repeated cooling and heating in high-temperature events (pers. comm. A. Müller, 2009) that did not allow the grains to equilibrate.

Discordant contacts between the host rock and the Göttemar Granite provide evidence for magmatic stoping that modified the roof and margins of the pluton (Cruden, 2008; Fig. 3.12). Although emplacement by prolonged magma injections is much less likely to produce xenoliths (Glazner and Bartley, 2006; Clarke and Erdman, 2008), autostoped blocks, observed in the eastern part of the Göttemar Pluton, suggest some modification by stoping and support a multistage emplacement of the pluton. In the case of the Göttemar Pluton, magmatic stoping was mainly caused by combined mechanisms of thermal-mechanical cracking (cf. Clarke et al., 1998), followed by porous flow (cf. Brown and Solar, 1998; Olsen et al., 2004). Bartley et al. (2006) state that discordant contacts but few xenolith occurrence, as it is described for the incrementally grown Göttemar Pluton, might be explained with a crack-seal mechanism, in which new cracks form within previously-

emplaced increments. Devolatilisation of blocks caused fracturing, the input of fresh magma and local pulsing of magma and volatiles contribute to further block sinking and enhanced a breaking off of (roof) blocks (e.g. Pignotta and Paterson, 2007).

Tectonically-controlled emplacement of the anorogenic Götömar Pluton?

Cruden (2008) proposed, based on the aeromagnetic anomaly alignment of plutons along the SE coast of Sweden, a NNE-SSW trending linear, deep-seated shear zone. Even though Cruden (2008) found no evidence of syn-emplacement faulting in the Götömar Pluton, the occurrence of the coeval plutons Götömar and Uthammar can be explained by a propagating shear zone, similar to the model proposed by Hutton (1982) for the Donegal Batholith, at the end of which the pluton is syn-tectonically emplaced. This is emphasised by the idea of Čečys (2004) that the Götömar Pluton is emplaced in a tensional stress regime triggered by far-field effects of the Danopolian Orogeny, and the absence of deformational pattern in the pluton itself.

The formation of laccoliths through upward inflation of tabular intrusions is regarded as being mechanically possible only at shallow depths. Buoyancy and volatile release effects control the magma pressure, and tectonic overpressuring increases a possible emplacement depth (de Saint-Blanquat et al., 2001), explaining a possible emplacement of the Götömar Pluton at depths between 4.5-8 km (Cruden, 2008). All field

evidences indicate that the pluton was not emplaced during regional deformation. Nevertheless the absence of synplutonic regional deformation of the host rock does not preclude the possibility that emplacement was subject to a regional deviatoric stress field at that time, as suggested by the occurrence of a propagating shear zone beneath the aligned plutons. The prevailing regional stress field had an influence on crustal migration of magma feeding into the pluton (e.g. feeder conduits, tectonic overpressuring) and on the final emplacement of the pluton. An inferred fast emplacement at rates of 10-15 cm/a for an average vertical growth rate were calculated by Cruden (1998) and Petford et al. (2000) for granitic plutons, and imply a vertical growth of 3 km of the pluton in 20 ka-30 ka, which is likely timeframe when evaluating the alternating injections of fine- and coarse-grained granite in the Götömar Pluton. A consequence of rapid emplacement is that more slowly accumulating regional tectonic strains were not recorded during pluton construction. This might explain why the Götömar Pluton appears to be undeformed and thus appear anorogenic, even though it was emplaced during waning stages of the Danopolian Orogeny and under influence of a propagating shear zone. It is possible that pluton assembly and regional-scale processes took place at different time rates, as shown by e.g. de Saint-Blanquat et al. (2001) for the Papoose Flat Pluton, USA.

3.7 Conclusions

The Götömar Pluton, located on the coast of SE Sweden, is a circular intrusion in map view with a diameter of 5 km. The asymmetrical, (geo) chemically homogeneous laccolith is structurally zoned in horizontal direction, with a feeder zone that fed the pluton from below. Sequential, subhorizontal injections of fine- and coarse-grained granitic magma were confirmed by borehole data. The model proposed in this study assumes at least two independent sources for the different granites. Structural field data, CLM studies on quartz, K-feldspar, and plagioclase and the occurrence of autoliths in the field support our model of an inflating sill and growth by episodic replenishment of silicic magma. Initial magma ponding was along structural and material heterogeneities in the TIB-batholith. Final emplacement of the Götömar Pluton was due to a combination of gradual minor floor subsidence and roof uplift as emplacement mechanisms. CL-analysis indicates a complex crystallisation history of the pluton with magma mixing in the deep magma chamber, repeated heating and recrystallisation of granite, and conditions of pressure decrease and variations in the temperature during rapid ascent of magma. Brittle deformation structures, healed microcracks, and recrystallisation of quartz imply a reheating history of the pluton triggered by several magma pulses, amalgamation and stacking of sills. The emplacement of the Götömar Pluton was tectonically controlled by a NNE-SSW

propagating shear zone along the coast of SE Sweden. Even though their coeval occurrence proves a genetic connection, the Götömar, Uthammar, and Jungfrun Plutons represent individual magma series in a proposed extensional setting at that time, expressing a rather distal influence of the igneous activity associated with the Danopolian Orogeny. A rapid emplacement of the Götömar Pluton offers an explanation for the lack of deformation in the “anorogenic” Götömar Pluton. We assume that the emplacement was subject to a regional deviatoric stress field, as is suggested by the occurrence of a propagating shear zone beneath the aligned coeval plutons. The prevailing regional stress field had an influence on the migration of magma feeding the three plutons (e.g. feeder conduits, tectonic overpressuring) and on their final emplacement.

Acknowledgments

We gratefully acknowledge discussion with A. Müller (NGU) and S. Burchardt (University of Göttingen). A. van den Kerhof (University Göttingen) is thanked for help with the CL-analysis and their discussion. A.R. Cruden (University of Toronto), and C.-H. Wahlberg, (SKB, Sweden), are acknowledged for their help with literature research.

4. Episodic formation of Cambrian clastic dykes – case study Southeast Sweden: preface

Clastic dykes are discordant, tabular bodies composed of weakly to strongly lithified arenaceous material, although breccia, gravel, clay, till, and bitumen are known (Röshoff and Cosgrove, 2002). These structures have a thickness in the range of centimetres to tens of meters and lengths of a few centimetres to several kilometers (Röshoff and Cosgrove, 2002). Clastic dykes do not only intrude sediments (e.g. Phillips and Alsop, 2000; Hillier and Cosgrove, 2002; Jolly and Lonergan, 2002; Andre et al., 2004; Levi et al., 2006; Heubeck, 2009), but also lava flows in volcanic environments (e.g. Harms, 1965; Sturt and Furnes, 1976; Schlische and Ackermann, 1995; Curtis and Riley, 2003) and basement rocks (e.g. Carlson and Holmquist, 1968; Bergman, 1982; Katzung and Obst, 1997; Beacom et al., 1999). Clastic dykes are also a common feature beneath glaciers (e.g. Åmark, 1986; Le Heron and Etienne, 2005; van der Meer et al., 2009).

From a tectonic point of view, extensive sandstone intrusions are common in tectonically active environments that are characterised by high sedimentation rates, mud-dominated sedimentary systems and where applied tectonic stresses afford the development of high fluid pressures, e.g. fold and thrust belts and strike-slip basins (e.g. Winslow, 1983; Thompson et al., 1999; Jolly and Lonergan, 2002).

The mechanism of clastic dyke formation is poorly understood, and interpretation of field observations are commonly ambiguous (e.g. Aspler and Donaldson, 1985). Two end-member mechanisms have been proposed: depositional or Neptunian clastic dykes formed by passive deposition (gravity-related) of clastic material into pre-existing fissures (e.g., Eyal, 1988; Stanton and Pray, 2004); and injection of clastic dykes formed dynamically by host-rock fracturing and injection of unlithified clastic sediment slurries from below (e.g. Larsson, 1975; Röshoff and Cosgrove, 2002; Heubeck, 2009) connected to high fluid pressures.

Considering actively injected clastic dykes, four principal intrusion triggers have been identified: (1) seismic-induced liquefaction (e.g. McCalpin, 1996; Galli, 2000); (2) tectonic stress (e.g. Winslow, 1983); (3) localised excess pore pressure generated by depositional processes (e.g. Truswell, 1972; Martel and Gibling, 1993), (4) overpressured fluid influx into a shallow sand body (e.g. Jenkins, 1930; Brooke et al., 1995). Le Heron and Etienne (2005) connect the downward injection of subglacial clastic dykes to meltwater-related hydraulic fracture processes. Jolly and Lonergan (2002) suggested that clastic dykes may also form by overpressure-induced hydraulic fracturing at depths greater than several hundred meters.

The following case study of a Cambrian sedimentary dyke in the Västervik area, Southeast Sweden, gives insight into the formation of a lithologically complex clastic dyke. Sedimentary dykes in crystalline basement that were formed by downward fracture opening and filled with siliciclastic material supplied from the surface are rarely described (e.g. Beacom et al. 1999). The field related example therefore closes a gap in literature by combining macro- and microfabric analyses to determine the evolutionary history of sedimentary dykes in basement rocks. Furthermore, the clastic dykes in the area of Southeast Sweden occupy pre-existing joint sets and are thus palaeostress indicators.

This work has been submitted in revision for publication to International Journal of Earth Sciences 2009 as: Friese, N., Vollbrecht, A., Leiss, B., Jacke, O. Cambrian sedimentary dykes in the Proterozoic basement of the Västervik area (Southeast Sweden): episodic formation inferred from macro and microfabrics.

4. Cambrian sedimentary dykes in the Proterozoic basement of the Västervik area (Southeast Sweden): episodic formation inferred from macro- and microfabrics

Nadine Friese, Axel Vollbrecht, Bernd Leiss and Olaf Jacke

Geoscience Centre, University of Göttingen, Goldschmidtstrasse 1-3, D-37077 Göttingen, Germany

Abstract

Fabrics of Cambrian sedimentary dykes formed in Proterozoic granites of the Västervik area (Southeast Sweden) evidence repeated opening/filling and mineralisation/cementation events under varying conditions. Diagnostic features include (1) wall-parallel boundaries between epiclastic fillings and (2) early-formed dyke sediments that appear as lithoclasts in subsequently-formed sedimentary fillings. The psammitic components mostly consist of well-rounded quartz grains related to a coastal environment and fragments from the granitic host rock. Platy calcitic fragments embedded in the epiclastic matrix originally formed as microveins within already-lithified dyke sediments and the adjacent host rock. Convex downward-pointing, internal sagging structures, together with the preferred orientation of compositional boundaries and long axes of grains/rock fragments parallel to the dyke walls, are interpreted as the result of suction-controlled flow of unconsolidated

fillings during episodes of downward dyke growth. Pressure solution of quartz grains is an evidence of extensional phases with dyke propagation that were interrupted by phases of horizontal compression normal to the dyke walls. The N-S and NE-SW striking sedimentary dykes formed by opening of a pre-existing joint set during NW-SE oriented rifting during the Cambrian.

4.1 Introduction

Sedimentary dykes in crystalline basement rocks have been described from different areas of the Baltic shield (e.g. Bergman, 1982; Carlson and Holmquist, 1968; Katzung and Obst, 1997). They have been interpreted to be of Cambrian age, although only a few fillings could be dated by fossils, which give the maximum age of fissure formation (e.g. Tynni, 1982). The age of dyke emplacement is generally accepted to be the age of the feeder bed (Röshoff and Cosgrove, 2002). Several mechanisms of the formation of sedimentary dykes have been

attributed to the dynamic environment and the physical properties of the host rocks (Röshoff and Cosgrove, 2002). Most frequent are Neptunian dykes which form by injection of soft sediments caused by pore pressure gradients (e.g. Smart et al., 1988; Winterer et al., 1991; Phillips and Alsop, 2000; André et al., 2004; Stanton and Pray, 2004; Levi et al., 2006; Heubeck, 2009). In contrast, sedimentary dykes in crystalline basement which were formed by downward fracture opening and filled with siliciclastic material supplied from the surface are rarely described (e.g. Beacom et al., 1999).

Geological mapping on the scale of 1:10 000, has been carried out in the Paleoproterozoic of the Västervik area (Southeast Sweden) by diploma students from the Geoscience Centre of the Georg-August-University of Göttingen (Germany). They have discovered several outcrops where sedimentary dykes cut granitoids (Fig. 4.1). A compilation of further locations concentrated along the coastline, south of Västervik, is given by Alm and Sundblad (2002). With respect to the study area around Västervik, sedimentary dykes have only been described in detail so far from one locality (Carlson and Holmquist, 1968), whereas the related microfabrics have only been discussed briefly. According to their strike, the dykes of the Västervik area can be divided into two sets (N-S and NE-SW striking, Figs. 4.2, 4.3), all of which are steeply inclined. Their thicknesses range between two and ten cm, and are relatively

constant throughout the outcrop. Cross-cutting relationships between the two dyke directions have not been observed. Since there are only vertical outcrop sections, possible strike-slip components could not be observed.

Detailed information about the evolutionary history of comparable sedimentary dykes based on comprehensive fabric analysis could not be found in the literature. The present study focuses on the macro- and microfabrics, which show a complex polyphase dyke formation under varying conditions and stress configurations, and hence contributes to the inferred geodynamic situation of SE Sweden in Cambrian times. The samples for this study were collected at a road cut at the E22, approximately 2.5 km NE of the village Gunnebo (Figs. 4.1, 4.2).

4.2 Geological setting

The study area around Västervik is part of the transition zone between the Svecofennian domain to the north and the Transscandinavian Igneous Belt (TIB) to the south (Fig. 4.1). Beunk and Page (2001) propose a back-arc environment for this crustal segment, which formed in response to Paleoproterozoic, northward-directed subduction beneath the Oskarshamn-Jönköping Belt (OJB; Fig. 4.1), approximately 100 km to the south (Mansfeld et al., 2005). Remnants of this back-arc basin are represented by the so-called Västervik formation, which mainly consists of

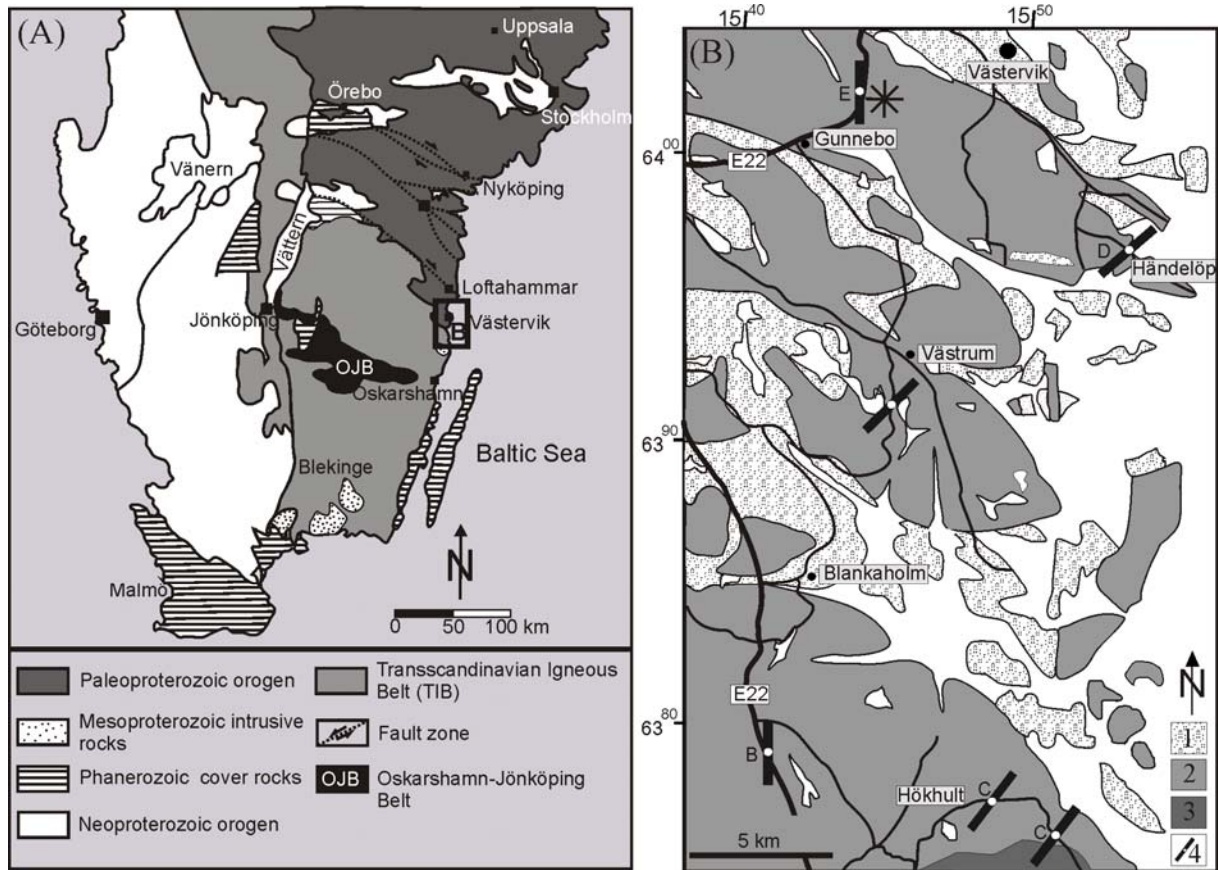


Figure 4.1: (A) Simplified geological map of South Sweden (modified after Beunk and Page, 2001). Study area in (B) is marked. (B) Simplified geological map of the Västervik area (after Lundegårdh et al., 1985; Carlson and Holmquist, 1968) with occurrences of sedimentary dykes. A: Frey (1997), B: Weiss (1994), C: Rudolph (1995), and E: Jacke (2000) occurrence each with one sedimentary dyke, D: Carlson and Holmquist (1968) describe three dykes. 1 Metasediments of the Västervik formation; 2 TIB-granites; 3 Götemar Granite; 4 Sedimentary dyke. Grid: Gauss projection.

metamorphic siliciclastics with intercalated basic flows and sills. The whole sequence was deposited between 1.88-1.85 Ga (U/Pb ages of detrital zircons) in a continental margin environment (Sultan et al., 2005; Sultan and Plink-Björklund, 2006).

Due to continued subduction, this back-arc basin closed and the Västervik formation was strongly deformed in a dextral transpressional regime associated with metamorphism under high-temperature/low-pressure conditions. Syn- to postkinematic intrusion of various generations of granitoids

occurred between 1.85 and 1.65 Ga (Åhäll and Larson, 2000; Nolte et al., 2008), which represent the southernmost part of the now-exposed TIB. This basement was deeply eroded by extensive lithospheric uplift and erosion during the late Proterozoic and probably Lower Paleozoic. At that time Baltica was affected by NW-SE extension with respect to the present geographic directions (e.g. Murnier and Talbot, 1993; Cocks and Torsvik, 2005). On the resultant peneplane, Lower Paleozoic platform sediments of several hundred metres

thickness were deposited. This cover was eroded during the Mesozoic and, to a minor amount, during the Quaternary by glacial erosion even below the Cambrian unconformity (Lidmar-Bergström, 1997). As a consequence, Cambrian sedimentary dykes, which formed within the Paleoproterozoic granitoids, were exposed.



Figure 4.2: Outcrop photograph showing the studied sedimentary dyke (white dashed line). View towards north, hammer for scale.

4.3 Macrofabrics

The steeply-inclined dykes display constant widths throughout the outcrop of two to ten cm (Fig. 4.4). Dyke filling contacts with the granitic wall rock are sharp and planar (Figs. 4.4A, C, and D). The dyke filling consists mainly of layers of sandstone with well-rounded quartz grains alternating with bands of sandy pelites (Fig. 4.4B). The

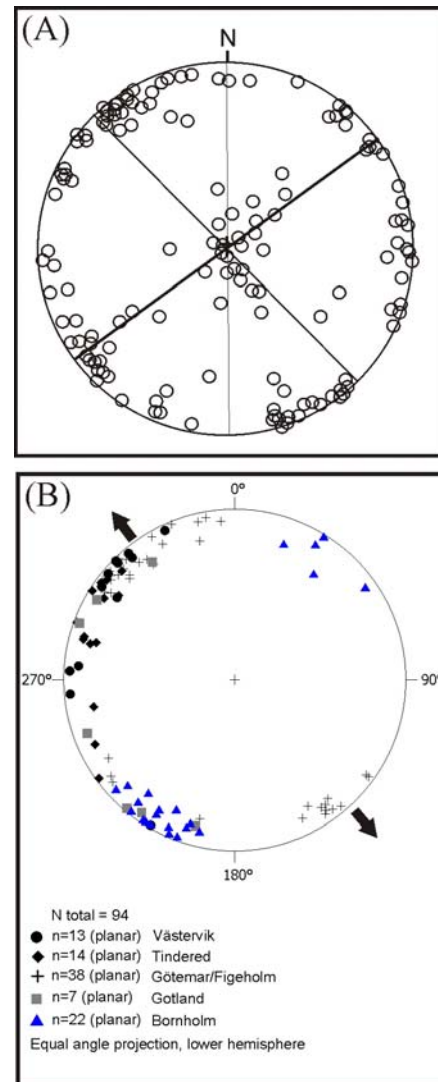


Figure 4.3: (A) Pole plot of the orientation of joints in granites and corresponding strike direction of main sets (source: 40 diploma mapping projects carried out by students of the University of Göttingen, Germany). (B) Pole plot of the orientation of 94 sedimentary dykes occurring in Scandinavia (Västervik area, Tindered area, Göttemar/ Figeholm, Gotland, and Bornholm). A prominent N-S strike is only observed for sedimentary dykes in the Västervik region, whereas NE-SW and NW-SE strike are prominent in all other areas, apart from Bornholm. There, only NW-SE strikes are documented. Data of sedimentary dykes from Carlson and Holmquist (1968), Larsson (1975), Weiss (1994), Rudolph (1995), Frey (1997), (continuation Figure 4.3) Katzung and Obst

(1997), Jacke (2000), Alm and Sundblad (2002), and Weidemann (2008). The arrows indicate the inferred NW-SE directed Cambrian extension.

boundaries between these two main lithological types are diffuse, slightly undulating and mostly sub-parallel to the dyke walls (Figs. 4.4C, E). Locally, the boundaries are sinusoidally curved with the convex arc pointing downwards (Fig. 4.4B). In a few cases, fragments of earlier-formed and at least partly-lithified sedimentary fillings were observed in zones of younger fillings (Fig. 4.4C). Some sections of the dykes contain larger amounts of angular fragments of the granitic wall rock, which are preferentially oriented with their long axis sub-parallel to the dyke boundaries (Fig. 4.4D). Smaller fragments of the wall rock occur mainly as reddish feldspar grains. A third component is represented by greyish platy calcitic grains that are accumulated in narrow wall-parallel zones in which individual plates are likewise preferentially oriented with their long axes parallel to the dyke walls (Fig. 4.4E). The platy calcitic grains are up to two cm long and three mm thick. These aligned plates seem to delineate boundaries between vein fillings of different composition. In the adjacent wall rock, similar carbonate plates of the same size appear as mineralisation in the form of en-echelon arranged (micro) veins (Fig. 4.4E). Corresponding veins are also observed in lithoclasts of the granitic wall rock (Fig. 4.4D).

4.4 Microfabrics

Thin sections of the sedimentary dyke were analysed with an optical microscope in plane and crossed polarised light. Thin sections were cut normal to the strike of the dykes. Carbonate veins were studied additionally with a “hot-cathode” cathodoluminescence (CL) microscope (HC3-LM apparatus; Neuser et al., 1995; Pagel et al., 2000) to investigate the in-situ formed fabrics of the calcite plates. Additional observations for three-dimensional interpretations were made on corresponding hand specimens.

4.4.1 Detrital components

The psammitic components are predominated by well-rounded monocrystalline quartz grains (Fig. 4.5A). The grains are mostly of plutonic origin, indicated by dark blue cathodoluminescence colours (Fig. 4.5B), and lack intragranular deformation structures. A contribution of vein quartz is questionable because grains displaying a diagnostic growth zoning by CL were not observed. A few non-luminescent grains may be derived from low temperature mineralisation in a diagenetic environment, probably from older Cambrian or Precambrian sandstones deposited in other areas. There are no other indications of sedimentary source rocks.

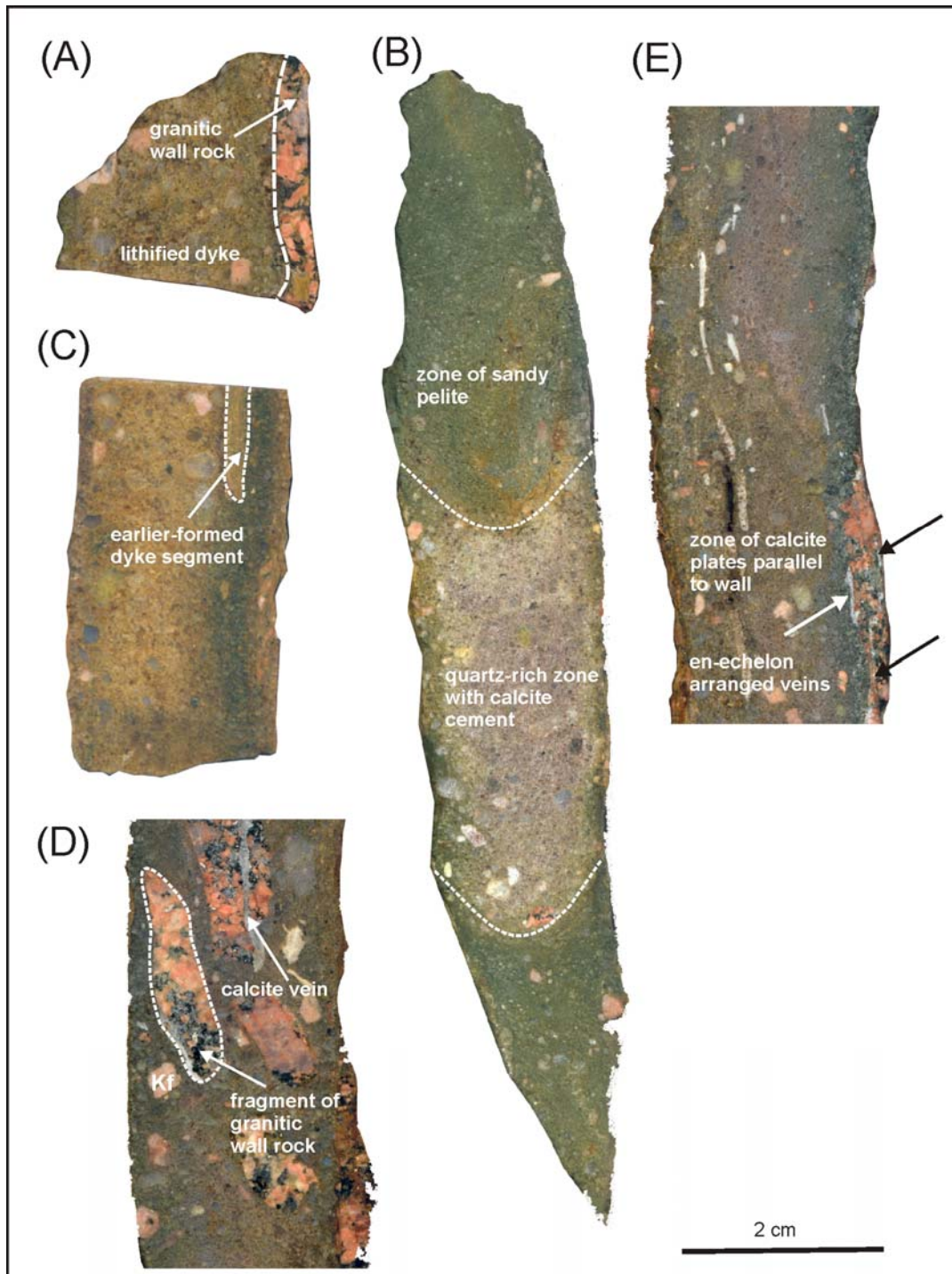


Figure 4.4: Macrob fabrics of sedimentary dyke as observed in hand specimens. (A) Dyke segment with sharp contact to the granitic wall rock. (B) Three generations of dyke filling; top and bottom: dark-coloured filling with high content of pelitic matrix; central segment: psammitic filling with calcite cement, convex arc (dashed line) pointing downwards. (C) Compositional zoning parallel to the dyke wall. Dark fine-grained zone contains a fragment of earlier-formed dyke sediment (arrow). (D) Dyke segment with abundant fragments of the granitic wall rock with long axes aligned sub-parallel to the dyke boundary. Fragments contain calcite (micro) veins. (E) Dyke segment with diffuse compositional zoning; zones of platy calcite plates are arranged parallel to the dyke wall, corresponding en-echelon calcite veins in the wall rock.

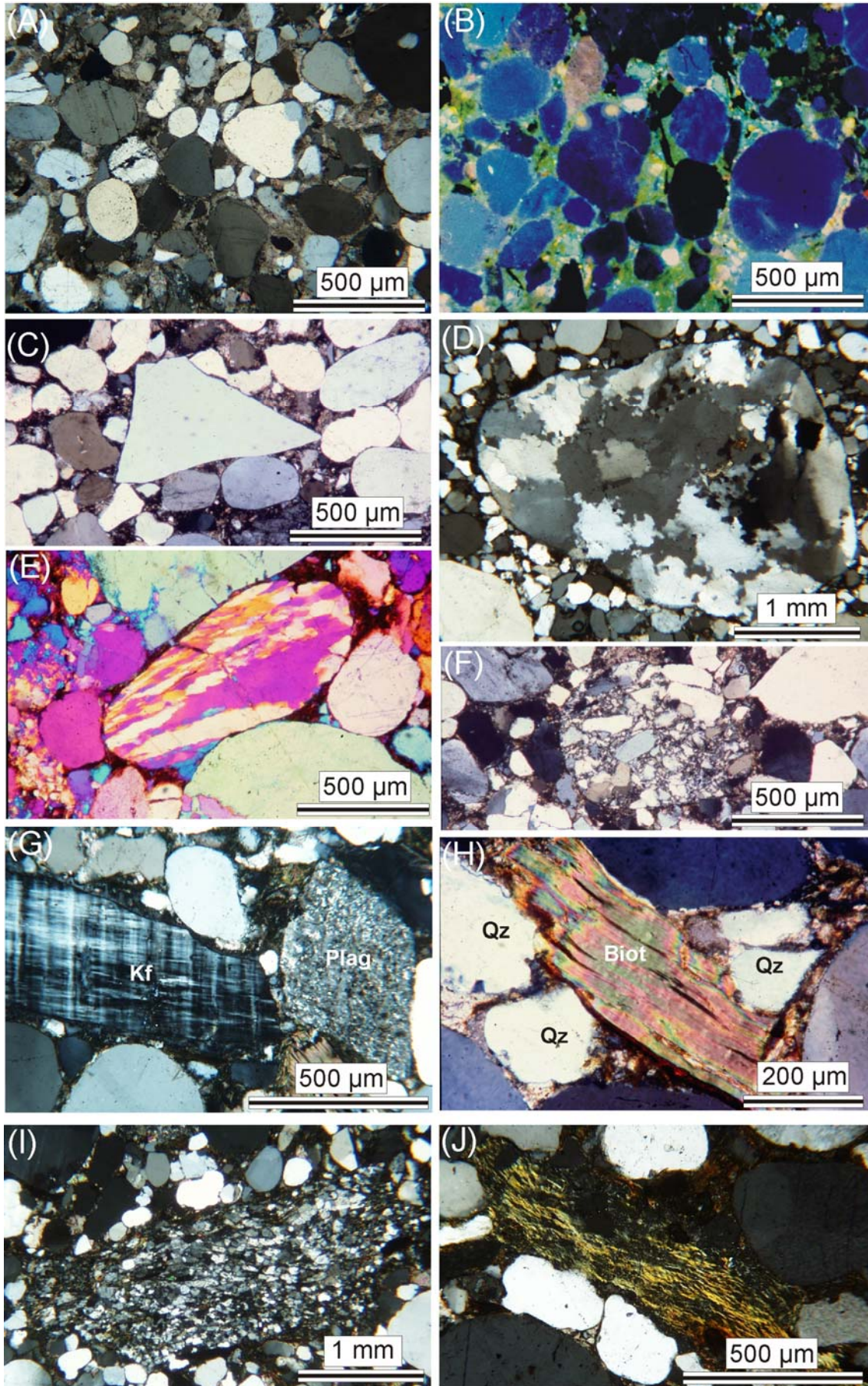


Figure 4.5 overpage: Spectrum of detrital components. (A) Well-rounded monocrystalline quartz grains embedded in calcite cement. (B) Cathodoluminescence image of a comparable fabric domain; blue colours point to plutonic source rocks of the quartz grains. (C) Example of rarely-observed angular quartz grains. (D) Polycrystalline quartz grain with strongly sutured crystal boundaries. (E) Quartz mylonite grain showing strong shape- and lattice-preferred orientation (crossed polars and gypsum plate). (F) Grain of coherent quartzitic breccia. (G) K-feldspar (Kf) with well-developed microcline twins, strongly-altered plagioclase (Plag). (H) Detrital biotite (Biot), slightly deformed by mechanical compaction between quartz grains (Qz); crossed polars. (I) Fragment of metaarkosic sandstone (crossed polars). (J) Fragment of micaschist (crossed polars).

Only very few monocrystalline quartz grains show angular shapes (Fig. 4.5C), which indicates fracturing shortly before or during deposition into the dyke. Polycrystalline quartz grains (Fig. 4.5D) are less frequent and display a wide range of crystal sizes and different shapes of internal grain boundaries, which both probably strongly depend on the angle of intersection. These components may have been mostly supplied from the Västervik formation where metaquartzites with a corresponding variety of microfibrils occur (Vollbrecht and Leiss, 2008). In rare cases, smaller grains of quartzitic mylonites with distinct textures (lattice-preferred orientations, Fig. 4.5E) and coherent micro breccias (cataclasites; Fig. 4.5F) were observed.

A second group of detrital components is represented by angular or weakly-rounded feldspars which are probably derived from granitic rocks in the vicinity or the immediate wall rock. Potassium feldspars are less common, but larger in size, and often display a hypidiomorphic shape with thin perthitic exsolution lamellae and diagenetic overgrowth zones. Microcline is abundant

with typical cross-twinning, showing only minor alteration, in contrast to plagioclase grains that are often strongly altered to sericite (Fig. 4.5G). Occasionally, larger flakes of brown biotite were observed in quartz/feldspar-rich fabric domains (Fig. 4.5H), as well as in the pelitic matrix. Zircon, rutile and apatite are the main accessory components.

With the exception of fragments from the granitic wall rock (see above), polymineralic components, for example, metaarkoses (Fig. 4.5I) or micaschists (Fig. 4.5J) are comparatively rare. Platy grains of calcite are regarded as fragments of microveins (details see below), which are mixed with the siliciclastic detrital material during later dyke opening and filling steps.

4.4.2 *In-situ* formed fabrics and mineralisations

Mechanical compaction by grain rotation associated with microbrecciation was one of the early processes in the unconsolidated sediment. Brecciation affected quartz grains in primarily porous or clay-rich domains, where rotation of grains

or fragments was possible. These domains are best documented by pockets of angular, well-fitting quartz fragments which display a similar crystallographic orientation (Fig. 4.6A).

In domains of early calcite cementation, mechanical compaction was prevented, indicated by the predominance of point contacts between quartz grains (Fig. 4.6A). Pressure solution as a second early process is documented by a significant number of quartz grains, which display concavo-convex or sutured boundaries (Figs. 4.6B, C), particularly in fabric domains poor in pelitic matrix. These boundaries preferentially show subvertical orientations (Fig. 4.6B) and hence could be related to phases, in which tensional stresses responsible for dyke propagation switched to subhorizontal compressive stresses acting normal to the dyke walls. A corresponding body rotation of elongated grains prior to pressure solution may have contributed to a shape-preferred orientation parallel to the dyke walls, in addition to the previously mentioned dyke-parallel mud-supported flow. Dissolved silica was probably the source for early-formed quartz cement which is, due to later replacement by calcite (see below), only preserved as relics (Fig. 4.6D). Part of the dissolved silica precipitated as cryptocrystalline quartz within the fine-grained pelitic matrix. In contact with quartz, parts of the previously mentioned detrital K-feldspar grains were also affected by pressure solution (Fig. 4.6E). Precipitation of

the dissolved material probably contributed to authigenic overgrowth on potassium feldspars in adjacent strain shadow areas or via mass transfer over longer distance on grains in other fabric domains (Fig. 4.6F). Corresponding potassium feldspars often display two zones of authigenic overgrowth separated by a dull rim (Fig. 4.6G). The fact that potassium feldspars with authigenic overgrowth also appear as displaced angular fragments within the matrix (Fig. 4.6H) is another clear sign of a polyphase dyke formation. Domains primarily poor in pelitic matrix are filled with sparry to microcrystalline calcite cement, which partly replaced marginal zones of detrital quartz grains and also earlier formed quartz cement (Fig. 4.7A). In rare cases two generations of sparry calcite cement are clearly discernable (Fig. 4.7B). Locally, transitions between microcrystalline cement and blocky calcite microveins in quartz were observed (Fig. 4.7C). The formation of the calcite veins must have affected the already solidified clastic dyke filling because vein propagation occurred not only along grain boundaries but also transgranular, for example by cross-cutting detrital grains of quartz and feldspar (Fig. 4.7D). Cathodoluminescence colours reveal a distinct growth zonation of individual calcite crystals within sealed microveins (Fig. 4.7E). This implies a free crystal growth into open fissures associated with an episodic variation in fluid influx during calcite cementation. Moreover, the incorporation of elongated clasts of the wall

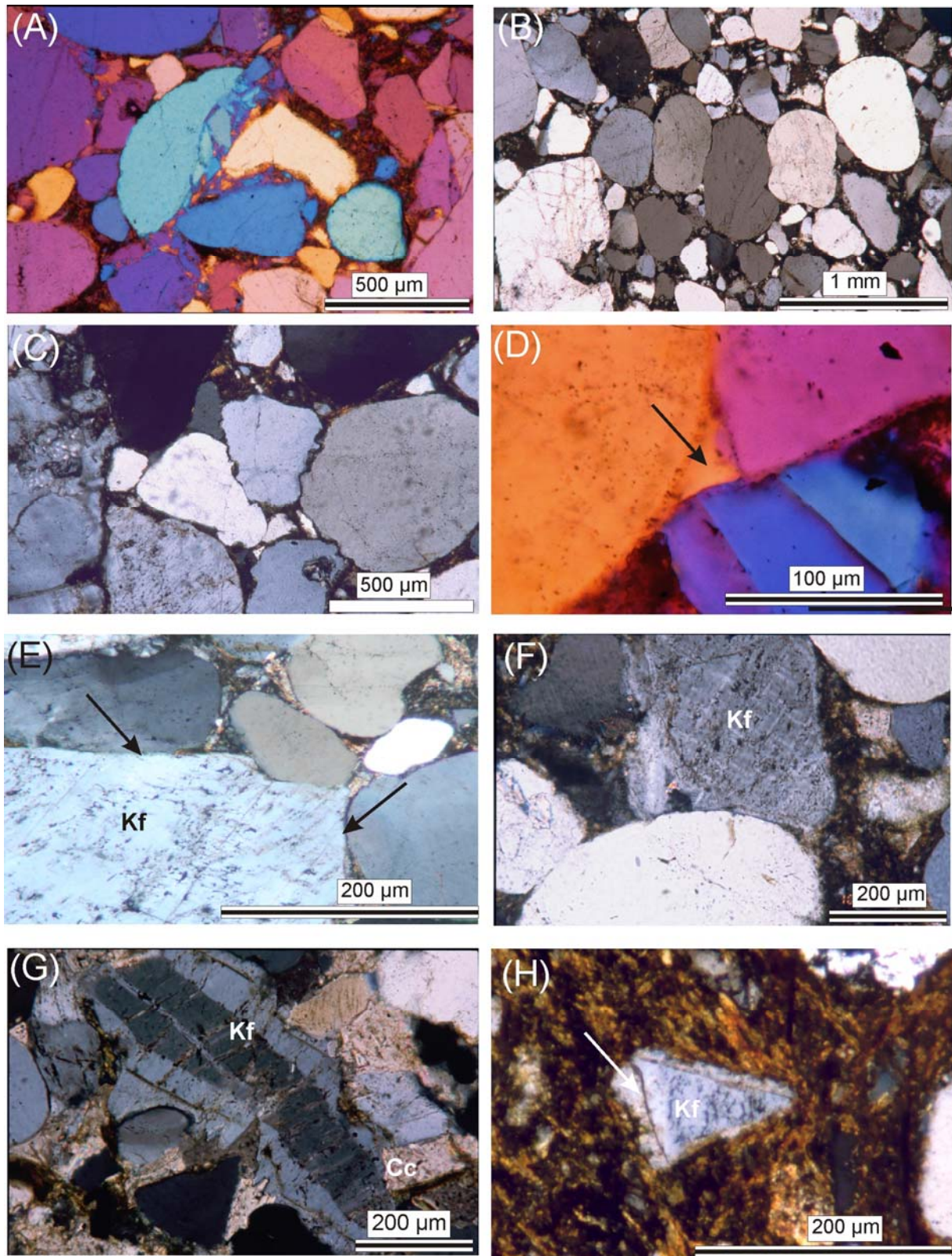


Figure 4.6: In-situ formed fabrics I: Mechanical compaction, pressure solution, and overgrowth. (A) Microbrecciation of quartz (crossed polars and gypsum plate). (B) Subvertical plane or concavo-convex boundaries between quartz grains (crossed polars). (C) Pressure solution of quartz indicated by sutured grain boundaries (crossed polars). (D) Relics of quartz cement (arrow; crossed polars and gypsum plate). (E) K-feldspar (Kf) affected by pressure solution in contact with quartz (arrows; crossed polars). (F) K-

(continuation Figure 4.6) feldspar overgrowth/cement and questionable pressure solution of K-feldspar in contact with quartz (crossed polars) (G) K-feldspar (Kf), displaying two zones of overgrowth, which are partly replaced by calcite (Cc). (H) Angular grain of K-feldspar with overgrowth on original boundaries, face without overgrowth (arrow) was produced by in-situ fragmentation; subsequent separation from counterpart due to flow of pelitic matrix.

(i.e. of the solidified sedimentary dyke) indicates that the considered calcite veins partly formed by repeated crack-sealing. Another evidence for a comparatively late formation of calcite microveins is that they crosscut the overgrowth rims of potassium feldspars (Fig. 4.7F).

In patches with higher clay content, quartz grains occasionally display a strong pseudomorphic replacement by sparry calcite with conservation of the original rounded grain shape (Fig. 4.7G). This kind of replacement preferentially-affected polycrystalline quartz grains along their boundaries, while monocrystalline grains are mostly preserved.

According to EDX analysis (Jacke, 2000), the matrix is mainly composed of microcrystalline aggregates of sericite/illite, chlorite, and probably cryptocrystalline quartz, in which larger, in-situ formed flakes of chlorite are embedded. Locally, these phyllosilicates display an orthogonal shape fabric symmetrically oriented to the dyke walls (Fig. 4.8A), particularly in domains with low content of coarse-grained detritus. Larger flakes of chlorite or strongly-altered detrital biotite are partly crenulated or marginally delaminated between hard components like quartz or feldspar

(Fig. 4.8B), which indicates mechanical compaction. Single crystals or aggregates of euhedral to subhedral pyrite represent another in-situ formed phase (Fig. 4.8C). Occasionally, the aggregates are elongated and outline the previously described, steeply inclined boundaries between different generations of detrital fillings. This may indicate that these compositional interfaces served as migration pathways for fluids.

In general, the significant in-situ processes comprise soft sediment flow in association with mechanical compaction by grain rotation and microbrecciation, pressure solution and re-precipitation, formation of microveins, authigenesis, and overgrowth (cementation) partly associated with replacement of pre-existing phases. Primary variations in composition and porosity, spatiotemporally variations in flow of different pore fluids, and local stress heterogeneities caused a heterogeneous distribution of different microfabric domains. Hence, a complete sequence of the dyke-forming processes cannot be reconstructed unequivocally, because unambiguous age relationships were established only for restricted fabrics domains and hence might not be valid for all the dyke fillings.

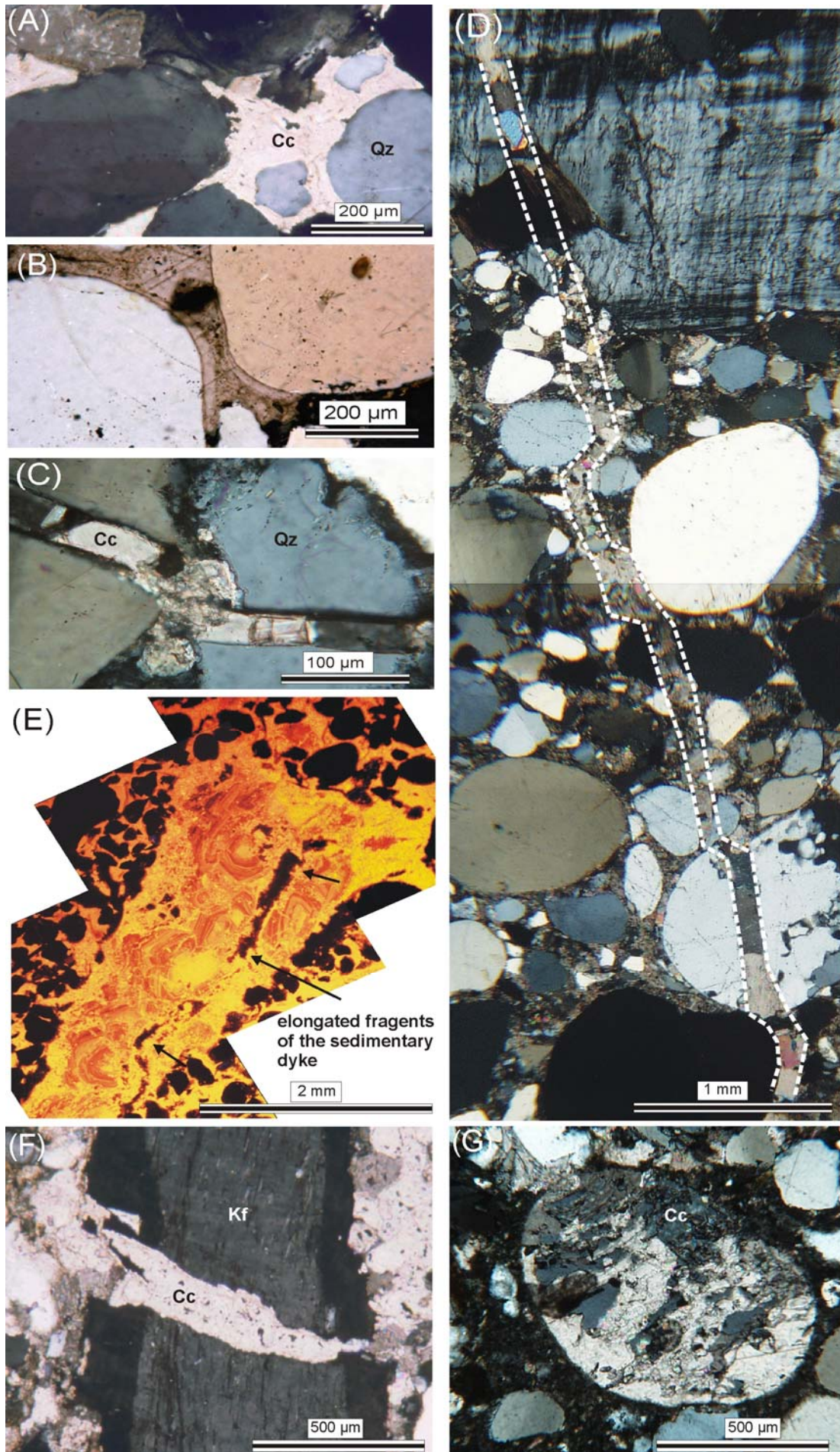


Figure 4.7 overpage: In-situ formed fabrics II: Calcite mineralisations (all photos taken with crossed polars). (A) Calcite cement partly replacing monocrystalline quartz grains and quartz cement. (B) Two generations of sparry calcite cement filling the interstitial between monocrystalline quartz grains. (C) Microveins of blocky calcite (Cc) transecting monocrystalline quartz grains (Qz). (D) Subvertical calcite microvein (dashed white line) with intra- and intergranular sections indicating a solidification of the dyke sediments prior to vein formation. (E) Cathodoluminescence image of a calcite vein fragment (see Figure 2e) showing growth zoning of individual crystals. Elongated fragments of a sedimentary dyke (arrows) indicate a calcite vein formation by repeated vein opening and sealing. (F) Calcite microvein crosscutting a K-feldspar grain (Kf) with in-situ overgrowth zone; fragments of K-feldspar within the calcite vein indicates crack-seal mechanism. (G) Polycrystalline quartz grain strongly replaced in-situ by calcite.

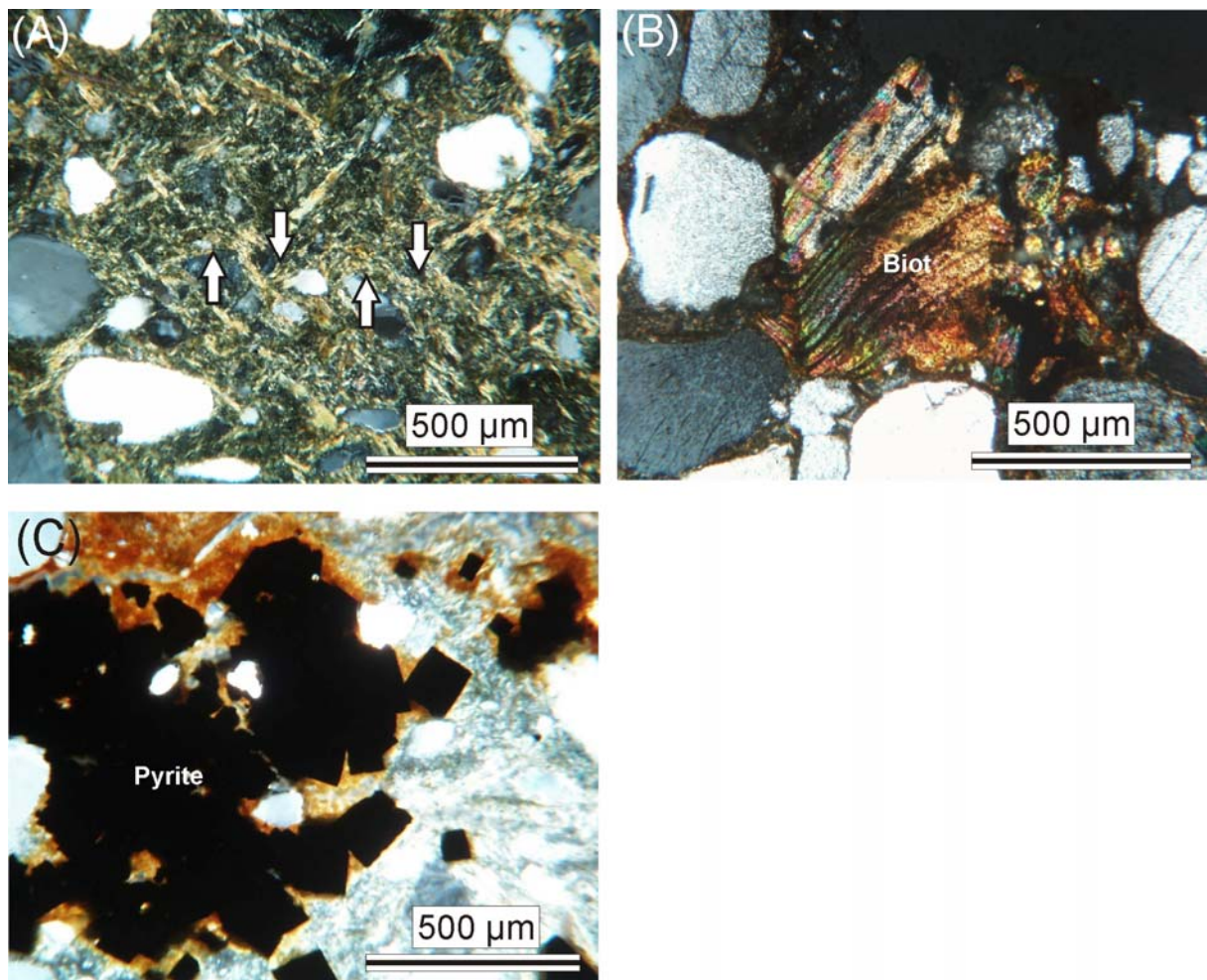


Figure 4.8: In-situ fabrics III: Matrix. (A) In-situ formed chlorite displaying two conjugate directions of shape-preferred orientations symmetrically inclined to the dyke wall; local crenulation (arrows) point to weak shortening normal to the dyke walls. (B) Detrital biotite (Biot) displaying in-situ crenulation due to horizontal compression. (C) Authigenesis of pyrite within the matrix (aggregates of single idiomorphic crystals).

4.5 Interpretation

According to their strike, dyke formation could be related to a NW-SE directed rifting, which affected Baltica during Early to Middle Cambrian (Fig. 4.9) and represented the latest stages of the break-up of the Precambrian super continent (e.g. Murnier and Talbot, 1993; Hartz and Torsvik, 2002; Cocks and Torsvik, 2005). This timing agrees with the paleogeographic reconstructions by Hagenfeldt (1989; see below). The simultaneous development of two sets of dykes was controlled by pre-existing subvertical joint sets (Figs. 4.1B, 4.3), both oriented at an obtuse angle to the supposed rifting direction. However, taking other regions of Baltica into account, the strike directions of comparable sedimentary dykes of Cambrian age cannot be attributed to this stress field (e.g., Katzung and Obst, 1997; dykes on Bornholm island strike 120-125°; Fig. 4.3). It follows from comparisons of Figure 4.3A and B that at regional scale all pre-existing steep joints were opened to form sedimentary dykes. This could be explained by a radial extensional regime due to a crustal up-doming, as described by e.g. Marco et al. (2002) for sedimentary dykes above a domal salt structure. Another possible explanation for additional dyke directions could be stress reorientations in the vicinity of faults. Other extensional structures like normal faults, which can be clearly correlated to the opening direction of the sedimentary dykes, have not been observed.

The described sedimentary dykes were only observed in granitic rocks and not in the Proterozoic metasediments of the Västervik formation. One probable explanation for this is that within the metasediments, the built-up of critical stress values necessary for dyke formation was prevented due to episodic stress relief by layer-parallel slip. The predominance of moderate to steep inclinations of the metasedimentary strata would be favourable for this process.

As described, K-feldspar displays zones of overgrowth which are later on replaced by calcite. For authigenic feldspar to occur, alkaline pore waters rich in Na⁺ or K⁺ are necessary to convert aluminosilicates in the sediment to feldspar during shallow burial (Kastner and Siever, 1979; Tucker 2001). Flehmig (1977) states that both the presence of alkali and silica in seawater are sufficient for feldspar and quartz to form, even during the deposition of sediments. Together with the predominance of well-rounded quartz grains, the formation of the sedimentary dykes can be attributed to a coastal environment which agrees with paleogeographic reconstructions of Hagenfeldt (1989). Clearly, only soft sediments were supplied from the surface, since (exotic) sandstone fragments, which could not be derived from older, already lithified dyke sediments, are absent.

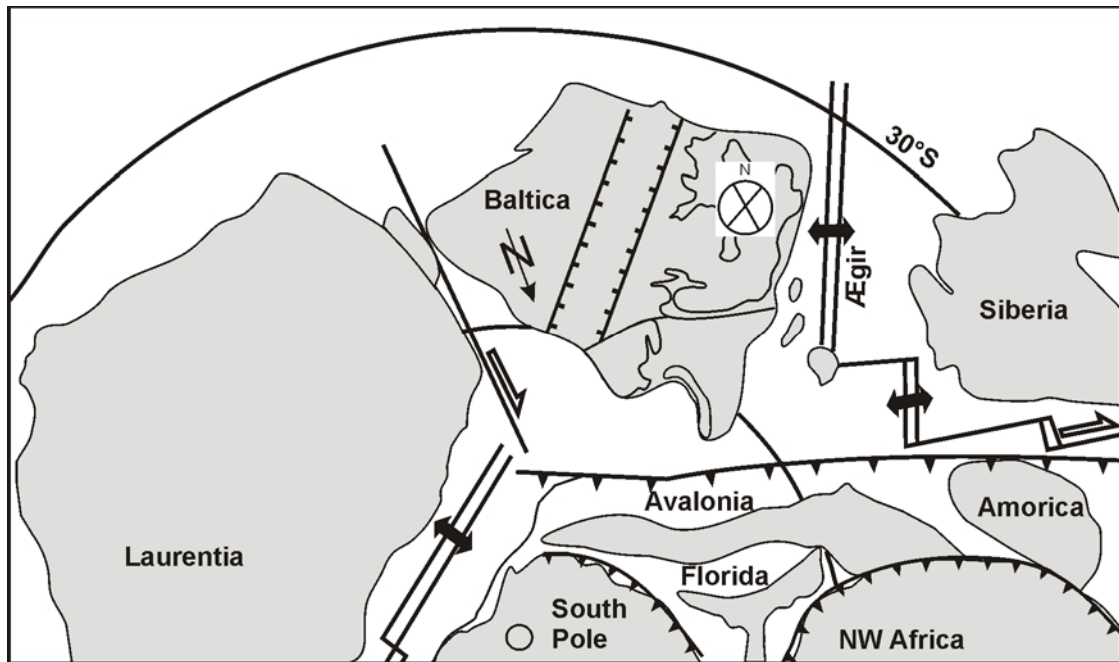


Figure 4.9: Schematic illustration of the Cambrian (550Ma) tectonic framework (modified from Cocks and Torsvik, 2005). Equal area polar projection, N gives the present N-direction with respect to Baltica. Rifting of Baltica marked by normal fault symbols. NE-SW and NW-SE striking trends of the joints in the Västervik area are indicated as simplified pole plot figure.

The following describes a sequence of events, which might have occurred repeatedly until individual dykes attained their final dimensions (Fig. 4.10):

- (1) Pre-existing joint formed by coalescence of microcracks during the early cooling and uplift history of the granite in a differential stress field (e.g. Nadan and Engelder, 2009 and references therein).
- (2) Lateral extension of joint and downward propagation of fracture. Simultaneous filling with wall rock fragments, detrital grains and mud from the surface.
- (3) Further downward fracture propagation caused a suction effect

leading to a downward flow of the unconsolidated fillings and re-orientation of elongated components and compositional boundaries (sub-) parallel to the subvertical dyke walls. Initial stages are represented by convex-downward boundaries between fillings.

- (4) Consolidation of fracture fillings due to combined mechanical compaction, pressure solution and precipitation of quartz or authigenesis of potassium feldspar (overgrowth), chlorite and pyrite. Horizontal compression normal to the dyke wall occurred at least temporarily during this consolidation phase.

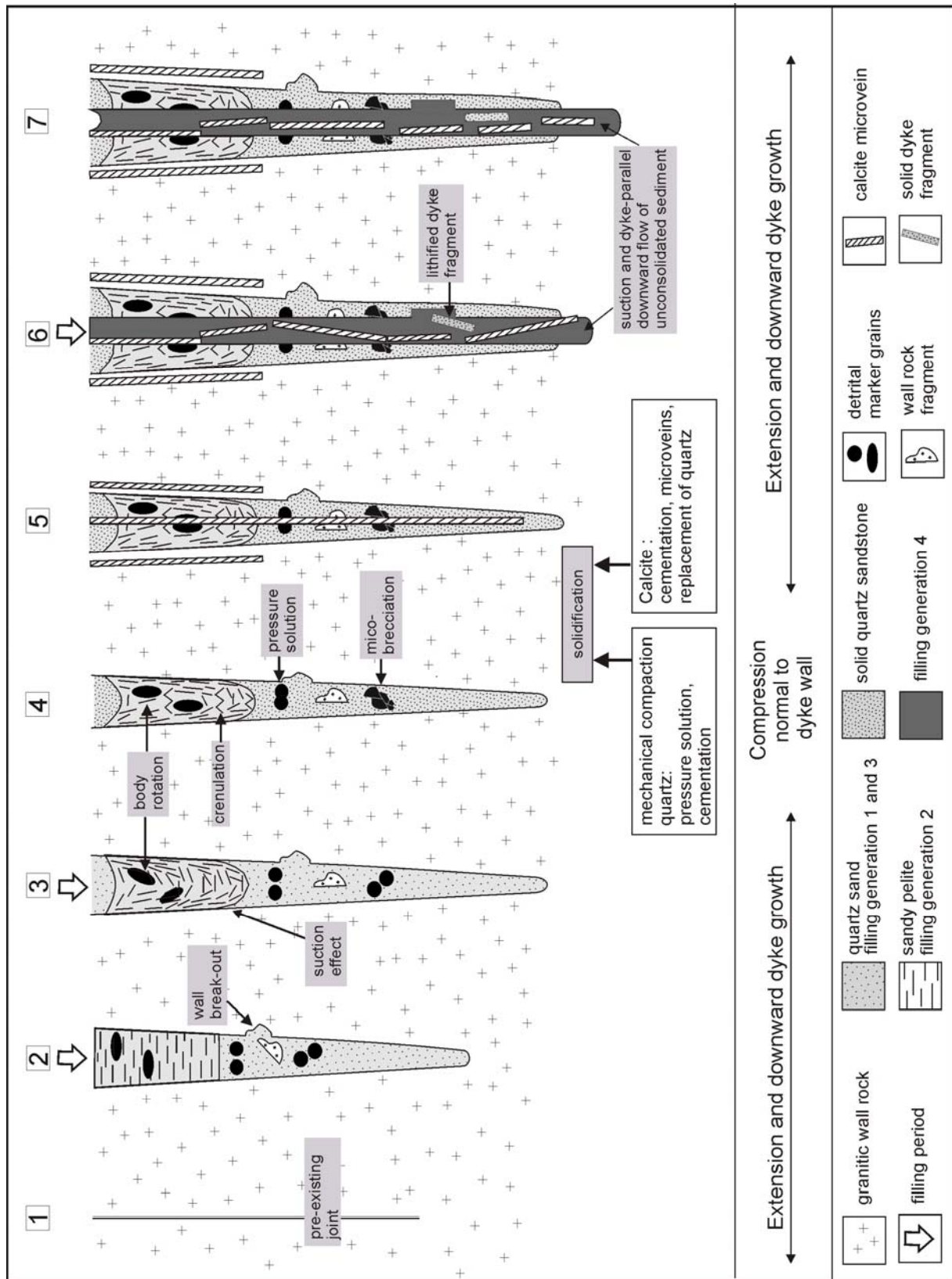


Figure 4.10: Model of polyphase dyke development. For explanation of the different stages see text. Structural elements not to scale.

(5) Formation of sub-vertical calcite microveins by calcite cementation in fractures through already lithified dyke fillings and the adjacent wall rock. Growth zoning indicates that calcite mineralisation occurred into open fissures. The absence of sediment input may reflect a lack of detritus supply from the surface or that these fissures formed in subsurface levels. Quartz cement and detrital quartz were partly replaced by calcite.

(6) Phase of dyke opening transecting already indurated sediments. The newly-introduced epiclastic sediments incorporated clasts of the partly-brecciated lithified dyke sediments, together with platy fragments of the calcite veins.

(7) Progressive downward dyke propagation and related subsidence of the latest sediment fillings, which caused a boudinage-like stretching and strong preferred orientation of the platy calcite fragments parallel to the dyke walls.

4.6 Conclusions

A closer look to the macro- and microfabrics of sedimentary dykes has revealed a multistage origin due to repeated fracture propagation under varying conditions. This may also imply that dyke formation lasted over a long time span with alternating periods of opening/filling,

cementation/lithification and alteration. Taken the results as a whole, a model of passive gravitational infill with unconsolidated sediment from the surface, associated with suction processes due to episodic downward dyke propagation is favoured, rather than injection under high fluid pressure as has been discussed for other sedimentary dykes in Southeast Sweden. Pressure solution of quartz and crenulation of phyllosilicates shows that extensional phases were interrupted by phases of horizontal compression normal to the dyke wall. The orientation of the sedimentary dykes agrees with the regional stress field during the Cambrian. The formation of two sets of dykes was controlled by pre-existing sets of joints, which were in suitable orientation to the extensional stress direction. Further analyses of the dyke-forming processes could implicate of the hosting environment and hence could help to reconstruct the paleogeographic situation and regional tectonics.

Acknowledgements

The authors gratefully acknowledge helpful discussions with colleagues from the Geoscience Centre of the Georg-August-University of Göttingen. The authors are grateful to Sven Egenhoff and an anonymous reviewer for their constructive comments on the manuscript. We thank David C. Tanner for revising the English.

5. Geological and tectonic framework of Iceland

5.1 Location of Iceland - mantle plume and Mid - Atlantic Ridge

The Iceland basaltic plateau is the product of the interaction between the spreading plate boundary and the mantle plume that influenced the region throughout

the opening of the North Atlantic (Wolfe et al., 1997; Allen et al., 2002). Iceland is located in the central North Atlantic and represents a subaerial part of the Mid-Atlantic Ridge between the ridge segments Reykjanes Ridge in the south and Kolbeinsey Ridge in the north, while separate the European and the North American Plate (Fig. 5.1).

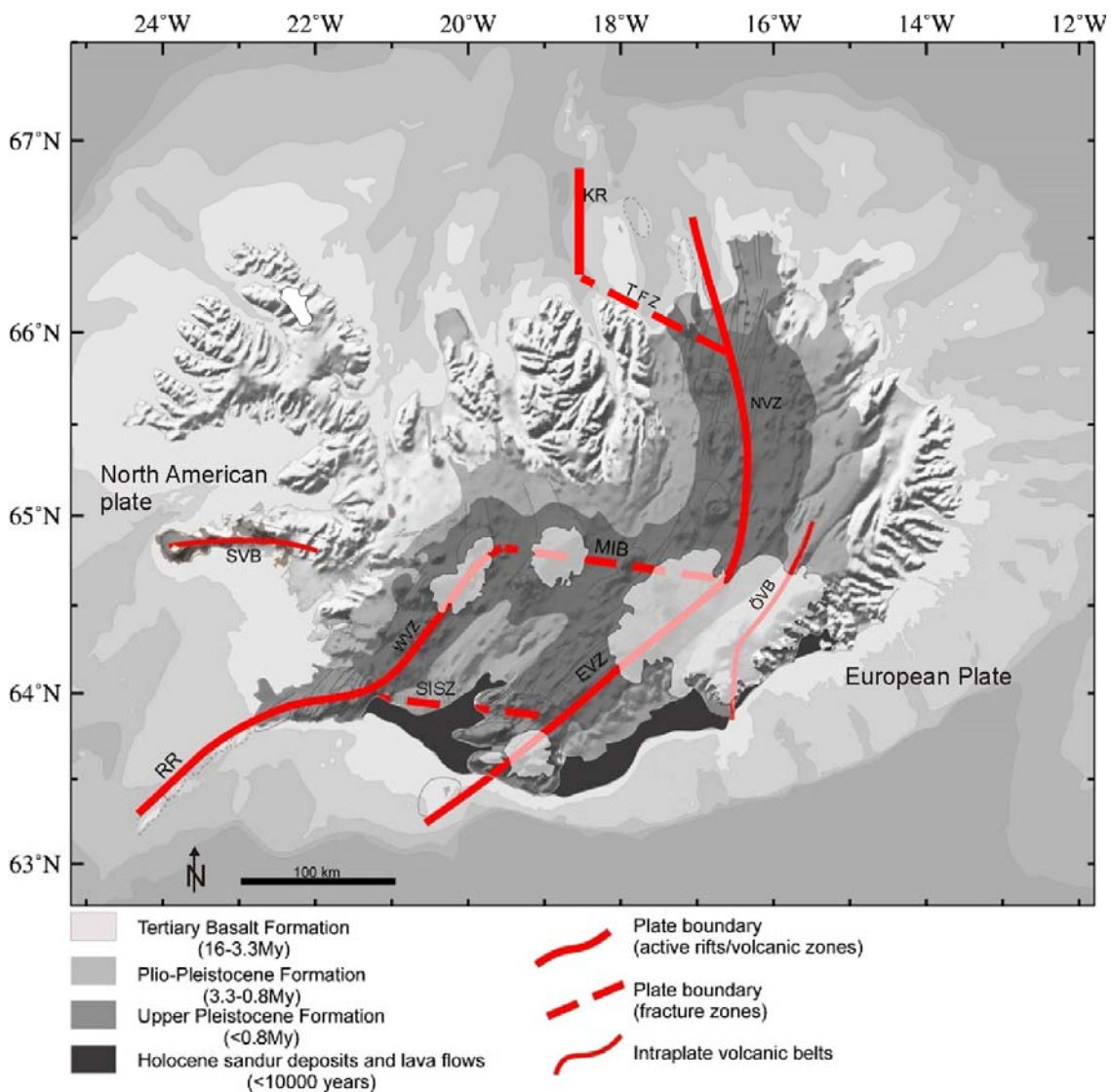


Figure 5.1: The principal elements of the geology in Iceland, outlining the distribution of the major geological subdivisions, including the main fault structures and volcanic zones and belts. RR, Reykjanes Ridge; SISZ, South Iceland Seismic Zone; WVZ, West Volcanic Zone; MIB, Mid-Iceland Belt; EVZ, East Volcanic Zone; NVZ, North Volcanic Zone; TFZ, Tjörnes Fracture Zone; KR, Kolbeinsey Ridge; ÖVB, Öraefi Volcanic Belt; SVB, Snæfellsnes Volcanic Belt (modified from Thordarson and Höskuldsson, 2002).

Spreading velocities across Iceland have been estimated at 18.3 mm/a over the last 3 Ma in a direction of 105°E (NUVEL-1A model of global plate motion; DeMets et al., 1994), whereas latest measurements reveal data of 21.9 mm/a in a direction 102°E (Geirsson et al., 2006) reflecting minor contributions from local processes such as on-going glacio-isostatic movements (Pagli et al., 2007). Due to widespread magma production caused by the mantle plume (estimated at 10^7 km³ in 2-3 Ma; e.g. White et al., 1987; White and McKenzie, 1989) flood basalts and volcanic centres in Greenland, the Faeroe Islands, and the British Isles have been formed.

Currently the mantle plume centre is located below south-central Iceland, beneath the glacier Vatnajökull (e.g. White and McKenzie, 1995; Fig. 5.2A). The high magma generation rates compared to mid-ocean ridges have led to the formation of an anomalously thick crust (up to 45 km below central Iceland; Darbyshire et al., 2000; Allen et al., 2002) and a high variation in geochemical and petrological signatures (e.g. Jonasson, 2007; Sigmarsson and Steinthorsson, 2007). However, the geochemical signature of Icelandic rocks reveals an origin by mixing of MORB and OIB sources (Oskarsson et al., 1985).

5.2 Geological structure and stratigraphy of Iceland

The Neovolcanic Zones in Iceland, which cover around 30 000 km², delineate

15–50 km-wide belts of active faulting and volcanism and is further divided into volcanic systems. More than 30 systems are identified by Johannesson and Saemundsson (1998; Fig. 5.2A). The spreading segments are divided further into fissure swarms. It is characterised by a volcano-tectonic architecture that includes a fissure (dyke) swarm associated mostly with a central volcano, with a typical lifetime of 0.5–1.5 Ma (e.g. Jakobsson et al., 1978; Jakobsson, 1979b; Saemundsson, 1978, 1979; Fig. 5.2B). The fissure swarms are elongate structures (5 to 20 km wide and 50 to 200 km long) which are normally aligned sub-parallel to the axis of the hosting volcanic zone. The central volcano, when present, marks the location of the main eruptive activity and characterised by the occurrence of felsic volcanic rocks, high-temperature geothermal fields, and, eventually, a collapse caldera (e.g. Thordarson and Larsen, 2007; Thordarson and Höskuldsson, 2008).

The Neovolcanic Zone, where lithospheric accretion takes place, is composed of an axial rift zone and three off-rift flank zones (Saemundsson, 1979). The flank zones are the Snaefellsness Volcanic Zone in West Iceland, the South Iceland Volcanic Flank Zone, and the Öraefajökull-Snaefell Flank Zone in East Iceland (Fig. 5.2A). Volcanic rift zones are characterised by extensive crustal spreading and the production of tholeiites, whereas flank zones exhibit little or no crustal spreading and are characterised by the production of alkali

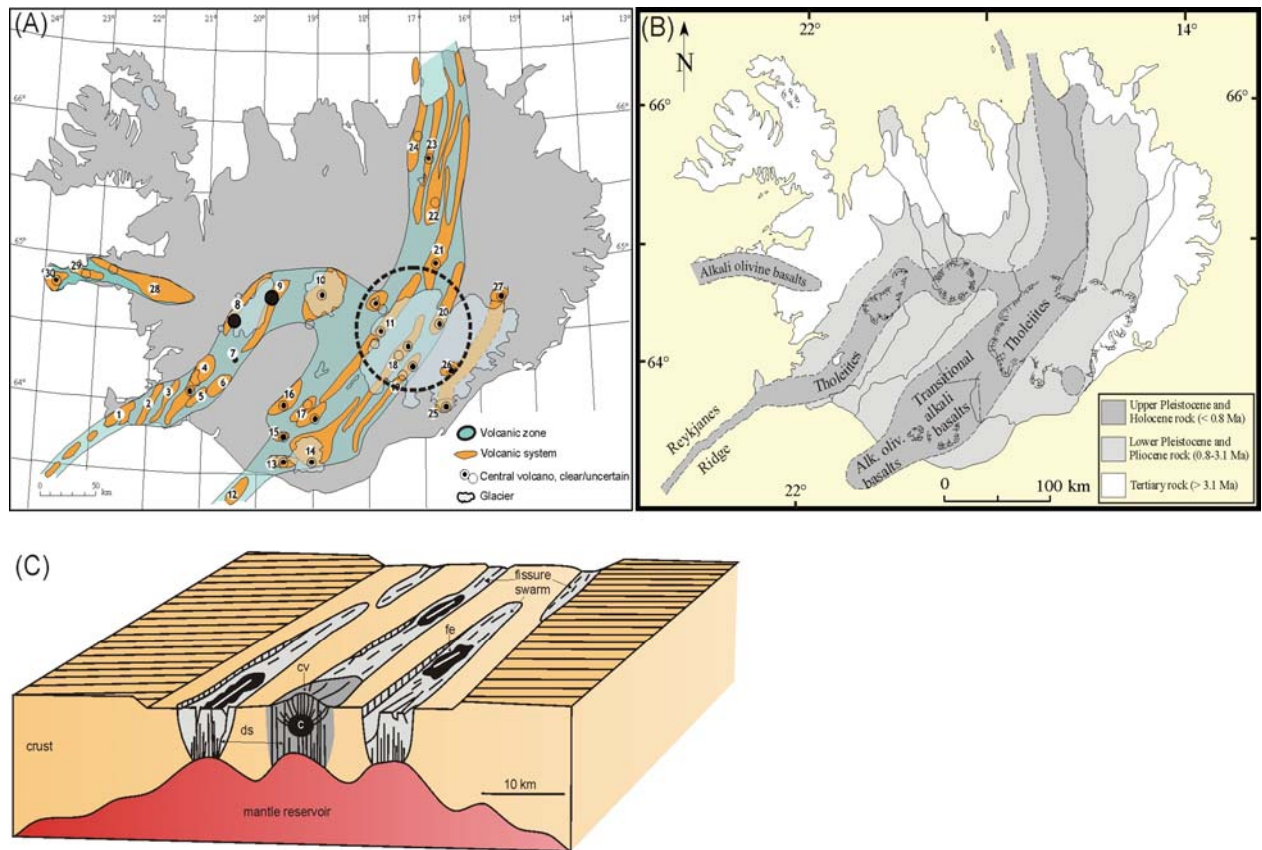


Figure 5.2 (A) Distribution of active volcanic systems among volcanic zones and belts in Iceland (modified after Johannesson and Saemundsson, 1998). (1) Reykjanes–Svartsengi, (2) Krisuvik, (3) Brennisteinsfjöll, (4) Hengill, (5) Hromundartindur, (6) Grimsnes, (7) Geysir, (8) Prestahnjukur, (9) Langjökull, (10) Hofsjökull, (11) Tungnafellsjökull, (12) Vestmannaeyjar, (13) Eyjafjallajökull, (14) Katla, (15) Tindfjöll, (16) Hekla–Vatnafjöll, (17) Torfajökull, (18) Bardarbunga–Veidivötn, (19) Grimsvötn, (20) Kverkfjöll, (21) Askja, (22) Fremrinamur, (23) Krafla, (24) Theistareykir, (25) Öraefajökull, (26) Esjufjöll, (27) Snæfell, (28) Ljosufjöll, (29) Helgrindur, (30) Snæfellsjökull. The large open circle indicates the approximate centre of the Iceland mantle plume/anomaly as depicted by Wolfe et al. (1997). (B) Key structures of volcanic systems: c-crustal magma chamber, ds-dyke swarm, cv-central volcano, fs-fissure swarm, fe-fissure eruption (modified from Thordarson and Höskuldsson, 2002). (C) Different petrological features of axial rift zones and flank zones (after Jakobsson, 1972; 1979a,b). Rift zones produce mainly tholeiites whereas flank zones produce alkali olivine basalt.

olivine basalts and transitional alkali basalts (Jakobsson, 1972, 1979a, b; Jonasson, 2007; Sigmarsson and Steinthorsson, 2007; Fig. 5.2C). Volcanic zones include the Reykjanes–Langjökull Volcanic Zone, in Southwest Iceland that has been active for at least 6 to 7Ma (Saemundsson, 1979, 1986), and consists of the Reykjanes Peninsula Oblique

Rift and the West Volcanic Zone (WVZ; Einarsson, 1991b; Figs. 5.1, 5.2A). With respect to data of Perlt and Heinert (2006), who reveal that 45 % of the total opening across the southern Iceland is accommodated along the WVZ, it would make it the slowest spreading volcanically active mid-ocean ridge presently known (Sinton et al., 2005). The

eastern part of the rift zone can be divided into the North Volcanic Zone (NVZ) and the East Volcanic Zone (EVZ; e.g. Oskarsson et al., 1985; Einarsson, 1991a,b). The North Volcanic Zone initiated about 8-8.5 Ma ago (Garcia et al., 2003), and its structural evolution appears to be closely related to rift jumps (Garcia et al., 2008). The East Volcanic Zone (EVZ) is with an age of 2 to 3 Ma years the youngest part of the Icelandic rift (Johannesson et al., 1990) and is currently propagating south (Johannesson, 1980).

The stratigraphic classification of Iceland is mainly based on absolute age dating, paleomagnetism (e.g. Kristjansson and Jonsson, 2007) and on the glacial-interglacial history of the country (e.g. Helgason and Duncan, 2001). According to Saemundsson (1979) and Thordarson and Hoskuldsson (2002), the succession of Iceland is grouped into the Tertiary basalts (16-3.3 Ma), the Plio-Pleistocene (3.3-0.7 Ma) and the Upper Pleistocene (< 0.7 Ma; Figs. 5.1, 5.2).

The oldest exposed rocks in Iceland occur in the Northwest and have an age of 14 to 16 Ma, while in East Iceland the oldest rocks have an age of 12 Ma (Ross and Mussett, 1976). The Tertiary pile mainly consists of 5 m to 15 m thick individual tholeiitic lava flows, basaltic breccias (hyaloclastite), and intermediate and acid rocks, which are restricted to central volcanoes (Saemundsson, 1979). The cumulative thickness of the Tertiary lava pile

is up to 12 km (Torfason, 1979) and composed of 1000s of individual flows (Watkins and Walker, 1977). Along the margins of the rift axis, the lava flows dip at low angles of 3°-10° towards the active rift zone, defining a synform-like structure (Garcia et al., 2003). The regional tilt varies with stratigraphic depth (Walker, 1964; Saemundsson et al., 1980) and is assumed to be the result of the gradual loading from volcanic production (Sigmundsson and Saemundsson, 2008). The exposure level ranges from 2000 m in Southeast Iceland (Walker, 1974) to around 1100 m in Northeast Iceland (Gustafsson, 1992) due to extensive erosion (Geirsdottir et al., 2007).

The Tertiary is conformably overlain by the Plio-Pleistocene, which covers around 25 000 km², predominantly in broad zones between Tertiary areas and the Neovolcanic zones. The boundary between Tertiary and Plio-Pleistocene series is fixed at the base of the Mammoth palaeomagnetic event 3.1-3.3 Ma ago, as the first tillites appear interstratified with the lavas in southwestern and northeastern Iceland (Sigmundsson, 2006; Sigmundsson and Saemundsson, 2008). Deposits of lacustrine sediments with dropstones, morainic material, hyaloclastites, pillow lavas interstratified in subaerial lava flows (Saemundsson, 1979) indicate alternating cold and warm periods with glaciations occurring every 100 000-130 000 a (e.g. Geirsdottir and Eiriksson, 1994); over 20 glaciations in the last 4-5 Ma were estimated by Geirsdottir et al. (2007).

The Upper Pleistocene covers an area of about 30 000 km² and is set between two magnetic epochs at 0.8 Ma (Sigmundsson and Saemundsson, 2008). The rocks are characterised by more voluminous hyaloclastites than that which occur in the Plio-Pleistocene, in addition, lavas erupted in interglacial periods that indicate more extensive and longer-lasting glaciations (Sigmundsson and Saemundsson, 2008).

The Postglacial period is not fixed but connected to the deglaciation before the Younger Dryas (around 11500 a BP; Thordarson and Hoskuldsson, 2002; Sigmundsson and Saemundsson, 2008). The Postglacial series constrain lava flows, pyroclastics, unconsolidated marine clays, fluvioglacial and fluvial outwash; eruptions of intermediate and acid magmas have occurred in some volcanic systems (e.g. Hekla). The intensity of volcanism has varied throughout the Postglacial, with much higher volcanic production rates in the first millennia after the deglaciation (e.g. Hardarson and Fitton, 1991; MacLennan et al., 2002; Thordarson and Larsen, 2007; Sigmundsson and Saemundsson, 2008).

5.3 Rift jumps and spreading episodes

As the North American-Eurasian plate boundary migrates westwards relative to the Icelandic hot spot (Burke et al., 1973; Fig. 5.3), eastwards jumps bring the volcanic zones of Iceland back to location of the mantle plume (Saemundsson, 1974). Rift-zone relocations have been proposed in the

past (Saemundsson, 1979; Hardarson et al., 1997; Kristjansson and Jonsson, 1998) and are evident from the location of monoclines created by the tilt of the lava pile towards the active rift zone (Johannesson, 1980). The unstable rift zones show evidence of relocation going back to at least 15 Ma (West Fjords; Jancin et al., 1985; Jonsson et al., 1991; Hardarson et al., 1997). The transition of activity of one rift zone to the next is characterised by a temporal overlap, similar to the present shift from the Reykjanes-Langjökull Volcanic Zone to the East Volcanic Zone.

Models explaining the mechanism of rift jumps were developed by e.g. Gibson and Piper (1972) and Helgason (1984). The model by Gibson and Piper (1972) involved lateral shifting of individual volcanic centres while others remain stationary, which in turn control the development of the new fissure and partially overlaps the earlier-formed lava flows. Helgason (1984) proposed, based on the distribution of volcanic centres in eastern Iceland that volcanic activity is not fixed to the plate boundary but shifts throughout the island. Helgason (1984) concluded that rift jumps occur frequently with small-scale jumps over 20 to 40 km approximately every 2 Ma, whereas large-scale rift jumps over 100 to 200 km can occur every 6 to 7 Ma. In addition, activity can also shift back to the area of an extinct rift zone, so that new rift segments can form in older crust with a higher proportion of evolved rocks.

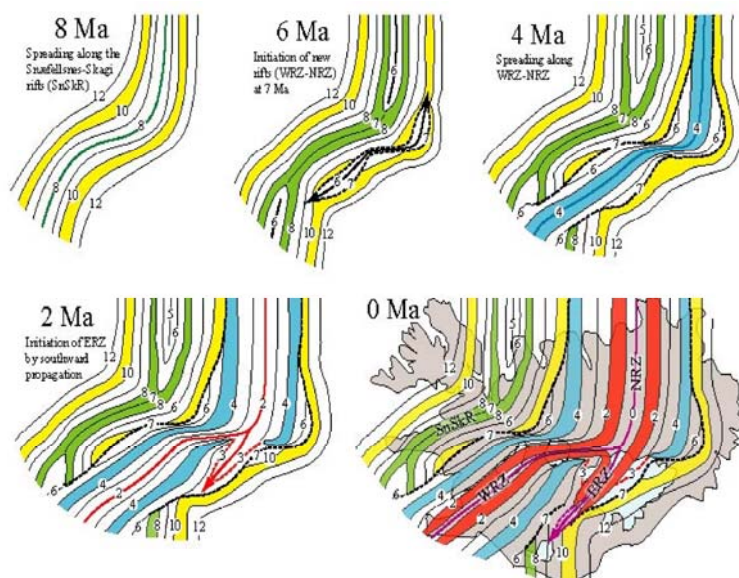


Figure 5.3: Crustal accretion, relocation and propagation of the Icelandic rift zones in the last 12 Ma (numbers in Ma). The panels show map views for 8, 6, 4, 2 and 0 Ma. The 8 Ma panel shows the spreading along the Snæfellsnes and Skagi rift zones. The 6 and 4 Ma panels demonstrate the incipient propagation and mature development of the Western and Northern Rift Zones after the new rift initiation at about 7 Ma. The 2 and 0 Ma panels show the southward propagation of the Eastern Rift Zone, initiated at about 3 Ma. Based on data from Sæmundsson (1979) and Johannesson (1980) and a synthesis by Ivarsson (1992), adapted from Trønnnes, R.G., (<http://www.hi.is>).

Rifting episodes are not a continuous process. Events on the volcanic systems are closely linked to plate movements (e.g. Sigurdsson and Sparks, 1978; Björnsson et al., 1979; Brandsdóttir and Einarsson, 1979; Björnsson, 1985).

Spreading takes place in distinct rifting episodes that usually are confined to a single volcanic system, although near-concurrent activity on two or more systems is known

(e.g. Einarsson and Johannesson, 1989; Sigurgeirsson, 1995; Larsen et al., 1998). The whole system is activated in these episodes and they can last for several years to decades. Constraints on the crustal spreading process are marked by build-up of extensional stress in the upper crust, decompressional melting in the mantle, stretching across the fissure swarm prior to

rifting causes subsidence. The stress is released in rifting episodes that occur irregularly, but are on the order of 100 to 1000 years at each location along the plate boundary (Sigmundsson and Saemundsson, 2008). The most recent rifting episodes occurred in north Iceland: 1618 Theistareykir event (without eruption), 1724-1729 Krafla Fissure Swarm, 1874-1875 Askja Fissure Swarm (Sigurdsson and Sparks, 1978; Buck et al., 2006; Hjartardóttir, 2008; Fig. 5.4) and 1975-1984 again in the Krafla swarm. It has been confirmed that the Krafla fissure swarm has been subjected to at least six major rifting events during the past 3000 years (Saemundsson, 1992). The latter magmatic-tectonic episode in the Krafla swarm was extensively studied and recorded and gave insights into the development of a rifting event (e.g. Einarsson, 1991a; Tryggvason, 1984, 1994; Brandsdóttir et al., 1997; Arnadóttir et al., 1998; Buck et al., 2006; Sigmundsson, 2006; Fig. 5.5). During most of the episode, magma ascended from depth and accumulated in a magma chamber at about

3 km depth. The inflation periods were characterised by sudden deflation events when the walls of the chamber were breached and magma was injected laterally into the adjacent fissure swarm where subsequently large-scale rifting took place (Fig. 5.5). Not every deflation episode results in an eruption (Fig. 5.5). Rifting episodes of the Krafla 1975–1984 type appear to take place in the northern rift zone of Iceland about every 100–150 years (Björnsson et al., 1977) and the eastern rift in South Iceland seems to have comparable frequency (Larsen, 1984).

The rifting process is a cyclic deformation process and can be subdivided into three phases (inter-, co- and post-rifting) with different deformation styles (Sigmundsson, 2006). Inter-rifting periods are characterised by continuous spreading with a velocity in agreement with NUVEL-1A model (DeMets et al., 1994). An inter-rifting period is followed by an active rifting event (co-rifting phase), where dykes are intruded into the upper crust to release extensional strain accumulation from the inter-rifting phase. The co-rifting phase is typically split up in a series of repeated large instantaneous displacements, giving a high, but short lived spreading velocity in the vicinity to the intruded dykes (Fig. 5.5).

A co-rifting phase is followed by post-rifting, where the rift perpendicular deformation rate near the rift axis decrease (Heki et al., 1993, Hofton and Foulger, 1996; Pollitz and Sacks, 1996). The duration of a post-rifting and the inter-rifting phase depend

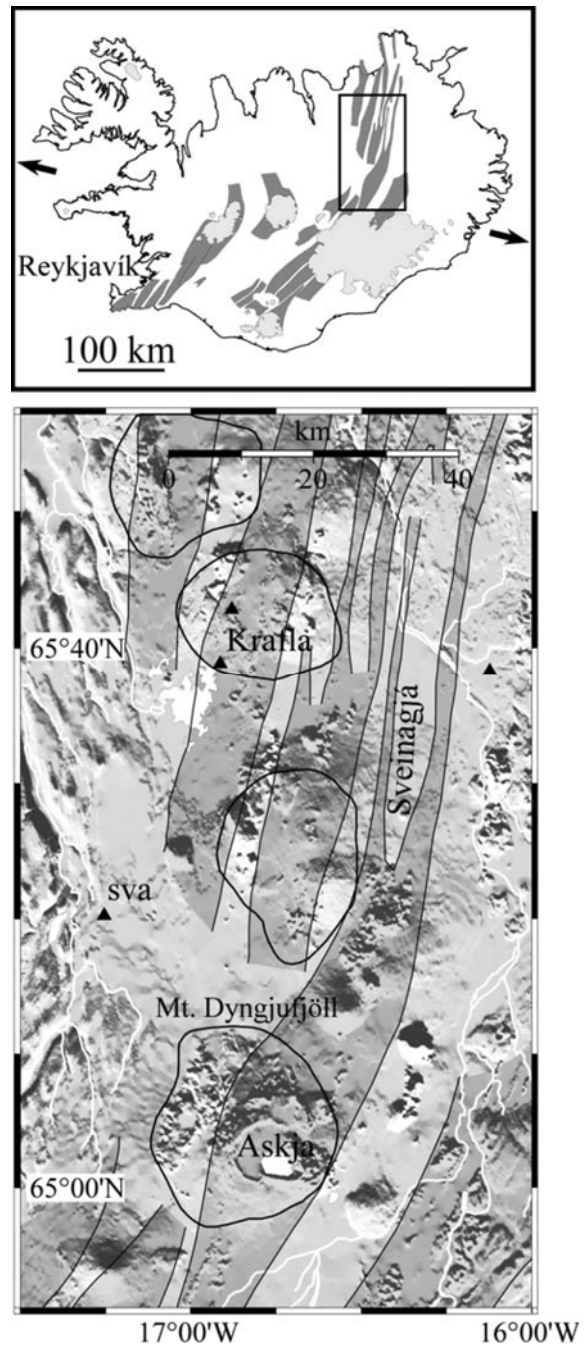


Figure 5.4: Location of the Askja and Krafla volcanoes and swarms of the same name at the divergent plate boundary in North Iceland. Seismic stations are shown with triangles (e.g. sva). The Sveinagja Graben, as part of the Askja fissure swarm, was part of the main fissure eruption during the Askja rifting episode 1874–1876 eruptive fissure was located 40–70 km north of Askja (figure reprinted from Sturkell et al. (2006), with kind permission from Springer Science and Business Media).

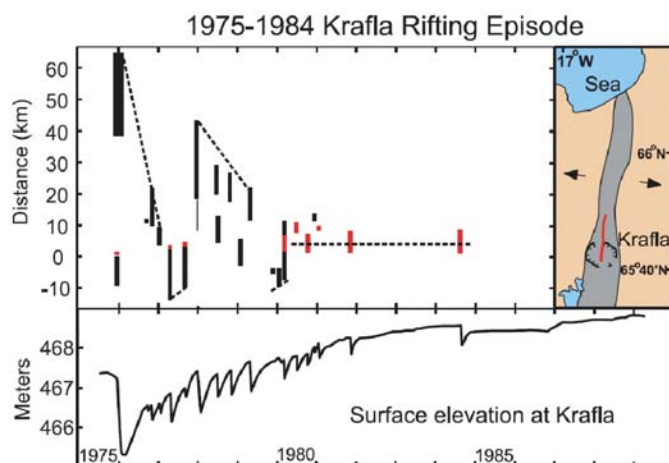


Figure 5.5: Observations with time during the Krafla rifting episode 1974–1989 (modified from Einarsson, 1991a). (top) Distance ranges for surface fissuring (black) or extrusion of lava (red) measured from the centre of the Krafla inflation (shown on the map, right). The thickness of the vertical lines gives the time duration of the activity. (bottom) Changes in the elevation near the centre of inflation in the Krafla caldera.

on the rheological properties of the materials underlying the recently activated spreading segment, and rheological variations within the en echelon arrangement of the fissure segment (Pedersen et al., 2009). Recent GPS measurements from the Krafla area indicate relaxation duration of a few decades (Arnadóttir et al., in press).

5.4 Case studies Iceland

Iceland is often named a “window” to study divergent plate tectonics and a laboratory to investigate fundamental processes such as magma flow processes, and eruption mechanics. Both are tectonically-controlled. The conditions in Iceland to study the interaction of magmatism and faulting offer interesting field examples supported by a rather uniform stress field conditions and a well-documented stratigraphy, that is exposed to up to 2 km depth in East Iceland (Walker, 1974).

In the northern rift zone the latest rifting episodes are documented (Krafla, 1975-1984), young eruptive fissures (eroded and intact) are present and the active

divergent plate movement can be studied. This is especially meaningful to determine actual hazard studies, not only referring to eruptive fissures, but also to various types of volcanoes. The interaction and feedback processes between magmatism and faulting, if and under what conditions a fault acts as pathway for an upward propagating dyke are relevant questions in terms of forecasting and understanding eruptions.

The northern rift zone of Iceland offers exposures of active systems, and therefore the conditions to study the tectonically-controlled emplacement of intrusive bodies in the upper, brittle crust in an area undergoing extension. The field examples of the area deal with the topics of (1) the interaction of dyke emplacement in graben and faulting, and (2) felsic magma movement and emplacement in an active rift zone.

6. Tectonic feedback on magma emplacement – case study Northeast Iceland: preface

Linear magmatic volcanoes or volcanic fissures form the Icelandic landscape. The monogenetic tightly packed crater cones are often distributed along rift zones and define a single fissure segment but most commonly the rows consist of multiple fissure segments arranged en echelon (e.g. Thorarinnsson, 1981; Thordarson and Self, 1993; Connor and Conway, 2000; Thordarson and Larsen, 2007). The basaltic volcanoes include spatter, scoria and mixed cone rows, which are constructed by weakly to vigorously fountaining, lava producing eruptions and volcanogenic chasms (e.g. Head and Wilson, 1989; Martin and Nemeth, 2006; Thordarson and Larsen, 2007). Spatter and scoria cones are typically formed by small-volume fissure eruptions ($\leq 0.5 \text{ km}^3$) in a short period of time (e.g. Vespermann and Schmincke, 2000), as for example observed during the eruption of the Parícutin cone (México; e.g. Luhr and Simkin, 1993) and assumed for scoria cones in the San Francisco Volcanic Field (USA; Holm and Moore, 1987; Elson et al., 2002; Ort et al., 2008; Riggs and Duffield, 2008).

Scoria cones, the focus of this case study, occur in all tectonic settings worldwide are commonly distributed along fault zones and are grouped parallel or en echelon to the strike of the faults, and can be thus indicators for the current stress field (Vespermann and Schmincke, 2000) and

infer mechanisms of shallow dyke injection in active volcanic areas (Connor and Conway, 2000). As regards volcanic hazard, the threat of scoria cones is often overlooked (Ort et al., 2008). Scoria-cone eruptions are typically low in volume, and are the most common landforms on Earth (Ort et al., 2008). Scoria-cone eruption effects vary due to eruption style, tephra extent, types of land use, the culture and complexity of the affected area.

Flow localisation along a fissure and conduit formation is not well understood (e.g. Wylie et al., 1999; Quarení et al., 2001; Petrovic and Dufek, 2005; Diller et al., 2006; Gaffney et al., 2007; Michieli Vittuni et al., 2008). The transition from fissure eruption to localised vents during basaltic volcanism is often explained as a function of cooling in narrow portions of dykes coupled with enhanced flow in thicker portions, resulting in isolated, long-lived vents. Along the selected 6 km long fissure in north Iceland, volcanic eruptions focused on several crater cones. The inner structure of such systems is rarely exposed.

The presented study sheds light on the interior of a crater cone row and helps to understand the feeding features, propagation and localisation of the magma flow.

This work was submitted to Journal of Volcanology and Geothermal Research 2009 as: Reconstruction of a monogenetic basaltic cinder cone row in the rift zone of North Iceland: tectonic control on magma emplacement and eruption dynamics, N. Friese, F. A. Bense, D. C. Tanner, L. E. Gustafsson, and S. Siegesmund

6. Reconstruction of a monogenetic basaltic cinder cone row in the rift zone of North Iceland: tectonic control on magma emplacement and eruption dynamics

Nadine Friese¹, Frithjof A. Bense¹, David C. Tanner², Ludvik E. Gustafsson³, Siegfried Siegesmund¹

¹ *Department of Structural Geology and Geodynamics, Geoscience Centre, University of Goettingen, Goldschmidtstrasse 3, 37077 Goettingen, Germany*

² *Leibniz Institute of Applied Geophysics, Stilleweg 2, 30655 Hannover, Germany*

³ *Icelandic Association of Local Authorities, Borgartuni 30, 105 Reykjavik, Iceland*

Abstract

A 6 km long, early Holocene cinder cone row in the rift zone of north Iceland, which is partly exposed to a depth of 200 m along the Jökulsa a Fjöllum river canyon, is reconstructed in three dimensions by using a precise, non-stationary GPS to investigate the fault control on emplacement and eruption style. The en-echelon arranged monogenetic volcanic structures in the Fremrinamur Volcanic System, show intensive water-magma interaction. Spatter, welded breccias, scoriaceous lapilli, welded and non-welded deposits, and the occurrence of different bombs and rounded river gravel point to phreatomagmatic and transitional eruptions between Strombolian and Hawaiian lava-fountaining episodes. An initial magma flow emission (effusive fountaining phase) from the fissure was responsible for the distinctive multi-tiered

curvi-columnar entablatures and colonnades in the eroded Hljodaklettur area. The chain is marked by “cone-in-cone” formation that reflects the irregular shape of the conduits. The magma transport between the eruptive vents is dominantly horizontal. Reactivation of pre-existing NNW-SSE trending faults, underlying the volcanic fissure caused the eruption frequency to be time-lapsed and hence resulted in the observed en-echelon segmentation of the vents. As regards the early Holocene age of the cones, the volcanic deposits in the Fremrinamur Volcanic System might represent a spatial and temporal link between compound lava shield formation just after the Weichselian Glaciation and the later common central eruptive fissures in the volcanic systems.

6.1 Introduction

Monogenetic volcanoes that have erupted only once in their history, such as the Raudholar tephra cones in the northern rift zone of Iceland with a volume of 0.1–1 km³, demonstrate the minimum amount of magma that is required to create a channel through the lithosphere (Walker, 1993). Spatter and scoria cones are the result of purely effusive to weakly fountaining, short lived, small (≤ 0.1 km³) to medium (0.1–1 km³) fissure eruptions (Thordarsson and Larson, 2007). Scoria-cone forming eruptions are commonly associated with Strombolian-type activity (Houghton et al., 1999; Vespermann and Schmincke, 2000; Martin and Nemeth, 2006), but often show a great variety in eruption styles, ranging from gradual transition between Hawaiian lava fountaining to moderate and violent Strombolian-type mechanisms, driven by a reduction in magma ascent speed (Parfitt and Wilson, 1995).

The physical connection between dyke-conduit systems and their associated eruptive products is rarely preserved or reported (Atkinson and Lambert, 1990; Goto et al., 1990; Houghton et al., 1999). Cinder cones are mostly studied in active volcanic zones, where the feeding conduits are often covered by lava flows, and as abundant features in volcanic fields (e.g. Head and Wilson, 1989; Martin and Nemeth, 2006; Rappich et al., 2007; Keating et al., 2008).

The monogenetic Raudholar crater cones (Figs. 6.1, 6.2) offer the opportunity to study an upper cross-section through the

inner workings of a crater row in a volcanic rift zone. Due to erosion of a large part of the vent system by the Jökulsa a Fjöllum river (Fig. 6.2), the interior of the cones is exposed to a depth of 200 m. The aim of this paper is to describe the exposed early Holocene eruptive fissure and its deposits, reconstruct the scoria cone row in three spatial dimensions and to demonstrate the geological evolution in terms of the coeval stress field, and the emplacement and propagation of magma under a small edifice. Furthermore, the importance of the tectonic control and the interplay between pre-existing structures and fissure eruption is outlined. A detailed 3D mapping of the volcanic construct was necessary because of a rather inaccurate digital elevation model (DEM) of the area. The 3D shape of the plugs is used as a tool to determine the magma flow and segmentation, localisation of the eruptive centres and give evidence for cone formation.

6.2 Regional setting

In the Northern Volcanic Zone, rift-related structures and eruptive fissures are common, but early postglacial and interglacial lava shields are responsible for the major amount of lava (MacLennan et al., 2002). The NNE-trending volcanic system Fremrinamur (Figs. 6.1, 6.2) is around 160 km long and 17 km wide. Its central volcano is constructed on the basaltic Ketildyngja shield volcano and is overlain in turn by two lava shields (Johannesson and Saemundsson,

1998; Tentler and Mazzoli, 2005; Hjartardottir, 2008), which last erupted approximately 4000 years ago (Thorarinsson, 1951).

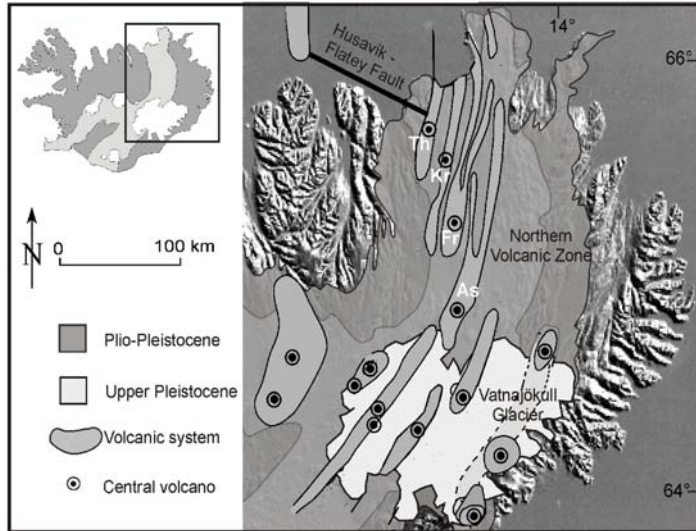


Figure 6.1: Geological map of the fissure swarms in Northeastern Iceland, after Johannesson and Saemundsson (1998). Encircled central volcanoes are: Th-Theistareykir, Kr-Krafla, Fr-Fremrinamur, and As-Askja. Background is a DEM of Iceland provided by the National Land Survey of Iceland.

The Fremrinamur Central Volcano contains a rhyolite extrusion and a prominent geothermal field (Sigurdsson and Sparks, 1978). It is a matter of debate which of the following eruptive fissures is assigned to the Fremrinamur system, as the Askja Fissure Swarm is so close by (Fig. 6.1). Whereas, for example, Tentler and Mazzoli (2005) attributed the fissures Kraeduborgir, Raudholar, Sveinar and Randarholar to the Fremrinamur system (Fig. 6.2); the Sveinar-Randarholar fissures were placed in the Askja Fissure Swarm by Johannesson and Saemundsson (1998) and Hjartardottir

(2008). In this paper, both the Randarholar and Raudholar crater cones are regarded as parts of the bifurcating Fremrinamur Volcanic System.

The Raudholar cones and its eroded southern part Hljodaklettur mark the easternmost branch of the Fremrinamur Fissure Swarm (Fig. 6.2, marked in red) and occur as fissure-aligned scoria cones. The approximately 6 km long crater row is aligned NNE, in and along the Jökulsargljúfur canyon, while its southern end bends slightly NNW, giving it an arcuate shape. The

unglaciated Raudholar scoria cones are situated along the narrow river canyon of Jökulsá a Fjöllum, a minor part of the cones are inside the canyon. As the cones underlie the Hekla tephra H5 deposits (dated to 7000 BP, Thorarinsson, 1971), the Raudholar eruption has an estimated early Holocene age of around 9000 years (Waitt, 2002 and references therein; Tentler and Mazzoli, 2005). It is associated with an intracanyon lava flow that fills an area of 2 km², just west of the prominent valley Vesturdalur (Fig. 6.2). The lava flow stratigraphy there shows that the Jökulsá river cut a canyon, nearly to present depth, before the Raudholar eruption.

The deposits surrounding the crater row, dating from the last interglacial, emanated mostly from shield volcanoes nearby, like for example, Grjóthals (Slater et al., 1998; Information Centre Jökulsargljúfur, Asbyrgi; Fig. 6.2).

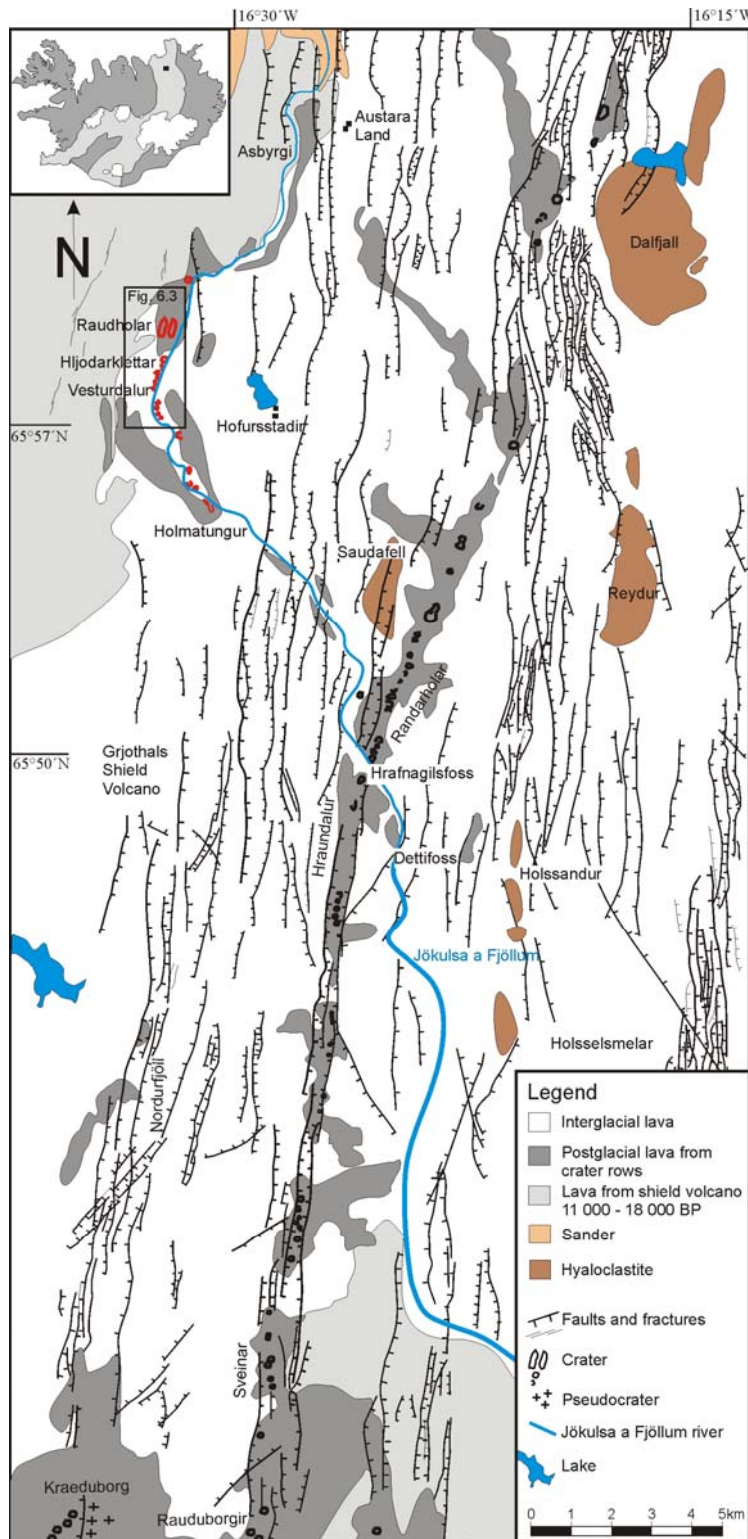


Figure 6.2: Detailed geological map of the northern part of the Fremrinamur Fissure Swarm modified after Sigurdsson et al. (1975). The studied Raudholar Cone Row and Hljodaklettur plugs are highlighted in red.

Hyaloclastite mountains and tillite deposits flank the eruptive fissure. The lava deposits east of the Hljodaklettur area have their origin in a 10 000 year old eruption from a shield volcano in the neighbored Theistareykir Fissure Swarm (Fig. 6.1; source: Information Centre Jökulsargljúfur, Asbyrgi).

A second, prominent NNE-trending crater row, the Randarholar-Rauborgir fissure, erupted slightly later, around 6000-8000 years ago (Thorarinsson, 1959; Sigurdsson et al., 1975; Tentler and Mazzoli, 2005; Fig. 6.2). This linear fissure chain is mainly controlled by (graben-bounding) normal faults, connected to the Fremrinamur Central Volcano. The lava poured northwards in a valley and joined with the lava of the Hljodaklettur eruption. The magma of both fissure eruptions is of primitive olivine tholeiitic composition.

It is assumed that the up to 120 m deep Jökulsa a Fjöllum canyon was excavated by gigantic glacial outburst floods (16 outbursts

were determined by stratigraphic methods near Vesturdalur; Waitt, 2002) that originated from the Vatnajökull Glacier to the south (Fig. 6.1). The best documented outbursts occurred in late Holocene (around 2500 BP), early Holocene (< 7100 BP),

Holocene (2900-2000 BP), and probably just after deglaciation 9000-8000 BP (Waitt, 2002; Alho et al., 2005 and references therein; Kirkbride et al., 2006). It has been argued that most of the Jökulsa canyon already existed in its present form before the Holocene series of floods, as the valley is cut into pre- to late glacial basalt (Kirkbride et al., 2006). A detailed canyon morphology, stratigraphy and glacial outburst history are described by Waitt (2002) and Alho et al. (2005).

6.3 Methodology

The Raudholar cones and eroded Hljodaklettur plugs were mapped with a non-stationary Trimble Pathfinder® Pro HX™ GPS system, including a 12-channel dual frequency GPS receiver, a Zephyr antenna, and a Ranger™ field computer, with an accuracy of 0.4 m in horizontal and 0.7 m in vertical direction, after post processing. The accuracy of mapping of the individual plugs in the field depended mainly on satellite availability and the geometry of the plugs. Mapped data of the plugs include the outline of the 3D structure of each individual conduit, data on individual dykes (including strike, dip, thickness), joints, scoria and hyaloclastite plane walls (contacts to the host rock), and faults in the vicinity of the crater row (Fig. 6.3A). Data were obtained by two different methods: point and line feature measurements. For a point measurement, a

structural feature is defined by a number of points with a known three dimensional position, and spatial orientation (strike and dip); dykes and contact to the host rock were measured in this way, for example. The second, line feature method, was used to map the complete outline of a plug or conduit, by continuously walking around and over the feature. The height of some inaccessible plugs was measured with a Silva levelling clinometer. Due to inaccessibility, the eroded area east of the Jökulsa a Fjöllum river could not be mapped (Fig. 6.3B, dashed lines), but is included in the overall interpretation of the cinder cone chain.

Inaccessible areas and overhanging parts of the geological structures were reconstructed with the help of aerial photographs in ArcGIS 9.1 and later added by hand in the 3D model of the crater chain. Aerial photographs at the scale of 1:30 000, a DEM of the area (cell size of 25 m) provided by the National Land Survey of Iceland, and several online available digital maps (National Land Survey Iceland) were used as a basis to plot field data and the individual plug outlines determined by the accurate GPS measurement. The digital maps and the DEM were also used for the 3D reconstruction and presentation of the crater row by modelling the point and surface structures using the software GoCad 2.0.8, 3D Move 5.0 and Move 2008.1 (Fig. 6.4).

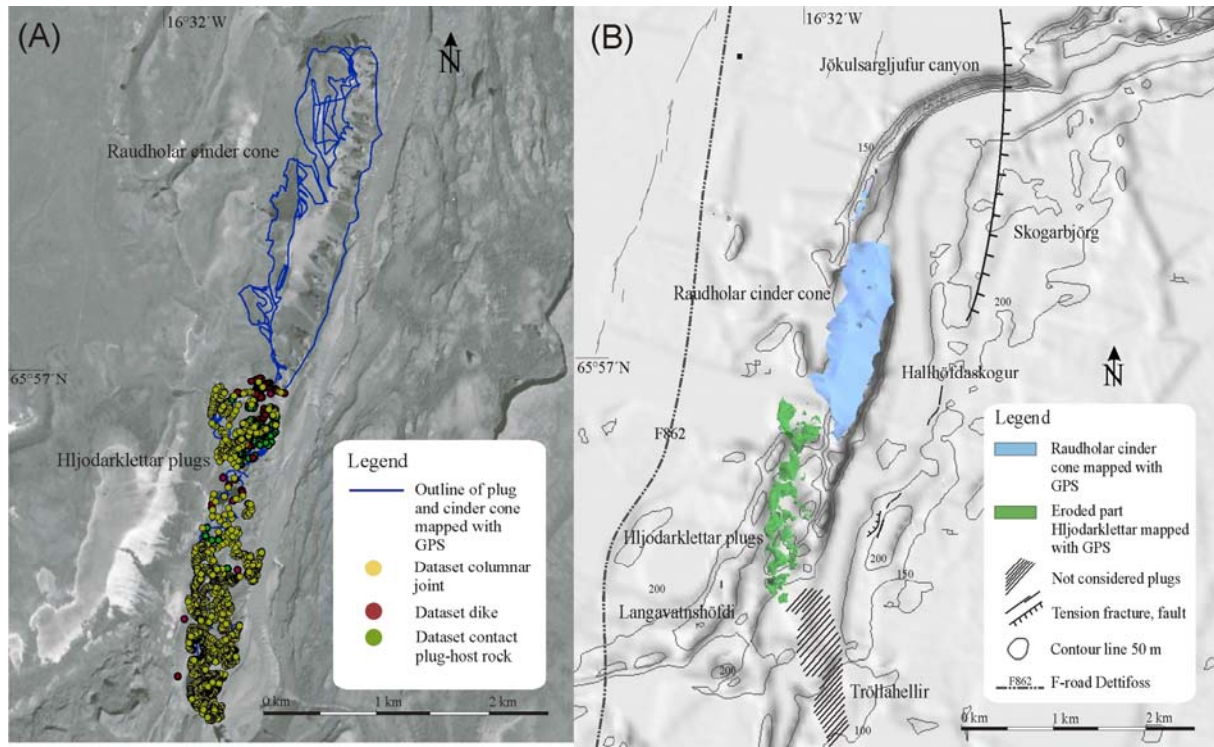


Figure 6.3: (A) Dataset of accomplished measurements in the field area. Two methods can be distinguished: point and line features (see text for further information). (B) DEM of the mapped area showing the reconstructed crater row in GoCad 2.0.8, as well as faults.

6.4 Results from the 3D mapping and reconstruction of the crater row

We inferred from the reconstructed 3D shape that the eruption vents were offset (left-lateral) and closely spaced, 50 m–300 m apart (Figs. 6.4B, C); the non-eroded Raudholar cones are spaced at 200 m in N-S direction and up to 800 m in E-W. The height of the plugs varies between 10 m–190 m and up to 205 m for the Raudholar cones (Fig. 6.4C). Several bigger plugs are flanked on their western side by small, aligned dyke conduits, which represent subsidiary vents or lava breakouts (Figs. 6.4B, C). The conduits are elongated in N-S direction, and are funnel-, horseshoe-, and irregular shaped, which indicates an overlapping of cones of the same age (Fig. 6.4C; see supplementary data,

Appendix CD). The lower cones merge at depth. From the shape of the intact cinder cone Raudholar we surmise that it consists of at least two buried, overlapping cones that may have resulted from a shift in vent location, or simultaneous activity at nearby vents on the fissure.

6.5 Raudholar and Hljodaklettur eruptive vents and deposits

The characteristics of pyroclastic deposits are influenced by factors like accumulation rate and cooling rate (Head and Wilson, 1989; Sumner et al., 2005). Among the studied eruptive centres, variation in the degree of welding in the eroded conduits of the volcanic edifice points to variable temperature conditions; weakly-welded

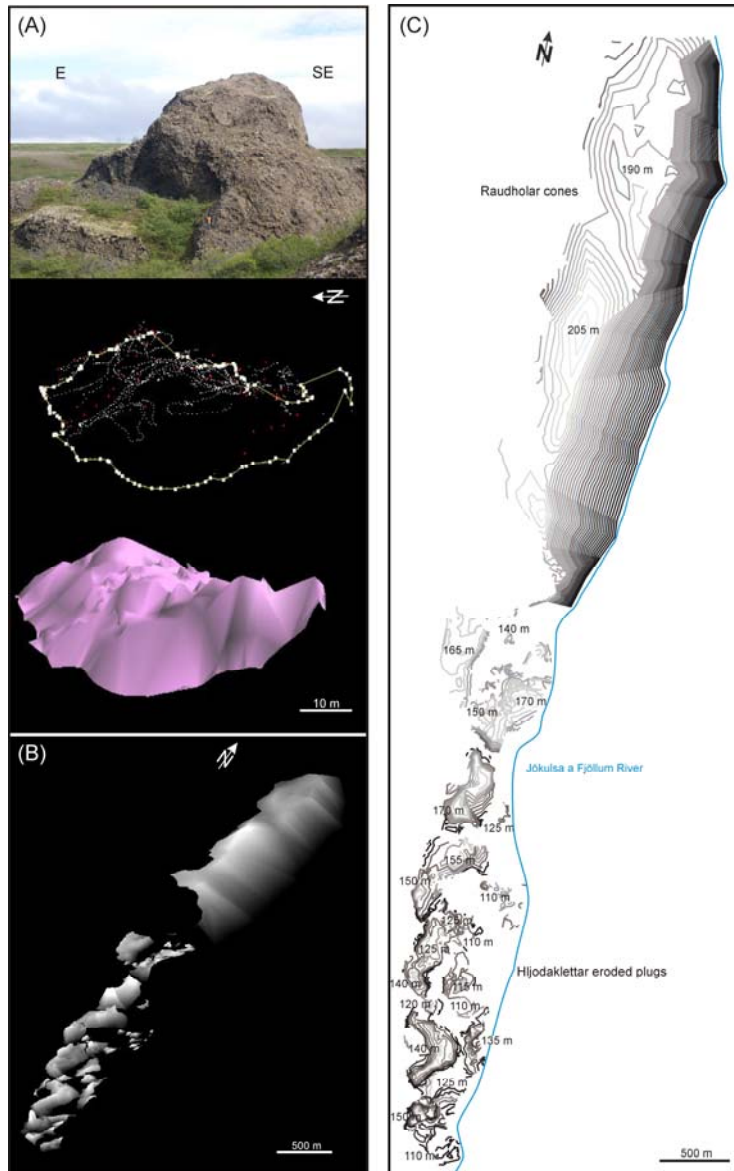


Figure 6.4: (A) Example of a mapped plug in the field, GPS data points and joint data were imported into GoCad 2.0.8. Point and line features were combined to a surface. (B) Complete reconstructed cone row that consists of 54 individual plugs and dykes measured with the non-stationary GPS system in the field. Oblique view. (C) Contour map of the crater cone, topology of the plugs is indicated by lines of different colours (dark–low altitude to light–higher altitude); each line represents 10 m in vertical section. The basic altitude of the area is at an elevation of 100 m, the river canyon has an average elevation of 50 m.

deposits represent low temperature deposits and agglutinated spatter beds point to a high temperature. Most common along the outcrop is an intermediate stage consisting of agglutinated spatters and non-flattened bombs. The deposits can be grouped by their size, shape of clasts and welding into (i) weakly welded, scoriaceous red and brown lapilli, (ii) twisted, fluidally-shaped, welded spatter and scoria, (iii) volcanic bombs, (iv) dykes and (v) lava flows.

6.5.1 Lithofacies of weakly welded, scoriaceous red and brown lapilli

The weakly welded, but well-sorted, red and dark scoriaceous lapilli-sized, fall-out deposits (Fig. 6.5) are only to be formed on the up to 205 m high and around 2 km long, 800 m wide Raudholar single spatter cone. This characterises the eruption as a discrete bubble outburst in the upper zone of the magma-filled conduit, partly interrupted by violent degassing of the near surface magma (Head and Wilson, 1989). The cone shows a coarse internal stratification and clasts-supported parallel, inward-dipping (angle of 20° - 50°) beds (Figs. 6.5A-C). Fine-grained black and red scoria ash units contain individual beds of massive, weakly-stratified scoria, as well as layers of ballistically-emplaced spindle bombs (Figs. 6.5B-E). Rootless lava flows, emitted

during an effusive episode, are embedded in loose scoria and spatter deposits in the cone (Figs. 6.5C-F).

6.5.2 Lithofacies of twisted, fluidally-shaped, welded spatter

Pyroclastic breccias and welded agglomerates (Figs. 6.6A, C), are exposed at the southern, eroded, steep part of the cinder cone Raudholar. The beds are rich in lava

bombs and welded vent breccia, and constitute the outer edifice wall (Fig. 6.6A). The agglutinated bombs, which have a diameter of up to 20 cm, are spindle and ribbon shaped. Welded deposits (Fig. 6.6B) along eruptive fissures and vent-forming spatter cones are dominant, rootless lava flows appear embedded in welded spatter (Fig. 6.6C).



Figure 6.5: Lithofacies of fallout deposits (A) Elongated Raudholar cinder cone. Pyroclastic beds are visible on the outer hinge, see person for scale. Jökulsargljúfur canyon is in the background. View to north-northeast. (B) View into eroded part of cinder cone. 1 m thick pyroclastic beds alternate with fall-out deposits. View to the northeast. (C) Inclined sheet above fall-out deposits ranging from scoria lapilli to smaller bombs, reflecting Strombolian-type eruption. View to the northeast. (D) Layered cinder-cone deposit. Scoria lapilli, fluidal-elongated small bombs and fragments of juvenile rocks. Compass for scale, (E) Layered cinder-cone deposit. Scoria lapilli, fluidal-elongated small bombs and fragments of juvenile rocks. Compass for scale, (F) Layered cinder-cone deposit. Scoria lapilli, fluidal-elongated small bombs and fragments of juvenile rocks. Compass for scale,

(continuation Figure 6.5) close-up view in E indicated by square. View to the north-northwest. (E) Close-up view of (D) showing scoria lapilli, fluidal small bombs and fragments of juvenile rocks. Compass for scale. (F) View north-northwest inside of the Raudholar cone, exposed by river outbursts. Columnar lava flow showing prominent entablature structure.



Figure 6.6: Lithofacies of welded spatter. (A) Welded agglutinates scoria fragments and bombs marking eruptive vent structures. (B) Welded lapilli and fractures building the resistant cone walls, signs for hot temperature and location for eruptive vent centres. (C) Lava flow over scoria breccia layer, embedding river gravel. View to the northeast.

6.5.3. Lithofacies of volcanic bombs

Volcanic bombs of all kinds of sizes and materials are present (Fig. 6.7) and give evidence of the eruption style, conduit composition and underlying rocks. Some rounded bombs are surrounded by scoria lapilli that are embedded on the bomb surface and indicate that still-molten bombs landed on the crater walls. Cored bombs are present (Fig. 6.7A), as well as fusiform (spindle shape) ones (Fig. 6.7B), angular tholeiitic

bombs (Fig. 6.7C) represent samples from the underlying basaltic lava flow in the canyon, as well as rounded, phenocryst-rich (plagioclase) fragments that originate from the nearby riverbed (Fig. 6.7D). The bombs, apart from river gravel, are only found at the base of Hljodaklettur; magmatic clasts are neither restricted to vertical nor horizontal sections of the eroded cones and implicate the contemporary activity of en-echelon volcanic segments.

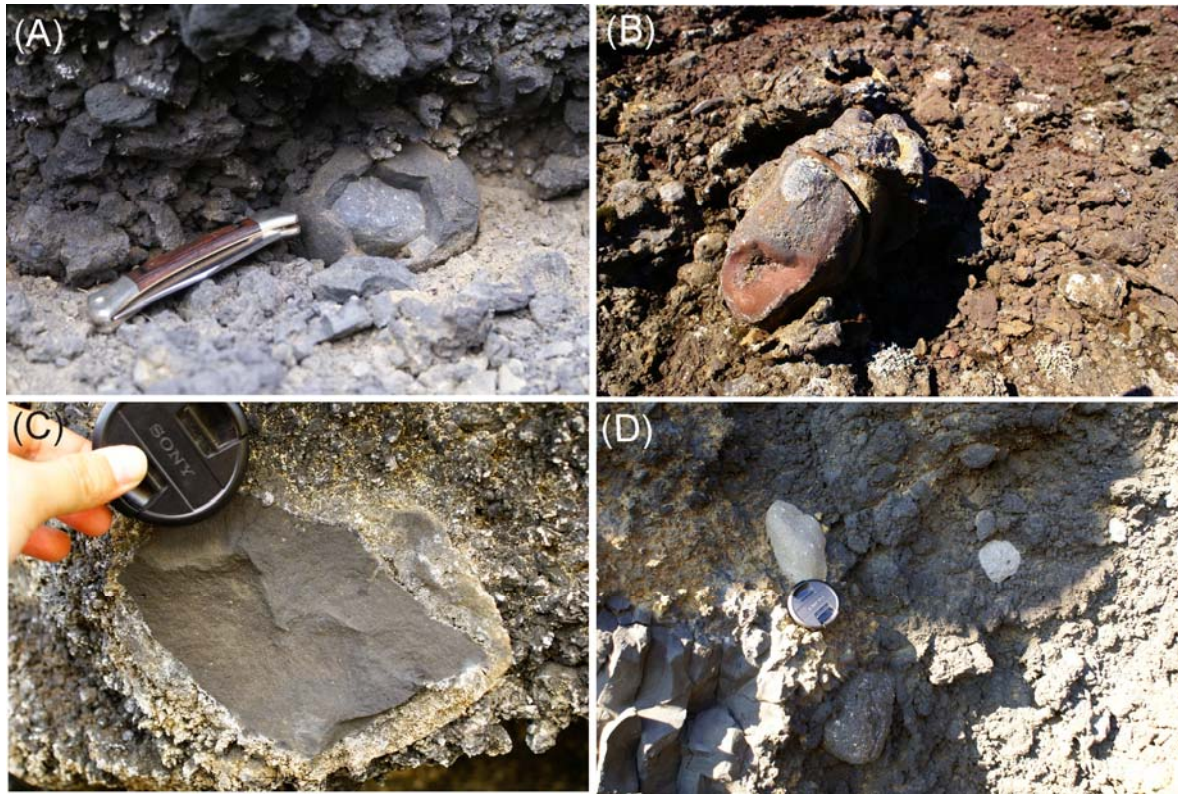


Figure 6.7: Lithofacies of volcanic bombs. (A) Cored bomb. River gravel bombs. (B) Elongated bomb on scoria cone. (C) Angular bomb with embedded molten scoria lapilli. (D) Rounded river gravel from nearby Jökulsa a Fjöllum river ballistically transported during phreatomagmatic eruption.

6.5.4 Dykes at the eroded part Hljodaklettur

A “transition zone” between the cinder cone and the exposed Hljodaklettur plugs is marked by the occurrence of numerous vertical dykes, which intersect each other (Figs. 6.8A, B). The geometry and widths of the cylindrical necks are remarkably constant (Fig. 6.8C); with increasing depth, they become elongated to a dyke form and are attached to the lava flows (e.g. Fig. 6.8D). Individual plugs are laterally interconnected by elongated plugs and narrow curving, vertically-jointed dykes, around 1-3 m thick. Funnel-shaped necks represent the convergence and intersection point of several dykes, since surrounded by individual dykes (Fig. 6.8A).

Within the plugs, the main transport is inferred to be lateral (Figs. 6.8A, B, D). One up to 5 m thick, NNE-SSW striking (feeder) dyke can be followed throughout the eroded outcrop and marks one of the major magma pathways that connect the plugs (Fig. 6.8A, dashed line). The dykes have a minimum thickness of 5 cm and coalesce to form thicker, multiple intrusions. The contact surfaces reveal typical brittle deformation structures such as breccias, tension gashes, and aligned vesicles (Figs. 6.8E, F) that point to a magma flow towards the individual conduits and a horizontal propagation of the magma flow.



Figure 6.8: Dykes and flow indicators. (A) View south, away from the cinder cone Raudholar. Some dykes (around 4 m-6 m wide) can be followed throughout the whole outcrop connecting single plugs (marked with dashed line) (B) Dykes marking the “transition zone” between plug dominated, eroded Hljodaklettur and Raudholar cinder cone. View NNW. Dyke-walls are approximately 15 m-20 m high. (C) View north-northwest into the labyrinth of plugs. Major plugs are always accompanied by smaller lava vent/breakouts on their sides. Person for scale. (D) View southeast to dykes next to river Jökulsa a Fjöllum, exposed underneath an eroded cone. Plugs are up to 40 m high. (E) En-echelon, sigmoidal-shaped cracks. Pencil for scale (F) Elongated, elliptical voids trace the magma flow path. Compass for scale.

The outer margins are covered with hyaloclastite breccia and scoria remnants (Figs. 6.8A, B). During flow of the magma, shearing occurred and caused a preferred orientation of platy crystals, flattening and elongation of gas bubbles parallel to the shearing surface (trachytic texture or foliation; see Fig. 6.10). The feeder dykes have sharp contacts to the overlying scoria and spatter deposits, and show chilled margins.

6.5.5 Lava flows at the eroded part Hljodaklettur

Columnar joints show a multi-tiered structure with a clear distinction into colonnade and entablature (Figs. 6.9A, C). The chaotically-jointed entablature (Fig. 6.9B, D) is marked by the occurrence of pipe vesicles, vesicle cylinders, and big spiracles (Fig. 6.9D). The largest amount of pahoehoe lava was discharged at the beginning of the cone-building episode (effusive fountaining episode), but rootless lava flows are also embedded in scoria and spatter deposits (Figs. 6.5, 6.6). Lava tubes (Fig. 6.9E) build prominent underground galleries. Prismatic joints in the colonnade (Fig. 6.9F) have striations (chisel structures) parallel to the cooling surface, which show crack initiation and arrest (Dance, 1997; Lyle, 2000 and references therein).

Thin sections (Fig. 6.10) to investigate the composition and texture were made from basaltic lava flows. The most frequent association of phenocrysts are plagioclase-olivine-clinopyroxene, with a high amount of glass in moderate vesicular lava flows (Figs. 6.10A, B) and agglutinates of opaque minerals that occur in the bombs. The variolitic basalt is a primitive olivine-tholeiite, showing corroded, subhedral to idiomorphic crystals with a serpentinitized network (chrysotile), emanating from the crystal edges, and partial replacement by iddingsite (pseudomorphic transformation of olivine; Figs. 6.10C, D). Skeletal plagioclase needles intergrown with olivine imply a high cooling rate of the lava flow (Lofgren et al., 1974; Fig. 6.10C).

Plagioclase is common in the groundmass and as subhedral, albite-carlsbad twinned crystals with oscillatory zoning (Fig. 6.10E). The fine-grained, holocrystalline groundmass is mainly represented by fanning intergrowths of skeletal plagioclase and dendritic clinopyroxene and glass (tachylite, sideromelan and its alteration product palagonite; Figs. 6.10A, B). Magma flow structures traced by oriented plagioclase lattes are common (Fig. 6.10F). Corroded and serpentinitised olivine implies alteration, plagioclase needles point to quick cooling and hence a reaction with water.

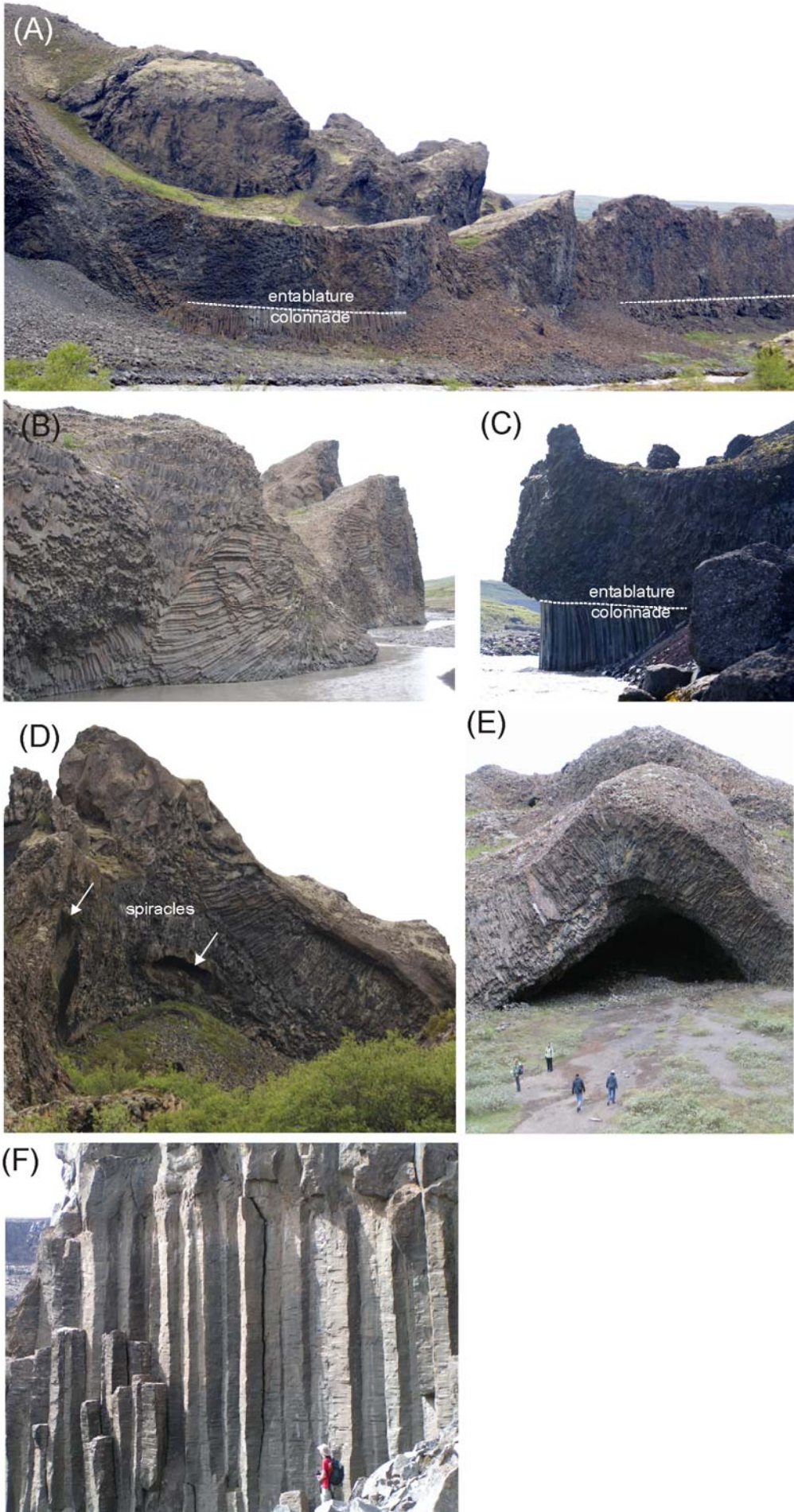


Figure 6.9 overpage: Lava flows. (A) Clear distinction between colonnade and entablature in the lava flow. Wall is around 15 m high. (B) Chaotic curvi-columnar joints of the entablature dominate the shape of the approximately 10 m wide necks. (C) Close-up view of 3 m high colonnade and entablature. (D) The entablature shows large spiracles (up to 5 m wide) that were filled with loose hyaloclastite material which has been eroded. (E) Lava tube in Hljodaklettur, the place is known as the “church”. Persons for scale. (F) Striations in vertical columnar joints in the lower colonnade marks joint growth and arrest (picture taken in the Sveinar fissure lava flow, south of Hljodaklettur). Person for scale.

6.6 Reconstruction of the eruption style

Elongated scoria cones that are built above fissures have a more complex subvolcanic vent system and are common in well-drained basaltic settings (Vespermann and Schmincke, 2000). The occurrence and eruption mechanisms give information about the paleoenvironment and sub-surface hydrology during the time of cone formation (Risso et al., 2008). A topographic profile (Fig. 6.11A; marked A-A', located in Fig. 6.3A) in direction 194° along the main vents of the linear cone row show a multiple vent activity (Fig. 6.11) indicated by a “cone-in-cone” geometry. This implies a horizontal magma transport direction (towards north as shown by deformation structures in the dykes), while the “fingers” that reach the surface now represent the eroded plugs.

The initial, vent-clearing, phase was a relatively short-lived phreatomagmatic eruption at shallow depths close to the river aquifer (Figs. 6.11B, C). Well-rounded river gravels and juvenile fragments were ballistically ejected and are found at various locations at the eroded base at Hljodaklettur. In the next stage, lava flows were emitted and formed the now prominent colonnade and entablature features of Hljodaklettur. A

variety of joint geometries (e.g. hexagons and polygons) have been documented in the field area, reflecting different cooling rates (Dance, 1997). Toramaru and Matsumoto (2004) carried out analogue experiments and found out that low order, polygonal-shaped joints are related to higher cooling rates, whereas at lower cooling rates, hexagons dominate. DeGraff and Aydin (1987) pointed out that colonnade joints propagated upwards from the lava base, while those of the entablature propagated downwards from the surface. The darker and more fine-grained “pitchstone or vitrophyre” are related to the faster cooling rate in the entablature (Saemundsson, 1970). The petrography of the olivine-plagioclase tholeiite (Fig. 6.10 see above) points to a high cooling rate.

The irregular top of these volcanic features is due to emplacement below its own cinder accumulation (Walker, 1993). The distinctive curvi-columnar entablature formed by water seepage into the lava interior (Lyle, 2000). Hyaloclastite breccia horizons are present at the outer margins of the magma flow and dykes, indicating that most lava flow interacted with water.

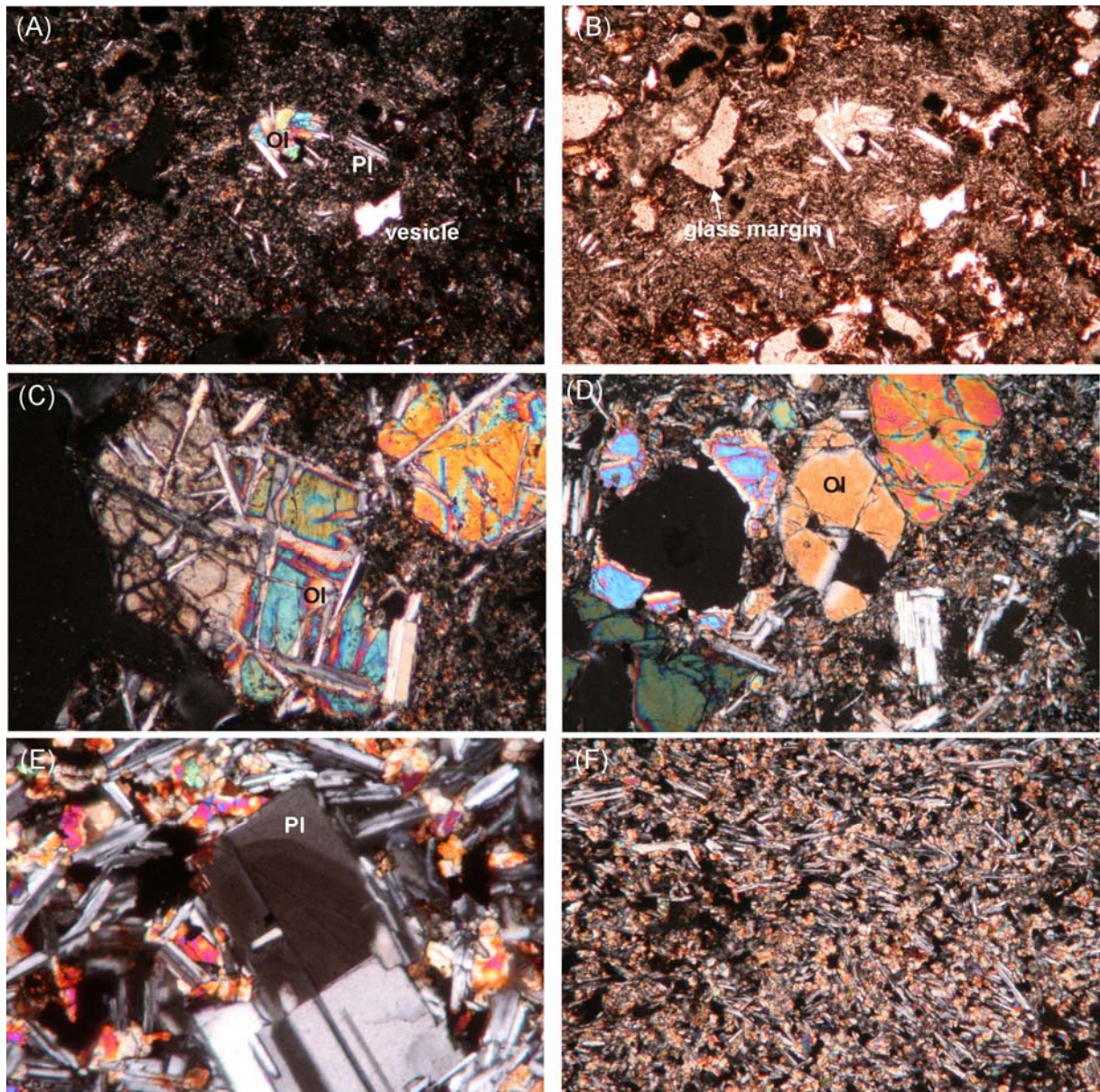


Figure 6.10: Thin sections of tholeiitic basalt from the field area. (A) Vent breccia containing fragments of tholeiitic basalt (olivine and plagioclase phenocryst embedded in microcrystalline, variolitic skeletal plagioclase in pyroxene groundmass), silicified glass rinds (brown colours) surround elongated segregation vesicles. Plane-polarized light, base of photo 1.8 cm. (B) Same view as in (A), crossed nicols. Interstitial brown basaltic glass is present. (C) Roundly-corroded olivine crystals with secondary plagioclase needles in tholeiitic fluidal bomb. Plane-polarised light, base of photo 9 mm. (D) Rounded embayment having their origin in magmatic corrosion that point to unstable conditions. Plane-polarized light, base of photo 9 mm. (E) Simple twinned plagioclase phenocryst with oscillatory zoning in the upper half of the crystal, surrounded by glomerophyric, skeletal, plagioclase needles and clinopyroxene (augite and pigeonite). Plane-polarized light, base of photo 9 mm. (F) Clusters of fine interstitial plagioclase needles intergrown with clinopyroxene in a microcrystalline groundmass of tholeiitic host rock exposed in the Jökulsa a Fjöllum canyon. Plagioclase shows slight magma flow alignment. Plane-polarised light, base of photo 1.8 cm.

Saemundsson (1970) and Long and Wood (1986) concluded that entablature jointing is the result of quick cooling of the upper part of the lava flow as the still hot flow surface becomes flooded by (river) water. The eruption environment favoured lava ponding and damming that resulted in a diversion of the river and induration of the lava flow surface (Saemundsson, 1970; Lyle, 2000).

We postulate that the eruption style was transitional between Strombolian and Hawaiian lava fountaining (Fig. 6.11D), which arose from an intermediate ascent of magma (Parfitt and Wilson, 1995). The agglutinates and spatter-rich tephra suggest that lava fountains may have erupted continuously (Wolff and Sumner, 2000). The Strombolian-style differs from the Hawaiian by the absence of glass fragments and the abundance of fine-grained tephra and non-welded clasts, whereas lava fountaining phases consist of larger portions of spatter (Vergnolle and Mangan, 2000; Parfitt, 2004; Bertotto et al., 2006). Spindle and fluidal spatter fragments, often welded together, were ejected from several contemporaneously active conduits. The lower facies of the eroded cones show a variety of coarse-grained, ragged ejecta.

The large variety in clasts (different vesicularity, density, shape) points to an extension of the vent system along the fissure, and hence to unstable discharge rates in magma and a varying extent of magma/water interaction between the vents

(Houghton et al., 1996, 1999). Alternating beds of welded and non-welded, fine- and coarser-grained lapilli are common (exposed on Raudholar cone), which show distinct inward-dipping bedding, and suggests repeated explosion driven by magmatic degassing in an open conduit. Deposits of well-sorted and rounded scoriaceous lapilli on Raudholar indicate that the final phase was Strombolian through a wide, unblocked conduit. Small lava flows (0.5 m thick) are embedded in Strombolian and Hawaiian-type related deposits. The lack of ash layers is explained by (1) an inferred low degree of fragmentation during Strombolian and Hawaiian eruptions (Chester et al., 1985; Vergnolle and Mangan, 2000) and (2) by the quick erosion after deposition, especially in an area characterised by numerous glacial outbursts (Fig. 6.11E).

A complex mixing of ejecta from different vents along the feeder system is typical for basaltic explosive eruptions (Self et al., 1980; Houghton et al., 1999). Together with a prominent linear arrangement of vents, it points to magma that intruded at shallow levels. Contrasting eruptive products and eruptions at various points in space and time are common (e.g. Walker et al., 1984; Thordarson and Self, 1993; Risso et al., 2008) and are caused by e.g. contrasts in the architecture of the fissure (elevation differences), development of local ponds and a non-uniform width of the conduits (Houghton et al., 1999).

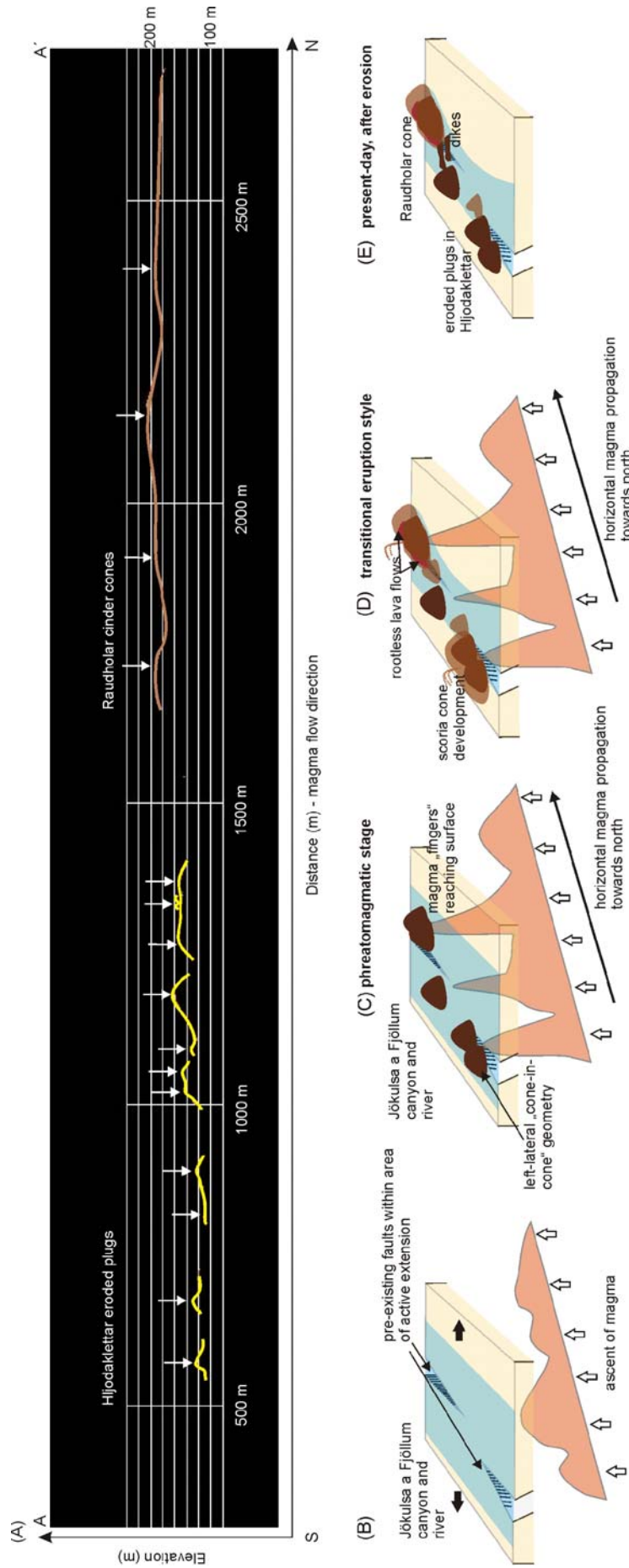


Figure 6.11 overpage: (A) Topographic profile (A-A') in N-S direction (194°) along the Raudholar Cone Row (see Fig. 6.3 for location). The z grid is 20 m beginning with an elevation of 80 m to 240 m; the x grid is 500 m. Arrows point to vents and thus feeder dykes as constrained by vent locations. (B) Initial stage before the eruption. Faults underlie the Jökulsa a Fjöllum canyon and river. (C) A phreatomagmatic eruption creates first deposits, where magma fingers reach the surface. The magma flow direction is assumed to be horizontal. The eruption produces left-lateral cones that present the now-eroded Hljodarklettur plugs. (D) The main eruption stage is transitional between Hawaiian lava fountaining and Strombolian eruption and produces scoria cones and rootless lava flows on top of the phreatomagmatic deposits. The river is partly dammed and diverted. (E) After erosion and glacial bursts, parts of the cone row are exposed, whereas the more northerly cones are intact.

6.7 Discussion

6.7.1 Structural control on eruptive fissure location

The Raudholar crater row is distinctly different compared to other eruptive fissures in the Northern Volcanic Zone. While the 70 km long, younger Randaholar fissure is located over wide areas inside a well-developed graben system, the Raudholar cones seem to lack a connection to superficial faults. Normal faults are numerous on the western and southern side of the crater row, which show a prominent downthrow to the west (Sigurdsson et al., 1975; Fig. 6.2).

The 3D model (Figs. 6.3, 6.4, additional movie in appendix), field observation and geological maps imply that crater cones at Hljodaklettur are segmented in a sinistral en-echelon manner, which follow the trend of the river canyon. For eruptive fissures located at rift zones, spreading stresses have been put forward as a cause of segmentation (Klügel et al., 2005) either by segmentation of individual dykes within the upper crust or by rotation of

subvertical axes during upwards propagation. The observed en-echelon arrangement indicates a time-lapsed eruption history along individual segments. This implies dyke segmentation (similar to observation during the Laki 1783 eruption, Thordarsson and Self, 1993; and Krafla rifting episode, Buck et al., 2006) at shallow depth from a main fracture/magma chamber or above lateral magma flow, controlled by slightly-changing regional stress field, under a small, developing volcanic edifice (Pinel and Jaupart, 2004) or/and due to oblique extension of the area (DeMets et al., 1994; Clifton and Schlichte, 2003).

In comparison with existing fault systems (Figs. 6.2, 6.12) surrounding the eruptive fissure, we suggest that the pre-existence and/or formation of en-echelon arranged faults, underlying the river, played a major role during fissure eruption. The cones thus follow the segmented fault trace (Connor and Conway, 2000). The presence of some conjugate NW-SE striking faults is evidence of a complex stress field pattern in the northern study area. The bending of the

eruptive fissure might reflect the meeting of two fault systems in the area, a NNE-SSW direction, similar to faults in its southern continuation that developed around 9000-8000 years ago (Sigurdsson et al., 1975; Sigvaldason et al., 1992), and a younger fault system striking NW-SE cross-cutting the older ones. The variation in strike might be connected to a change of the axial rift zone from NNE in the vicinity of the Vatnajökull glacier to N on the north coast of Iceland and, secondly, a far-field influence from the Tjörnes fracture zone (Sigurdsson and Sparks, 1978; Rögnvaldsson et al., 1998).

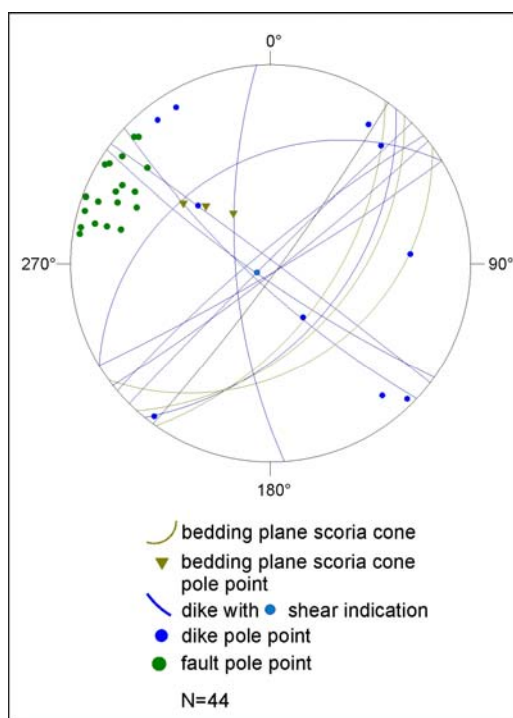


Figure 6.12: Stereogram of structural data in Raudholar and Hljodaklettur. Equal area projection, lower hemisphere. Great circles show surfaces and kinematic indicator. Isolated dots represent poles of fault and dike orientation, and the triangles are poles to bedding planes on Raudholar cone.

As most of the conduits are cylindrical in shape once they became established, the maximum horizontal compression was radial and the minimum horizontal compression circumferential, thus σ_1 was subvertical and σ_3 was subhorizontal in the fissure swarm. The surface-near, exposed plugs show the dominant influence of the stress field, since the maximum principal stress σ_1 is responsible for the larger superficial opening of conduits. However, the overall tectonics (Fig. 6.12) shows a dominant NNE-SSW structure, with σ_H parallel to the rift axis.

6.7.2 Plumbing system of the eruptive fissure

Although only the first two hundred metres of the shallow feeding system of dykes and conduits of the Raudholar-Hljodaklettur row are exposed, field observations of the inner workings of the conduits suggest that magma transport was mostly vertical with lateral offshoots in the fissure interconnecting the individual plugs. Dykes below 250 m are not exposed in the working area. Further south, in the Sveinar Graben, which belongs to the 70 km long Raudholar fissure, a slightly-deeper feeding system and the connection to the overlying cone is exposed in three dimensions (Fig. 6.13; Gudmundsson et al., 2008; Chapter 7). We use this outcrop as an analogue for the cones of Raudholar, as the formation and tectonic setting are comparable. Combining both areas, we conclude that the transition between tabular dykes to cylindrical flaring

conduits was gradual and started in the upper exposed 100 m-50 m of the vent system, similar to results and field observation by Keating et al. (2008). The width of the feeder dykes is about 4 m-12 m at depth to 200 m (outcrop Raudholar-Hljodaklettur) and decrease with depth, as observed at the Sveinar Graben.

6.7.3 Magma source and vertical versus horizontal magma flow in the fissure swarm

The age of the Raudholar-Hljodaklettur fissure eruption (around 9000 years) can be correlated with higher magma productivity after the Weichselian Glaciation (10 000-7000 a BP; MacLennan et al., 2002). With regards to the age and the remote location of the Raudholar fissure at the branch of the fissure swarm, the cone row might be temporally related to the formation of compound lava shields in the area (Sigvaldason et al., 1992). Both, lava shields and fissure eruptions, have similar formation histories (Rossi, 1996) and their magma source is at the deep roots of the crustal-mantle boundary, with vertical-feeding channels supplying them with magma. Volcanic activity in the last 7000 years was dominantly fissure eruption (MacLennan et al., 2002), located in central segments of the volcanic systems. We therefore assumed that the formation of the Raudholar-Hljodaklettur

fissure marks an intermediate step between the high eruption rates after Weichselian Glaciation between 10 000–7000 BP and the dominant fissure eruptions after 7000 BP. Phreatomagmatic eruptions are enhanced, not only by the location in proximity of the Jökulsa a Fjöllum river, but after the ice retreat, a higher groundwater level is postulated as well (Sigvaldason et al., 1992), suggesting shallow magma fragmentation. Magma transport along fissure swarms is often described as a horizontal process from a magma chamber underneath a central volcano, as observed and monitored in other swarms, such as Krafla and Grimsvötn (Thordarson and Self, 1993; Buck et al., 2006; Paquet et al., 2007). The long, discontinuous crater row of the Holocene Randaholar fissure probably has its origin in a rifting episode of the Fremrinamur Volcano.

In contrast, the Raudholar cones represent a single eruptive event, unconnected to the 70 km long Randarholar eruptive fissures. However, further geochemical sampling of fissures, lava flows of similar age and the lava shields in this area is needed to clarify the source of magma and hence the deep magma movement.

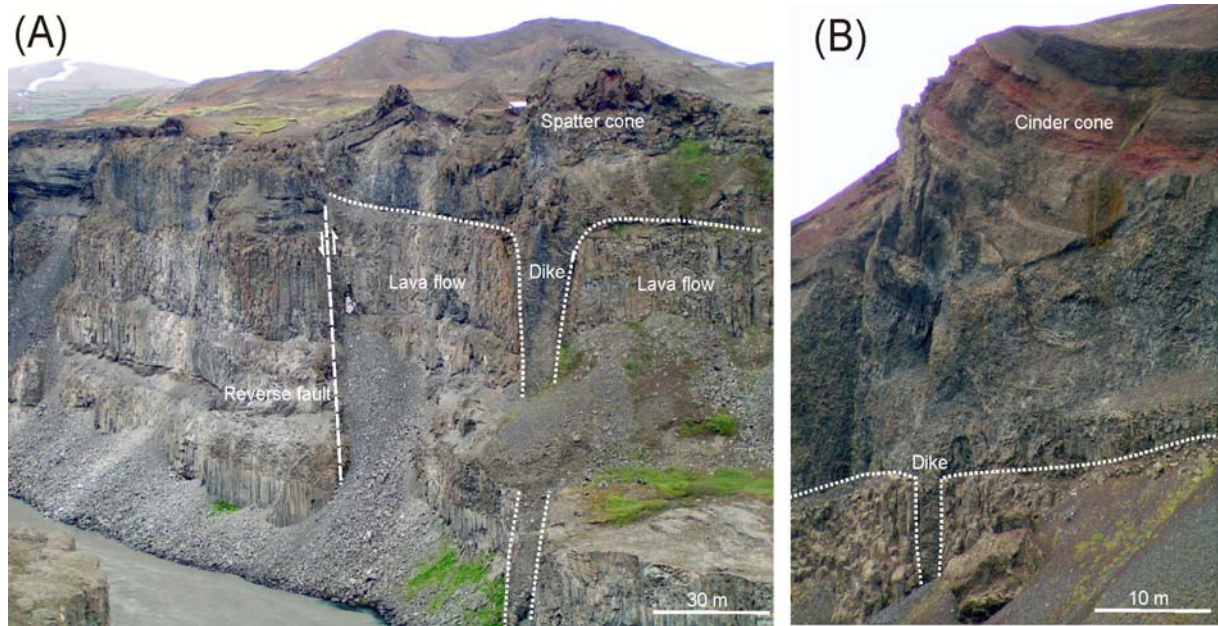


Figure 6.13: Field example of Sveinar cone row, southwest of Raudholar Cone Row. (A) Dyke in Sveinar Graben widens near the surface and feeds a spatter cone. View is north across the Jökulsargljúfur canyon. (B) Dyke feeding basaltic lava flow. View northwest.

6.8 Conclusions

The 6 km long roughly NNE-trending Raudholar-Hljodaklettur fissure is divided into left-lateral arranged segments, dominated by (eroded) remnants of scoria cones. Detailed field studies and GPS mapping of the crater row allow us to reconstruct the eruption and to evaluate the reasons for its location and shape. The eruption began with a short-lived phreatomagmatic phase as magma came into contact with the Jökulsá river. Evidence for this is the multi-tiered, columnar basaltic lava flow (curvi-columnar entablature and colonnade), hyaloclastite breccia and rounded gravel, which have their source in the river bed. The main eruptive episode was transitional, between Strombolian-type eruption, that produced spatter ramparts,

partly-welded deposits and fluidal bombs, and an Hawaiian lava fountaining phase, that produced cinder cones, among them the Raudholar cone, with well-sorted, bedded, scoriaceous lapilli and embedded rootless lava flows. The linear arrangement, multiple vents and mixed ejecta resulting from a change in eruption style point to shallow-seated controls on degassing and magma fragmentation in the short-lived vents. Data collection shows a dominant NNE-SSW structure, with σ_H parallel to the rift axis.

The monogenetic Raudholar fissure is located on the outer branch of the Fremrinamur Fissure Swarm, controlled by pre-existing (reactivated) or newly-formed NNE-SSW trending faults. Faulting and an inferred time-lapsed eruption history are

responsible for the en-echelon segmentation of the 9000 year old eruptive fissure. Due to its remote location, on the outer rim of the fissure swarm and without any observed evidence for a connection to the Randaholar-Sveinar fissure, the magma source is assumed to be the crust-mantle boundary. Flow indicators point to horizontal magma transport between the eruptive vents along the fissure. A gradual transition from tabular dykes to cylindrical flaring conduits, starting in the upper exposed 100 m-50 m of the vent system, is observed. Whereas the Randaholar fissure marks a typical “central volcano-eruptive fissure connection”, the Raudholar cones represent individual eruptive segments, temporally connected to a glacial rebound effect and enhanced mantle melting in early Holocene times.

Acknowledgements

We are grateful to the managers S.S. Jóhannsdóttir and Th. Hymer and the staff of the Jökulsargljúfur National Park for their kind permission to work in the Hljodarklettur area and support during our field studies. Especially the Rangers Jóna and Kristin are thanked for their company in the Ranger House and introducing to us the cultural highlights in Asbyrgi. A. Höskuldsson is acknowledged for help with the literature research, and S. Steinþórsson for support with formalities at the beginning of the field work. We thank S. Burchardt and M. Hartley for very helpful discussions. We are grateful for the financial support from the Structural

Geology and Geodynamics Department of the University of Göttingen. Midland Valley is acknowledged for providing a free educational license for their software Move 2008.1.

7. Dyke-induced reverse faulting in a graben—case study Northeast Iceland: preface

Extension of the Earth's lithosphere at rift zones can result in both faulting and magmatism. Within rifts, dykes may accommodate an equal or possibly larger proportion of strain than is accommodated by normal faults (e.g. Ebinger and Casey, 2001; Buck et al., 2006; Keir et al., 2006; Rowland et al., 2007; Ebinger et al., 2008). The process of dyke intrusion and strain partitioning between faulting and magmatism remains poorly understood, because magma rarely reaches the surface and surface deformation is interlinked with faulting triggered by dyke intrusion (e.g. Rubin and Pollard, 1988; Rubin, 1992; Bursvik et al., 2003; Gudmundsson and Loetveit, 2005; Calais et al., 2008).

Dyking events result in localised extension marked by intensive swarms of earthquakes, with or without effusive volcanism (e.g. Einarsson and Brandsdottir, 1980; Rubin et al., 1998; Buck et al., 2006). Thus earthquake swarms and geophysical measurements (e.g. InSAR, satellite geodetic techniques) allow to estimate vertical and lateral migration of magma during tectono-magmatic episodes and the response of the plate to stresses induced by dyke intrusion (e.g. the 9-year Krafla rifting period in Iceland; e.g. Sigmundsson, 2006; Afar rift, Africa; Ebinger et al., 2008).

Active magma reservoirs are known to trigger faulting in their vicinity (e.g. Walter

and Troll, 2001) in normal and reverse slip directions (e.g. Gargani et al., 2006; Hampel and Hetzel, 2008). The stress transfer between volcanic activity and dyke intrusions may enhance or suppress seismicity (e.g. Troise, 2001; Bursvik et al., 2003; Walter and Amelung, 2004) whereas dyke intrusion itself may be aseismic (Ebinger et al., 2008). In rift zones, lateral dyke intrusion at shallow levels can trigger normal faulting and subsidence (Brandsdottir and Einarsson, 1979; Sigurdsson, 1980; Saemundsson, 1992). Observations of dyke intrusions, which cause fault slip have been reported e.g. at Kilauea volcano, Hawaii, and demonstrated by field observation and InSAR data revealing coeval slip on a normal fault system (Cervelli et al., 2002). Dyke-induced deformation and graben formation is not only constricted to the terrestrial surface but can be found on other planets, e.g. Mars (e.g. Ernst et al., 2001; Schultz et al., 2004; Goudy and Schultz, 2005; Wyrick and Smart, 2008).

Existing (volcano-tectonic) grabens in rift zones may capture upward-propagating dykes (e.g. Gudmundsson and Loetveit, 2005). Rubin (1992) demonstrates a relationship between displacement on boundary faults with dyke emplacement at depth by models of matching data from the Krafla event in 1975-1984, Iceland, as well as experimental models by Mastin and Pollard (1988). They showed that faults far from the dyke are within a zone of dyke-induced compression and are effectively

locked during the dyke event, whereas faults that would intersect the dyke close to its top will slip until they intersect the dyke at depth. Gaffney et al. (2007) state that dyke capture by faults is most common at high angle faults and restricted to shallow depths. Dyke-induced faulting at oceanic spreading centres is assumed to be responsible for narrow (10m-100 m) grabens (e.g. Chadwick and Embley, 1998; Carbotte et al., 2006). Thus, observed dyke-induced graben displacements, not only in Iceland, best fit with dyke- and normal fault-induced displacements, instead of dyke-induced displacements alone (Rubin and Pollard, 1988).

One of the key questions in the formation of volcano-tectonic grabens is, whether the boundary faults already existed before the eruption and thus captured the associated dyke, or if the feeder dyke was responsible for the graben formation. Several examples from Iceland, e.g. during the Krafla unrest events in 1975-1984 (Rubin, 1992; Rubin et al., 1998), in the Thingvellir Graben, western rift (Bull et al., 2003), and in the Laki fissure (Gudmundsson et al., 2007) indicate that dykes may have been captured by (boundary graben) faults and subsidence occurred ahead of a laterally propagating dyke. This adds additional mechanisms for seismic components of volcanic risk assessment along with fault motion due to transient stresses around a propagating dyke top (e.g. Rubin and Pollard, 1988; Rubin, 1992; Chadwick and

Embley, 1998) and due to magma-induced stress changes along parts of faults (e.g. Parsons et al., 2006).

In the following example, the focus is on normal fault-dyke interaction in the northern rift zone of Iceland. Field observations and a two-dimensional numerical model suggest that dyke emplacement can cause reverse slip due to dyke overpressure exerting horizontal compression along a nearby normal fault, rather than generating a graben or triggering normal fault slip on the existing boundary graben faults.

Numerical models are a helpful tool to simulate physical problems and to simplify complex geometries with heterogeneous material properties. Numerical models are divided into boundary-element (BEM, Brebbia and Dominguez, 1992), discrete elements (e.g. DEM, Egholm, 2007) and finite- element (FEM, Logan, 2000) models whereas the difference between them is the way of discretisation of a problem in either volumetric or surface elements. To run a numerical model, the boundary conditions have to be known, i.e. the inferred geometry of the feature, the thickness of the model layers, the applied stress field, and the mechanical properties of the rock and its surrounding layers (most commonly Young's modulus and Poisson's ratio; Hudson and Harrison, 1997). The BEM, as used in the following study, gives accurate solutions for boundary problems, like surface stresses.

This work has been published as: Gudmundsson, A., Friese, N., Galindo, I., Philipp, S.L., 2008. Dyke-induced reverse faulting in a graben. Geology 36, pages 123-126.

7. Dyke-induced reverse faulting in a graben

Agust Gudmundsson¹, Nadine Friese¹, Ines Galindo², Sonja L. Philipp¹

¹*Department of Structural Geology and Geodynamics, Geoscience Centre, University of Göttingen, Goldschmidtstrasse 3, D-37077 Göttingen, Germany*

²*Instituto Geológico y Minero de España, Oficina de Proyectos de Las Palmas de Gran Canaria, Alonso Alvarado, 43, 2^ªA, 35003 Las Palmas de Gran Canaria, Spain*

Abstract

Normal-fault slip of the boundary faults of a graben is commonly attributed to dyke-induced stresses. Here, however, we report for the first time clear field evidence of a large dyke-induced reverse-fault slip on a fault associated with a volcano-tectonic graben. The measured reverse faulting, reaching at least 5 m occurs in the Holocene rift zone of North Iceland. The reverse slip has apparently occurred on an existing normal fault as a result of overpressure of a nearby 6 m–13-m-thick 8000 yr-old feeder dyke. A numerical model of the dyke-fault interaction supports our interpretation. The results indicate that dykes, particularly potential feeder dykes, may cause large reverse slips on nearby normal faults. This conclusion should improve the general understanding of geodetic deformation during volcanic unrest periods and may help forecast dyke-fed eruptions.

7.1 Introduction

One principal aim of volcanology is to provide a theoretical understanding, on

which we can base reliable forecasting of eruptions. Worldwide, several hundred million people live in the vicinity of active volcanoes (Chester et al., 2002). Accurate forecasting of eruptions is thus a basic concern in many countries. Some eruptions have been predicted, many more have not. Also, many unrest periods have caused false alarm since they have, eventually, not lead to eruptions (Newhall and Dzurisin, 1988; Scarth and Tanguy, 2001).

Most volcanic eruptions are supplied with magma through dykes. A dyke propagating toward the surface induces stresses and displacements at the surface (Pollard and Holzhausen, 1979; Pollard et al., 1983; Rubin and Pollard, 1988; Bonafede and Olivieri, 1997; Rubin, 1995; Bonafede and Danesi, 1997; Gudmundsson, 2003). Dykes in rift zones are commonly associated with grabens (Rubin and Pollard, 1988; Rubin, 1995; Gudmundsson and Loetveit, 2005). The effects of dyke-induced stresses on the boundary faults of the grabens and the associated fissure swarms must be understood if we are to infer correctly the

volcano-tectonic processes associated with volcanic unrest periods. The surface effects of an approaching dyke can often be detected by geodetic and other measurements (Pollard et al., 1983; Rubin and Pollard, 1988; Bonafede and Olivieri, 1997; Bonafede and Danesi, 1997; Meriaux and Jaupart, 1998; Gudmundsson, 2003; Houlie et al., 2006; Wright et al., 2006). When dyke-induced surface deformation and related signals are understood, we should be able to infer if, and then when and where, a dyke-fed eruption is likely to occur.

In this paper, we present the results of field observations and numerical modelling indicating that dykes that enter rift zones may occasionally generate reverse slip on existing normal faults. We focus on a feeder dyke associated with the Holocene Sveinar Graben in the rift zone of North Iceland. The emplacement of the dyke (at ~8000 B.P.) apparently generated a 5 m reverse slip on a nearby fault associated with the continuation of the Sveinar Graben.

7.2 Graben and feeder dyke

The Sveinar Graben forms a part of the volcanic rift zone of North Iceland (Fig. 7.1). Traditionally, the Sveinar Graben has been assigned to the Fremrinamur Volcanic System (Gudmundsson and Backström, 1989), but some recent studies assign it to the Askja Volcanic System (Johannesson and Saemundsson, 1998). The graben is composed of major, discontinuous normal faults, the fault segments commonly being

offset laterally by 25–50 m. The main graben is ~20 km long and mostly 0.5–1 km wide (Fig. 7.2). Normal faults north of the canyon of the river Jökulsa a Fjöllum (Fig. 7.1) are clearly a continuation of the Sveinar Graben, but they do not form such a clear-cut, single main graben (Fig. 7.2).

The vertical displacement was measured at many points along the boundary faults of the Sveinar Graben. The displacement is generally similar on the eastern and western faults, commonly 2–7 m, but increases to ~20 m as the graben approaches the river canyon. The maximum measured throw, the same on both the boundary faults, is 22 m. On approaching the river canyon, the graben thus deepens, but also becomes more complex in structure. Thus, the western boundary fault splits into two segments (not shown in the schematic illustration in Fig. 7.2). Also, there are many faults and fractures inside the graben where it meets with the canyon, both on the western and the eastern side of the canyon (Sigurdsson et al., 1975; Gudmundsson and Backström, 1989; this study).

Part of the Sveinar Graben is the site of a Holocene volcanic fissure (Figs. 7.1, 7.2). The fissure has given rise to the Sveinar-Randarholar Crater Row. The total length of the crater row is ~75 km, but it consists of separate segments many of which are spaced far apart (Fig. 7.1).

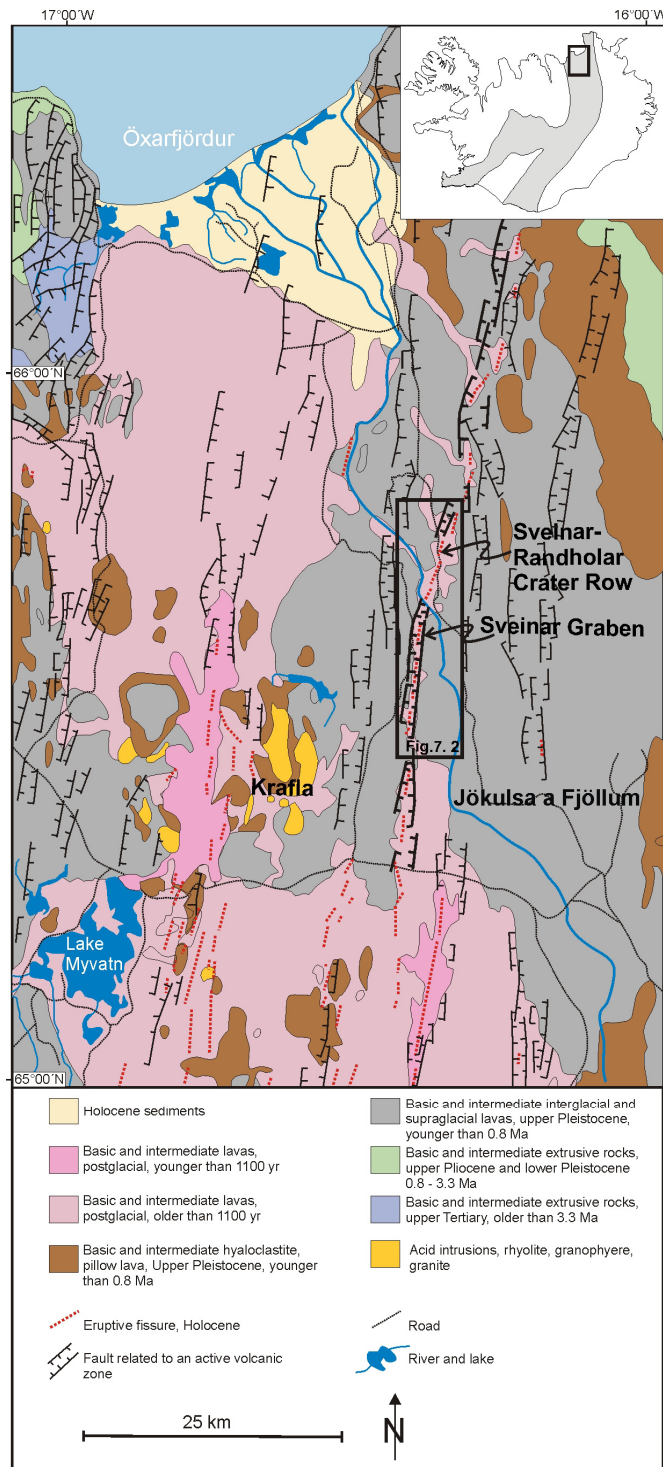


Figure 7.1: Location of the Sveinar Graben and Sveinar-Randarholar Crater Row in the Holocene rift zone of northern Iceland (modified from Johannesson and Saemundsson, 1998). Inset map of Iceland shows location of research area within the Neovolcanic zone (covered by rocks younger than 0.8 Ma). Also shown is location of Figure 7.2.

The age of the Sveinar-Randarholar Crater Row is estimated to be at least 6 000 yrs and more likely about 8000 yr (Thorarinsson, 1959; Sigurdsson et al., 1975; Gudmundsson and Backström, 1989). It is not known if the entire fissure was simultaneously active.

South of the river canyon, the Sveinar-Randarholar Crater Row is partly inside the Sveinar Graben (Figs. 7.1, 7.2). North of the canyon, however, most of the crater row does not follow a clear, narrow graben; in fact, the Sveinar-Randarholar lava flows cover some of the faults (Figs. 7.1, 7.3). Similarly, the southernmost part of the crater row is not associated with a graben (Fig. 7.1). Indeed, most of the narrow grabens in this part of the rift zone of Iceland cannot be related to crater rows (Fig. 7.1).

The feeder dyke to the Sveinar-Randarholar Crater Row is exposed in both the walls of the canyon of Jökulsá a Fjöllum. Where the dyke crosses the canyon it consists of two overlapping segments. The eastern dyke segment strikes N5°W, dips 86–89°E, and is 2 m thick on both sides of the canyon.

In the western wall of the canyon the dyke segment is directly connected with a spatter cone of the Sveinar-Randarholar Crater Row. The western dyke segment, some 85 m west of the eastern segment, is more variable in attitude and thickness. Thus, in the western canyon wall, its attitude is N30°E/85°W, but in the eastern wall the

attitude changes from N5°W/82°W (deep in the canyon) to N9°E/84°W close to the surface (Fig. 7.3). Similarly, in the western wall the segment thickness varies from 8.5 m close to the river to 2 m far from the river. In the eastern canyon wall, the segment thickness is 4.5 m close to the river but gradually increases with altitude to 6–7 m, and then to ~13 m where the dyke connects with the spatter cone (Fig. 7.3). In all the outcrops of both segments, the dyke rock is the same: very fine-grained and dense basalt, without phenocrysts or large vesicles, even close to the surface. The dyke segments have clear cooling joints; some parts are essentially cube jointed, whereas others have typical horizontal joints forming two main columnar rows.

7.3 Dyke-induced reverse faulting

Where the dyke meets with the crater cone in the eastern wall of the canyon, it is very close to a fault (Fig. 7.3). The attitude of this fault, labelled A in Figure 7.4, indicates that it is a reverse fault. Major reverse faults, however, are very rare in Iceland (Gudmundsson and Loetveit, 2005). Where the dyke dissects the paleosurface and connects with the crater cone, the dyke is 13 m thick and its centre is only 40 m from fault A. We propose that fault A was earlier a normal fault and that its present reverse slip is induced by the dyke emplacement.

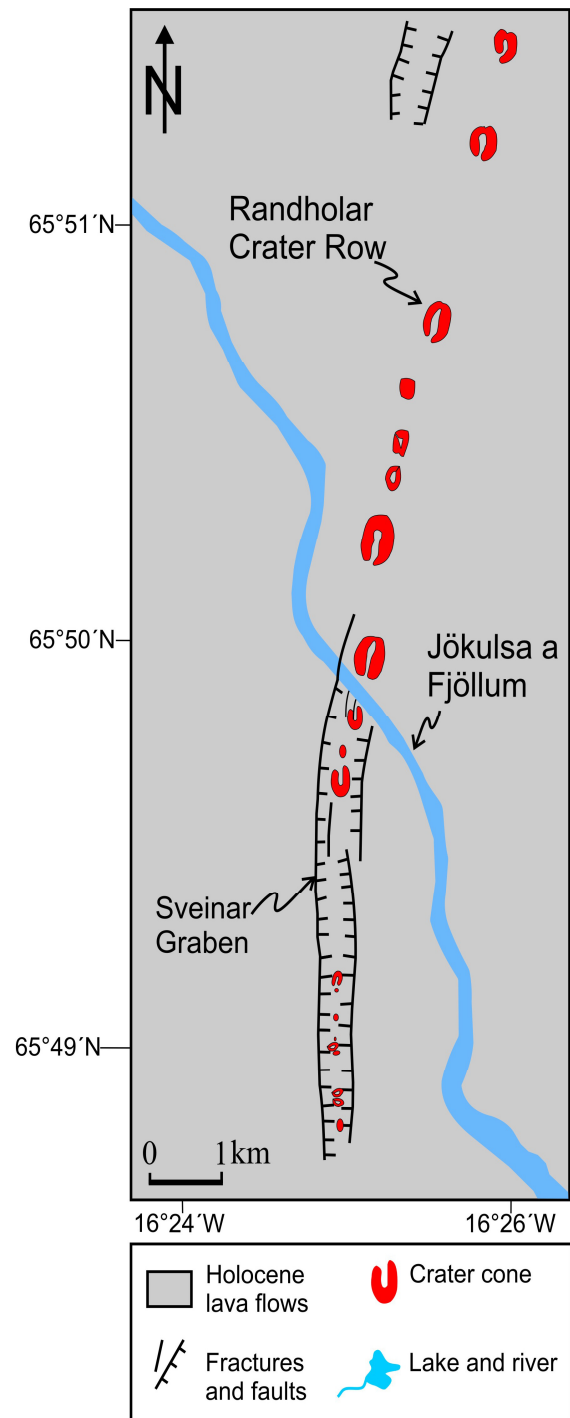


Figure 7.2: Schematic illustration (located in Fig. 7.1) of part of the 8000 yr old Sveinar-Randholar Crater Row and Sveinar Graben where they meet with the canyon of the Jökulsá a Fjöllum.

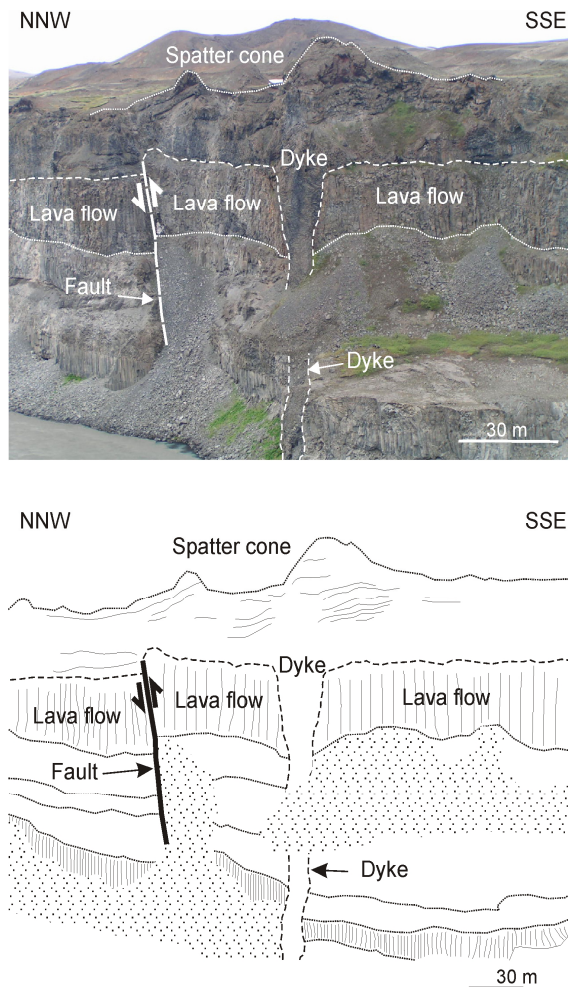


Figure 7.3: Photograph and drawing show the western feeder-dyke segment to the Sveinar-Randarholar Crater row being connected to one of its spatter cones. View is north across the canyon of the river Jökulsa a Fjöllum. At connection labelled “Dyke”, the thickness is of the dyke is 13 m, whereas close to the river, this thickness is 4.5 m (Dyke with arrow). Also shown is the reverse fault (Fault, arrow), with a displacement of 5 m, only 40 m from the centre of the dyke. Host rock is primarily composed of interglacial basaltic lava flows.

To test this idea, we made several simple numerical models using the boundary-element program Beasy (Brebbia and Dominguez, 1992; www.beasy.com). In

the models, the dip of fault A is 75°E and it is located at a distance of 40 m from the dyke fracture (Figs. 7.3-7.4). There are several faults east of the dyke, the closest one being ~ 80 m from the dyke. This fault B is also included in the model (Figs. 7.4). The host rock is modelled as homogeneous and isotropic with a typical in situ Young’s modulus (stiffness) for basaltic lava flows of 10 GPa and a Poisson’s ratio of 0.25 (Oddson, 1984; Egilsson et al., 1989; Bell, 2000). In estimating the static in situ Young’s modulus, account has been taken of the common fractures (mainly cooling joints) in the basaltic lava flows (Fig. 7.3), which tend to lower the effective Young’s modulus (Priest, 1993; Nemat-Nasser and Hori, 1999).

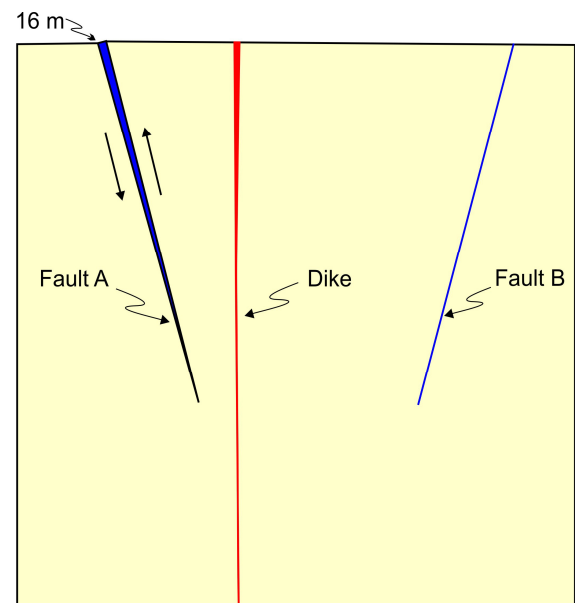


Figure 7.4: Boundary-element model of effects of a dyke with a magmatic overpressure of 10 MPa on nearby graben faults A and B. Fault A is identified in Figure 7.3, whereas fault B is outside the area of Figure 7.3. In the model, the faults are taken as open, friction-free normal

(continuation Figure 7.4) faults that extend from the free surface to a depth of around 100 m. Subsequent dyke emplacement has insignificant effects on fault B, but causes reverse slip of as much as 16 m on fault A.

Based on their length/thickness ratios, many regional dykes in Iceland exposed in the uppermost 1 km of the crust formed with an overpressure of $\sim 4\text{--}21$ MPa, with a common value of ~ 10 MPa (Gudmundsson, 1986). Using this value for the feeder-dyke overpressure in the uppermost 100 m of the crust and the above elastic constants, the numerical model in Figure 7.4 indicates that the dyke has little effects on fault B but induces reverse slip on fault A by as much as 16 m. Thus, when the dyke entered the Sveinar Graben and, eventually, propagated to the surface its overpressure resulted in a large reverse slip on the normal fault closest to the dyke, namely fault A. Thus, even if fault A may initially have had a normal displacement of, say, 10 m, as is common in the Sveinar Graben, the dyke overpressure presumably changed it to a reverse fault with a slip of ~ 5 m. For some faults, however, the reverse slip due to a dyke may not exceed the previous normal throw. Many normal faults near dykes may thus at one time have had larger throws than presently observed.

7.4 Discussion

There is little doubt that the Sveinar Graben captured the feeder-dyke to the Sveinar-Randarholar Crater Row.

Thorarinsson (1959) argues that the Sveinar-Randarholar eruption started north of the canyon of Jökulsa a Fjöllum and gradually propagated laterally to the south and became captured by the Sveinar Graben. Gudmundsson and Backström (1989) also found evidence of the Sveinar-Randarholar lava flow being faulted in a brittle manner at some localities along the Sveinar Graben. This observation suggests that the graben continued to develop during rifting episodes younger than the one that generated the 8000 yr-old Sveinar-Randarholar lava flow.

Further evidence that fault A existed at the time of the feeder-dyke emplacement is the great increase in the dyke thickness close to the surface (Fig. 7.3). While the free-surface effect increases a mode I fracture opening at the surface (Gray, 1992), the dyke-thickness increase from 6 m at the depth of 30 m below the surface to 13 m at the surface (Fig. 7.3) is likely to be partly related to the reverse slip on fault A during dyke emplacement. Not only does the slip provide space for the accommodation of the dyke opening, but fractures of any kind, and particularly slipping faults, also lower the effective Young's modulus of the rock in a direction perpendicular to the loading (Priest, 1993; Nemat-Nasser and Hori, 1999). Thus, part of the great increase in the dyke thickness in the uppermost 30 m of the canyon wall is presumably due to the associated reverse slip on fault A (cf. Gudmundsson and Loetveit, 2005).

7.5 Conclusion

The field observations reported here show that dyke-induced surface deformation during unrest periods in volcanoes and rift zones may be complex and that existing grabens may capture potential or actual feeder dykes. The field data and the numerical model indicate that dykes entering rift-zone grabens may cause large reverse displacements on nearby boundary faults and that the displacements, in turn, may contribute to an increasing dyke thickness close to and at the surface. We believe that these results add significantly to our general understanding of geodetic deformation during periods of volcanic unrest and may help forecast dyke-fed eruptions.

Acknowledgements

We thank the reviewers, Nicolas Houlié and Michele Cooke, for very helpful comments. The work reported here was supported by a Marie Curie Fellowship (for IG) contract number MEIF-CT-2006-0250007, from the European Commission.

8. Discussion and conclusions

The case studies (Chapters 3-4 and 6-7) presented in this thesis contribute to an enhanced understanding of tectonically-controlled emplacement mechanisms of different features at different levels in the upper crust. The field studies deal with the conditions of the opening of tectonic fractures in the upper crustal level, their propagation, interaction, and final emplacement. Features addressed in the case scenarios include clastic, eruptive, and plutonic bodies, which were studied using field work, 2D numerical and 3D geometrical modelling, and macro- and microstructural fabric analysis. The results of the field-based studies attempt to address the following points: (1) the influence of pre-existing tectonic features on emplacement mechanisms in the upper crust; (2) tectonic effect on magma movement and location of eruption sites; (3) the feedback between faulting and magmatism; and (4) conditions and mechanisms of (clastic) dyke emplacement.

The following discussion of the main results is grouped according to the emplacement depth of the features, starting with the Göttemar granitic laccolith, SE Sweden (see Chapter 3), followed by the Holocene scoria cone row Raudholar in the northern rift zone of Iceland (see Chapter 6). The second part of the discussion deals with the feedback between magmatic bodies and faulting (dyke-induced reverse faulting in the northern rift zone of Iceland, see Chapter 7).

The fourth field study examines a combination of active and passive emplacement at the Earth's surface using the example of a sedimentary dyke located in SE Sweden (see Chapter 4).

8.1 Multi-stage emplacement of the Göttemar Pluton, Southeast Sweden

Chapter 3 describes the results of a field study of the Mesoproterozoic Göttemar Pluton located in SE Sweden. The emplacement is suggested to be episodic with repeated magma injections that build up a layered intrusion with alternating fine- and coarse-grained granite for the upper third of the body, based on borehole data. Gravity data and field observations show that space creation was mainly by roof uplift and minor floor subsidence. CL-analysis indicate a complex crystallisation history of the pluton with magma mixing in a deep magma chamber, repeated heating and recrystallisation of the growing granite succession, and conditions of pressure decrease and variations in the temperature during rapid ascent of magma. Brittle deformation structures, healed microcracks, and recrystallisation of quartz imply a reheating history of the pluton triggered by several magma pulses, amalgamation and stacking of sills. The final, idealised emplacement history is illustrated in Figure 8.1. For further explanation see Chapter 3.

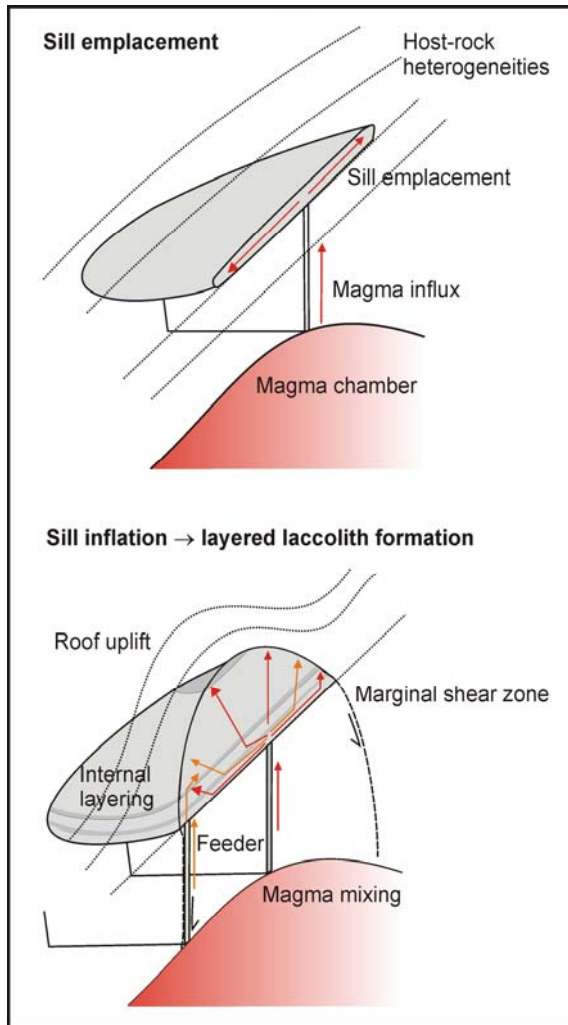


Figure 8.1: Schematic emplacement history of the Göttemar Pluton. Initial pluton formation involved magma ascent in a vertical feeder dyke, which was arrested at stratigraphically-controlled mechanical discontinuities in the host rock, leading to the formation of a sill. Subsequent sill inflation, accompanied by horizontal infilling from several magma sources via fractures and a feeder dyke at the base of the laccolith, resulted in deformation of previously emplaced magma pulses and raising of the roof.

The study of the Göttemar Pluton joins a series of studies that investigate the formation of intrusions as result of incremental growth by pulsed injections of silicic and/or mafic magmas (e.g. McNulty et

al., 2000; Petford et al., 2000; de Saint-Blanquat et al., 2001; 2006; Coleman et al., 2004; Pupier et al., 2008; Slaby and Martin, 2008, to name a few). Tabular plutons that grew by vertical stacking of magma increments formed by dyke and coeval sill amalgamation might serve furthermore as conduits for vertical transport of magma (Bartley et al., 2006).

Emplacement of granite plutons in areas of local extension associated with strike-slip faults and shear zones is a mechanism consistent with the main structural and petrological features of many batholiths (e.g. Castro, 1987; Tikoff and Teyssier, 1992; Vigneresse, 1995a,b). The case study emphasises that the emplacement of the Göttemar Pluton was tectonically controlled by a NNE-SSW propagating shear zone along the coast of SE Sweden, similar to the proposed tectonic model by Hutton (1982) for the emplacement of round and deformed plutons ahead of a propagating shear zone and filling of pull-apart structures.

A major point of debate about the applicability of this mechanism arises from the comparison between the time scale of granite emplacement and the common rates of regional deformation (Paterson and Fowler, 1993a,b; Hanson and Glazner, 1995; Vigneresse, 1995a,b). Ascent velocities of magmas are typically faster than tectonic strain rates (Fernandez and Castro, 1999). As shown with this field example, a rapid emplacement offers an explanation for the lack of deformation in an inferred

“anorogenic” pluton. The emplacement was subject to a regional deviatoric stress field, as is suggested by the occurrence of a propagating shear zone beneath the aligned coeval plutons. The prevailing regional stress field had an influence on the migration of magma feeding the several plutons (e.g. feeder conduits, tectonic overpressuring) and on their final emplacement (cf. de Saint-Blanquat et al., 2001). Several Mesoproterozoic plutons in Fennoscandia, and outside (cf. Anderson and Morrison, 2005), are described as anorogenic intrusions predating the orogenic construction of Rodinia. Some plutons, however, are shown to be syntectonic (e.g. Motuza et al., 2006; Skridlaite et al., 2007; Čečys and Benn, 2007, Bogdanova et al., 2008; Brander and Söderlund, 2008; Zarins and Johansson, 2008), and are assumed to be connected to reactivated shear zones at that time (Selverstone et al., 2000; Anderson and Morrison, 2005; Chapter 3), other plutons are anorogenic although it is recognised that the same conditions leading to their formation may have occurred during extensional phases of orogens (Karlstrom et al., 2001; Anderson and Morrison, 2005). Nevertheless, the discussion regarding anorogenic versus orogenic origin continues, but the fact that most of these intrusions postdate prior orogenic events is regarded as significant (Åhäll et al., 2000; Andersson and Morrison, 2005). That some intrusions have been shown to be coeval with regional deformation does

not necessarily provide evidence for an orogenic setting.

With regards to the Götemar granite many questions remain unanswered that might be solved by further intensive geochemical and isotope analyses. These questions include (1) the source depth of the magma formation; (2) further implications for magma mixing, or/and fractional crystallisation and heating of Transcandinavian Igneous Belt (TIB) granite; (3) classification of granites forming the TIB in a broader view to the regional tectonics of SE Sweden (e.g. Nolte et al., in preparation).

8.2 Reconstruction of a crater cone row in the northern rift zone of Iceland

The field example, presented in Chapter 6, describes a Holocene segmented row of monogenetic crater cones in the northern rift zone of Iceland that offers the opportunity to study a cross-section through the inner workings of the uppermost few hundred metres of a crater row in an active volcanic rift zone. The 3D reconstruction based on high-precision GPS mapping of the plugs and scoria cones, is used as a tool to determine the magma flow under a small edifice, segmentation, influence of the reactivation, and the influence of pre-existing faults underlying the crater row on the localisation of the eruptive centres. Volcanic deposit analysis suggests a diversified eruption style (Fig. 8.2).

As common in Iceland, aligned eruptive fissures are initially active along

entire segments, while eruption later focuses on central points to build up cones (Fig. 8.2). To explain and model the transition from a fissure eruption to a central vent eruption has been a major research field in the last years (Ida, 1992; Wylie et al., 1999; Quarenì et al., 2001; Petcovic and Dufek, 2005; Diller et al., 2006; Gaffney et al., 2007; Michieli Vittuni et al., 2008). The presented study also discusses the occurrence of magmatic plumbing systems connected to tectonic features.

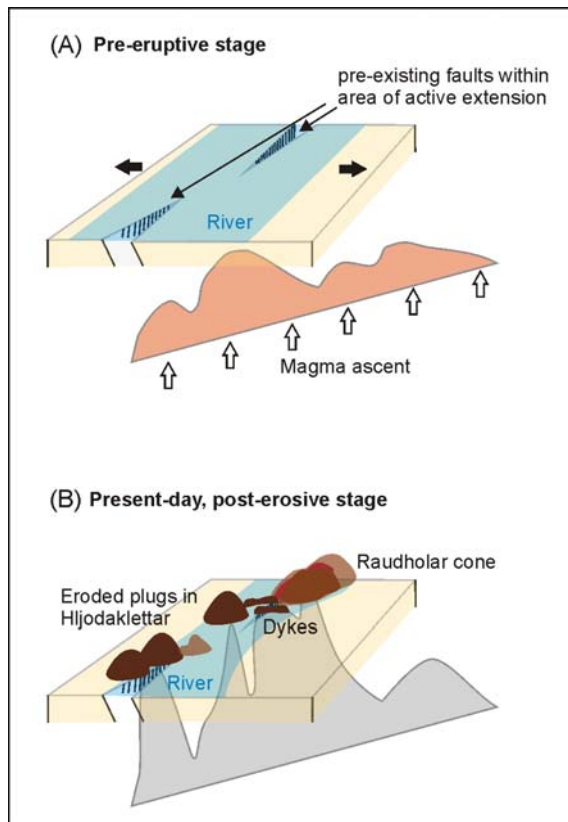


Figure 8.2: Intrusion of magma and opening of tectonic fractures perpendicular to rift extension. The magma flow direction between the Raudholar single cone segments is assumed to be horizontal. The eruption produces left-lateral cones that present the now-eroded Hljodarklettur plugs.

The formation of crater rows during fissure eruptions has received scientific

attention mainly because of its significance for hazard assessment (e.g. Martin and Nemeth, 2006; Valentine and Keating, 2007; Keating et al., 2008; Ort et al., 2008) and associated environmental and climatic issues that arise from large eruptions as for example the Laki eruption 1783-1784 AD (e.g. Thordarson et al., 2001; Thordarson and Self, 2003; Chenet et al., 2005; Grattan, 2005), as well as the formation of flood basalts (e.g. Mege and Kome, 2004; Grattan, 2005; Petcovic and Dufek, 2005; Wignall, 2005; Bryan and Ernst, 2008). Furthermore, crater rows play a significant role in the analysis of the paleoenvironment (e.g. syn-volcanic rivers, fluvial deposits; Risso et al., 2008), and palaeostress and current stress situation (e.g. Vespermann and Schmincke, 2000).

The direction of magma transport is important for the formation of volcanic edifices and the morphology of rift zones (Ishizuka et al., 2008). While vertical propagation is imagined for a conduit between source depth and magma plumbing locality underneath large volcanic centres (e.g. Pinel and Jaupart, 2004; Geshi, 2008; Soriano et al., 2008), lateral magma transport has been recognised along volcanic rift zones of ocean-island volcanoes (e.g. Hawaii, Canary Islands; Iceland; e.g. Sigurdsson and Sparks, 1978a,b; Ryan, 1988; Soriano et al., 2008), mid oceanic ridges (e.g., Dziak et al., 1995; Smith and Cann, 1999; Sinton et al., 2002) and continental rift zones (e.g., Wright et al., 2006). Eruptive fissures that occur independently from a central volcano, as seen

in this field example in Iceland (Fig. 8.2), might be fed from the dykes that directly propagate from the deeper a magma chamber (e.g. Geshi, 2008).

8.3 Dyke-induced reverse faulting in the northern rift zone of Iceland

The field study presented in Chapter 7, located in the rift zone of Iceland, represents an example of the interconnection between faulting and magmatism and provides valuable insight into magma feeding relationships, the mechanical conditions of dyke emplacement, and the mechanical effect of its emplacement on the surroundings. It thus defines the feedback between dyke emplacement and fault slip processes. The results of the field study show that dyke-induced surface deformation during unrest periods in volcanoes and rift zones are complex, and that existing grabens may capture feeder dykes (Fig. 8.3). The field observations and a numerical model also indicate that a dyke entering a rift-zone graben may cause large reverse displacement on a nearby boundary fault, and that the displacement, in turn, may contribute to an increasing dyke thickness close to and at the surface (Fig. 8.3).

Reverse faults are rarely observed in grabens associated with dykes. Field observation presented in this case study suggests two possible reasons for that. One explanation is that reverse throw often

simply does not exceed the previous normal throw of the fault. This suggests in turn that normal faults near dykes, which intrude after the faulting, may have experienced greater normal slip than presently observed.

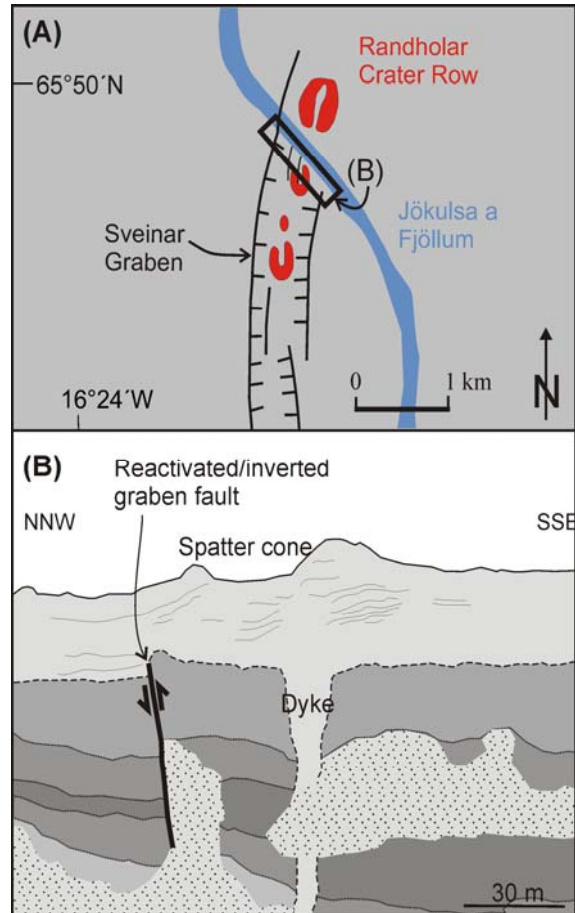


Figure 8.3: Schematic illustration (A) of part of the 8000 yr old Sveinar-Randarholar Crater Row and Sveinar Graben where they meet with the canyon of the Jökulsa a Fjöllum. (B) Drawing showing the western feeder-dyke segment of the Sveinar-Randarholar View is north across the canyon of the river Jökulsa a Fjöllum. At connection labelled “Dyke”, the thickness is of the dyke is 13 m, whereas close to the river, this (continuation Figure 8.3) thickness is 4.5 m. Also shown is the reverse fault (Fault, arrow), with a displacement of 5 m, only 40 m from the centre of the dyke. Host rock is primarily composed of interglacial basaltic lava flows.

A second reason is that the faults outside a critical distance to the dyke cannot be reactivated (e.g. Rubin and Pollard, 1988). According to Gaffney et al. (2007), the ability of magma to intrude a fault depends on the fault dip; while high-angle faults are often occupied by dykes, shallow dipping faults are not (Keating et al., 2008). The results of the case study suggest that a significant fault slip can occur due to magma lubrication when a dyke is captured by a fault. This adds additional mechanisms for seismicity along with fault motion due to transient stresses around a propagating dyke top (e.g. Rubin and Pollard, 1988; Rubin, 1992) and due to magma-induced stress changes along parts of faults (e.g. Parsons et al., 2006).

Although the primary cause of dyke injection in a volcano-tectonic context remains unclear, it is accepted that dyke intrusions trigger faulting and not vice versa (cf. Rubin and Pollard, 1988). The slip magnitude is roughly equal to the dyke thickness, which agrees with displacement rates measured and modelled in the field example in northwest Iceland (Pollard et al., 1983). Khodayar and Einarsson (2004) present several field examples from Iceland of reverse motion associated with dykes, sills or cone sheets and suggest local bends of steeply-dipping fractures, and/or magma intrusion as a likely origin. The results of this study are thus of a general significance, not only from a hazard point of view, but can be applied to other volcanic areas, such as Etna, Nyiragongo and Fogo (e.g. Houlie et al.,

2006; Acocella and Neri, 2008) in connection with the triggering of landslides and the monitoring of seismic events.

8.4 Episodic formation of Cambrian clastic dykes in the basement of Southeast Sweden

Chapter 4 presents the results of the multi-stage emplacement of clastic dykes in the Paleoproterozoic basement in SE Sweden. Macro- and microfabric analyses and a conceptual model of the formation of a selected dyke reveal that the downward propagation of the dyke was controlled by an alternating stress regime. Pre-existing joints in the basement rocks were used as pathways for dyke intrusion, and dyke orientation can thus be used as a palaeostress indicator.

Further results indicate that clastic dyke formation can last over a long time span with episodic propagation. Changing stress conditions result in alternating periods of opening/filling, cementation/lithification and alteration. The analyses of micro- and macrofabrics are therefore not only a helpful tool to distinguish between Neptunian and actively emplaced sedimentary dykes (Fig. 8.4), but can also help to determine the host tectonic environment, and thus the paleogeographic and tectonic conditions during dyke formation. The existence of joints and other heterogeneities in the host rock are thus potential locations for intrusions (Fig. 8.4), not only of clastic material, but also for magma. In this context, the presented field study attempts to close a gap in literature, providing a combination of detailed

macro- and microfabric studies for the downward propagation of clastic intrusions in basement rocks (Fig. 8.4).

This study joins a series of examples that reflect the general increase in attention on clastic dyke intrusion that have not only an implications for fluid flow processes through hydrocarbon reservoirs (e.g. Jolly and Lonergan, 2002; Hurst and Cartwright, 2007) and applications in waste disposal and groundwater remediation (e.g. Pearce et al., 2001), but also use sedimentary dykes as excellent palaeostress indicators. Current research activities focus intensively on these fields. For example, Beacom et al. (1999) use clastic dykes to date fault movements in context of a syn-rifting palaeostress system in northern Scotland. Andre et al. (2004) use sedimentary dykes in the Paris Basin to reconstruct the E-W extension of the western European platform during the late Jurassic. Winslow (1983) describes clastic dykes in relation to thrusting in the southern Andes. Eyal (1988) presents sandstone dykes captured within fault breccias, located in the eastern Sinai. Levi et al. (2006) present a method based on AMS, to provide a petrofabric tool to distinguish between passively-filled dykes and injection dykes that provide an useful addition to paleoseismic records (see also e.g. Obermeier, 1996; Becker et al., 2005).

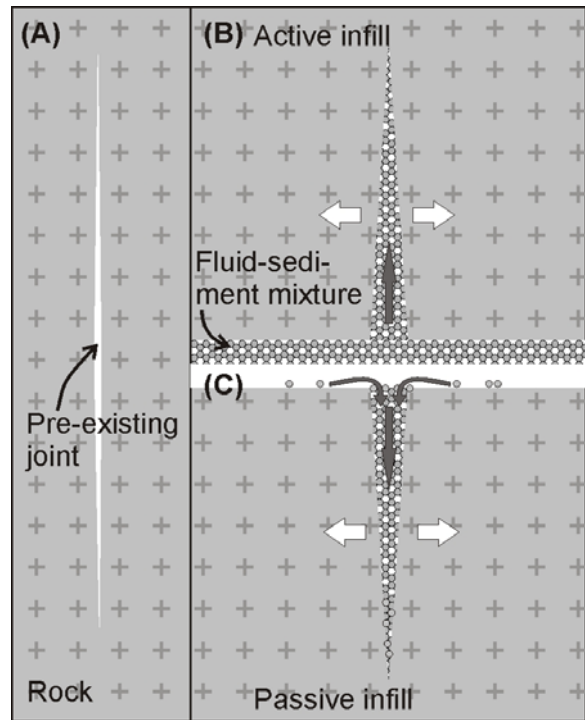


Figure 8.4: (A) Initial pre-existing joint serves as location for dyke in crystalline basement. Sedimentary dyke emplacement is divided into active intrusion (induced by fluid pressure, B) and passive (so called Neptunian dyke; driven by gravity infill, C). The described dyke in SE Sweden features active downward propagation and passive infill of sediment form above.

Ancient fluid seeps and intrusions related to hydrocarbon migration were studied by e.g. Mazzini et al. (2003a,b) and Aiello (2005). The main trigger identified for the sandstone intrusion were earthquake induced liquefaction or a large fluid pressure increase caused by hydrocarbon-rich fluids (Fig. 8.4; e.g. Mazzini et al., 2003a,b; Duranti and Mazzini, 2005; Huuse et al., 2005). Seismic studies often detect large (clastic) intrusions from offshore petroleum provinces e.g. in the North Sea, West Africa, and offshore Mid Norway (e.g. Møller et al.,

2001; Davies, 2003; Hurst et al., 2003). Sandstone intrusions with a similar geometry to magmatic saucer-shaped sills are under intensive study in terms of hydrocarbon potential and fluid pathways by e.g. Cartwright et al. (2008) and Polteau et al. (2008a,b) in the North Sea and the Faroe-Shetland Basins.

Regardless of the material the tectonic fractures were filled with, the field-based examples show that conditions for the opening and further development of tectonic fractures are similar. The stress field determines the opening direction (along planes perpendicular to the minor stress component) and rate, controls the fluid flow and the location of final emplacement. All presented examples are thus palaeostress indicators. General implications that arise from the presented case scenarios include

- Pre-existing structural heterogeneities (mainly lithological boundaries, faults and joint systems) determine the location of dyke/sill emplacement (see Chapter 3-4, 6-7), eruptive cone localisation and alignment (see Chapter 6).
- Fluid ascent is not related to a special type of deformation (see Chapters 3, 6-7). The simplest way is extraction of fluid from a matrix by compression and shear, but it always connected to an extensional near-field setting (see Chapters 3-4, 6-7).
- Faults can be reactivated during dyke emplacement and can change their sense of slip in addition (see Chapter 7).
- Dykes can be captured by faults. This is not only applicable to magma, but also for clastic intrusions (see Chapter 4, Chapter 7).
- The interplay between tectonic forces and emplacement has to be considered as an important parameter for analogue, numerical and geometrical modelling (e.g. Chapter 6-7).
- The feedback between tectonics and emplacement contributes significantly to geological hazard assessment (Chapter 6 and Chapter 7).

- Åberg, G., 1978. Precambrian geochronology of southeastern Sweden. *GFF* 100, 125-154.
- Åberg, G., 1988. Middle Proterozoic anorogenic magmatism in Sweden and worldwide. *Lithos* 21, 279–289.
- Åberg, G., Löfvendahl, R., Levi, B., 1984. Radiometric dating of the Jungfrun granite. *GFF* 105, 191-198.
- Åberg, G., Löfvendahl, R., Levi, B., 1985. The Götömar granite-isotropic and geochemical evidence for a complex history of an anorogenic granite. *GFF* 106, 327-333.
- Åhäll, K. I., Larson, S. Å., 2000. Growth related 1.85-1.55 Ga magmatism in the Baltic shield; a review addressing two tectonic characteristics of Svecofennian, TIB 1-related, and Gothian events. *GFF* 122, 193-206.
- Åhäll, K.-I., Connelly, J. N., Brewer, T. S., 2000. Episodic rapakivi magmatism due to distal orogenesis? Correlation of 1.69–1.50 Ga orogenic and inboard anorogenic events in the Baltic shield. *Geology* 28, 823–826.
- Åhall, K.-I., 2001. Åldersbestämning av svårdaterade bergarter i sydöstra Sverige. SKB-R-01-60, Swedish Nuclear Fuel and Waste Management Co, Stockholm, Sweden, pp. 24.
- Åhall, K.-I., Gower, C. F., 1997. The Gothian and Labradorian orogens: variations in accretionary tectonism along a late Paleoproterozoic Laurentia-Baltica margin. *GFF* 119, 181-191.
- Acocella, V., Neri, M., 2008. Dyke propagation in volcanic edifices: overview and possible developments. *Tectonophysics* doi:10.1016/j.tecto.2008.10.002.
- Aiello, I. W., 2005. Fossil seep structures of the Monterey Bay region and tectonic/structural controls on fluid flow in an active transform margin. *Palaeogeogr Palaeoclimatol Palaeoecol* 227, 124–142.
- Alho, P., Russell, A. J., Carrivick, J. L., Käyhkö, J., 2005. Reconstruction of the largest Holocene jökulhlaup within Jökulsá a Fjöllum, NE Iceland. *Quat Sci Rev* 24, 2319-2334.
- Allen, R. M., Nolet, G., Morgan, W. J., Vogfjord, K., Bergsson, B. H., Eriendsson, P., Foulger, G. R., Jakobsdottir, S., Julian, B. R., Pritchard, M., Ragnarsson, S., Stefansson, R., 1999. The thin hot plume beneath Iceland. *Geophys J Int* 137, 51–63.
- Allen, R. M., Nolet, G., Morgan, W. J., Vogfjord, K., Nettles, M., Ekström, G., Bergsson, B. H., Erlendsson, P., Foulger, G. R., Jakobsdottir, S., Julian, B., Pritchard, M., Ragnarsson, S., Stefansson, R., 2002. Plume-driven plumbing and crustal deformation in Iceland. *J Geophys Res* 107, doi: 10.1029/2001JB000584.
- Alm, E., Sundblad, K., 2002. Fluorite-calcite bearing fractures in the countries of Kalmar and Blekinge, Sweden. SKB-R-02-42, Swedish Nuclear Fuel and Waste

- Management Co, Stockholm, Sweden, pp. 116.
- Alm, E., Sundblad, K., Huhma, H., 2005. Sm-Nd Isotope determination of low-temperature fluorite-calcite-galena mineralization in the margins of the Fennoscandian Shield. SKB-R-05-55, Swedish Nuclear Fuel and Waste Management Co, Stockholm, Sweden, pp. 48.
- Åmark, M., 1986. Clastic dykes formed beneath an active glacier. *GFF* 108, 13-20.
- Anderson, E. M., 1936. The dynamics of the formation of cone-sheets, ring dikes, and cauldron-subsidence: *Proc R Soc Edinburgh* 56, 128-156.
- Anderson, E. M., 1938. The dynamics of sheet intrusions. *Proc R Soc Edinburgh* 58, 242-251.
- Anderson, J. L., Morrison, J., 2005. Ilmenite, magnetite, and peraluminous Mesoproterozoic anorogenic granites of Laurentia and Baltica. *Lithos* 80, 45-60.
- Andersson, U. B., 1991. Granitoid episodes and mafic-felsic magma interaction in the Svecofennian of the Fennoscandian shield, with main emphasis in the 1.8 Ga plutonics. *Precambrian Res* 51, 127-149.
- Andersson, U. B., Sjöström, H., Högdahl, K., Eklund, O., 2004. The Transscandinavian Igneous Belt, evolutionary models, In: Högdahl, K., et al. (eds.). *The Transscandinavian Igneous Belt (TIB) in Sweden: A review of its character and evolution: Geol Surv Finland, Spec Paper 37, 104-112.*
- Andersson, U. B., Rutanen, H., Johansson, Å., Mansfeld, J., Rimša, A., 2007. Characterization of Paleoproterozoic mantle beneath the Fennoscandian Shield: geochemistry and isotope geology (Nd, Sr) of ~ 1.8 Ga mafic plutonic rocks from the Transscandinavian Igneous Belt in Southeastern Sweden. *Int Geol Rev* 49, 587-625.
- Andre, G., Hibsich, C., Beaudoin, B., Carpentier, C., Fourcade, S., Cathelineau, M., Élion, P., 2004. Oxfordian sedimentary dykes: tectonic and diagenetic implications for the eastern Paris basin. *Bull Soc Geol France* 175, 595-605 (in French with English abstract).
- Andronico, D., Scollo, S., Cristaldi, A., Ferrari, F., 2009. Monitoring ash emission episodes at Mt Etna: the 16 November 2006 case study. *J Vol Geotherm Res* 180, 123-134.
- Annen, C., Blundy, J.D., Sparks, R.S.J., 2006. The genesis of intermediate and silicic magmas in deep crustal hot zones. *J Petrol* 47, 505-539.
- Aranguren, A., Larrea, F. J., Carracedo, M., Cuevas, J., Tubia, J. M., 1997. The Los Pedroches batholith (southern Spain): Polyphase interplay between shear zones in transtension and setting of granites. In: Bouchez, J. L., Hutton, D. H. W., Stephens, W. E., (eds). *Granite: From segregation of melt to emplacement fabrics: Amsterdam, Netherlands,*

- Kluwer Academic Publishers, p. 215–229.
- Arnadóttir, Th., Sigmundsson, F., Delaney, P. T., 1998. Sources of crustal deformation associated with the Krafla, Iceland, eruption in September 1984. *Geophys Res Lett* 25, 1043-1046.
- Arnadóttir, Th., Lund, B., Jiang, W., Geirsson, H., Einarsson, P., Sigurdsson, T., in press. Glacial rebound and plate spreading: results from the first countrywide GPS observations in Iceland, *Geophys. J. Int.* doi:10.1111/j.1365-246X.2008.
- Aspler, L. B., Donaldson, J. A., 1985. Penecontemporaneous sandstone dykes, Nonacho Basin (Early Proterozoic, Northwest Territories): horizontal injection in vertical, tabular fissures. *Can J Earth Sci* 23, 827–838.
- Atkinson, S. S., Lambert, R. J., 1990. The Roza Member feeder dyke system, Columbia River Basalt Group, USA: compositional variation and emplacement. In: Parker, A. J., Rickwood, P. C., Tucker, D. H. (eds.). *Mafic dykes and emplacement mechanisms*, Balkema, Rotterdam, 447-459.
- Bachl, C. A., Miller, C. F., Miller, J. S., Faulds, J. E., 2001. Construction of a pluton: evidence from an exposed cross-section of the Searchlight pluton, Eldorado Mountains, Nevada. *GSA Bull* 113, 1213–1228.
- Bachmann, O., Bergantz, G. W., 2004. On the origin of crystal-poor rhyolites: extracted from batholithic crystal mushes. *J Petrol* 45, 1565–1582.
- Bachmann, O., Miller, C. F., de Silva, S. L., 2007. The volcanic-plutonic connection as a stage for understanding crustal magmatism. *J Volcanol Geotherm Res* 167, 1-23.
- Bahorich, M., Farmer, S., 1995. 3-D seismic discontinuity for faults and stratigraphic features: The coherence cube: The Leading Edge 14, 1053–1058, doi: 10.1190/1.1437077.
- Bambauer, H. U., 1961. Spurenelementgehalt und Farbzentren in Quarzen aus Zerrklüften der Schweizer Alpen. *Schweiz Mineral Petrogr Mitt* 43, 259–268.
- Barker, D. S., 2000. Emplacement of a xenolith-rich sill, Lajitas, Texas. *J Volcanol Geotherm Res* 104, 153-168.
- Barnes, C. G., Allen, C. M., Hoover, J. D., Brigham, R. H., 1990. Magmatic components of a tilted plutonic system, Klamath Mountains, California. In Anderson, J. L. (Ed.), *The Nature and Origin of Cordilleran Magmatism*. *Geol Soc Am Memoir* 174, 331–46.
- Barnes, C. G., Dumond, G., Yoshinobu, A. S., Prestvik, T., 2004. Assimilation and crystal accumulation in a mid-crustal magma chamber: The Sausfjellet pluton, north-central Norway: *Lithos*, 75, 389–412.
- Bartley, J. M., Coleman, D. S., Glazner, A. F., 2006. Incremental pluton

- emplacement by magmatic crack-seal. *Trans R Soc Edinburgh: Earth Sci* 97, 383-396.
- Bateman, R., 1985. Aureole deformation by flattening around a diapir during in situ ballooning: the Cannibal Creek Granite. *J Geol* 93, 293 -310.
- Beacom, L. E., Anderson, T. B., Holdsworth, R. E., 1999. Using basement-hosted clastic dykes as syn-rifting palaeostress indicators: an example from the basal Stoer Group, northwest Scotland. *Geol Mag* 136, 301-310.
- Becker, A., Ferry, M., Monecke, K., Schnellmann, M., Giardini, D., 2005. Multiarchive paleoseismic record of late Pleistocene and Holocene strong earthquakes in Switzerland. *Tectonophysics* 400, 153-177.
- Behlau, J., Mingerzahn, G., 2001. Geological and tectonic investigations in the former Morsleben salt mine (Germany) as a basis for the safety assessment of a radioactive waste repository. *Eng Geol* 61, 83–97.
- Bell, F. G., 2000. *Engineering Properties of Rocks*, 4th ed. Blackwell, Oxford.
- Bergman, L., 1982. Clastic dykes in the Åland Islands, SW Finland and their origin. In: Bergman, L., Tynni, R., Winterhalter, B., (eds.) *Palaeozoic sediments in the Rapakivi area of the Åland Islands*. *Bull Geol Soc Finland* 317, 8-32.
- Bergman, S., Hogdahl, K., Nironen, M., Ogenhall, E., Sjöstrom, H., Lundqvist, L., Lathinen, R., 1998. Timing of Palaeoproterozoic intra-orogenic sedimentation in the central Fennoscandian Shield: evidence from detrital zircon in metasandstone. *Precambrian Res* 161, 231-249.
- Bergman, T., Isaksson, H., Johansson, R., Lindèn, A. H., Lindroos, H., Rudmark, L., Stephens, M., 1999. Förstudie Tierp. Jordarter, bergarter och deformationszoner. Swedish Nuclear Fuel and Waste Management Company. SKB-R-99-53. Stockholm, Sweden.
- Bertotto, G. W., Bjerg, E. A., Cingolani, C. A., 2006. Hawaiian and Strombolian style monogenetic volcanism in the extra-Andean domain of central-west Argentina. *J Volcanol Geotherm Res* 158, 430-444.
- Beunk, F. F., Page, L. M., 2001. Structural evolution of the accretional continental margin of the Paleoproterozoic Svecofennian orogen in South Sweden. *Tectonophysics* 339, 67-92.
- Bingen, B., Andersson, J., Söderlund, U., Möller, C., 2008. The Mesoproterozoic in the Nordic countries. In: Gee, D. G., Ladenberger, A. (eds.). *Nordic Geosciences and 33rd IGC 2008*, Episodes 31, 29-34.
- Björnsson A., Saemundsson K., Einarsson P., Tryggvason E., Grönvold K., 1977. Current rifting episode in North Iceland. *Nature* 266, 318–323.
- Björnsson, A., Johnsen, G., Sigurdsson, S., Thorbergsson G., Tryggvason, E., 1979. Rifting of the plate boundary in North

- Iceland 1975–1978. *J Geophys Res* 84, 3029–3038.
- Björnsson, A., 1985. Dynamics of crustal rifting in NE Iceland. *J Geophys Res* 90 (B12), 10151–10162.
- Blinova, V. N., Ivanov, M. K., Bohrmann, G., 2003. Hydrocarbon gases in deposits from mud volcanoes in the Sorokin Trough, north-eastern Black Sea. *Geo Mar Lett* 23, 250-257.
- Bogdanova, S. V., 2001. Tectonic setting of 1.65-1.4Ga AMCG magmatism in the western East European Craton (western Baltica). *J Conf Abstr* 6 (1). 769.
- Bogdanova, S. V., Page, L. M., Skridlaite, G., Taran, L. N., 2001. Proterozoic tectonothermal history in the western part of the East European Craton: $^{40}\text{Ar}/^{39}\text{Ar}$ geochronological constraints. *Tectonophysics* 339, 39-66.
- Bogdanova, S. V., Bingen, B., Gorbatshev, R., Kheraskova, T. N., Kozlov, V. I., Puchkov, V. N., Volozh, Y. A., 2008. The East European Craton (Baltica) before and during the assembly of Rodinia. *Precambrian Res* 160, 23-45.
- Bonafede, M., Olivieri, M., 1997. Displacement and gravity anomaly produced by a shallow vertical dyke in a cohesionless medium. *Geophys J Int* 130, 435-448.
- Bonafede, M., Danesi, S., 1997. Near-field modifications of stress induced by dyke injection at shallow depth. *Geophys J Int* 130, 435-448.
- Bonini, M., 2008. Elliptical mud volcano caldera as stress indicator in an active compressional setting (Nirano, Pedemontane margin, northern Italy). *Geology* 36, 131-134.
- Bradley, J., 1965. Intrusion of major dolerite sills. *Trans R Soc New Zealand* 3, 27-55.
- Brander, L., Söderlund, U., 2008. Mesoproterozoic (1.47-1.44Ga) orogenic magmatism in Fennoscandia, Baddelyite U-Pb dating of a suite of massif-type anorthosite in S Sweden. *Int J Earth Sci*, doi: 10.1007/S0053100702810.
- Brandstottir, B., Einarsson, P., 1979. Seismic activity associated with the September 1977 deflation of Krafla Volcano in north-eastern Iceland. *J Volcanol Geotherm Res* 6, 197-212.
- Brandstottir, B., Menke, W., Einarsson, P., White, S., Staples, R. K., 1997. Faroe-Iceland ridge experiment 2. Crustal structure of the Krafla central volcano. *J Geophys Res* 102, 7867-7886.
- Brebbia, C. A., Dominguez, J., 1992. *Boundary Elements: An Introductory Course*, 2nd ed, McGraw-Hill, New York.
- Breitkreuz, C., Mock, A., 2004. Are laccolith complexes characteristic of transtensional basin systems? Examples from the Permo-Carboniferous of Central Europe. In: Breitkreuz, C., Petford, N. (eds.). *Physical geology of high-level magmatic systems*. *J Geol Soc London, Special Pub* 234, 13-31.
- Breitkreuz, C., Petford, N., 2004. Physical geology of high-level magmatic systems: introduction. In: Breitkreuz, C.,

- Petford, N. (eds.). Physical geology of high-level magmatic systems. *J Geol Soc, London, Special Pub 234*, 1-4.
- Brewitz, W., Rothfuchs, S. T., 2007. Concepts and technologies for radioactive waste disposal in rock salt. *Acta Montanistica Slovaca 12*, 67-74.
- Bridgwater, D., Coe, K., 1969. The role of stoping in the emplacement of the giant dykes of Isortoq, South Greenland. In: Newall, G., Rast, N. (eds.). *Mechanism of Igneous Intrusion*. Gallery Press, Liverpool, 67– 78.
- Brooke, C-M., Trimble, T. J., Mackay, T. A., 1995. Mounded shallow gas sands from the Quaternary of the North Sea: analogues from the formation of sand mounds in deep water Tertiary sediments? In: Hartley, A. J., Prosser, D. J. (eds.). *Characterisation of deep marine clastic systems*. Geol. Soc. London, Special Pub 94, 95-101.
- Brown, M., Solar, G. S., 1998. Shear zone systems and melts: feedback relations and self-organization in orogenic belts. *J Struct Geol 20*, 211-227.
- Brown, E. H., McClelland, W. C., 2000. Pluton emplacement by sheeting and vertical ballooning in part of the southeast Coast Plutonic Complex, British Columbia. *GSA Bull 112*, 708-719.
- Bryan, S. E., Ernst, R. E., 2008. Revised definition of Large Igneous Provinces (LIPs). *Earth-Sci Rev 86*, 175-202.
- Buck, R. W., Einarsson, P., Brandsdottir, B., 2006. Tectonic stress and magma chamber site as controls on dike propagation: constraints from the 1975-1984 Krafla rifting episode. *J Geophys Res 111*, B122404. doi: 10.1029/2005JB003879.
- Bull, J. M., Minshull, T. A., Mitchell, N. C., Thors. K., Dix, J. K., Best, A. I., 2003. Fault and magmatic interaction within Iceland's western rift over the last 9 kyr. *Geophys J Int 154*, F1-F8.
- Burchardt, S., 2008. New insights into the mechanics of sill emplacement provided by field observations of the Njardvik Sill, Northeast Iceland. *J Vol Geotherm Res 173*, 280-288.
- Burchardt, S., Walter, T. R., 2009. Miyakejima caldera collapse simulated in experiments: digital image correlation analyses reveal caldera ring fault propagation, linkage, and interaction. *Bull Volcanol*, accepted manuscript.
- Burchardt, S., Tanner, D. C., Krumbholz, M., 2009. Mode of emplacement of the Slaufudalur Pluton, Southeast Iceland inferred from three-dimensional GPS mapping and model building. *Tectonophysics*, accepted manuscript.
- Burg, J.-P., Gerya, T. V., 2008. Modelling intrusions of mafic and ultramafic magma into the continental crust: numerical methodology and results. *Ital J Geosci 127*, 1-6.
- Burke, K., Kidd, W. S. F., Wilson, J. T., 1973. Plumes and concentric plume traces of the Eurasian Plate. *Nature 241*, 128-129.

- Bursvik, M., Renshaw, C., McCalpin, J., Berry, M., 2003. A volcanotectonic cascade: Activation of range front faulting and eruptions by dyke intrusion, Mono Basin-Long Valley Caldera, California, *J Geophys Res* 108(B8), 2393, doi:10.1029/2002JB002032.
- Calais, E., d'Oreye, N., Albaric, J., Deschamps, A., Delvaux, D., Déverchère, J., Ebinger, C., Ferdinand, R. W., Kervyn, F., Macheyeke, A., Oyen, A., Perrot, J., Saria, E., Smets, B., Stamps, D. S., Wauthier, C., 2008. Strain accommodation by slow slip and dyking in a youthful continental rift, East Africa. *Nature* 456, 783-788.
- Capozzi, R., Picotti, V., 2002. Fluid migration and origin of a mud volcano in the Northern Apennines (Italy): the role of deeply rooted normal faults. *Terra Nova* 14, 363-370.
- Carbotte, S. M., Detrick, R. S., Harding, A., Canales, J-P., Babcock, J., Kent, G., Van Ark, E., Nedimovic, M., Diebold, J., 2006. Rift topography linked to magmatism at the intermediate spreading Juan de Fuca Ridge. *Geology* 34, 209-212.
- Carlson, L., Holmquist, A., 1968. Ett nytt fynd av sanstengångar i Västervikstrakten. *GFF* 90, 519-528.
- Carlsson, A., Christiansson, R., 2007. Construction experiences from underground works at Oskarshamn, Swedish Nuclear Fuel and Waste Management Company, SKB-R-07-66, Stockholm, Sweden.
- Cartwright, J., Hansen, D. M., 2006. Magma transport through the crust via interconnected sill complexes. *Geology* 34, 929-932.
- Cartwright, J., James, D., Huuse, M., Vetel, W., Hurst, A., 2008. The geometry and emplacement of conical sandstone intrusions. *J Struct Geol* 30, 854-867.
- Castro, A., 1987. On granitoid emplacement and related structures: A review. *Geol Rundsch* 76, 101-124.
- Čečys, A., 2004. Tectonic implications of a 1.45 Ga granitoid magmatism at the southwestern margin of the East European Craton, PhD thesis, University of Lund, 25p.
- Čečys, A., Benn, K., 2007. Emplacement and deformation of the ca. 1.45 Ga Karlshamn granitoid pluton, southeastern Sweden, during ENE-WSW Danopolian shortening. *Int J Earth Sci* 96, 397-414.
- Čečys, A., Bogdanova, S., Janson, C., Bibikova, E., Kornfält, K.-A., 2002. The Stenshuvud and Tåghusa granitoids. New representatives of Mesoproterozoic magmatism in southern Sweden. *GFF* 124, 149-162.
- Černý, P., 1971. Graphic intergrowths of feldspars and quartz in some Czechoslovak pegmatites. *Contrib Min Petrol* 30, 343-355.
- Cervelli, P., Segall, P., Amelung, F., Garbeil, H., Meertens, C., Owen, S., Miklius, A., Lisowski, M., 2002. The September 12,

- 1999 Upper East Rift Zone dyke intrusion at Kilauea Volcano, Hawaii. *J Geophys Res* 106, doi: 10.1029/2001JB000602.
- Chadwick, W.W., Embley, R. W., 1998. Graben formation associated with recent dyke intrusions and volcanic eruptions on the mid-ocean ridge. *J Geophys Res* 103 (B5), 9807-9825.
- Chenet, A.-L., Fluteau, F., Courtillot, V., 2005. Modelling massive sulphate aerosol pollution, following the large 1783 Laki basaltic eruption. *Earth Planet Sci Lett* 236, 721– 731.
- Chester, D. K., Duncan, A. M., Guest, J. E., Kilburn, C. R., 1985. Mount Etna: Anatomy of a volcano. Chapman and Hall, London, 404 pp.
- Chester, D. K., Dikken, C. J. L., Duncan, A. M., 2002. Volcanic hazard assessment in Western Europe. *J Volcanol Geotherm Res* 115, 411-435.
- Ciavarella, V., Wyld, S. J., 2008. Wall rocks as recorders of multiple pluton emplacement mechanisms-examples from Cretaceous intrusions of northwest Nevada. *GSA Spec Paper* 438, 517-550, doi:10.1130/2008.2438.
- Clari, P., Cavagna, S., Martire, L., Hunziker, J., 2004. A Miocene mud volcano and its plumbing system: a chaotic complex revisited (Monferrato, NW Italy). *J Sed Res* 74, 662-676; doi: 10.1306/022504740662.
- Clarke, D. B., Erdmann, S., 2008. Is stoping a volumetrically significant pluton emplacement process? *Comment. GSA Bull* 120, 1072-1074.
- Clarke, D. B., Henry, A. S., White, M. A., 1998. Exploding xenoliths and the absence of “elephant’s graveyards” in granite batholiths. *J Struct Geol* 20, 1325-1343.
- Clemens, J. D., Mawer, C. K., 1992. Granitic magma transport by fracture propagation. *Tectonophysics* 204, 339-360.
- Clemens, J. D., 1998. Observations on the origins and ascent mechanisms of granite magmas. *J Geol Soc London* 155, 843-851.
- Clifton, A. E., Schlische, R. W., 2003. Fracture propagation on the Reykjanes Peninsula, Iceland: comparison with experimental clay models of oblique spreading. *J Geophys Res* 108 (B2), 2074, doi: 10.1029/2001JB000635.
- Clough, C. T., Brantwood Maufe, H., Battersby Bailey, E., 1909. The cauldron-subsidence of Glen Coe, and the associated igneous phenomena. *Quart J Geol Soc, London* 65, 611-678.
- Cocks, L. R., Torsvik, T. H., 2005. Baltica from the late Precambrian to mid-Palaeozoic times: the gain and loss of a terrane’s identity. *Earth Sci Rev* 72, 39-66.
- Coleman, D.S., Glazner, A.F., Miller, J.S., Bradford, K.J., Frost, T.P., Joye, J.L., Bachl, C.A., 1995. Exposure of a Late Cretaceous layered mafic-felsic magma system in the central Sierra Nevada

- batholith, California: *Contrib Mineral Petrol* 89, 30–38.
- Coleman, D. S., Gray, W., Glazner, A. F., 2004. Rethinking the emplacement and evolution of zoned plutons: geochronologic evidence of incremental assembly of the Tuolumne Intrusive Suite, California. *Geology* 32, 433-436.
- Collins, W. J., Sawyer, E. W., 1996. Pervasive granitoid magma transport through the lower-middle crust during non-coaxial compressional deformation. *J Metamorph Geol* 14, 565-579.
- Collins, W. J., Wiebe, R. A., Healy, B., Richards, W., 2006. Replenishment, crystal accumulation and floor aggradation in the megacrystic Kameruka Suite, Australia. *J Petrol* 47, 2073-2104.
- Condon, D.J., Bowring, S.A., Pitcher, W.S., Hutton, D.W. 2004. Rates and tempo of granitic magmatism: a U–Pb geochronological investigation of the Donegal Batholith (Ireland). *Geological Society of America, Abstracts with Programs* 46, 406.
- Connor, C. B., Conway, M., 2000. Basaltic Volcanic Fields. In: Sigurdsson, H., Houghton, B., McNutt, S., Rymer, H., Stix, J. (eds.). *Encyclopedia of volcanoes*. Academic Press, San Diego, CA, pp. 331-343.
- Corry, C. E., 1988. Laccoliths: mechanics of emplacement and growth. *Geol Soc Am Special Pub* 220, 110 pp.
- Cosgrove, J. W., 2001. Hydraulic fracturing during the formation and deformation of a basin: a factor in dewatering of low-permeability sediments. *AAPG Bull* 85, 737-748.
- Coulson, I. M., Villeneuve, M. E., Dipple, G. M., Duncan, R. A., Russell, J. K., and Mortensen, J. K., 2002. Time-scales of assembly and thermal history of a composite felsic pluton; constraints from the Emerald Lake area, northern Canadian Cordillera, Yukon: *J Volcanol Geotherm Res* 114, 331–356, doi: 10.1016/S03770273
- Crowe, B., Self, S., Vaniman, D., Amos, R., Perry, F., 1983. Aspects of potential magmatic disruption of a high-level radioactive waste repository in southern Nevada. *J Geol* 91, 259-276.
- Cruden, A., 1998. On the emplacement of tabular granites. *J Geol Soc London* 155, 853-862.
- Cruden, A. R., 2008. Emplacement mechanisms and structural influences of a younger granite intrusion into older wall rock—a principal study with application to the Götemar and Uthammar granites. SKB-R-08-138, Swedish Nuclear Fuel and Waste Management Co, Stockholm, Sweden, pp. 48.
- Cruden, A. R., Aaro, S., 1992. The Ljugaren granite massif, Dalarna, central Sweden. *GFF* 114, 209-225.
- Cruden, A. R., McCaffrey, K. J. W., 2001. Growth of plutons by floor subsidence: Implications for rates of emplacement, intrusion spacing and melt-extraction

- mechanisms. *Physics Chem Earth (A)* 26, 303-315.
- Cruden, A. R., Wahlgren, C.-H., 2008. Form and emplacement of two anorogenic granite plutons, SE Sweden: laccoliths, sills or what? LASI III Conference, Abstract, Elba Island.
- Cruden, A. R., Sjöstrom, H., Aaro, S., 1999. Structure and geophysics of the Gåsborn granite, Central Sweden: an example of fracture-fed asymmetric pluton emplacement. In: Castro, A., Fernandez, C., Vigneresse, J. L. (eds.). *Understanding Granites: integrating new and classical techniques*. Geol Soc London, Spec Pub 168, 141-160.
- Cruden, A.R., et al., 2005. Timescales of incremental pluton growth: theory and a field-based test. 2005 Annual Meeting, Abstracts and Programs 56 (9). Geological Society of America, Abstracts p. 131.
- Curtis, M.L., Riley, T.R., 2003. Mobilization of fluidized sediment during sill emplacement, western Dronning Maud Land, East Antarctica. *Antarctic Sci* 15, 393-398.
- Cymerman, Z., 2004. Precambrian structures of Bornholm and their relationships in the Kaszuby region (N Poland). *Przeegl ad Geologiczny* 52, 593–602 (Polish with English abstract).
- Daly, R. A., 1903. The mechanics of igneous intrusion. *Am J Sci* 15, 269-298.
- Dance, M., 1997. Fracture and fracturing of lava. PhD Thesis, University of Bristol, Bristol, Great Britain.
- Darbyshire, F.M.A., White, R. S., Priestley, K. F., 2000. Structure of the crust and uppermost mantle of Iceland from a combined seismic and gravity study. *Earth Planet Sci Lett* 181, 409-428.
- Davies, R. J., 2003. Kilometer-scale fluidization structures formed during early burial of a deepwater slope channel on the Niger Delta. *Geology* 31, 949–952.
- Davies, R. J., Stewart, S. A., 2005. Emplacement of giant mud volcanoes in the South Caspian Basin: 3D seismic reflection imaging of their root zones: *J Geol Soc London* 162, 1–4, doi: 10.1144/0016-764904-082.
- Davies, R. J., Swarbrick, R. E., Evans, R. J., Huuse, M., 2007. Birth of a mud volcano, East Java, 29 May 2006. *GSA Today* 17, doi:10.1130/GSA TO1702A.1.
- Davies, R. J., Brumm, M., Mangan, M., Rubiandini, R., Swarbrick, R., Tingay, M., 2008. The East Java mud volcano (2006 to present): an earthquake of drilling trigger. *Earth Planet Sci Lett* 272, 627-638.
- Davison, I., Alsop, G. I., Evans, N. G., Safaricz, M., 2000. Overburden development patterns and mechanisms of salt diapir penetration in the Central Graben, North Sea. *Marine Petrol Geol* 17, 601-618.

- DeGaff, J. M., Aydin, A., 1987. Surface morphology of columnar joints and its significance to mechanism and direction of joint growth. *GSA Bull* 99, 605-617.
- DeMets, C., Gordon, R. G., Argus, D. F., Stein, S., 1994. Effect of recent revisions to the geomagnetic reversal time scale on estimates of current plate motions. *Geophys Res Lett* 21, 2191-2194.
- Dempster, T. J., Jenkin, G. R. T., Rogers, G., 1994. The origin of rapakivi texture. *J Petrol* 35, 963-981.
- De Saint-Blanquat, M., Tikoff, B., Teyssier, C., Vigneresse, J. L., 1998. Transpressional kinematics and magmatic arcs. In: Holdsworth, R. E., Strachan, R. A., Dewey, J. F. (eds.). *Continental transpressional and transtensional tectonics*. Geol Soc London, Special Pub 135, 327-340.
- De Saint-Blanquat, M., Law, R. D., Bouchez, J.-L., Morgan, S. S., 2001. Internal structure and emplacement of the Papoose Flat pluton: An integrated structural, petrographic, and magnetic susceptibility study. *GSA Bull* 113, 976-995.
- De Saint-Blanquat, M., Habert, G., Horsman, E., Morgan, S. S., Tikoff, B., Launeau, P., Gleizes, G., 2006. Mechanisms and duration of non-tectonically assisted magma emplacement in the upper crust: The Black Mesa pluton, Henry Mountains, Utah. *Tectonophysics* 428, 1-31.
- Diller, K., Clarke, A. B., Voight, B., Neri, A., 2006. Mechanisms of conduit plug formation: implications for vulcanian explosions. *Geophys Res Lett* 33, L20302.
- Dimitrov, L. I., 2002. Mud volcanoes-the most important pathway for degassing deeply buried sediments. *Earth Sci Review* 59, 49-76.
- Dobnikar, M., Dolenc, T., Bellieni, G., 2002. Rapakivi texture in porphyritic dikes within the Karavanke granitic massif (Slovenia). *Bull Geol Soc Finland* 74, 147-157.
- Doubik, P., Hill, B. E., 1999. Magmatic and hydromagmatic conduit development during the 1975 Tolbachik Eruption, Kamchatka, with implications for hazards assessment at Yucca Mountain, NV. *J Volcanol Geotherm Res* 91, 43-64.
- Drachenfels, von, M-V., 2004. *Petrographie und Gefüge von Granitoiden der Västervik Region (SE-Schweden)*. Diploma thesis, University of Göttingen, Germany (in German).
- Drake, H., Tullborg, E.-L., 2006. Fracture mineralogy of the Götemar granite: results from drill cores KKR01, KKR02 and KKR03. SKB-P-06-04, Swedish Nuclear Fuel and Waste Management Co, Stockholm, Sweden, pp. 54.
- Drake, H., Page, L., Tullborg, E.-L., 2007. $^{40}\text{Ar}/^{39}\text{Ar}$ dating of fracture minerals. SKB-P-07-27, Swedish Nuclear Fuel and Waste Management Co, Stockholm, Sweden, pp. 42.
- Drake, H., Tullborg, E.-L., Page, L., 2009. Distinguished multiple events of fracture

- mineralisation related to far-field orogenic effects in Paleoproterozoic crystalline rocks, Simpevarp area, SE Sweden. *Lithos*, doi: 10.1016/j.lithos.2008.003
- Dumond, G., Yoshinobu, A. S., Barnes, C. G., 2005. Midcrustal emplacement of the Sausfjellet pluton, central Norway: ductile flow, stoping, and in situ assimilation. *GSA Bull* 117, 383-395.
- Duranti, D., Mazzini, A., 2005. Large-scale hydrocarbon-driven sand injection in the Paleogene of the North Sea. *Earth Planet Sci Lett* 239, 327–335.
- Dziak, R. P., C. G. Fox, C. G., Schreiner, A. E., 1995. The June –July 1993 seismo-acoustic event at Co-Axial segment, Juan de Fuca Ridge: Evidence for a lateral dike injection. *Geophys Res Lett* 22, 135-138, doi:10.1029/94GL01857.
- Ebinger, C., Casey, M., 2001. Continental break-up in magmatic provinces: an Ethiopian example. *Geology* 29, 527-530.
- Ebinger, C. J., Keir, D., Ayele, A., Calais, E., Wright, T. J., Belachew, M., Hammond, J. O. S., Campbell, E., Buck, W. R., 2008. Capturing magma intrusions and faulting process during continental rupture: seismicity of the Dabbahu (Afar) rift. *Geophys J Int* 174, 1138-1152.
- Eckstrand, O. R., Hulbert, L. J., 2007. Magmatic nickel-copper-platinum group elements deposits. In: Goodfellow, W. D. (ed.). *Mineral Deposits of Canada: A Synthesis of Major Deposit Types, District Metallogeny, the Evolution of Geological Provinces, and Exploration Methods*. Geol Ass Canada, Mineral Deposits Division, Special Pub 5, 205-222.
- Egholm, D.L., 2007. A new strategy for discrete element numerical models: 1. Theory. *J Geophys Res* 112, B05203, doi:10.1029/2006JB004557.
- Egilsson, D., Hardarson, B. A., Jonsson, B., 1989. Dynamic properties of rock: Yearbook of the Engineering Association of Iceland, 226-233 (in Icelandic).
- Einarsson, P., 1991a. The Krafla rifting episode 1975–1989. In: Gardarsson, A., Einarsson, P. (eds.). *Nattura Myvatns (The Nature of Lake Myvatn)*. Icelandic Nature Sci. Soc., Reykjavik, pp. 97–139.
- Einarsson, P., 1991b. Earthquakes and present-day tectonism in Iceland. *Tectonophysics* 189, 261–279.
- Einarsson, P., Brandsdottir, B., 1980. Seismological evidence for lateral magma intrusion during the July 1978 deflation of the Krafla volcano in NE Iceland. *J Geophys* 47, 160-165.
- Einarsson, S., Johannesson, H., 1989. Aldur Arnarseturshrauns a Reykjanesskaga (Age of the Arnarseturshraun lava flow, Reykjanes peninsula, SW-Iceland). *Náttúrufræðistofnunar* 8, 15.
- Elson, M. D., Ort, M. H., Hesse, S. J., Duffield, W. A., 2002. Lava, corn, and ritual in the northern Southwest.

- American Antiquity 67,119–135, doi: 10.2307/2694881.
- England, R.W., 1990. The identification of granitic diapirs. *J Geol Soc London* 147, 931-933.
- Erlstöm, M., Sivhed, U., 2001. Intra-cratonic dextral transtension and inversion of southern Kattegat on the southwest margin of Baltica-seismostratigraphy and crustal development. *Sveriges Geologiska Undersökning C832*.
- Ernst, R. E., Grosfils. E. B., Mège, O., 2001. Giant dyke swarms: Earth, Venus and Mars. *Annu Rev Earth Planet Sci* 29, 489-534.
- Eyal, Y., 1988. Sandstone dyke as evidence of localized transtension in a transpressive regime, Br Zreir area, eastern Sinai. *Tectonics* 7, 1279-1289.
- Fahlbusch, W., 2008. Structural geology analyses of joints and mineral veins in the Götemar pluton and its bedrock. Bachelor of Science thesis (written in German), University of Göttingen, pp. 52.
- Fernandez, C., Castro, A., 1999. Pluton accommodation of high strain rates in the upper continental crust. The example of the Central Extremadura batholith, Spain. *J Struct Geol* 21, 1143-1149.
- Filho, A. T., Mizusaki, A. M. P., Antonioli, L., 2008. Magmatism and petroleum exploration in the Brazilian Paleozoic basins. *Marine Petrol Geol* 25, 143-151.
- Flehmig, W., 1977. The synthesis of feldspar at temperatures between 0°-80°C, their ordering behavior and twinning. *Contrib Mineral Petrol* 65, 1-9
- Flodén, T., 1980. Seismic stratigraphy and bedrock geology of the central Baltic. *Stockholm Contrib Geol* 35.
- Fowler, T. K., Paterson, S. R., 1997. Timing and nature of magmatic fabrics from structural relations around stoped blocks. *J Struct Geol* 19, 209–224.
- Francis, E. H., 1982. Magma and sediment-1. Emplacement mechanism of late Carboniferous tholeiite sills in northern Britain. *J Geol Soc London* 139, 1–20.
- Frey, M., 1997. Mittelproterozoische Magmatite und Metamorphite des Transskandinavischen Magmatit-Gürtels, SW' Västrum, S' Västervik, SE Schweden. Diploma mapping thesis, University of Göttingen, Germany (in German).
- Friese, N., Vollbrecht, A., Leiss, B., Jacke, O., submitted in revision. Cambrian sedimentary dykes in the Proterozoic basement of the Västervik area (Southeast Sweden): episodic formation inferred from macro- and microfabrics. *Int J Eart Sci*.
- Gaal, G., Gorbatshev, R., 1987. An outline of the Precambrian evolution of the Baltic Shield. *Precambrian Res* 35, 15-52.
- Gaffney, E. S, Damjanac, B., Valentine, G. A., 2007. Localization of volcanic activity: 2. effects of pre-existing structure. *Earth Planet Sci Lett* 263, 323-338.

- Gagnevin, D., Daly J. S., Poli, G., Morgan, D., 2005. Microchemical and Sr isotopic investigation of zoned K-feldspar megacrysts: insights into the petrogenesis of a granitic system and disequilibrium crystal growth. *J Petrol* 46, 1689-1724.
- Galadi-Enriquez, E., Galindo-Zaldivar, J., Simancas, F., Exposito, I., 2003. Diapiric emplacement in the upper crust of a granitic body: the la Bazana granite. *Tectonophysics* 361, 83-96.
- Galerne, C. Y., Neumann, E.-R., Planke, S., 2008. Emplacement mechanisms of sill complexes: information from the geochemical architecture of the Golden Sill Complex, South Africa. *J Volcanol Geotherm Res* 177, 425-440.
- Galland, O., Planke, S., Neumann, E.-R., Malthe-Sørensen, A., 2009. Experimental modelling of shallow magma emplacement: application to saucer-shaped intrusions. *Earth Planet Sci Lett* 227, 373-383.
- Galli, P., 2000. New empirical relationships between magnitude and distance for liquefaction, *Tectonophysics* 324, 169–187.
- Garcia, S., Arnaud, N. O., Angelier, J., Bergerat, F., Homberg, C., 2003. Rift jump process in northern Iceland since 10 Ma from $^{40}\text{Ar}/^{39}\text{Ar}$ geochronology. *Earth Planet Sci Lett* 214, 529-544.
- Garcia, S., Angelier, J., Bergerat, F., Homberg, C., Dauteuil, O., 2008. Influence of rift jump and excess loading on the structural evolution of northern Iceland. *Tectonics* 27, doi: 10.1029/2006TC002029
- Gargani, J., Geoffroy, L., Gac, S., Cravoisier, S., 2006. Fault slip and Coulomb stress variations around a pressured magma reservoir: consequences on seismicity and magma intrusion. *Terra Nova* 18, 403-411.
- Geirsdottir, A., Eiriksson, J., 1994. Growth of an intermittent ice sheet in Iceland during the late Pliocene and early Pleistocene. *Quat Res* 42, 115-130.
- Geirsdottir, A., Miller, G. H., Andrews, J. T., 2007. Glaciation, erosion, and landscape evolution of Iceland. *J Geodyn* 43, 170-186.
- Geirsson, H., Arnadottir, Th., Völksen, C., Jiang, W., Sturkell, E., Villemin, T., Einarsson, P., Sigmundsson, F., Stefansson, R., 2006. Current plate movements across the Mid-Atlantic ridge determined from 5 years of continuous GPS measurements in Iceland. *J Geophys Res* 111, B09407.
- Geshi, N., 2008. Vertical and lateral propagation of radial dykes inferred from the flow-direction analysis of the radial dyke swarm in Komochi Volcano, Central Japan. *J Vol Geotherm Res* 173, 122-134.
- Gibson, I. L., Piper, J. D. A., 1972. Structure of the Iceland basalt plateau and the process of drift. *Phil Trans R Soc London Series A* 271, 141-150.
- Ginibre, C., Wörner, G., Kronz, A., 2002. Minor- and trace-element zoning in plagioclase: implications for magma

- chamber processes at Parinacota volcano, northern Chile. *Contrib Mineral Petrol* 143, 300–315.
- Girard, G., van Wyk de Vries, B., 2005. The Managua Graben and La Sierras-Masaya volcanic complex (Nicaragua); pull-apart localization by an intrusive complex: results from analogue modelling. *J Volcanol Geotherm Res* 144, 37-57.
- Gorbatshev, R., Bogdanova, S., 1993. Frontiers in the Baltic Shield. *Precambrian Res* 64, 3-22.
- Goto, Y., Gouchi, N., Itaya, T., 1990. Radial dyke swarms and reconstruction of the Pleistocene submarine volcanoes in the Shiretoko Peninsula, Japan. In: Parker, A. J., Rickwood, P. C., Tucker, D. H. (eds.). *Mafic dykes and emplacement mechanisms*. Balkema, Rotterdam, pp. 25-33.
- Götze J., Plötze M., Habermann D., 2001. Origin, spectral characteristics and practical applications of the cathodoluminescence (CL) of quartz: a review. *Mineral Petrol* 71, 225–250.
- Goudy, C. L., Schultz, R. A., 2005. Dyke intrusion beneath grabens of Arsia Mons, Mars. *Geophys Res Lett* 32, doi: 10.1029/2004GL021977.
- Gouly, N. R., 2005. Emplacement mechanism of the Great Whin and Midland Valley dolerite sill. *J Geol Soc London* 162, 1047–1056.
- Glazner, A. F., Miller, D. M., 1997. Late-stage sinking of plutons. *Geology* 25, 1099–1102, doi: 10.1130/00917613.
- Glazner, A. F., Bartley, J. M., 2006. Is stopping a volumetrically significant pluton emplacement process? *GSA Bull* 118, 1185-1195.
- Glazner, A. F., Bartley, J. M., Coleman, D. S., Taylor, R. Z., 2004. Are plutons assembled over millions of years by amalgamation from small magma chambers? *GSA Today* 14, doi: 10.1130/1052-5173
- Grattan, J., 2005. Pollution and paradigms: lessons from Icelandic volcanisms for continental flood basalt studies. *Lithos* 79, 343-353.
- Gray, T. G. F., 1992. *Handbook of Crack Opening Data*. Abington Publishing, Cambridge UK.
- Gregersen, S., 1992. Crustal stress regime in Fennoscandia from focal mechanisms. *J Geophys Res* 97, B8. 11.821–11.827.
- Grocott, J., Brown, M., Dallmeyer, R.D., Taylor, G.K., Treloar, P., 1994. Mechanisms of the continental growth in extensional arcs: a example from the Andean plate-boundary zone. *Geology* 22, 391-394.
- Grogan, S. E., Reavy, R. J., 2002. Disequilibrium textures in the Leinster Granite complex, SE Ireland: evidence for acid-acid magma mixing. *Mineral Mag* 66, 929-939.
- Gudmundsson, A., 1986. Formation of crustal magma chambers in Iceland. *Geology* 14, 164-166.
- Gudmundsson, A., 2003. Surface stresses associated with arrested dykes in rift zones: *Bull Volcanol* 65, 606-619.

- Gudmundsson, A., Backström, K., 1989. The grabens of Sveinar and Sveinagja, NE Iceland. Nordic Volcanological Institute, Reykjavik, Report 8901.
- Gudmundsson, A., Loetveit, I.F., 2005. Dyke emplacement in a layered and faulted rift zone. *J Volcanol Geotherm Res* 144, 311-327.
- Gudmundsson, A., Andrew, R. E. B., Letourneur, L., 2007. Tectonics of the 1783 Laki Crater Row and associated graben, South Iceland. AGU Fall Meeting Abstract V52B05.
- Gudmundsson, A., Friese, N., Galindo, I., Philipp, S., 2008. Dyke-induced reverse faulting in a graben. *Geology* 36, 123-126.
- Guilbaud, M.-N., Siebe, C., Agusti-Flores, J., 2009. Eruptive style of the young high-Mg basaltic-andesite Pelagatos scoria cones, southeast of Mexico City. *Bull Volcanol*, doi: 10.1007/s00445-009-0271-0
- Gustafsson, L. E., 1992. Geology and Petrography of the Dyrfjöll Central Volcano, Eastern Iceland. *Berliner Geowissenschaftliche Abhandlungen, Reihe A, Band 138*.
- Habert, G., de Saint-Blanquat, M., 2004. Rate of construction of the Black Mesa bysmalith, Henry Mountains, Utah. In: Breitzkreuz, C., Petford, N. (eds.). *Physical geology of high-level magmatic systems*. *J Geol Soc, London, Special Pub 234*, 163-173.
- Hagenfeldt, S. E., 1989. Lower and Middle Cambrian acritarchs from the Baltic Depression and south-central Sweden taxonomy, stratigraphy and palaeographic reconstruction. Ph.D. thesis, University of Stockholm, Stockholm, Sweden, 32 pp.
- Hampel, A., Hetzel, R., 2008. Slip reveals on active normal faults related to inflations and deflation of magma chambers: numerical modeling with application to the Yellowstone-Teton region. *Geophys Res Lett* 35, doi: 10.1029/2008GL033226.
- Hanson, R. B., Glazner, A. F., 1995. Thermal requirements for extensional emplacement of granitoids. *Geology* 23, 213-216.
- Hansen, D. M., Cartwright, J., 2006. Saucer-shaped sill with lobate morphology revealed by 3D seismic data: implications for resolving a shallow-level sill emplacement mechanism. *J Geol Soc, London* 163, 509-523.
- Hardarson, B. S., Fitton, J. G., 1991. Increased mantle melting beneath Snaefellsjökull volcano during Late Pleistocene deglaciation. *Nature* 353, 62-64.
- Hardarson, B. S., Fitton, J. G., Ellam, R. M., Pringle, M. S., 1997. Rift relocation - a geochemical and geochronological investigation of a palaeo-rift in Northwest Iceland. *Earth Planet Sci Lett* 153, 181-196.
- Härmä, P., Selonen, O., 2008. Surface weathering of rapakivi granite outcrops-

- implications for natural stone exploration and quality evaluation. *Estonian J Earth Sci* 57, 135-148.
- Harms, J. C., 1965. Sandstone dikes in relation to Laramide faults and stress distribution in the Southern Front Range, Colorado. *GSA Bull* 76, 981-1002.
- Hartz, E. H., Torsvik, T. H., 2002. Baltica upside down: a new plate tectonic model for Rodinia and the Iapetus Ocean. *Geology* 30, 255-258.
- Hawkesworth, C. J., Turner, S., Gallagher, K., Hunter, A., Bradshaw, T. and Roger, N., 1995. Calc-alkaline magmatism, lithospheric thinning and extension in the Basin and Range. *J Geophys Res* 100, 10271–10286.
- Hawkins, D. P., Wiebe, R. A., 2004. Discrete stoping events in granite plutons; a signature of eruptions from silicic magma chambers? *Geology* 32, 1021–1024.
- Head, J. W., Wilson, L., 1989. Basaltic pyroclastic eruptions: influence on gas-release patterns and volume fluxes on fountain structure, and the formations of cinder cones, spatter cones, rootless flows, lava ponds, and lava flows. *J Volcanol Geotherm Res* 37, 261-271.
- Heimpel, M., Oison, P., 1994. Buoyancy-driven fracture and magma transport through the lithosphere: models and experiments. In: Ryan, M.P. (ed.). *Magmatic systems*, 223–240.
- Heki, K., Foulger, G. R., Julian, B. R., Jahn, C. H., 1993. Plate dynamics near divergent boundaries: geophysical implications of post-rifting crustal deformation in NE Iceland. *J Geophys Res* 98 (B8), 14279–14297.
- Helgason, J., 1984. Frequent shifts of the volcanic zone in Iceland. *Geology* 12, 212–216.
- Helgason, J. Duncan, R. A., 2001. Glacial-Interglacial history of the Skaftafell Region, Southeast Iceland, 0-5 Ma. *Geology* 29, 179-182
- Heubeck, C., 2009. Gravel-filled dykes of the Eisenach Formation (Oberrotliegend, Early Permian): modified artesian injections at the base of alluvial fans? *ZDGG* 160, 41-56 (in German with English abstract).
- Hibbard, M. J., 1981. The magma mixing origin of mantled feldspars. *Contrib Mineral Petrol* 76, 158 - 170.
- Hibbard, M. J., 1987. Deformation of incompletely crystallized magma systems: Granite gneisses and their tectonic implications. *J Geol* 95, 543–561.
- Hibbard, M. J., 1991. Textural anatomy of twelve magma mixed granitoid systems. In: Didier, J., Barbarin, B., (eds.). *Enclaves and Granite Petrology*. Elsevier, Amsterdam, p. 431 - 444.
- Hildreth, W., 2004. Volcanological perspectives on Long Valley, Mammoth Mountain, and Mono Craters: several contiguous but discrete systems. *J Volcanol Geotherm Res* 136, 169–198.
- Hillier, R. D., Cosgrove, J. W., 2002. Core and seismic observations of overpressure-related deformation within

- Eocene sediments of the Outer Moray Firth, UKCS. *Petrol Geosci* 8, 141-149.
- Hjartardottir, A. R., 2008. The fissure swarm of the Askja central volcano. MSc thesis, University of Iceland, pp. 121.
- Ho, C.-H., Smith, E. I., Keenan, D. L., 2006. Hazard area and probability of volcanic disruption of the proposed high-level radioactive waste repository at Yucca Mountain, Nevada, USA. *Bull Volcanol* 69, 117-123.
- Hoffmann, A., Siegesmund, S., 2007. Investigation of dimension stones in Thailand: overview and granite site investigations. *Geol Soc London, Spec Pub* 271, 43-54.
- Hofton, M. A., Foulger, G. R., 1996. Postrifting anelastic deformation around the spreading plate boundary, north Iceland. 1. Modeling of the 1987–1992 deformation field using a viscoelastic Earth structure. *J Geophys Res* 101 (B11), 25403–25421.
- Hogan, J. P., Price, J. D., Gilbert, M. C., 1998. Magma traps and driving pressure: consequences for pluton shape and emplacement in an extensional regime. *J Struct Geol* 20, 1155-1168.
- Hogan, J. O., Gilbert, M. C., Price, J. D., 2000. Crystallisation of fine and coarse grained A-type granite sheets at the Southern Oklahoma Aulacogen, USA. *GSA Special Paper* 350, The Fourth Hutton Symposium on the origin of granite and related rocks, p. 139-150.
- Högdahl, K., Andersson, U. B., Eklund, O., 2004. The Transscandinavian Igneous Belt (TIB) in Sweden: a review of its character and evolution. *Geol Surv Finland, Spec Paper* 37, 125 pp.
- Holdsworth, R.E., McErlan, M.A., Strachan, R.A., 1999. The influence of country structural architecture during pluton emplacement: the Loch Loyal syenite, Scotland. *J Geol Soc* 156, 163-175.
- Holm, R. F., Moore, R. B., 1987. Holocene scoria cone and lava flows at Sunset Crater, northern Arizona. In: Beus, S. (ed.). *GSA Centennial Field Guide*. Boulder, GSA Rocky Mountain Section, 393–397.
- Holness, M. B., Humphreys, M. C. S., 2003. The Traigh Bhàn na Sgura sill, Isle of Mull: flow localization in a major magma conduit. *J Petrol* 44, 961–1976.
- Holohan, E. P., Troll, V. R., Errington, M., Donaldson, C. H., Nicoll, G. R., Emeleus, C. H., 2009. The Southern Mountains Zone, Isle of Rum, Scotland: volcanic and sedimentary process upon an uplifted and subsided magma chamber roof. *Geol Mag* 146, 400-418.
- Hornschemeyer, F. G., 2008. Final storage of radioactive waste in Germany by international comparison. *ATW - Int J Nuclear Power* 53, 600 pp.
- Horsman, E., Tikoff, B., Morgan, S., 2005. Emplacement-related fabric and multiple sheets in the Maiden Creek sill, Henry Mountains, Utah, USA. *J Struct Geol* 27, 1426-1444.
- Houghton, B. F., Wilson, C. J. N., Rosenberg, M. D., Smith, I. E. M., Parker, R., 1996. Mixed deposits of

- complex magmatic and phreato-magmatic volcanism: an example from Crater Hill. Auckland, New Zealand. *Bull Volcanol* 58, 59-66.
- Houghton, B. F., Wilson, C. J. N., Smith, I. E. M., 1999. Shallow seated controls of explosive basaltic volcanism: a case study from New Zealand. *J Volcanol Geotherm Res* 91, 97-120.
- Houlié, N., Komorowski, J. C., de Michele, M., Kasereka, M, Ciraba, H., 2006. Early detection of eruptive dykes revealed by normalized difference vegetation index (NDVI) on Mt. Etna and Mt. Nyiragongo. *Earth Planet Sci Lett* 246, 231-240.
- Hjartardottir, A.R., 2008. The fissure swarm of the Askja central volcano. MSc thesis, University of Iceland, Reykjavik, Iceland, 121 pp.
- Hubbert, M. K., Willis, D. G., 1957. Mechanics of hydraulic fracturing. *J Pet Technol* 9, 153-168.
- Hudec, M. R., Jackson, M. P. A. 2007. Terra infirma: understanding salt tectonics. *Earth Sci Rev* 82, 1-24.
- Hudson, J.A., Harrison, J.P., 1997. *Engineering Rock Mechanics: an introduction to the principles*. Pergamon, Oxford.
- Huffman, A. C., Jr., Taylor, D. J., 1998. Relationship of Basement Faulting to Laccolithic Centers of Southeastern Utah and Vicinity. In: Friedman, J. D., Huffman, A. C., Jr (eds.). *Laccolith Complexes of Southeastern Utah: Tectonic Control and Time of Emplacement*. Workshop. Proc USGS Bull 2158, 41-43.
- Hurst, A., Cartwright, J., Huuse, M., Jonk, R., Schwab, A., Duranti, D., Cronin, B., 2003. Significance of large-scale sand injectites as long-term fluid conduits: evidence from seismic data. *Geofluids* 3, 263-274.
- Hurst, A., Cartwright, J. A., 2007. Sand injectites: implications for hydrocarbon exploration and production. AAPG Mem 87 (Tulsa).
- Hutton, D. H. W. 1982. A tectonic model for the emplacement of the Main Donegal Granite, NW Ireland. *J Geol Soc London* 139, 615-31
- Hutton, D. H. W., 1988. Granite emplacement mechanisms and tectonic controls: inferences from deformation studies. *Trans R Soc Edinburgh: Earth Sci* 79, 245-255.
- Hutton, D.H.W., 1992. Granite sheeted complexes: evidence for the dyking ascent mechanisms. *Trans R Soc Edinburgh: Earth Sci* 83, 377-382.
- Hutton, D. H. W., 1997. Syntectonic granites and the principle of effective stress: A general solution to the space problem? In: Bouchez, J. L., Hutton, D. H. W., Stephens, W. E. (eds.). *Granite: from Segregation of Melt to Emplacement Fabrics*. Kluwer Academic, London, pp. 189-197.
- Hutton, D. H. W., Siegesmund, S., 2001. The Ardara Granite: reinflating the balloon hypothesis. *ZDGG* 152, 309-323.

- Hutton, D. H. W., Dempster, T. J., Brown, P. E., Becker, J. M., 1990. A new mechanism of granite emplacement: rapakivi intrusions in active shear zones. *Nature* 343, 452-454.
- Huuse, M., Duranti, D., Steinsland, N., Guargena, C., Prat, P., Holm, K., Cartwright, J. A., Hurst, A., 2004. Seismic characteristics of large scale sandstone intrusions in the Paleogene of the South Viking Graben, UK and Norwegian North Sea. In: Davies, R., Cartwright, J. A., Stewart, S. A., Underhill, J. R., Lappin, M. (eds.). *3D Seismic Data: Application to the Exploration of Sedimentary Basins* 29. *Geol Soc London Memoir* pp. 263–277.
- Huuse, M., Cartwright, J., Gras, R., Hurst, A., 2005. Kilometre-scale sandstone intrusions in the Eocene of the Outer Moray Firth (UK North Sea): migration paths, reservoirs and potential drilling hazards. In: Dore, A. G., Vining, B. A. (eds.). *Petroleum Geology: North-West Europe and Global Perspectives*. *Proc 6th Petrol Geol Conf. Geol Soc London*, pp. 1577–1594.
- Ida, Y., 1992. Width change of a planar magma path: implication for the evolution and style of volcanic eruptions. *Phys Earth Planet Inter* 74, 127-138.
- Irvine, T.N., 1980. Magmatic infiltration metasomatism, double-diffusive fractional crystallization and adcumulus growth in the Muskox intrusion and other layered intrusions. In: Hargreaves RB (ed). *Physics of Magmatic Processes*. Princeton University Press: 245-306
- Ishizuka, O., Geshi, N., Itoh, J., Kawanabe, Y., TuZino, T., 2008. The magmatic plumbing of the submarine Hachijo NW volcanic chain, Hachijojima, Japan: Long-distance magma transport? *J Geophys Res* 113, B08S08, doi:10.1029/2007JB005325.
- Ivarsson, G., 1992. *Geology and Petrochemistry of the Torfajökull Central Volcano in Central South Iceland, in Association with the Icelandic Hot Spot and Rift Zones*, PhD thesis, Univ. Hawaii, USA.
- Jacke, O., 2000. *Petrographie und Gefüge von Sedimentgängen im Granit der Västervik-Region/SE-Schweden*. Diploma thesis, University of Göttingen, Göttingen, Germany.
- Jackson, M. P. A., Talbot, C. J., 1991. A glossary of salt tectonics. *Geological Circular*, vol. 91-4. The University of Texas at Austin, Bureau of Economic Geology, 44 pp.
- Jaeger, C. M., 1972. *Rock Mechanics and Engineering*. Cambridge University Press, Cambridge.
- Jakobsson, S. P., 1972. Chemistry and distribution pattern of recent basaltic rocks in Iceland. *Lithos* 5, 365–386.
- Jakobsson, S. P., 1979a. Petrology of recent basalts in the Eastern Volcanic Zone, Iceland. *Acta Naturalia Islandica* 26, 1-103.

- Jakobsson, S. P., 1979b. Outline of the petrology of Iceland. *Jökull* 29, 57-73.
- Jakobsson, S. P., Jonsson, J., Shido, F., 1978. Petrology of the western Reykjanes Peninsula, Iceland. *J Petrol* 19, 669–705.
- Jancin, M., Young, K. D., Voight, B., 1985. Stratigraphy and K/Ar ages across the west flank of the northeast Iceland axial rift zone, in relation to the 7 Ma volcano-tectonic reorganization of Iceland. *J Geophys Res* 90, 9961-9985.
- Jenkins, O. P., 1930. Sandstone dikes as conduits for oil migration through shales. *AAPG Bull* 14, 411-421.
- Johannes W., Holtz F., 1996. Petrogenesis and experimental petrology of granitic rocks. Springer, Berlin Heidelberg New York, 335 p.
- Johannesson, H., 1980. Evolution of rift zones in western Iceland. *Naturufraedingurinn* 50, 13–31 (in Icelandic with English summary).
- Johannesson H., Saemundsson, K., 1998. Geological map of Iceland, 1: 500,000, tectonics. Iceland Institute of Natural History, Reykjavik.
- Johannesson, H., Jakobsson, S. P., and Saemundsson, K., 1990. Geological map of Iceland. Sheet 6, South-Iceland. Icelandic Museum of Natural History and Icelandic Geodetic Survey. Reykjavik. 3rd edition.
- Johansson, Å, Bogdanova, S. V., Taran, L., 2004. Gneisses and granitoids of Bornholm. *GG* 126, 24.
- Johansson Å, Bogdanova, S. V., Čečys, A., 2006. A revised geochronology for the Blekinge Province, southern Sweden. *GFF* 128, 287-302.
- John, B. E., 1988. Structural reconstruction and zonation of a tilted midcrustal magma chamber: the felsic Chemehuevi Mountains Plutonic Suite. *Geology* 16, 613 - 617.
- John, B. E., Blundy, J. D., 1993. Emplacement-related deformation of granitoid magmas, southern Adamello Massif, Italy: *GSA Bull* 105, 1517–1541, doi: 10.1130/0016-7606.
- Johnson, A. M., Pollard, D. D., 1973. Mechanics of growth of some laccolithic intrusions in Henry Mountains, Utah. 1. Field observations, Gilbert's model, physical properties and flow of magma. *Tectonophysics* 18, 261-309.
- Johnson, C. M., Czamanske, G. K., Lipman, P. W., 1990. H, O, Sr, Nd, and Pb isotope geochemistry of the Latir volcanic field and cogenetic intrusions, New Mexico, and relations between evolution of a continental magmatic center and modifications of the lithosphere. *Contrib Mineral Petrol* 104, 99–124.
- Jolly, R. J. H., Lonergan, L., 2002. Mechanisms and control on the formation of sand intrusions. *J Geol Soc London* 159, 605-617.
- Jonasson, K., 2007. Silicic volcanism in Iceland: composition and distribution within the active volcanic zones. *J Geodyn* 43, 101-117.
- Jones, S. F., Wielens, H., Williamson, M.-C., Zentilli, M., 2007. Impact of magmatism

- on petroleum systems in the Sverdrup Basin, Canadian Arctic Islands, Nunavut: a numerical modelling study. *J Petrol Geol* 30, 237-256.
- Jonsson, G., Kristjansson, L., Sverrisson, M., 1991. Magnetic surveys of Iceland. *Tectonophysics* 189, 229-247.
- Kalakay, T. J., John, B. E., Lageson, D.R., 2001. Fault-controlled pluton emplacement in the Sevier fold-and-thrust belt, SW Montana. *J Struct Geol* 23, 1151-1165.
- Kalvig, P., Knudsen, C. N. & Rasmussen, T. V. 2002: Potentialer for facadesten og skærver i Grønland. Danmarks og Grønlands Geologiske Undersøgelse Rapport 2002/11, 104 pp.
- Karlstrom, K. E., Åhall, K.-I., Harlan, S. S., Williams, M. L., McLelland, J., Geissman, J. W., 2001. Long-lived (1.8–1.0 Ga) convergent orogen in southern Laurentia, its extensions to Australia and Baltica, and implications for refining Rodinia. *Precambrian Res* 111, 5-30.
- Kastner, M., Siever, R., 1979. Low temperature feldspar in sedimentary rocks. *Am J Sci* 279, 435-479.
- Katzung, G., Obst K., 1997. The sandstone dyke swarm of Vang, Bornholm (Denmark). *Bull Geol Soc Denmark* 44, 161-171.
- Kavanagh, J. L., Menand, T., Sparks, R. S. J., 2006. An experimental investigation of sill formation and propagation in layered elastic media. *Earth Planet Sci Lett* 245, 799-813.
- Keating, G. N., Valentine, G. A., Krier, D. J., Perry, F. V., 2008. Shallow plumbing systems for small-volume basaltic volcanoes. *Bull Volcanol* 70, 563-582.
- Keir, D., Ebinger, C., Stuart, G. W., Daly, E., Ayele, A., 2006. Strain accommodation by magmatism and faulting at continental break-up: seismicity of the northern Ethiopian rift. *J Geophys Res* 111, doi: 10.1785/0120060051.
- Kemp, A. I. S., Hawkesworth, C. J., Paterson, B. A., Forster, G. L., Kinny, P. D., Whitehouse, M. J., Maas, R. J., EIMF, 2006. Exploring the plutonic-volcanic link: a zircon U-Pb, Lu-Hf and O isotope study of paired volcanic and granitic units from southeastern Australia. *Trans R Soc Edinburgh: Earth Sci* 97, 337-355.
- Khodayar, M., Einarsson, P., 2004. Reverse-slip structures at oceanic diverging plate boundaries and their kinematic origin: data from Tertiary crust of west and south Iceland. *J Struct Geol* 26, 1945-1960.
- Kirkbride, M. P., Dugmore, A. J., Brazier, V., 2006. Radiocarbon dating of mid-Holocene megaflood deposits in the Jökulsa a Fjöllum, north Iceland. *The Holocene* 16, 605-609.
- Klügel, A., Walter, T. R., Schwarz, S., Geldmacher, J., 2005. Gravitational spreading causes en-echelon diking along a rift zone of Madeira Archipelago: an experimental approach and implications for magma transport. *Bull Volcanol* 68, 37-46.

- Komorowski, J. C., Legendre, Y., Caron, B., Boudon, G., 2008. Reconstruction and analysis of sub-plinian tephra dispersal during the 1530 AD Soufrière (Guadeloupe) eruption: implications for scenario definition and hazards assessment. *J Vol Geotherm Res* 178, 491-515.
- Komuro, H., 1987. Experiments on cauldron formation: a polygonal cauldron and ring fractures. *J Volcanol Geotherm Res* 31, 139-149.
- Kopf, A., Stegmann, A., Delisle, G., Panahi, B., Aliyev, C. S., Guliyev, I., 2008. In situ cone penetration tests at the active Dashgil mud volcano, Azerbaijan: evidence for fluid pressure, updoming, and possible future violent eruption. *Marine and Petrol Geol*, doi: 10.1016/j.marpetgeo.2008.11.005.
- Kornfält, K.-A., Vaasjoki, M., 1999. U-Pb zircon dating of Småland and Karlshamn granites from the southeasternmost Sweden. In: Bergman, S. (ed.), *Radiometric Dating Results*, 4. SGU C831. Swedish Geological Survey, Uppsala, Sweden, pp. 33-41.
- Kornfält, K.-A., Persson, P.-O., Wikman, H., 1997. Granitoids from the Äspö area, southeastern Sweden-geochemical and geochronological data. *GFF* 119, 109-114.
- Koyi, H. A., 2001. Modeling the influence of sinking anhydrite blocks on salt diapirs targeted for hazardous waste disposal. *Geology* 29, 387-390.
- Kresten, P., Chyssler, J., 1976. The Götemar massif in south-eastern Sweden: A reconnaissance survey. *GFF* 98, 155-161.
- Kristjansson L., Jonsson, G., 1998. Aeromagnetic results and the presence of an extinct rift zone in western Iceland. *J Geodyn* 25, 99-108.
- Kristjansson, L., Jonsson, G., 2007. Paleomagnetism and magnetic anomalies in Iceland. *J Geodyn* 43, 30-54.
- Krumbholz, M., 2009. Natural Electromagnetic Radiation (NEMR) as indicator of lithospheric stresses - Case studies in different structural environments. PhD thesis, University of Göttingen, Germany.
- Kusumoto, S., Takemura, K., 2003. Numerical simulation of caldera formation due to collapse of a magma chamber. *Geophys Res Lett* 30, 2278.
- Küstner, W., 1997. Mesoproterozoic magmatite in the Transscandinavian Igneous Belt, NE' of Lake Götemar, SE Sweden, Diploma mapping, University of Göttingen, Germany, pp 65 (in German).
- Lafrance, B., John, B. E., 2001. Sheeting and dyking emplacement of the Gunnison annular complex, SW Colorado. *J Struct Geol* 23, 1141-1150.
- Lahtinen, R., Korja, A., Nironen, M., 2005. Paleoproterozoic tectonic evolution. In: Lehtinen, M., Nurmi, P. A., Rämö, O. T. (eds.). *Precambrian Geology of Finland-Key to the Evolution of the*

- Fennoscandian Shield. Elsevier, Amsterdam, pp. 481–532.
- Langer, M., 1999. Principles of geomechanical safety assessment for radioactive waste disposal in salt structures. *Eng Geol* 52, 257-269.
- Langmuir, C. H., 1989. Geochemical consequences of in situ crystallization. *Nature* 340, 199-205.
- Larsen, O., 1971. K/Ar age determinations from Precambrian of Denmark. *Geol Surv Denmark. II Series* 97.
- Larsen, G., 1984, Recent volcanic history of the Veidivötn fissure swarm, southern Iceland—An approach to volcanic risk assessment: *J Volcanol Geotherm Res* 22, 33–58.
- Larsen, G., Gudmundsson, M. T., Björnsson, H., 1998. Eight centuries of periodic volcanism at the center of the Icelandic hotspot revealed by glacier tephrostratigraphy. *Geology* 26, 943–946.
- Larson, S. Å., Berglund, J., 1992. A chronical subdivision of the Transscandinavian Igneous Belt: three magmatic episodes? *GFF*, 114, 459-461.
- Larson, S. Å., Tullborg, E.-L., Cederbom, C., Stiberg, J. P., 1999. Sveconorwegian and Caledonian foreland basins in the Baltic Shield revealed by fission-track thermochronology. *Terra Nova* 11, 210-215.
- Larsson, K., 1975. Clastic dykes from the Burgsvik Beds of Gotland. *GFF* 97, 125-134.
- Lee, G. H., Kwon, Y. I., Yoon, C. S., Kim, H. J., Yoo, H. S., 2006. Igneous complexes in the eastern Northern South Yellow Sea Basin and their implications for hydrocarbon systems. *Marine Petrol Geol* 23, 631-645.
- Le Heron, D. P., Etienne, J. L., 2005. A complex subglacial clastic dyke swarm, Sólheimajökull, southern Iceland. *Sediment Geol* 181, 25-37.
- Lentz, D. R., Fowler, A. D., 1992. A dynamic model for graphic quartz-feldspar intergrowths in granitic pegmatites in the Southwestern Greenville Province. *Can Min* 30, 571-585.
- Levi, T., Weinberger, R., Aïfa, T., Eyal, Y., Marco, S., 2006. Earthquake-induced clastic dykes detected by anisotropy of magmatic susceptibility. *Geology* 34, 69-72
- Li, Z. X., Bogdanova, S. V., Collins, A. S., Davidson, A., De Weale, B., Ernst, R. E., Fritsimons, I. C. W., Fuck, R. A., Gladkochub, D. P., Jabobs, J., Karlstrom, K. E., Lu, S., Natapov, L. M., Pease, V., Pisarewsky, S. A., Thrane, K., Vernikovsky, V., 2008. Assembly, configuration and break-up history of Rodinia: a synthesis. *Precambrian Res* 160, 179-210.
- Lidmar-Bergström K, 1994. Morphology of the bedrock surface. In Fredén, C. (ed.), *Geology. National Atlas of Sweden*, 1st Edition, 44–54.
- Lidmar-Bergström, K., 1996. Long-term morphotectonic evolution in Sweden. *Geomorphology* 16, 33-59.

- Lidmar-Bergström, K., 1997. A long-term perspective of glacial erosion. *Earth Surf Processes and Landforms* 22, 297-306
- Lipman, P. W., 1984. The roots of ash flow calderas in western North America: windows into the tops of granitic batholiths. *J Geophys Res* 89, 8801–8841.
- Lister, J. R., Kerr, R. C., 1991. Fluid-mechanical models of crack propagation and their application to magma transport in dykes. *J Geophys Res* 96, 10049–10077.
- Lofgren, G., Donaldson, C. H., Williams, R., Mullins, O. J., Usselman, T. M., 1974. Experimentally reproduced textures and mineral chemistry of Apollo 15 quartz-normative basalts. *Proc Lunar Sci Conf* 5th, p. 549-567.
- Logan, D. L., 2000. A first course in the finite element method. 3rd edition. Brooks and Cole.
- Long, P. E., Wood, B. J., 1986. Structures, textures and cooling history of Columbia River basalt flows. *GSA Bull* 97, 1144-1155.
- Lorenz, J. C., Teufel, L. W., Warpinski, N. R., 1991. Regional fractures 1: a mechanism for formation of regional fractures at depth in flat-lying reservoirs. *AAPG Bull* 75, 1714-1737.
- Luhr, J. F., Simkin, T., 1993. Parícutin, the volcano born in a Mexican cornfield: Phoenix, Geosci Press, 427 p.
- Lundberg, E., Sjöström, H., 2006. Oskarshamn site investigation. Kinematic analysis of ductile and brittle/ductile shear zones in Simpevarp and Laxemar subarea. Swedish Nuclear Fuel and Waste Management Company. SKB-P-06-118. Stockholm, Sweden.
- Lundegårdh, P. H., Wikström, A., Bruun, Å., 1985. Provisoriska översiktliga Berggrundskartan Oskarshamn. Sveriges Geologiska Undersökning Ba34.
- Lundqvist, Th., Vaasjoki, M., Persson, P.-O., 1998. U-Pb ages of plutonic and volcanic rocks in the Svecofennian Bothnian Basin, Central Sweden, and their implications for the Palaeoproterozoic evolution of the Basin. *GFF* 120, 357-363.
- Lyle, P., 2000. The eruption environment of multi-tired columnar basalt lava flows. *J Geol Soc London* 157, 715-722.
- Løseth, H., Gading, M., Wensaas, L., 2008. Hydrocarbon leakage interpreted on seismic data. *Marine Petrol Geol*, doi:10.1016/j.marpetgeo.2008.09.008.
- Macedonio, G., Costa, A., Folch, A., 2008. Ash fallout scenario at Vesuvius: numerical simulations and implications for hazard assessment. *J Vol Geotherm Res* 178, 366-377.
- MacLennan, J., Jull, M., McKenzie, D., Slater, L., Grönvold, K., 2002. The link between volcanism and deglaciation in Iceland. *Geochem Geophys Geosyst* 3, 1062, doi: 10.1029/2001GC000282.
- Mahood, G. A., 1990. Evidence for long residence times of rhyolitic magma in the Long Valley magmatic system: The isotopic record in precaldera lavas of

- Glass Mountain. Reply. *Earth Planet Sci Lett* 99, 395–399.
- Mansfeld, J., Beunk, F. F., Barling, J., 2005. 1.83–1.82 Ga formation of a juvenile volcanic arc—implications from U–Pb and Sm–Nd analyses of the Oskarshamn–Jönköping Belt, south-eastern Sweden. *GFF* 127, 149–157.
- Marco, S., Weinberger, R., Agnon, A., 2002. Radial clastic dykes formed by salt diapir in the Dead Sea Rift, Israel. *Terra Nova* 14, 288–294.
- Marsh, B. D., 1982. On the mechanics of igneous diapirism, stoping, and zone melting. *Am J Sci* 282, 808–855.
- Martel, A.T., Gibling, M.R., 1993. Clastic dykes of the Devonian–Carboniferous Horton Bluff Formation, Nova Scotia; storm-related structures in shallow lakes. *Sedimentary Geology* 87, 103–119.
- Marti, J., Aspinall, W. P., Sobradelo, R., Felpeo, A., Geyer, A., Ortiz, R., Baxter, P., Cole, P., Pacheco, J., Blanco, M. J., Lopez, C., 2008. A long-term volcanic hazard event tree for Teide–Pico Viejo stratovolcanoes (Tenerife, Canary Islands). *J Vol Geotherm Res* 178, 543–552.
- Martin, U., Nemeth, K., 2006. How Strombolian is a “Strombolian” scoria cone? Some irregularities in scoria cone architecture from the Transmexican Volcanic Belt, near Volcán Ceboruco, (Mexico) and Al Haruj (Libya). *J Volcanol Geotherm Res* 155, 104–118.
- Mastin, L. G., Pollard, D. D., 1988. Surface deformation and shallow dyke intrusion processes at Inyo Craters, Long Valley, California. *J Geophys Res* 93, 13221–13235.
- Mathieu, L., van Wyk de Vries, B., Holohan, E. P., Troll, V. R., 2008. Dykes, cups, saucers, and sills: analogue experiments on magma intrusion into brittle rock. *Earth Planet Sci Lett* 271, 1–13.
- Matzel, J. E. P., Bowring, S. A., and Miller, R. B., 2006. Time scales of pluton construction at differing crustal levels; examples from the Mount Stuart and Tenpeak Intrusions, north Cascades, Washington: *GSA Bull* 118, 1412–1430, doi: 10.1130/B25923.1.
- Mazzini, A., Jonk, R., Duranti, D., Parnell, J., Crain, B., Hurst, A., 2003a. Fluid escape from reservoirs: implications from cold seeps, fractures and injected sands Part I. The fluid flow system. *J Geochem Exploration* 78–79, 293–296.
- Mazzini, A., Duranti, D., Jonk, R., Parnell, J., Cronin, B.T., Hurst, A., Quine, M., 2003b. Palaeo-carbonate seep structures above an oil reservoir, Gryphon Field, Tertiary, North Sea. *Geo Mar Lett* 23, 323–339.
- Mazzini, A., Svensen, H., Akhmanov, G. G., Aloisi, G., Planke, S., Malthe-Sørensen, A., Istadi, B., 2007. Triggering and dynamic evolution of the LUSI mud volcano, Indonesia. *Earth Planet Sci Lett* 261, 375–388.
- Mazzarini, F., Corti, G., Muscumecci, G., Innocenti, F., 2004. Tectonic control on laccolith emplacement in the northern Apennines fold-thrust belt: the

- Gavorrano intrusion (southern Tuscany, Italy). In: Breikreuz, C., Petford, N. (eds.). Physical geology of high-level magmatic systems. *J Geol Soc London*, Special Pub 234, 151-161.
- McBirney, A. R., 1996. The Skaergaard Intrusion. In: Cawthorn, R. G. (Ed.) *Layered Intrusions*. Amsterdam, Elsevier, pp. 147–180.
- McCaffrey, K. J. W., Petford, N., 1997. Are granite intrusions scale invariant? *J Geol Soc London* 154, 1-4.
- McCalpin, J.P., ed., 1996. *Paleoseismology: International Geophysical Series 62*. San Diego, California, Academic Press, p. 588
- McNulty, B. A., Tobisch, O. T., Cruden, A. R., Gilder, S., 2000. Multistage emplacement of the Mount Givens pluton, central Sierra Nevada batholith, California. *GSA Bull* 112, 119-135.
- Meert, J. G., Torsvik, T. H., 2003. The making and unmaking of a supercontinent: Rodinia revisited. *Tectonophysics* 375, 261-288.
- Mege, D., Kome, T., 2004. Fissure eruptions of flood basalt from statistical analysis of dyke fracture length. *J Vol Geotherm Res* 131, 77-92.
- Menand, T., 2008. The mechanics and dynamics of sills in layered elastic rocks and their implications for the growth of laccoliths and other igneous complexes. *Earth Planet Sci Lett* 267, 93-99.
- Meriaux, C., Jaupart, C., 1998. Dyke propagation through an elastic plate. *J Geophys Res* 103, 18295-18314.
- Metcalf, R. V., 2004. Volcanic-plutonic links, plutons as magma chambers, and crust-mantle interaction: a lithospheric scale view of magma systems. *Trans R Soc Edinburgh: Earth Sci* 95, 357-374.
- Michel, J., Baumgartner, L., Putlitz, B., Schaltegger, U., Ovtcharova, M., 2008. Incremental growth of the Patagonian Torres del Paine laccolith over 90 k.y. *Geology* 36, 459-462.
- Michieli Vittuni, M. de, Clarke, A. B., Neri, A., Voight, S., 2008. Effects of conduit geometry on magma ascent dynamics in dome-shaped eruptions. *Earth Planet Sci Lett* 272, 567-578.
- Middleton, M. F., Tullborg, E.-L., Larson, S.-A., Björklund, L., 1996. Modelling of a Caledonian foreland basin in Sweden: petrophysical constraints. *Mar Petrol Geol* 13, 407–413.
- Miller, C. F., Miller, J. S., 2002. Contrasting stratified plutons exposed in tilt blocks, Eldorado Mountains, Colorado River Rift, NV, USA. *Lithos* 61, 209–224.
- Miller, R. B., Paterson, S. R., 1999. In defense of magmatic diapirs. *J Struct Geol* 21, 1161-1173.
- Möller, C., Andersson, J., Lundqvist, I., Hellström, F. A., 2007. Linking deformation, migmatite formation and zircon U-Pb geochronology in polymetamorphic gneisses, Sveconorwegian province, Sweden. *J Metamorph Geol* 25, 727–750.
- Molyneux, S. J., Hutton, D. H. W., 2000. Evidence for significant granite space creation by the ballooning mechanism:

- The example of the Ardara pluton, Ireland. *GSA Bull* 112, 1543-1558.
- Morgan, S.S., Law, R.D., Nyman, M.W., 1998. Laccolith like emplacement model for the Papoose Flat pluton based on porphyroblast-matrix analysis. *GSA Bull* 110, 96–110.
- Morgan, S. S., Horsman, E., Tokoff, B., de Saint-Blanquat, M., Habert, G., 2005. Sheet-like emplacement of satellite laccoliths, sills and bysmaliths of the Henry Mountains, Southern Utah. In: Pederson, J., Dehler, C. M. (eds.). Interior Western United States, Volume 6 of GSA Field Guide. doi:10.1130/2005.fld006(14).
- Morley, C. K., Crevello, P., Zulkifli, A., 1998. Shale tectonics-deformation associated with active diapirism: the Jerudong Anticline, Brunei Darussalam. *J Geol Soc London* 155, 475–490.
- Morley, C. K., 2003. Outcrop examples of mudstone intrusions from the Jerudong anticline, Brunei Darussalam and inferences for hydrocarbon reservoirs, In: Van Rensbergen, P., Hillis, R. R., Maltman, A. J., Morley C. K. (eds.). Subsurface Sediment Mobilization. *Geol Soc London, Special Pub* 216, 381–394.
- Morris, G. A., Hutton, D. H. W., 1993. Evidence for sinistral shear associated with the emplacement of the early Devonian Etive dyke swarm. *Scott J Geol* 29, 69–72.
- Motuza, G., Čečys, A., Kotov, A.B., Salnikova, E. B., 2006. The Zemaičiu Naumiestis granitoids: new evidences for Mesoproterozoic magmatism in western Lithuania. *GFF* 128, 209–272.
- Mudge, M. R., 1968. Depth control of some concordant intrusions. *GSA Bull* 79, 315–332.
- Müller, A., 2000. Cathodoluminescence and characterisation of defect structures in quartz with applications to the study of granitic rocks. PhD thesis, University of Göttingen, Germany.
- Müller, A., Lennox, P., Trzebski, R., 2002. Cathodoluminescence and microstructural evidence for crystallisation and deformation processes of granites in Eastern Lachlan Fold Belt (SE Australia). *Contrib Mineral Petrol* 143, 510-524.
- Müller, A., Rene, M., Behr, H.-J., Kronz, A., 2003. Trace elements and cathodoluminescence of igneous quartz in topaz granites from the Hub Stock (Slavkovsky Les Mts, Czech Rep). *Min Petrol* 79, 167-191.
- Müller, A., Breiter, K., Seltmann, R., Pécskay, Z., 2005. Quartz and feldspar zoning in the eastern Erzgebirge volcano-plutonic complex (Germany, Czech Republic): evidence of multiple magma mixing. *Lithos* 80, 201-227.
- Müller, A., Seltmann, R., Kober, B., Eklund, O., Jeffries, T., Kronz, A., 2008. Compositional zoning of Rapakivi feldspars and coexisting quartz phenocrysts. *Can Min* 46, 1417-1442.
- Murnier, R., Talbot, C. J., 1993. Segmentation, fragmentation, and jostling of cratonic basement in and near

- Äspo, Southeast Sweden. *Tectonics* 12, 713-727.
- Møller, N. K., Kjaernes, P. A., Martinsen, O. J., Charnock, M. A., 2001. Remobilised sands at the Cretaceous/Tertiary boundary in the Ormen Lange Field, offshore mid Norway, Subsurface Sediment Mobilisation Conference, September 2001. Abstract Vol, Gent, Belgium, p. 13.
- Nadan, B. J., Engelder, T., 2009. Microcracks in New England granitoids: A record of thermoelastic relaxation during exhumation of intracontinental crust. *GSA Bull* 121, 80-99
- Nance, R. D., Linnemann, U., 2008. The Rheic Ocean: origin, evolution, and significance. *GSA Today* 18, doi: 10.1130/GSATG24A.1.
- National Land Survey Iceland <http://www.lmi.is>
- Nemat-Nasser, S., Hori, M., 1999. *Micromechanics: Overall Properties of Heterogeneous Materials*. 2nd ed. Elsevier, Amsterdam.
- Neumann, E. R., Olsen, K. H., Baldrige, W. S., Sundvoll, B., 1992. The Oslo Rift: a review. *Tectonophysics* 208, 1-18.
- Neuser, R. D., Bruhn, F., Habermann, D., Richter, D. K., 1995. Kathodolumineszenz: Methodik und Anwendung. *Zbl Geol Paläont I*, 1/2, 287-306
- Newhall, C. G., Dzurisin, D., 1988. Historical Unrest of Large Calderas of the World: USGS Bull 1855, Reston, VA.
- Nicoll, G. R., Holness, M. B. Troll, V. R., Emeleus, C. H., Chew, D., 2009. Early mafic magmatism and crustal anatexis on the Isle of Rum: evidence from the Am Mam intrusion breccia. *Geol Mag* 146, 368-381.
- Nironen, M., 1997. The Svecofennian Orogen: a tectonic model. *Precambrian Res* 86, 21-44.
- Nolte, N., Kleinhans, I. C., Bairo, W., Hansen, B. T., 2008. An evolutionary model of 1.8 Ga granitoids of the Västervik area (SE Sweden) based on a refined geological map. 86th Annual Meeting of the German Mineralogical Society, DMG, Berlin, September 14th -17th 2008, Abstract S07-275.
- Nolte, N., Kleinhans, I. C., Bairo, W., Hansen, B. T., in preparation. Refined classification of Västervik granitoids-a petrographic and geochemical study.
- Obermeier, S. F., 1996. Using liquefaction-induced features for paleoseismic analysis. In: McCalpin, J. P. (ed.). *Paleoseismology*. Academic Press, London, pp 331-396.
- Obst, K., Hammer, J., Katzung, G., Korich, D., 2004. The Mesoproterozoic basement in the southern Baltic Sea: insights from the G 14-1 off-shore borehole. *Int J Earth Sci* 93, 1-12.
- Oddson, B., 1984. Geology and geotechnical behavior of the young volcanic rocks of Iceland with emphasis on the effects of petrography. PhD thesis, ETH, Zurich (in German).

- O'Driscoll, B., Troll, V. R., Reavy, R. J., Turner, P., 2006. The Great Eucrite intrusion of Ardnamurchan, Scotland: reevaluating the ring dike concept. *Geology* 34, 189-192.
- Olsen, S. N., Marsh, B. D., Baumgartner, L. P., 2004. Modelling mid-crustal migmatite terrains as feeder zones for granite plutons: the competing dynamics of melt transfer by bulk versus porous flow. *Trans R Soc Edinburgh: Earth Sci* 95, 49-58.
- Ort, M. H., Elson, M. D., Andersson, K. C., Duffield, W. A., Hooker, J. A., Champion, D. E., Waring, G., 2008. Effects of scoria-cone eruption upon nearby human communities. *GSA Bull* 120, 476-486.
- Oskarsson, N., Steinthorsson, S., Sigvaldason, G. E., 1985. Iceland geochemical anomaly: origin, volcanotectonics, chemical fractionation and isotope evolution of the crust. *J Geophys Res* 90, 10011-10255.
- Oyhantçabal, P., Siegesmund, S., Stein, K.-J., Spoturno, J., 2007. Dimensional stones in Uruguay: situation and perspectives. *ZDGG* 158, 417-428.
- Page, L., Söderlund, P., Wahlgren, C.-H., 2007. $^{49}\text{Ar}/^{39}\text{Ar}$ and (U-Th)/He geochronology of samples from the cored boreholes KSH03A, KSH03B, KLX01, KLX02 and the access tunnel to the Äspö Hard Rock Laboratory. SKB-P07-160, Swedish Nuclear Fuel and Waste Management Co, Stockholm, Sweden.
- Pagel, M., Barbin, V., Blanc, P., Ohnstedter, D., 2000. Cathodoluminescence in Geosciences. Springer Verlag, Berlin.
- Pagli, C., Sigmundsson, F., Lund, B., Sturkell, E., Geirsson, H., Einarsson, P., Arnadóttir, Th., Hreinsdóttir, S., 2007. Glacio-isostatic deformation around the Vatnajökull ice cap, Iceland, induced by recent climate warming: GPS observation and Finite Element Modeling. *J Geophys Res* 112, B08405.
- Paquet, F., Dauteuil, O., Hallot, E., Moreau, F., 2007. Tectonics and magma dynamics coupling in a dyke swarm of Iceland. *J Struct Geol* 29, 1477-1493.
- Parfitt, E. A., 2004. A discussion of the mechanisms of explosive basaltic eruptions. *J Volcanol Geotherm Res* 134, 77-107.
- Parfitt, E. A., Wilson, L., 1995. Explosive volcanic eruptions: IX. The transition between Hawaiian-style lava fountaining and Strombolian explosive activity. *Geophys J Int* 121, 226-232.
- Parsons, T., Thompson, G. A., Cogbill, A. H., 2006. Earthquake and volcano clustering via stress transfer at Yucca Mountain, Nevada. *Geology* 34, 785-788.
- Paterson, S. R., Fowler, T. K., 1993a. Extensional pluton-emplacement models: Do they work for large plutonic complexes? *Geology* 21, 781-784.

- Paterson, S. R., Fowler, T. K., 1993b. Re-examining pluton emplacement processes. *J Struct Geol* 15, 191 - 206.
- Paterson, S. R., Vernon, R. H., 1995. Bursting the bubble of ballooning plutons; A return to nested diapirs emplaced by multiple processes. *GSA Bull* 107, 1356 - 1380.
- Paterson, S. R., Pignotta, G. S., Farris, D., Memeti, V., Miller, R. B., Vernon, R. H., Zak, J., 2008. Is stopping a volumetrically significant pluton emplacement process? Discussion. *GSA Bull* 120, 1075-1079.
- Pearce, J. M., Hough, E., Williams, G. M., Wealthall, G. P., Tellam, J. H., Herbert, A., 2001. Sediment-filled fractures in Triassic sandstones-pathways or barriers to contaminant migration? In: Kueper, B. H., Novakowski, K. S., Reynolds, D. A. (eds.). *Conference Proceedings of Fractured Rock 2001*, Toronto, Ontario, Canada.
- Pedersen, R., Sigmundsson, F., Masterlak, F., 2009. Rheologic controls on inter-rifting deformation of the Northern Volcanic Zone, Iceland. *Earth Planet Sci Lett* 281, 14-26.
- Perlt, J., Heinert, M., 2006. Kinematic model of the South Icelandic tectonic system. *Geophys J Int* 164, 168-175.
- Petford, N., 1996. Dykes or diapirs? *Trans R Soc Edinburgh: Earth Sci* 87, 105-114.
- Petford, N., McCaffrey, K. J. M., 2003. Hydrocarbons in Crystalline Rocks. *J Geol Soc London, Spec Pub* 214, 1-5.
- Petford, N., Kerr, R. C., Lister, J. R., 1993. Dike transport of granitoid magmas. *Geology* 21, 845-848.
- Petford, N., Lister, J. R., Kerr, R. C., 1994. The ascent of felsic magmas in dykes. *Lithos* 32, 161-168
- Petford, N., Cruden, A. R., McCaffrey, K. J. W., Vigneresse, J.-L., 2000. Granite magma formation, transport and emplacement in the Earth's crust. *Nature* 408, 669-673.
- Petcovic, H. L., Dufek, J. D., 2005. Modeling magma flow and cooling in dikes: implications for emplacement of Columbia River flood basalts. *J Geophys Res* 110, B10201, doi: 10.1029/2004JB00343
- Phillips, C. A., Alsop, G. I., 2000. Post-tectonic clastic dykes in the Dalradian of Scotland and Ireland: implications for delayed lithification and deformation of sediments. *Geol J* 35, 99-110
- Pickering, K. T., 2008. The destruction of Iapetus and Tornquist's Ocean. *Geology Today* 5, 160-166.
- Pignotta, G. S., Paterson, S. R., 2007. Voluminous stopping in the Mitchell Peak granodiorite, Sierra Nevada Batholith, California. *Can Mineral* 45, 87-106.
- Pinotti, L. P., Coniglio, J. E., Esparza, A. M., D'Eramo, F. J., Llambias, E. J., 2002. Nearly circular plutons emplaced by stopping at shallow crustal levels, Cerro Aspero batholith, Sierras Pampeanas de Cordoba, Argentina. *J South Am Earth Sci* 15, 251-265.

- Pitcher, W. S., Berger, A. R., 1972. The geology of Donegal Wiley: A study of granite emplacement and unroofing. Wiley Interscience, New York, pp 135.
- Pinel, V., Jaupart, C., 2004. Magma storage and horizontal dyke injection beneath a volcanic edifice. *Earth Planet Sci Lett* 221, 245-262.
- Planke, S., Svensen, H., Hovland, M., Banks, D. A., Jamtveit, B., 2003. Mud and fluid migration in active mud volcanoes in Azerbaijan. *Geo-Mar Lett* 23, 258-268.
- Pollard, D. D., 1973. Derivation and evolution of a mechanical model for sheet intrusions. *Tectonophysics* 19, 233-269.
- Pollard, D. D., Holzhausen, G., 1979. On the mechanical interaction between a fluid-filled fracture and the Earth's surface. *Tectonophysics* 53, 27-57.
- Pollard, D. D., Johnson, A. M., 1973. Mechanics of growth of dome laccolithic intrusions in Henry Mountains, Utah. 2. Bending and failure of overburden layers and sill formation. *Tectonophysics* 18, 311-354.
- Pollard, D. D., Delaney, P. T., Duffield, W. A., Endo, E. T., Okamura, A. T., 1983. Surface deformation in volcanic rift zones. *Tectonophysics* 94, 541-584.
- Pollitz, F. F., Sacks, I. S., 1996. Viscosity structure beneath northeast Iceland. *J. Geophys. Res.* 101 (B8), 17771-17793.
- Polteau, S., Mazzini, A., Galland, O., Planke, S., Malthe-Sørensen, A., 2008a. Saucer-shaped intrusions: occurrence, emplacement and implications. *Earth Planet Sci Lett* 266, 195-204.
- Polteau, S., Ferré, E. C., Planke, S., Neumann, E.-R., Chevallier, L., 2008b. How are saucer-shaped sills emplaced? Constraints from the Golden Valley, South Africa. *J Geophys Res* 113, B12104, doi: 10.1029/2008JB005620.
- Poprawa, P., Šliaupa, S., Stephenson, R., Lazauskiene, C., 1999. Late Vendian-Early Paleozoic tectonic evolution of the Baltic Basin: regional tectonic implications from subsidence analysis. *Tectonophysics* 314, 219-239.
- Priest, S. D., 1993. *Discontinuity Analysis for Rock Engineering*. Chapman and Hall, London.
- Pupier, E., Barbey, P., Toplis, M., Bussy, F., 2008. Igneous layering, fractional crystallization, and growth of granitic plutons: the Dolbel Batholith in SW Niger. *J Petrol* 49, 1043-1068. doi: 10.1093/petrology/egn017.
- Quareni, F., Ventura, G., Mulgaria, F., 2001. Numerical modelling of the transition from fissure- to central-type activity on volcanoes: a case study from Salina Island, Italy. *Phys Earth Planet Interiors* 124, 213-221.
- Raposo, M. I. B., Gastal, M. C. P., 2009. Emplacement mechanism of the main granite pluton of the Lavras do Sul intrusive complex, South Brazil, determined by magmatic anisotropies. *Tectonophysics* 466, 18-31.

- Rapprich, V., Cajz, V., Kostak, M., Pecskey, Z., Ridkos, I. T., Raskar, P., Radon, M., 2007. Reconstruction of eroded monogenetic Strombolian cones of Miocene age: A case study on character of volcanic activity of the Jicin Volcanic Field (NE Bohemia) and subsequent erosional rates estimation. *J Geosci* 52, 169-180.
- Ramirez, L. E., Palacios, C., Townly, B., Parada, M. A., Sial, A. N., Fernandez-Turiel, J. L., Gimeno, D., Garcia-Valles, M., Lehmann, B., 2006. The Mantos Blancos copper deposit: an upper Jurassic breccia-style hydrothermal system in the coastal range of Northern Chile. *Miner Depos* 41, 246-258.
- Ramsay, J. G. 1989. Emplacement kinematics of a granite diapir: The Chindamora batholith, Zimbabwe. *J Struct Geol* 11,191-209.
- Rasmussen, T. V., Olsen, H. K. 2003. Dimension stone prospecting in West and South Greenland 2003. Danmarks og Grønlands Geologiske Undersøgelse Rapport 2003/107, pp 67.
- Richter, D., 1966. On the New Red Sandstone neptunian dykes of the Tor Bay Area (Devonshire). *Proc Geol Assoc* 77, 173–86.
- Riggs, N. R., Duffield, W. A., 2008. Record of complex scoria cone eruptive activity at Red Mountain, Arizona, USA, and implications for monogenetic mafic volcanoes. *J Volcanol Geotherm Res* 178, 763-776.
- Risso, C., Nemeth, K., Combina, A. M., Nullo, F., Drosina, M., 2008. The role of phreatomagmatism in a Plio-Pleistocene high-density scoria cone field: Llacanelo Volcanic Field (Mendoza), Argentina. *J Volcanol Geotherm Res* 169, 61-86.
- Roberts, J. L., 1970. The intrusion of magma into brittle rocks. In: Newall, G., Rast, N. (eds.). *Mechanism of Igneous Intrusion*. *Geol J Special Issues* 2, 287-338.
- Rocchi, S., Westerman, D. S., Dini, A., Innocenti, F., Tonarini, S., 2002. Two-stage growth of laccoliths at Elba Island, Italy. *Geology* 30, 983-986.
- Rohrman, M., 2007. Prospectivity of volcanic basins: trap delineation and acreage de-risking. *AAPG Bull* 91, 915-939.
- Roman, D. C., Moran, S. C., Power, J. A., Cashman, K. V., 2004. Temporal and spatial variation of local stress fields before and after the 1992 eruptions of Crater Peak Vent, Mount Spurr volcano, Alaska. *Bull Seismol Soc Am* 94, 2366-2379.
- Rögnvaldsson, S. T., Gudmundsson, A., Slunga, R., 1998. Seismotectonic analysis of the Tjörnes Fracture Zone, an active transform fault in north Iceland. *J Geophys Res* 103 (B12), 30117-30129.
- Röshoff, K., Cosgrove, J., 2002. Sedimentary dykes in the Oskarshamn-Västervik area: a study of the mechanisms of formation. SKB-R-02-37, Swedish

- Nuclear Fuel and Waste Management Company, Stockholm, Sweden, pp 98.
- Ross, J. G., Mussett, A. E., 1976. $^{40}\text{Ar}/^{39}\text{Ar}$ dates for spreading rates in eastern Iceland. *Nature* 259, 36-38.
- Rossi, M. J., 1996. Morphology and mechanism of eruptions of postglacial shield volcanoes in Iceland. *Bull Volcanol* 57, 530-540.
- Rowan, M. G., Ratliff, R., Trudgill, Bruce D., Duarte, J. B., 2001. Emplacement and evolution of the Mahogany salt body, central Louisiana outer shelf, northern Gulf of Mexico. *AAPG Bull* 85, 947-969.
- Rowan, M. G., Lawton, T. F., Giles, K. A., Ratcliffe, R. A., 2003. Near-salt deformation in La Popa basin, Mexico, and the northern Gulf of Mexico: A general model for passive diapirism. *AAPG Bull* 87, 733-756.
- Rowland, J. R., Baker, E., Ebinger, C., Keir, D., Kidane, T., Biggs, J., Hayward, N., Wright, T., 2007. Fault growth at a nascent slow-spreading ridge: 2005 Dabbahu rifting episode, Afar. *Geophys J Int* 171, 1226-1246.
- Rubin, A. M., 1992. Dyke-induced faulting and graben subsidence in volcanic rift zones. *J Geophys Res* 97, 1839-1858.
- Rubin A., 1993. Tensile fracture of rock at high confining pressure: Implications for dike propagation. *J Geophys Res* 98, 15919-15935
- Rubin, A. M., 1995. Propagation of magma-filled cracks. *Annu Rev Earth Planet Sci* 23, 287-336.
- Rubin, A. M., Pollard, D. D., 1988. Dyke-induced faulting in rift zones. *Geology* 16, 413-417.
- Rubin, A., Gillard, D., Got, J-L., 1998. Re-interpretation of seismicity associated with the January 1983 dyke intrusion at Kilauea volcano, Hawaii. *J Geophys Res* 103, 10003-10015.
- Rudolph, S., 1995. Mittelproterozoische Magmatite des "Transscandinavian Granite-Porphyr Belt" E'Adriansnäs, Västervikgebiet, SE Schweden. Diploma mapping thesis, University of Göttinge, Germany (in German).
- Rutland, R. W. R., Williams, I. S., Korsman, K., 2004. Pre-1.91 Ga deformation and metamorphism in the Palaeoproterozoic Vammala migmatite belt, southern Finland, and implications for Svecofennian tectonics. *Bull Geol Soc Finland* 76, 93-140.
- Ryan, M. P., 1988. The mechanics and three-dimensional internal structure of active magmatic systems: Kilauea Volcano, Hawaii. *J Geophys Res* 93, 4213-4248.
- Saemundsson, K., 1970. Interglacial lava flows in the lowlands of southern Iceland and the problem of two-tiered columnar jointing. *Jökull* 20, 62-77.
- Saemundsson, K., 1974. Evolution of the axial rifting zone in northern Iceland and the Tjörnes fracture zone. *GSA Bull* 85, 495-504.
- Saemundsson, K., 1978. Fissure swarms and central volcanoes in the Neovolcanic zones of Iceland. In: Bowes, D. R.,

- Leake, B. E. (eds.). Crustal evolution in NW-Britain and adjacent regions. *Geol J Spec Issue* 10, 415-432.
- Saemundsson, K., 1979. Outline of the geology of Iceland. *Jökull* 29, 7-28.
- Saemundsson, K., 1986. Subaerial volcanism in the western North Atlantic. In: Vogt, P. R., Tucholke, B. E. (eds.). *The Geology of North America, Volume M, The Western North Atlantic Region*. *Geol Soc Am*, 69-86.
- Saemundsson, K., 1992. Geology of the Thingvallavatn area. *Oikos* 64, 40-68.
- Saemundsson K., Kristjansson L., McDougall I., Watkins N. D., 1980. K-Ar dating, geological and palaeomagnetic study of a 5-km lava succession in northern Iceland. *J Geophys Res* 85, 3628-3646.
- Salonsaari, P. T., Haapala, I., 1994. The Jaala-Iitti Rapakivi Complex. An example of bimodal magmatism and hybridisation in the Wiborg rapakivi batholith, southeastern Finland. *Mineral Petrol* 50, 21-34.
- Sanderson, D. J., Meneilly, A. W., 1981. Analysis of three-dimensional strain modified uniform distributions: Andalusite fabrics from a granite aureole. *J Struct Geol* 3, 109-116.
- Saunders, S. J., 2001. The shallow plumbing system of Rabaul caldera: a partially intruded ring fault? *Bull Volcanol* 63, 406-420.
- Scarth, A., Tanguy, J. C., 2001. *Volcanoes of Europe*. Terra Publishing, Harpenden, Hertfordshire.
- Schmeling, H., Cruden, A. R., Marquart, G., 1988. Finite deformation in and around a fluid sphere moving through a viscous medium: implications for diapiritic ascent. *Tectonophysics* 149, 17 - 34.
- Scherman, S., 1978. Förarbeten för platsval, berggrundsundersökningar. SKB Technical report 60, Swedish Nuclear Fuel and Waste Management Co, Stockholm, Sweden, pp. 223.
- Schliche, R.W., Ackermann, R.V., 1995. Kinematic significance of sediment-filled fissures in the North Mountain basalt, Fundy rift basin, Nova Scotia, Canada. *J Struct Geol* 17, 987-996.
- Schultz, R. A., Okubo, C. H., Goudy, C. L., Wilkins, S. J., 2004. Igneous dykes on Mars revealed by Mars Orbiter Laser Altimeter topography. *Geology* 32, 889-892.
- Schutter, S. R., 2003. Occurrence of hydrocarbons in and around igneous rocks. In: Petford, N., McCaffrey, K.J.W. (eds.). *Hydrocarbons in crystalline rocks*. *Geol Soc London, Spec Publ* 214, 35-68.
- Self, S., Kienle, J., Huot, J. P., 1980. Ukinrek maars, Alaska: II. Deposits and formation of the 1977 craters. *J Volcanol Geotherm Res* 7, 39-65.
- Selverstone, J., Hodgins, M., Aleinikoff, J. N., Fanning, C. M., 2000. Mesoproterozoic reactivation of a Paleoproterozoic transcurrent boundary in the northern Colorado Front Range: implications for ~1.7- and 1.4-Ga

- tectonism. *Rocky Mountain Geol* 35, 139–162.
- Siebe, C., Rodriguez-Lara, V., Schaaf, P., Abrams, M., 2004. Radiocarbon ages of Holocene Pelado, Guespalpa, and Chichinautzin scoria cones, south of Mexico City: implications for archaeology and future hazards. *Bull Volcanol* 66, 203-225.
- Siegesmund, S., Becker, J. K. 2000. Emplacement of the Ardara pluton (Ireland): new constraints from magnetic fabrics, rock fabrics and age dating. *Int J Earth Sci* 89, 307–27.
- Sigmarsson, O., Steinthorsson, S., 2007. Origin of Icelandic basalts: a review of their petrology and geochemistry. *J Geodyn* 43, 87- 100.
- Sigmundsson, F., 2006. Iceland Geodynamics: crustal deformation and divergent plate tectonics. Springer-Praxis, Chichester, UK, pp 228.
- Sigmundsson, F., Saemundsson, K., 2008. Iceland: a window on North-Atlantic divergent plate tectonics and geological processes. *Episodes* 31, 92-97.
- Sigurdsson, O., Zophoniasson, S., Hannesdottir, L., Thorgrimsson, S., 1975. Geological report on the proposed hydroelectric power plant at Dettifoss. National Energy Authority (Orkustofnun), Reykjavik, report OS-ROD-7526 (in Icelandic).
- Sigurdsson, H., Sparks, S. R. J., 1978a. Lateral magma flow within rifted Icelandic crust. *Nature* 274, 126-130.
- Sigurdsson, H., Sparks, R. S. J., 1978b. Rifting episode in north Iceland in 1874-1875 and the eruption of Askja and Sveinagja. *Bull Volcanol* 41, 149-167.
- Sigurdsson, O., 1980. Surface deformation of the Krafla fissure swarm in two rifting events. *J Geophys* 47, 154-159.
- Sigurgeirsson, M. A., 1995. Yngra-Stampagosið á Reykjanesi. *Náttúrufræðingurinn* 64, 211–230 (in Icelandic).
- Sigvaldason, G. E., Annertz, K., Nilsson, M., 1992. Effect of glacier loading/deloading on volcanism: Postglacial volcanic production rate at Dyngjufjöll area, Central Iceland. *Bull Volcanol* 54, 385-392.
- Sinton, J., E. Bergmanis, K. Rubin, R. Batiza, T. K. P. Gregg, K. Grönvold, K. C. Macdonald, White, S. M., 2002. Volcanic eruptions on mid-ocean ridges: New evidence from the superfast spreading East Pacific Rise, 17°–19°S. *J Geophys Res* 107, 2115, doi: 10.1029/2000 JB000090.
- Sinton, J., Grönvold, K., Saemundsson, K., 2005. Postglacial eruptive history of the West Volcanic Zone. *Geochem Geophys Geosyst* 6, Q12009, doi: 10.1029/2006GQ001021.
- SKB report, 2002. Simpevarp-site descriptive model version 0. Swedish Nuclear Fuel and Waste Management Company. SKB-R-02-35. Stockholm, Sweden.
- SKB report, 2006. Hydrogeochemical evaluation, preliminary site description

- Laxemar subarea-version 1.2. Swedish Nuclear Fuel and Waste Management Company. SKB-R-06-12. Stockholm, Sweden.
- SKB report, 2008. Söderbäck, B. (ed.), Geological evolution, palaeo-climate and historical development of the Forsmark and Laxemar–Simpevarp areas, Site descriptive modelling, SDM-Site. Swedish Nuclear Fuel and Waste Management Company. SKB-R-08-19. Stockholm, Sweden
- Skelhorn, R. R., Elwell, R. W. D., 1971. Central subsidence in the layered Hypersthene-gabbro of Centre II, Ardnamurchan, Argyllshire. *J Geol Soc* 127, 535-551.
- Skridlaite, G., Whitehouse, M. J., Rimša, A., 2007. Evidence for a pulse of 1.45 Ga anorthosite-mangerite-charnockite-granite (AMCG) plutonism in Lithuania: implications for the Mesoproterozoic evolution of the East European Craton. *Terra Nova* 19, 294–301.
- Slabunov, A. I., et al., 2006. The Archean nucleus of the Fennoscandian (Baltic) Shield. In: Gee, D. G., Stephenson, R. A. (eds.). *European Lithosphere Dynamics*. *Geol Soc London Memoirs* 32, 627–644.
- Slaby, E., Götze, J., 2004. Feldspar crystallization under magma-mixing conditions shown by cathodoluminescence and geochemical modelling—a case study from the Karkonosze pluton (SE Poland). *Mineral Mag* 68, 561-577.
- Slaby, E., Martin, H., 2008. Mafic and felsic magma interaction in granites: the Hercynian Karkonosze Pluton (Sudetes, Bohemian Massif). *J Petrol* 49, 353-391, doi: 10.1093/petrology/egm085.
- Słaby, E., Galbarczyk-Gasiorowska, L., Baszkiewicz, A., 2002. Mantled alkali-feldspar megacrysts from the marginal part of the Karkonosze granitoid massif (SW Poland). *Acta Geologica Polonia* 52, 501-519.
- Słaby, E., Galbarczyk-Gasiorowska, L., Seltmann, R., Müller, A., 2007. Alkali feldspar megacryst growth: geochemical modelling. *Mineral Petrol* 89, 1–29.
- Slater, L., Jull, M., McKenzie, D., Grönvold, K., 1998. Deglaciation effects on mantle melting under Iceland: Results from the northern volcanic zone. *Earth Planet Sci Lett* 164, 151-164.
- Slunga, R., 1989. Analysis of the earthquake mechanisms in the Norrbottom area. In: Bäckblom, Stanfors (eds.). *Interdisciplinary study of postglacial faulting in the Lansjörn area northern Sweden, 1986-1988*. Swedish Nuclear Fuel and Waste Management Company. SKB TR-89-31. Stockholm, Sweden.
- Smart, P. L., Palmer, R. J., Whitaker, F., Wright, V. P., 1988. Neptunian dikes and fissure fills: an overview and account of some modern examples. In: James N. P., Choquette P. W. (eds.). *Paleokarst*. Springer, New York, pp 149-163
- Smith, D. K., Cann, J. R., 1999. Constructing the upper crust of the Mid-Atlantic Ridge: A reinterpretation based on the

- Puna Ridge, Kilauea Volcano. *J Geophys Res* 104, 25379–25399.
- Söderbäck, B., 2008. Geological evolution, palaeoclimate and historical development of the Forsmark and Laxemar-Simpevarp areas. Swedish Nuclear Fuel and Waste Management Company. SKB-R-08-19, Stockholm, Sweden.
- Söderlund, U., Möller, C., Andersson, J., Johansson, L., Whitehouse, M., 2002. Zircon geochronology in poly-metamorphic gneisses in the Sveconorwegian orogen, SW Sweden: ion microprobe evidence for 1.46–1.42 and 0.98–0.96 Ga reworking. *Precambrian Res* 113, 193.
- Söderlund, U., Isachsen, C. E., Bylund, G., Heaman, L. M., Patchett, P. J., Vervoort, J. D., Andersson, U. B., 2005. U–Pb baddeleyite ages and Hf, Nd isotope chemistry constraining repeated mafic magmatism in the Fennoscandian Shield from 1.6 to 0.9 Ga. *Contrib Mineral Petrol* 150, 174–194.
- Söderlund, P., Page, L., Söderlund, U., 2008. $^{40}\text{Ar}/^{39}\text{Ar}$ biotite and hornblende geochronology from the Oskarshamn area, SW Sweden: discerning multiple Proterozoic tectonothermal events. *Geol Mag* doi: 10.1017/S0016756808005001.
- Soriano, C., Beamud, E., Garces, M., 2008. Magma flow in dykes from rift zones of the basaltic shield of Tenerife, Canary Islands: implications for the emplacement of buoyant magma. *J Vol Geotherm Res* 173, 55–68.
- Smart, P. L., Palmer, R. J., Whitaker, F., Wright, V. P., 1988. Neptunian dykes and fissure fills: an overview and account of some modern examples. In: James, N. P., Choquette, P. W. (eds). *Paleokarst*. Springer, New York, pp 149–163.
- Sparks, R. S. J., 1988. Petrology and geochemistry of the Loch Ba ring-dyke, Mull (NW Scotland): an example of the extreme differentiation of tholeiitic magmas. *Contrib Mineral Petrol* 100, 446–461.
- Sparks, R. S. J., Sigurdsson, H., Wilson, L., 1977. Magma mixing; a mechanism for triggering acid explosive eruptions. *Nature* 267, 315–318.
- Sparks, R. S. J., Baker, L., Brown, R.J., Field, M., Schumacher, J., Stripp, G., Walters, A., 2006. Dynamical constraints on kimberlite volcanism. *J Vol Geotherm Res* 155, 18–48.
- Spence, D. A., Turcotte, D. L., 1990. Buoyancy-driven magma fracture: a mechanism for ascent through the lithosphere and the emplacement of diamonds. *J Geophys Res* 95, 5133–5139.
- Sprunt, E., 1981. Causes of quartz cathodoluminescence colours. *Scan Electron Microsc* 1981, 525–535.
- Stanton, R. J., Pray, L. C., 2004. Skeletal-carbonate neptunian dykes of the Capitan Reef: Permian, Guadalupe Mountains, Texas, USA. *J Sed Res* 74, 805–816.
- Stephens, M. B., Wahlgren, C.-H., Weijermars, R., Cruden, A. R., 1996.

- Left-lateral transpressive deformation and its tectonic implications, Sveconorwegian orogen, Baltic Shield, southwestern Sweden. *Precambrian Res* 79, 261–279.
- Stephens, M., Wahlgren, C.-H., 2008. Bedrock evolution. In: Söderbäck, B. (ed.). *Geological evolution, palaeoclimate and historical development of the Forsmark and Laxemar–Simpevarp areas, Site descriptive modelling, SDM-Site*. Swedish Nuclear Fuel and Waste Management Company. SKB-R-08-19. Stockholm, Sweden
- Stevenson, C. T. E., Owens, W. H., Hutton, D. H. W., Hood, D. N., Meighan, I. G., 2007. Laccolithic, as opposed to cauldron subsidence, emplacement of the Eastern Mourne pluton, N. Ireland: evidence from anisotropy of magmatic susceptibility. *J Geol Soc* 164, 99–110.
- Stewart, S. A., Davies, R. J., 2006. Structure and emplacement of mud volcano systems in the Southern Caspian Basin. *AAPG Bull* 90, 771–786.
- Ström, A., Andersson, J., Skagius, K., Winberg, A., 2008. Site descriptive modelling during characterization of a geological repository for nuclear waste in Sweden. *App Geochem* 23, 1747–1760.
- Stull, R. J., 1979. Mantled feldspars and synneusis. *Am Min* 64, 514–518.
- Sturkell, E., Sigmundsson, F., Slunga, R., 2006. 1983–2003 decaying rate of deflation at Askja Caldera: pressure decrease in an extensive magma plumbing system at a spreading plate boundary. *Bull Volcanol* 68, 727–735, doi: 10.1007/s00445-005-0046-1
- Sturt, B. A., Furnes, H., 1976. Spatial and temporal relationships of intrusive limestones from Las Palmas, Canary Islands. *J Sed Petrol* 46, 555–562.
- Sultan, L., Claesson, S., Plink-Björklund, P., 2005. Proterozoic and Archean ages of detrital zircon from the Paleoproterozoic Västervik Basin, SE Sweden: Implications for provenance and timing of deposition. *GFF* 127, 17–24
- Sultan, L., Plink-Björklund, P., 2006. Depositional environments at a Palaeoproterozoic continental margin, Västervik Basin, SE Sweden. *Precambrian Res* 145, 243–271
- Sumner, J. M., Blake, S., Matela, R. J., Wolff, J. A., 2005. Spatter. *J Volcanol Geotherm Res* 142, 49–65.
- Sylvester, A. G., Oertel, G., Nelson, C. A., Christie, J. M., 1978. Papoose Flat pluton: A granitic blister in the Inyo Mountains, California. *GSA Bull* 89, 1205–1219.
- Takada, A., 1994. Development of a subvolcanic structure by the interaction of liquid filled cracks. *J Volcanol Geotherm Res* 62, 207–224.
- Talbot, C. J., Medvedev, S., Alavi, M., Sharivar, H., Heidari, E. 2000. Salt extrusion at Kuh-e-Jahani, Iran, from June 1994 to November 1997. In: Vendeville, B., Mart, Y., Vigneresse, J. L. (eds.). *Salt Shale and Igneous Diapirs*

- in and around Europe. Geol Soc London, Spec Pub 174, 93–110.
- Tentler, T., Mazzoli, S., 2005. Architecture of normal faults in the rift zone of central north Iceland. *J Struct Geol* 27, 1721-1739.
- Thomas, R., 1992. Results of investigations on melt inclusions in various magmatic rocks from the northern border of the Bohemian Massif. In: Kukal Z. (ed.). *Proceed 1st Internat Conf Bohemian Massif in Prague 1988*, Czech Geol Surv Prague, 298-306.
- Thompson, B.J., Garrison, R.E., Casey Moore, J., 1999. A late Cenozoic sandstone intrusion west of Santa Cruz, California: fluidized flow of water- and hydrocarbon saturated sediments. In: Garrison, R.E., Aiello, I.W., Casey Moore, J. (Eds.), *Late Cenozoic fluid seeps and tectonics along the San Gregorio fault zone in the Monterey Bay region, California GB-76*, Annual Meeting of the Pacific Section AAPG, Monterey, California, pp. 53–74.
- Thomson, K., Hutton, D., 2004. Geometry and growth of sill complexes: insight using 3d seismic from the North Rockall Trough. *Bull Volcanol* 66, 364-375.
- Thorarinsson, S., 1951. Laxárgljúfur and Laxarhraun. A tephrochronological study. *Geografiska Annaler A*, 1-1, 1-89.
- Thorarinsson, S., 1959. Some geological problems involved in the hydroelectric development of the Jökulsa a Fjöllum, Iceland. Reykjavik, Iceland, Report to the State Electricity Authority.
- Thorarinsson, S., 1971. Aldur ljösugjöskulaganna úr Heklu sanikvacmt leidrettu geislakolstimali. *Natturufrædingurinn* 41, 99-105 (in Icelandic).
- Thorarinsson, S., 1981. Greetings from Iceland: ash-falls and volcanic aerosols in Scandinavia. *Geografiska Annaler* 63A, 109-118.
- Thordarson, T., Self, S., 1993. The Laki (Skaftar Fires) and Grimsvötn eruptions in 1783-1785. *Bull Volcanol* 55, 233-263.
- Thordarson, T., Höskuldsson, A., 2002. Iceland. *Classic Geology in Europe 3*. Terra Publishing, Harpenden, UK, 200 pp.
- Thordarson, T., Self, S., 2003. Atmospheric and environmental effects of the 1783-1784 AD Laki eruption: a review and reassessment. *J Geophys Res* 108, D14011, doi: 10.1029/2001JD002042.
- Thordarson, T., Larsen, G., 2007. Volcanism in Iceland in historical time: volcano types, eruption style and eruptive history. *J Geodyn* 43, 118-152.
- Thordarson, T., Höskuldsson, A., 2008. Postglacial volcanism in Iceland. *Jökull* 58, 197-228.
- Thordarson, T., Miller, D. J., Larsen, G., Self, S., Sigurdson, H., 2001. New estimates of sulphur degassing and atmospheric mass loading by the 934 AD Eldgja eruption, Iceland, *J Volcanol Geotherm Res* 108, 33–54.
- Tikoff, B., Teyssier, C., 1992. Crustal-scale, en echelon “P-shear” tensional bridges; a possible solution to the batholithic room

- problem: *Geology* 20, 927–930, doi: 10.1130/0091-7613.
- Timmermann, M. J., 2004. Timing, geodynamic setting and character of Permo-Carboniferous magmatism in the foreland of the Variscan Orogen, NW Europe. *Geol Soc London, Special Pub* 223, 41-74.
- Tiren, S. A., Askling, P., Wanstedt, S., 1999. Geologic site characterization for deep nuclear waste disposal in fractured rock based on 3D data visualization. *Eng Geol* 52, 319-346.
- Titus, S.J., Clark, R., Tikoff, B., 2005. Geologic and geophysical investigation of two fine-grained granites, Sierra Nevada Batholith, California: evidence for structural controls on emplacement and volcanism. *GSA Bull* 117, 1256-1271.
- Tobisch, O. T., Cruden, A. R., 1995. Fracture-controlled magma conduits in an obliquely convergent continental magmatic arc. *Geology* 23, 941–944.
- Tommasi, A., Vauchez, A., Fernandes, L. A. D., Porcher, C. C., 1994. Magma-assisted strain localization in an orogen-parallel transcurrent shear zone of southern Brazil. *Tectonics*, 2, 421-437.
- Toramaru, A., Matsumoto, T., 2004. Columnar joint morphology and cooling rate: a starch-water mixture experiment. *J Geophys Res* 109, B02205, doi: 10.1029/2003BJ 002686.
- Torfason, H., 1979. Investigations into the structure of southeastern Iceland. PhD-thesis, University of Liverpool.
- Triumf, C.-A., 2004. Gravity measurements in the Laxemar model area with surrounding. Swedish Nuclear Fuel and Waste Management Company. SKB-P-04-128, Stockholm, Sweden.
- Troise, C., 2001. Stress changes associated with volcanic sources: constraints on Kilauea rift dynamics. *J Volcanol and Geotherm Res* 109, 191-203.
- Trønnes, R. G., 2004. Geology and Geodynamics of Iceland. Nordic Volcanological Institute, University of Iceland. <http://www.hi.is>.
- Troll, V. R., Emeleus, C. H., Donaldson, C. H., 2000. Caldera formation in the Rum Central Igneous Complex, Scotland. *Bull Volcanol* 62, 301-317.
- Truswell, J., 1972. Sandstone sheets and related intrusions from Coffee Bay, Transkei, South Africa. *J Sediment Petrol* 42, 578-583.
- Tryggvason, E., 1984. Widening of the Krafla fissure swarm during the 1975-1981 volcano-tectonic episode. *Bull Volcanol* 47, 47-69.
- Tryggvason, E., 1994. Surface deformation at the Krafla volcano, north Iceland. *Bull Volcanol* 56, 98-107.
- Tucker, M. E., 2001. *Sedimentary Petrology*. 3rd edition. Blackwell Science, London.
- Tucker, M. E., 2003. *Sedimentary rocks in the field*. John Wiley and sons, Chichester.
- Tullborg, E-L., Larsson, S. A., Björklund, L., Samuelsson, L., Stigh, J., 1995. Thermal evidence of a Caledonide Foreland Molasse Sedimentation, Swedish

- Nuclear Fuel and Waste Management Company. SKB TR 95-18.
- Tynni, R., 1982. On palaeozoic microfossils in clastic dykes in the Åland Islands and in the core samples of Lumparn. In: Bergman, L., Tynni, R., Winterhalter, B. (eds.). Palaeozoic sediments in the Rapakivi area of the Åland Islands. Bull Geol Soc Finland 317, 35-114
- Valentine, G. A., Krogh, K. E. C., 2006. Emplacement of shallow dikes and sills beneath a small basaltic volcanic center –The role of pre-existing structure (Paiute Ridge, southern Nevada, USA). Earth Planet Sci Lett 246, 217-230.
- Valentine, G. A., Keating, G. N., 2007. Eruptive styles and inferences about plumbing systems at Hidden Cone and Little Black Peak scoria cone volcanoes (Nevada, U.S.A.). Bull Volcanol 70, 105-113.
- Vance, J. A., 1969. Zoning in igneous plagioclase: patchy zoning. J Geol 73, 636-651.
- Van der Meer, J. J. M., Kjaer, K. H., Kruger, J., Rabassa, J., Kilfeather, A. A., 2009. Under pressure: classic dykes in glacial settings. Quart Sci Rev 28, 708-720.
- Vasquez, J. R., Reid, M. R. 2005. Probing the accumulation history of the voluminous Toba Tuff. Science 305, 991–994.
- Vendeville, B. C., Jackson, M. P. A., 1992a. The rise of diapirs during thin-skinned extension. Marine Petrol Geol 9, 331–353.
- Vendeville, B.C., Jackson, M.P.A., 1992b. The fall of diapirs during thin-skinned extension. Marine Petrol Geol 9, 354–371.
- Vergnolle, S., Mangan, M., 2000. Hawaiian and Strombolian eruptions. In: Sigurdsson, H., Houghton, B. F., McNutt, S. R., Rymer, H., Stix, J. (eds.). Encyclopedia of Volcanoes. Academic Press, San Diego, CA, pp. 447-461.
- Vespermann, D., Schmincke, H.-U., 2000. Scoria cones and tuff rings. In: Sigurdsson, H., Houghton, B. F., McNutt, S. R., Rymer, H., Stix, J. (Eds.). Encyclopedia of Volcanoes. Academic Press, San Diego, pp. 683-694.
- Vignerresse, J.-L., 1995a. Control of granite emplacement by regional deformation. Tectonophysics 249, 173-186.
- Vignerresse, J.-L., 1995b. Crustal regime of deformation and ascent of granitic magma. Tectonophysics 249, 187-202.
- Vignerresse, J.-L., 2004. A new paradigm for granite generation. Trans R Soc Edinburgh: Earth Sci 95, 11-22.
- Vignerresse, J.L., 2007. The role of discontinuous magma inputs in felsic magma and ore generation. Ore Geol Rev 30, 181-216.
- Vignerresse, J. L., Clemens, J. D. 2000. Granitic magma ascent and emplacement: neither diapirism nor neutral buoyancy. In: Vendeville, B., Mart, Y., Vignerresse, J.-L. (eds.). Salt, Shale and Igneous Diapirs in and around Europe. Geol Soc London, Spec Pub 174, 1–19.

- Vignerresse, J.-L., Cuney, M., Barbey, P., 1991. Deformation assisted crustal melt segregation and transfer. *Geol Assoc Can Mineral Assoc Canada Abstract* 16, A128.
- Vignerresse, J.-L., Tikoff, B., Améglio, L., 1999. Modification of the regional stress field by magma intrusion and formation of tabular granitic plutons. *Tectonophysics* 302, 203-224.
- Vollbrecht, A., Leiss, B., 2008. Complex fabric development in Paleoproterozoic metaquartzites of the Västervik Basin, SE Sweden. *GFF* 130, 41-45.
- Wahlgren, C.-H., Ahl, M., Sandahl, K.-A., Berglund, J., Petersson, J., Ekström, M., Persson, P.-O., 2004. Oskarshamn site investigation. Bedrock mapping 2003–Simpevarp subarea. Outcrop data, fracture data, modal and geochemical classification of rock types, bedrock map, radiometric dating. Swedish Nuclear Fuel and Waste Management Company. SKB-R-04-102. Stockholm, Sweden.
- Wahlgren, C.-H., Hermanson, J., Forssberg, O., Curtis, P., Triumph, C.-A., Drake, H., Tullborg, E.-L., 2006. Geological description of rock domains and deformation zones in the Simpevarp and Laxemar subareas. Preliminary site description Laxemar subarea-version 1.2. Swedish Nuclear Fuel and Waste Management Company. SKB-R-05-69, Stockholm, Sweden.
- Wahlgren, C.-H., Curtis, P., Hermanson, J., Forssberg, O., Öhman, J., Drake, H., Fox, A., Triumph, C.-A., Mattsson, H., Thunehed, H., 2008. Geology Laxemar, Site descriptive modelling, SDM-Site Laxemar. Swedish Nuclear Fuel and Waste Management Company. SKB-R-08-54. Stockholm, Sweden.
- Waitt, R. B., 2002. Great Holocene floods along Jökulsa a Fjöllum, north Iceland. In: Martini, I.P., Baker, V.R., Garzón, G. (Eds.), *Flood and megaflood processes and deposits: recent and ancient examples*. *Special Pub Int Ass Sed* 32, 37-51.
- Walker, G. P. L., 1964. Geological investigation in eastern Iceland. *Bull Volcanol* 27, 351-363.
- Walker, G. P. L., 1974. The structure of eastern Iceland. In: Kristjansson, L. (ed.). *Geodynamics of Iceland and the North Atlantic Area*. Reidel Publishing Company, Dordrecht, Holland, pp 177-188.
- Walker, G. P. L., 1993. Basaltic-volcano systems. *Geol Soc London, Spec Pub* 76, 3-38.
- Walker, G. P. L., Self, S., Wilson, L., 1984. Tarawera 1886, New Zealand—a basaltic plinian fissure eruption. *J Volcanol Geotherm Res* 21, 61-78.
- Walter, T. R., Amelung, F., 2004. Influence of volcanic activity at Mauna Loa, Hawaii, on earthquake occurrence in the Kaoiki Seismic Zone. *Geophys Res Lett* 31, LO7622, doi: 10.1029/2003GL019131.

- Walter, T. R., Troll, V. R., 2001. Formation of caldera periphery faults: an experimental study. *Bull Volcanol* 63, 191-203.
- Wang, T., Wang, X., Li, W., 2000. Evaluation of multiple emplacement mechanisms: the Huichizi granite pluton, Qinling orogenic belt, central China. *J Struct Geol* 22, 505-518.
- Wark, D. A., Stimac, J. A., 1992. Origin of mantled (rapakivi) feldspars: experimental evidence of a dissolution- and diffusion-controlled mechanism. *Contrib Mineral Petrol* 111, 345-361.
- Watkins, N. D., Walker, G. P. L., 1977. Magnetostratigraphy of eastern Iceland. *Am J Sci* 277, 513-584.
- Weidemann, M., 2008. Structural geology analyses of dykes in the Göttemar pluton and its bedrock. Bachelor of Science thesis, University of Göttingen, Germany (in German).
- Weil J. A., 1984. A review of electron spin spectroscopy and its application to the study of paramagnetic defects in crystalline quartz. *Phys Chem Minerals* 10, 149-165.
- Weiss, T., 1994. Mittelproterozoische Magmatite im "Transscandinavian Fold Belt" S' Blankaholm, SE Schweden. Diploma mapping thesis, University of Göttingen, Germany (in German).
- Wells, S. G., McFadden, L. D., Renault, C. E., 1990. Geomorphic assessment of Quaternary volcanism in the Yucca Mountain area, southern Nevada: implications for the proposed high-level radioactive waste repository. *Geology* 18, 549-553.
- Westerman, D. S., Dini, A., Innocenti, F., Rocchi, S., 2004. Rise and fall of a nested Christmas-tree laccolith complex, Elba Island, Italy. In: Breitkreuz, C., Petford, N. (eds.). *Physical geology of high-level magmatic systems*. *J Geol Soc London, Special Pub* 234, 195-213.
- Whalen, J. B., Currie, K. L., Chappell, B. W., 1987. A-type granites: geochemical characteristics, discrimination, and petrogenesis. *Contrib Mineral Petrol* 95, 407-419.
- White, R. S., McKenzie, D., 1989. Magmatism at rift zones: The generation of volcanic continental margins and flood basalts. *J Geophys Res* 94, 7685-7729.
- White, R. S., McKenzie, D., 1995. Mantle plumes and flood basalts. *J Geophys Res* 100, 17543-17585.
- White, R. S., Spence, G. D., Fowler, S. R., McKenzie, D. P., Westbrook, G. K., Bowen, N., 1987. Magmatism at rifted continental margins. *Nature* 330, 439-444.
- Wiebe, R. A., Smith, D., Sturm, M., King, E. M., Seckler, M. S., 1997. Enclaves in the Cadillac Mountain Granite (Coastal Marine): samples of hybrid magma from the base of the chamber. *J Pet* 38, 393-423.
- Wiebe, R. A., Collins, W. J., 1998. Depositional features and stratigraphic sections in granitic plutons: implications for the emplacement and crystallization

- of granitic magma. *J Struct Geol* 20, 1273-1289.
- Wiebe, R. A., Wark, D. A., Hawkins, D. P., 2007. Insights from quartz cathodoluminescence zoning into crystallisation of the Vinalhaven granite, coastal Maine. *Contrib Mineral Petrol* 154, 439-453.
- Wignall, P., 2005. The link between Large Igneous Province eruptions and mass extinctions. *Elements* 1, 293-297.
- Wikman, H., Kornfält, K.-A., 1995. Updating of a lithological model of the bedrock of the Aspo area. Swedish Nuclear Fuel and Waste Management Company. SKB-PR 25-95-04.
- Wilson, J., Ferré, E.C., Lespinasse, P., 2000. Repeated tabular injection of high-level alkaline granites in the eastern Bushveld, South Africa. *J Geol Soc London* 157, 1077-1088
- Winslow, M. A., 1983. Clastic dyke swarm and the structural evolution of the foreland fold and thrust belt of the southern Andes. *GSA Bull* 94, 1073-1080.
- Winterer, E. L., Metzler, C. V., Sarti, M., 1991. Neptunian dykes and associated breccias (southern Alps, Italy and Switzerland): role of gravity sliding in open and closed systems. *Sedimentology* 38, 381-404
- Wood, C. A., 1980. Morphometric evolution of cinder cones. *J Volcanol Geotherm Res* 7, 387-413.
- Wolfe, C. J., Bjarnason, I. T., VanDecar, J. C., Solomon, S. C., 1997. Seismic structure of the Iceland mantle plume. *Nature* 385, 245-247.
- Wolff, J. A., Sumner, J. M., 2000. Lava fountains and their products. In: Sigurdsson, H., Houghton, B. F., McNutt, S. R., Rymer, H., Stix, J. (eds.). *Encyclopedia of volcanoes*. Academic Press, San Diego, CA, pp. 321-329.
- Wright, T. J., Ebinger, C., Biggs, J., Ayele, A., Yirgu, G., Keir, D., Stork, A., 2006. Magma-maintained rift segmentation at continental rupture in the 2005 Afar dyking episode. *Nature* 442, 291-294.
- Wylie, J. J., Helfrich, K. R., Dade, B., Lister, J. R., Salzig, J. F., 1999. Flow localization in fissure eruption. *Bull Volcanol* 60, 432-440.
- Wyrick, D. Y., Smart, K. J., 2008. Dyke-induced deformation and Martian graben systems. *J Volcanol Geotherm Res*, doi: 10.1016/j.volgeores.08.11.022.20
- Yoshinubo, A. S., Barnes, C. G., 2008. Is stoping a volumetrically significant pluton emplacement process? Discussion. *GSA Bull* 120, 1080-1081.
- Yoshinubo, A. S., Fowler, T. K., Paterson, S. R., Llambias, E., Tickyi, H., Sato, A. M., 2003. A view from the roof: magmatic stoping in the shallow crust, Chita pluton, Argentina. *J Struct Geol* 25, 1037-1048.
- Zak, J., Paterson, S. R., 2006. Roof and walls of the Red Mountain Creek pluton, eastern Sierra Nevada, California (USA): implications for process zones

- during pluton emplacement. *J Struct Geol* 28, 575-587. <http://lmi.is>
<http://www.skb.se>
- Zak, J., Holub, F. V., Kachlik, V., 2006. Magmatic stoping as an important emplacement mechanism of Variscan plutons: Evidence from roof pendants in the Central Bohemian plutonic complex (Bohemian Massif). *Int J Earth Sci* 95, 771-789.
- Zarins, K., Johansson, Å., 2008. U-Pb geochronology of gneisses and granitoids from the Danish island of Bornholm: new evidence for 1.47-1.45 Ga magmatism at the southwestern margin of the East European Craton. *Int J Earth Sci*, doi: 10.1007/s00531-008-0333-0.
- Zeck, H. P., Andriessen, P. A. M., Hansen, K., Jensen, P. K., Rasmussen, B. L., 1988. Paleozoic paleo-cove of the southern part of the Fennoscandian Shield: fission track constraints. *Tectonophysics* 149, 61-66.
- Zhigulev, V. V., Gurinov, M. G., Ershov, V. V., 2008. Deep structure of the Yuzhno-Sakhalinsk mud volcano: results of multidisciplinary seismic surveys. *Russ J Pacific Geol* 2, 294-298.
- Zieg, M. J., Marsh, B. D., 2005. The Sudbury igneous complex: viscous emulsion differentiation of a superheated impact melt sheet. *GSA Bull* 117, 1427-1450.

Websites:

- <http://www.beasy.com>
<http://en.wikipedia.org>
<http://www.hi.is>

PERSÖNLICHE ANGABEN

Name: Nadine Friese

Geburtsdatum: 26.08.1980

Geburtsort: Leinefelde

Staatsangehörigkeit: deutsch

AUSBILDUNG

06/2006 – 06/2009

*Georg-August Universität
Göttingen*

**Wissenschaftliche Mitarbeiterin am
Geowissenschaftlichen Zentrum (GZG) der Georg-
August Universität Göttingen, Promotionsstudium**

Promotion mit dem Thema: Tectonically-controlled
emplacement mechanisms in the upper crust under
specific stress regimes: case studies

05/2006

*Georg-August Universität
Göttingen*

Diplom Abschluss Geowissenschaften

Diplomarbeit: Field and remote sensing studies of fault
development and fluid transport (groundwater) in the
Thingvellir Graben, Southwest Iceland

Diplomkartierung: Lithologische und Struktur-
geologische Kartierung in dem Gebiet NW´ Ankersrum,
W´ des Långsjön (Västervik Region), SE Schweden

04/2003:

*Georg-August Universität
Göttingen*

Bachelor of Science Abschluss Geowissenschaften

Bachelorarbeit: Mineralogische und Geochemische
Charakterisierung von „Cold Seep“ Karbonaten aus dem
Nordwestlichen Teil des Schwarzen Meeres

10/1999 – 06/2009:

*Georg-August Universität
Göttingen*

Studium der Geowissenschaften

07/1999:

Abitur am Staatlichen Gymnasium „Marie Curie“,
Worbis

Ort, Datum

Unterschrift